


For Reference

NOT TO BE TAKEN FROM THIS ROOM

Ex LIBRIS
UNIVERSITATIS
ALBERTAENSIS





Digitized by the Internet Archive
in 2023 with funding from
University of Alberta Library

<https://archive.org/details/Miller1982>

THE UNIVERSITY OF ALBERTA

"The metallogeny of uranium in the Great Bear Batholith complex, Northwest Territories"

by



Richard George Miller

A THESIS

SUBMITTED TO THE FACULTY OF GRADUATE STUDIES AND RESEARCH

IN PARTIAL FULFILMENT OF THE REQUIREMENTS FOR THE DEGREE

OF Doctor of Philosophy

Geology

EDMONTON, ALBERTA

Spring, 1982

Dedication

to all those who never dedicated their theses to themselves,
in recognition of the price they have paid.

Abstract

The Great Bear Batholith Complex is a late Aphebian (1850–1875 Ma) volcano–plutonic terrain east of Great Bear Lake in the Northwest Territories of Canada, comprising 20,000 km² of the Bear Structural Province. Elongated north–south, it is separated by the Wopmay Fault from the more deeply eroded, 1890 Ma old Hepburn Batholith to the east. It is overlain to the north and west by the Helikian Hornby Bay Group of marine sandstones, dolostones and shales, and to the south and west by a predominantly carbonate marine succession of early Cambrian to late Devonian age, with minor Cretaceous marine outliers. Post-orogenic diabbases were emplaced at 1392±48 Ma, 1250–1200 Ma and approximately 675 Ma. A regional north–east grain is imparted by dykes, faults and giant quartz veins.

The complex is a uranium metallogenic province, and uranium deposits occur within and around the batholith and in the overlying sedimentary rocks. They include the U–Ag deposits of the Echo Bay and Eldorado mines, and the pitchblende deposit of the Rayrock mine, all now exhausted. Some forty sites were visited, of which about thirty had uranium mineralisation; these sites are under active exploration or were selected after consulting government assessment records. The deposits, mostly previously undescribed, may be broadly classified as, (a) supergene veinlets; (b) sandstone–hosted deposits within Helikian strata; (c) hydrothermal veins; and (d) xerogenic deposits (placers and/or duricrust–hosted deposits, formed under desert conditions and now regionally metamorphosed to amphibolite facies).

(a) A group of small pitchblende deposits along the Coppermine River straddles the Wopmay Fault. 400–660 Ma old, they are regarded as supergene in origin, and occur immediately beneath the Helikian unconformity.

(b) Helikian Hornby Bay Group sandstones host several deposits. At Mountain Lake, stratiform pitchblende with Cu, Ni and minor Co and Ag arsenides and sulphides is 1076±96 Ma old, possibly remobilised at about 450 Ma. Barite occurs in the sandstone matrix. At Dease Lake, narrow stratiform bands of metazeunerite ($\text{Cu}(\text{UO}_2)_2(\text{AsO}_4)_2 \cdot 8\text{H}_2\text{O}$) in sandstone may represent a similar but oxidised deposit, again with minor associated

barite. On Leith Peninsula, a swamp at Naga Lake contains an unidentified source of radioactivity, and there are slightly radioactive redox interfaces in sandstones tentatively correlated with the basal Hornby Bay Group. Leith Peninsula also shows minor syngenetic, strata-bound copper sulphide deposits in a sandstone–dolostone sequence. It is suggested that similar copper sulphide deposits at Mountain Lake caused the precipitation of pitchblende by the reduction of percolating hexavalent uranyl solutions; in the process, barite replaced some of the original carbonate cement.

(c) The hydrothermal deposits investigated include showings at Echo Bay, Achook Island and Dog Island (all 1500 ± 10 or 1424 ± 29 Ma old); on the JD claims at the Wopmay Fault (1092 ± 115 and 535 ± 164 Ma old); at the PITCH 8–10 and 27–28 claims on Hottah Lake (440 ± 57 and 1450 ± 150 Ma old respectively); at Beaverlodge Lake (440 ± 57 Ma old, but indicating an event as much as 2058 ± 34 Ma old); at Mazenod Lake (457 ± 26 Ma old); and at the Rayrock mine, where pitchblende 511 ± 86 Ma old is hosted by a much older giant quartz vein. Correlations were sought amongst the hydrothermal deposits between such factors as age, host-rock lithology, vein orientation, geography and mineralogy, but few were found. The mineralogy ranges from simple pitchblende–quartz–hematite deposits to the complex Ag–U–Cu–Co–Ni–Bi–As suite at Echo Bay. Chlorite is not a common accessory mineral, but carbonates, copper minerals and pyrite or hematite are common, and quartz almost ubiquitous. Wall-rock potassium metasomatism occurs at the Echo Bay and Mazenod Lake deposits, and sodium metasomatism at the Rayrock deposit, while the JD deposit group is associated with minor episyenitic alteration of a granite. Such metasomatic reactions between feldspars and phyllosilicates may serve to buffer the pH of hydrothermal solutions during pitchblende precipitation. Ferrous silicates or magnetite are probably the commonest reductants for the $U^{6+} : U^{4+}$ transition, explaining the frequent association of pitchblende with hematite, and the marked frequency of diabase in the vein wall-rocks.

(d) A narrow belt of feldspathic paragneisses adjacent to the Wopmay Fault hosts deposits of uraninite associated with magnetite, and sometimes hydroxyapatite, scapolite, tourmaline, rare earths, molybdenite or zircon. They have many characteristics of placer sands, such as apparently detrital uraninite and zircon-rich laminae. The Cl- and B-bearing minerals also suggest an evaporitic influence, and the occurrences are interpreted as

metamorphosed desert or "xerogenic" deposits. These deposits include those on the JACKPOT, HAM, JONES, JLD, NORI/RA and UGI/DV claims.

The isotopic dating showed periods of hydrothermal mineralisation 1400–1500 Ma, 1050–1200 Ma and 400–660 Ma ago. These intervals coincide both with the known periods of tropical palaeolatitude, derived from published palaeomagnetic studies, and with major igneous or tectonic events, and these two factors are suggested to be major controls upon the regional mobilisation and local deposition of uranium. Deeply penetrative tropical weathering has not occurred during the past 200 Ma, uranium has thus not been rapidly released for transport into hydrothermal systems, and no pitchblende deposits younger than some 200 Ma are therefore predicted to occur in the batholith. Isotopic analyses of secondary uranium minerals, and of lead from certain sulphides and sedimentary carbonates, were also undertaken. The secondary minerals gave ages similar to their parental pitchblende. Although the results from the sedimentary rocks were inconclusive, they suggest that this method has potential for the common–lead dating of carbonate rocks.

Country rock samples were analysed for U and Th by neutron activation by Dr. E. Hoffman of McMaster University, Ontario. The felsic igneous rocks comprising the bulk of the batholith are enriched in U, Th and K compared to the rest of the known Canadian Shield. The source of uranium for any deposit can rarely, if ever, be proved, but these rocks have probably directly provided the metal for a minority of the deposits. It is thought that pre–batholithic cover sequences, such as those containing the xerogenic deposits, are a source of uranium for some others, and probably supplied U, Th and K to at least some of the igneous suites by anatectic processes. Isotopic studies suggest that some uranium deposits were created by the remobilisation of older, post–batholithic deposits, whose radiogenic lead they have inherited.

Proterozoic meta–pelites have often been suggested as a source of uranium in unconformity–coincident deposits overlying Proterozoic metamorphic terrains, as in the Athabasca Basin; it would now seem that placer and xerogenic deposits of this age are also a possible precursor in some cases.

Acknowledgements

Theses are the result of the co-operation of many people. Ron Oxburgh first had the faith to recommend my application, and Richard Lambert accepted it, sight unseen. Roger Morton then taught me the fundamental principles of economic geology in all its facets, and first suggested a regional study of uranium mineralisation. To him is owed the greatest debt. Within the department, practically all the faculty have submitted patiently to questions of varying sensibility at one time or another. Particular thanks go to Bud Baadsgaard for instructing me in the theory and practice of U-Pb isotopic systems, to Fred Longstaffe for the freedom of the X-ray laboratory, to Dorian Smith for allowing me a free rein on the electron microprobe and to Steve Launspach for the microprobe data reduction.

Many others have helped in various ways, with active assistance or by intimating that this study could *not* be done! Bill Padgham of the Department of Indian Affairs and Northern Development gave solid financial and logistical support in the field, and his staff were a constant resource. Stu Roscoe of the Geological Survey asked the most pertinent questions, and Sunil Gandhi and Bob Hildebrand supplied answers. The field geologists of numerous companies housed, fed, transported and educated me in the field, and I particularly thank the employees of S.E.R.U. Nucleaire (Canada) Ltd., B.P. Minerals Ltd., Esso Minerals Canada, Gulf Minerals Canada Ltd., AGIP Canada Ltd., Highwood Resources Ltd., Echo Bay Mines Ltd. and Aquitaine Company of Canada Ltd.

Friends and family helped me retain my sanity through the darker days; Don Blackadar, Mike Cunningham, Fred Longstaffe, Garth Milvain, Lauren Pudsey, Jock Slater and Bob St Louis deserve special mention. Last but not least, my parents provided every encouragement throughout the ups and downs, and this thesis is a testimony to their faith, love and support.

Table of Contents

Chapter	Page
I. INTRODUCTION	1
II. GEOLOGY OF THE BEAR PROVINCE	3
A. General Geology	3
B. Great Bear Batholith	6
The exotic terrain	11
C. Epworth Basin	12
D. Great Slave and Kilohigok Basins	12
E. Coppermine Homocline	15
F. Metamorphism	15
G. Non-granitic Intrusions	16
H. Folding and Faulting	17
I. Giant quartz veins	18
J. Deep Structure	19
K. Palaeohistory	20
III. URANIUM: ASPECTS OF GENERAL GEOCHEMISTRY AND DEPOSITION	23
A. Uranium Geochemistry	23
Uranium solubility	24
Mechanisms of uranium precipitation	25
B. Uranium deposits: classification and origins	33
IV. THE DEPOSITS	39
Foreword	39
A. The Coppermine River deposits	41
The MAC U-Fe-Cu-S-(Co-As-carbonate) showing	41
The BESS U-Co-Cu-As showing	43
The CAM showing	43
The CON showing	43
The FALCON U-Si-Cu-Fe-Pb-(carbonate) showing	43
The ECHO, FLOW and SOUTH U-carbonate-(Cu-Fe-S-Ag) showings	44

	The BEAR showing	45
	The FC U-Fe-Cu-S showing	45
	The TABB U-Si-Fe-S-(Co-As) showing	46
	Discussion of the Coppermine River deposits	46
B.	The Mountain Lake U-(Cu-Co-Ni-Fe-Ag-S-As-Ba) deposit	47
C.	The Dease Lake U-Cu-Fe-As-S deposits	54
D.	Leith Peninsula	55
	Naga Lake	55
	Leith Showing	58
	The Raspberry Ridge Cu-Fe-S showing	58
E.	The Echo Bay Ag-U-Bi-Cu-Co-Ni-Fe-Pb-As-S-Si-carbonate (-Te-Se-Mn-Zn-Ba) deposits	60
	Echo Bay and Eldorado mines	62
	Camsell River	65
F.	The Achook Island U-Cu-S-Si(-Fe-Co-Ni-Zn-As) deposits	66
G.	The Dog Island U-Si-Fe-carbonate deposit	69
H.	Models of mineralisation for the Echo Bay, Achook Island and Dog Island deposits	72
I.	The JD claims group	74
	The JD Zone U-Cu-Fe-Pb-S-Si-carbonate deposit	74
	The T1 Zone U-Fe-Pb-S-Si deposit	77
	The Main Zone U-Fe-Cu-Pb-S-Si deposit	77
	The episyenite	78
	Discussion of the JD deposit group	80
J.	Hottah Lake	82
	The PITCH 8-10 U-Cu-Fe-Bi-Pb-Ag-S-Se-Si-carbonate deposits	82
	The PITCH 27-28 U-Mo-Bi-Pb-Cu-Zn-REE-S-Te-Si deposit	85
K.	The Beaverlodge Lake U-Fe-Si(-Bi-S) deposits	86
	The quartzite-hosted deposits	89
	The gabbro-hosted deposits	90
	The adit	90

	Discussion of the Beaverlodge Lake deposits	92
L.	The Mazenod Lake Cu-U-Bi-Cu-Pb-Fe-S-Se-Te(-Ag) deposits	93
M.	The Rayrock mine U-Cu-Ni-S-As-Si(-Co-Bi) deposits	98
	Adjacent deposits	102
	The proposed paragenesis	102
N.	The metamorphosed palaeo-placer deposits	103
	Introduction	103
	The JACKPOT claims	104
	The HAM and JONES claims	114
	The JLD claims	120
	De Vries Lake: the NORI/RA claims	122
	De Vries Lake: the UGI/DV claims	130
	The genesis of the metamorphosed palaeo-placer deposits	135
	Other genetic models	138
	The source-rock potential of the meta-placer deposits	141
V.	ISOTOPIC ANALYSES	142
A.	Uranium-lead dating	142
B.	Sulphide lead analyses	147
C.	Carbonate lead analyses	149
VI.	DEPOSITIONAL CORRELATIONS AND CONTROLS	151
A.	Foreword: the isotopic ages	151
B.	Genetic, geological, geographical and structural comparisons	153
	The Helikian sandstone-hosted deposits	153
	The late Aphebian palaeo-placer deposits	154
	The hydrothermal and supergene deposits	155
C.	The mineralogical and geochemical correlations	158
	A digression on copper mineralisation	161
D.	The tectonic and climatic correlations	161
VII.	THE SOURCES OF URANIUM	164
A.	The limitations of $^{208}\text{Pb}/^{204}\text{Pb}$ and $^{208}\text{Pb}/^{206}\text{Pb}$ ratios	164
	Uranogenic lead contamination and precursor uranium deposits	165

B.	The geographical location of the sources and deposits	166
C.	The dispersed uranium content of the batholith: local enrichment	166
	"S-type" and "I-type" granitoids	167
	Whole-rock sampling and analysis for U and Th	169
	Weathering and loss of U and Th	170
	Analytical results	175
D.	Regional uranium enrichment	178
E.	Conclusions on the source of uranium	179
VIII.	THE CONTINUITY OF PROCESS : WEATHERING AND OXIDATION	182
A.	Oxidation and secondary uranium minerals	183
	The identification of secondary uranium minerals	184
	The "autunite" and "uranophane" group minerals	186
	The uranyl oxide hydrate minerals	192
	The uranyl carbonate minerals	193
	Other uranyl minerals	193
	Controls on the formation of uranyl minerals	193
B.	The age and isotopic composition of the secondary mineralisation ..	194
C.	Present day uranium deposition	197
IX.	SUMMARY AND CONCLUSIONS	199
X.	REFERENCES CITED	203
XI.	APPENDIX I: KEY TO SAMPLE NUMBERING	221
XII.	APPENDIX II: ANALYTICAL TECHNIQUES	222
	Electron microprobe analyses	222
	Reflectivity and hardness measurements	222
	Neutron activation analysis	222
XIII.	APPENDIX III: ISOTOPIC AGES OF THE DEPOSITS	224
A.	Introduction	226
B.	Regional geology	226
C.	Sample sites and geology	228
	Echo Bay Geochronology	230
D.	Techniques: Sampling	232

Pb and U Isotope Measurements	233
Treatment of Lead Isotope Data	234
E. Results	235
Meta-placer Deposits	242
Other Isotopically Simple Deposits: Mountain Lake	246
Coppermine River	246
Echo Bay, Achook Island, Dog Island	246
Rayrock Mine	252
Isotopically Complex Deposits: Mazenod Lake	252
JD Claims Group	257
Hottah and Beaverlodge Lakes	261
F. Conclusions	264
G. Acknowledgements	268
XIV. APPENDIX IV: MAZENOD LAKE DEPOSIT MINERALOGY	272

Tables

Table 1: Classification of the principal uranium deposit associations	35
Table 2: Electron microprobe analyses of uraninite and pseudobrookite from the meta-placer deposits	105
Table 3: Lead isotope analyses of sulphide and sedimentary carbonate samples	148
Table 4: Orientations of uranium-mineralised veins	157
Table 5: The elemental chemistry of the uranium deposits	159
Table 6: Criteria for distinguishing "S-type" and "I-type" granites	168
Table 7: Uranium-thorium analyses of rocks from the Great Bear Batholith and adjacent areas	171-174
Table 8: Average uranium and thorium contents of Canadian Shield areas	180
Table 9: Secondary uranium minerals reported from the Great Bear Batholith and adjacent areas	185
Table 10: Anomalous and unidentified X-ray diffraction patterns of uranium secondary minerals	187-190
Table 11: Isotopic data of uranium secondary minerals	196

Figures

Figure 1: The structural elements of the Bear–Slave area	4
Figure 2: Location map of deposits visited	8
Figure 3: Stratigraphic columns for the Great Slave Basin, Epworth Basin and Coppermine Homocline	13
Figure 4: Plot of palaeolatitude against time	21
Figure 5: Eh values for important redox reactions and uraninite dissolution	26
Figure 6: Eh – pH diagram for the system $U-O_2-CO_2-H_2O$	28
Figure 7: Eh – pH diagram of iron sulphides and oxides and dissolved sulphur species in water	31
Figure 8: Eh – pH diagram of iron sulphides, oxides, carbonates and dissolved iron species in water	32
Figure 9: Electrochemical deposition of uraninite	34
Figure 10: Geology of the Coppermine River deposits	42
Figure 11: Regional geology of Mountain Lake	48
Figure 12: Detailed geology and stratigraphic position of the Mountain Lake deposits	49
Figure 13: Geology of the Leith Peninsula showings	57
Figure 14: Echo Bay – Camsell River area and the Mystery Island plutons	61
Figure 15: Geology of the Echo Bay and Eldorado mines	63
Figure 16: Geology of the Achook Island showings (RHY and SHORE claims)	67
Figure 17: Geology of the Dog Island showings (BERNI claims)	70
Figure 18: Geology of the JD claims group showings	75
Figure 19: Geology of the PITCH 8–10, PITCH 27–28, JB and LOIS showings	83

Figure 20: Geology of the Beaverlodge Lake occurrences88

Figure 21: Geology of the Mazenod Lake area94

Figure 22: Geology of the Marion River Fault (Rayrock mine)99

Figure 23: Geology of the JACKPOT occurrence 106

Figure 24: Geology of the HAM and JONES occurrences 115

Figure 25: Geology of the JLD occurrence 121

Figure 26: Geology of the NORI/RA and UGI/DV occurrences 124

Figure 27: Generalised concordia plot illustrating the effect of contaminant
radiogenic lead 145

Figure 28: Correlation diagram of uranium mineralisation events, tectonism and
palaeolatitudes in the Great Bear Batholith 163

Plates

Plate 1: Mineralised Hornby Bay Group sandstone, Bear Mountain (Dease Lake)	56
Plate 2: Naga Lake radioactive swamp, Leith Peninsula	56
Plate 3: Dog Island; scintillometer survey of radioactive tuff	71
Plate 4: Episyenite, T1 Zone (JD deposit group)	79
Plate 5: Episyenite, T1 Zone (JD group)	79
Plate 6: Pitchblende deposited with dolomite, PITCH 8–10; thin section	87
Plate 7: Pitchblende and molybdenite, PITCH 27–28; polished section	87
Plate 8: Unconformity in Snare Group rocks, Beaverlodge Lake	91
Plate 9: Pitchblende–hematite mineralisation in quartzite, Beaverlodge Lake; thin section	91
Plate 10: Chess–board albite replacing plagioclase, Mazenod Lake; thin section	95
Plate 11: Microcline replacing plagioclase, Mazenod Lake; thin section	95
Plate 12: Plagioclase and microcline altering to albite, Rayrock mine; thin section	101
Plate 13: Pitchblende–chlorite–hematite mineralisation replacing country rock, Rayrock mine; thin section	101
Plate 14: The JACKPOT occurrence; view of stripped outcrop	108
Plate 15: The JACKPOT occurrence; boudins of the conformable magnetite in paragneiss	108
Plate 16: The JACKPOT occurrence; deformed paragneiss cut by magnetite vein	110
Plate 17: The JACKPOT occurrence; magnetite vein hosting brecciated paragneiss	110
Plate 18: Fluorite in biotite, JACKPOT occurrence; thin section	111
Plate 19: Xenotime, JACKPOT occurrence; thin section	111

Plate 20: Pseudobrookite replacing ilmenite, JACKPOT occurrence; polished section ..	113
Plate 21: Uraninite in pseudobrookite, JACKPOT occurrence; polished section	113
Plate 22: Zircons in paragneiss, JONES occurrence; thin section	118
Plate 23: Massive magnetite outcrop, HAM occurrence	118
Plate 24: Uraninite in magnetite, JONES occurrence; polished section	119
Plate 25: Quartz pebble in laminated, radioactive paragneiss, JONES occurrence	119
Plate 26: Magnetite remobilised into veinlets, JLD occurrence	123
Plate 27: Magnetite augen in paragneiss country rocks, NORI/RA occurrence	126
Plate 28: Magnetite-rich laminae in paragneiss country rocks, NORI/RA occurrence	126
Plate 29: Apatite-biotite rock, NORI/RA occurrence; thin section	128
Plate 30: Detrital uraninite grains in biotite, NORI/RA occurrence; polished section	128
Plate 31: Detrital uraninite grains in biotite, NORI/RA occurrence; polished section	129
Plate 32: Xenoliths in "porphyritic" paragneiss, UGI/DV occurrence	133
Plate 33: Hornblende-apatite rock, UGI/DV occurrence	133
Plate 34: Hornblende-apatite rock, UGI/DV occurrence; thin section	134
Plate 35: Uraninite in paragneiss, UGI/DV occurrence; polished section	134

I. INTRODUCTION

The Great Bear Batholith Complex comprises some 20,000 km² of the Canadian Shield, east of Great Bear Lake. It is a late Aphebian (~1850–1875 Ma) volcano–plutonic complex forming the western sector of the Bear structural province, which in turn lies on the west flank of the Archaean Slave province, and extends from Great Slave Lake to the Arctic coast. The batholith and some adjacent rocks form a uraniferous metallotect of modest importance; for example, the Manhattan Project was fuelled with uranium from the Eldorado mine at Port Radium, which produced at least 6300t of uranium. The Rayrock mine, 150 kilometres north–west of Yellowknife, produced another 150t of uranium, and other less successful mining operations have been attempted. Under present market conditions, and with richer deposits now being exploited elsewhere in Canada, commercial interest in uranium in the area is waning, although at least two deposits are undergoing feasibility studies. Gandhi (1978a) reports the existence of over two hundred occurrences of uranium mineralisation in the Bear and Slave area, principally from the East Arm of Great Slave Lake, the Goulburn Basin, the Coppermine Homocline and the Great Bear Batholith. These areas all flank the Bear–Slave block, and contain rocks of late Aphebian to early Helikian age. This perimetric distribution is not just a function of ease of access, since airborne surveys indicate a similar pattern of radiometric anomalies. In a broader context, rocks of late Aphebian age, and especially unconformities involving such rocks, have uraniferous associations throughout Canada and the world.

Some intensive studies have been conducted on specific deposits in and around the batholith complex, such as the theses of Withers (1979), Bloy (1979), Walker (1977), Badham (1973a), Robinson (1971), Jory (1964) and Campbell (1955), and most of the significant occurrences have been investigated commercially, with reports being lodged with the Department of Indian Affairs and Northern Development (DIAND or DINA), Yellowknife. The purpose of this thesis is to commence the welding of this disseminated information into a cohesive structure. The questions considered are the broad ones, of where the uranium came from, when and how it was transported, and where and how it was trapped. These pages present a history of uranium in this area, a framework to

orient any aspect of uranium mineralisation into a regional context. Like all broadly based studies, time will prove this to have its errors, but nevertheless it will give a necessary perspective to studies within the batholith complex, and provide a comparison for other late Archean uranium provinces.

Some forty separate sites have been visited and sampled, few of which have been presented previously in accessible literature. Of more direct interest is the inter-comparison of these deposits. The approach taken has been to find, as far as possible, the similarities rather than the differences, using such criteria as age, mineralogy, structure, geological setting and geophysical signatures to emphasize relationships. Since the detailed study of individual deposits is beyond the scope of this work, techniques such as fluid inclusion studies, stable isotope analyses and multi-element geochemistry have not been used. One detailed mineralogical study was undertaken on the Mazenod Lake deposit, however, and published separately (Miller 1981) (Appendix IV). In addition, problems peculiar to the isotopic dating of pitchblende and uraninite have been considered, to explain the techniques which evolved and the interpretation of the results, which are now in press (Miller 1982, Canadian Journal of Earth Sciences) (Appendix III).

II. GEOLOGY OF THE BEAR PROVINCE

A. General Geology

The Bear Province covers about 90,000 km², east of Great Bear Lake, of which about 50,000 km² comprise rocks of late Aphebian age. The remainder is Helikian (1750 to 950 Ma) or Hadrynian (950 Ma to the Palaeozoic). The Brock Inlier, south of Banks Island, the Minto Inlier on Victoria Island, and the post-Aphebian rocks at the mouth of Bathurst Inlet, are also parts of the province but outside the region of interest.

Since 1968, Paul Hoffman (of the Geological Survey of Canada) and co-workers have radically revised the interpretation of the Bear Province, and have established three tectonic divisions (Fig. 1). From oldest to youngest, these are:

(1) *The Coronation Geosyncline*, comprising the Hepburn (and Wentzel) Batholiths and the Epworth, Goulburn and Great Slave basins, all areas of Aphebian geosynclinal sedimentation. Comparatively unmetamorphosed relicts of the geosyncline are still preserved in the basins, which were probably originally contiguous with broadly similar successions and depositional environments.

(2) *The Wopmay Orogen*, consisting of the Great Bear Batholith complex, the Hepburn and Wentzel Batholiths and the Epworth Basin (or Fold Belt), the areas affected by the Hudsonian orogeny (ending the Aphebian era at about 1800 Ma). All three batholiths are aggregates of granitoid plutons. The Hepburn Batholith is the root of a granitic structure, and the isograds around it are inverted (*i.e.* hot-side up) and dip towards it; it partly surrounds the Wentzel Batholith, the roof of a similar structure with normal adjacent isograds (St. Onge and Hoffman 1980; Hoffman *et al.* 1980). The Wentzel Batholith plutons are highly variable, and generally became more basic with time (Hoffman *et al.* 1980). This discordant batholith has a strong contact metamorphic aureole, and was emplaced during a period of folding and continental collision (Hoffman *et al.*, *op. cit.*). The more basic and mesozonal Hepburn Batholith was unroofed before the Great Bear Batholith was emplaced (Hoffman and McGlynn 1977). No distinction will be made hereafter between the Wentzel and Hepburn Batholiths. The entrenched term "Great Bear Batholith" will be retained for what is in fact a complex volcano-plutonic terrain.

(3) *The Amundsen Basin*, a post-Hudsonian structure comprising the Brock and Minto

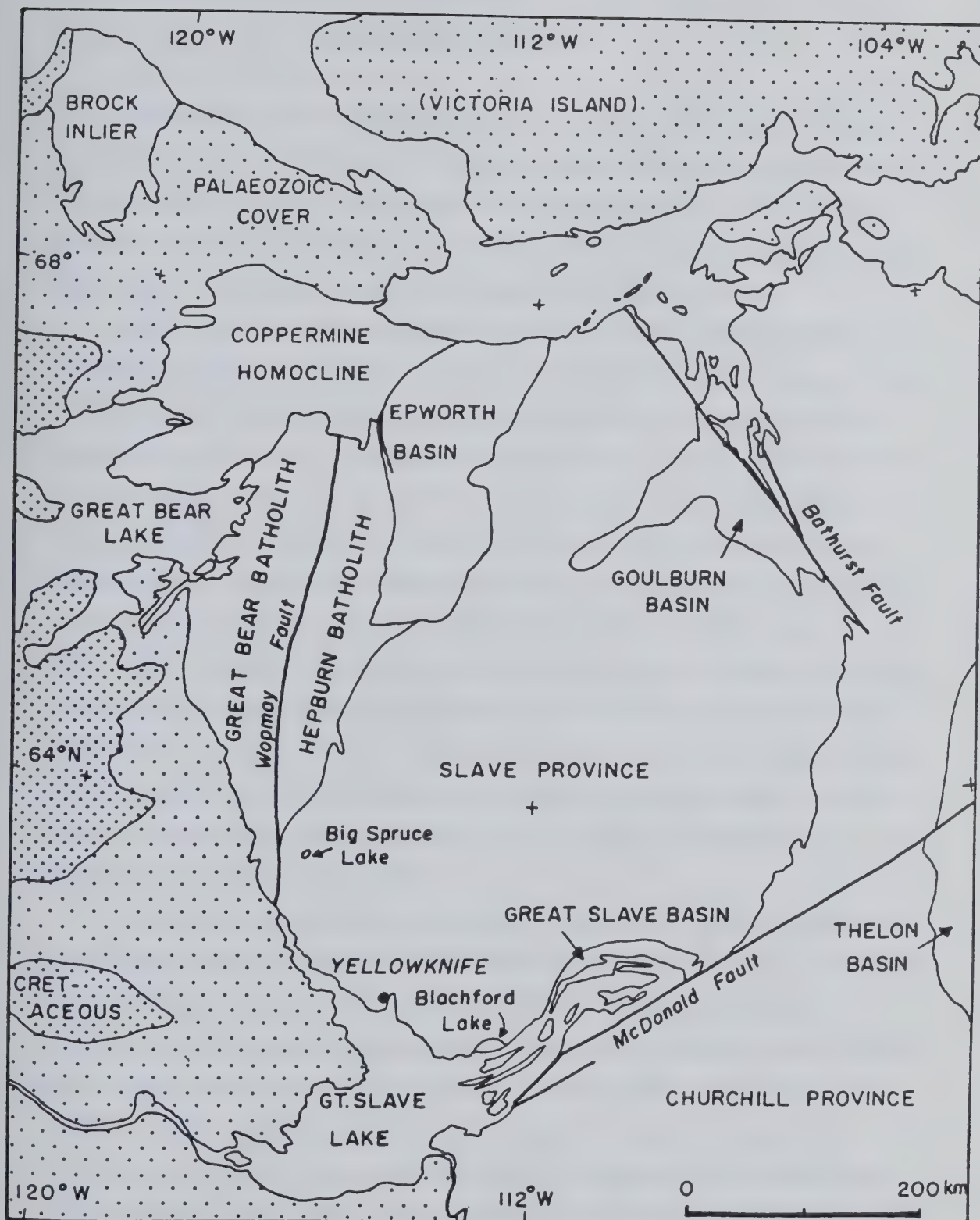


Figure 1: The principal structural elements of the Bear-Slave area.

inliers and the Coppermine Homocline. This basin accumulated shallow marine sediments throughout much of the Helikian and Hadrynian eras.

The southern part of the Bear Province extends westwards beneath Palaeozoic cover rocks for an uncertain distance. However, unpublished gravity data assembled by G. Ross (pers. comm. 1981) strongly suggest that it does not extend west of its present exposure at Great Bear Lake. Helikian sedimentary rocks of the Hornby Bay and overlying groups cover it to the north west, and to the east lies the Slave province.

The province is defined by a preponderance of radiometric ages¹ equivalent to the Hudsonian Orogeny². Plutons of the Hepburn Batholith have a general zircon U–Pb age of 1890 ± 20 Ma (van Schmus and Bowring 1980), although its southeastern sector is remobilised Archaean crust, forming mantled gneiss domes with cores 2655 ± 218 Ma old by Rb–Sr dating (after Frith *et al.* 1977). The Great Bear Batholith is the youngest sector, with a general zircon U–Pb age of 1850–1875 Ma (van Schmus and Bowring 1980), which is markedly older than was suggested by earlier K–Ar and Rb–Sr studies (see the various reports of Wanless *et al.* 1964–1979; Stockwell 1973, 1964; Lowdon 1960–1963; Loveridge 1980; Wanless and Loveridge 1972). Loss of argon during burial metamorphism to zeolite facies may explain the low K–Ar dates (Robinson and Morton 1972). Some of the igneous rocks studied by the author and others (*e.g.* Badham 1973b) have also undergone alkali metasomatism, converting the groundmass into diffuse alkali feldspar mosaics. Since such metasomatism may be prevalent in the batholith, the zircon ages are probably the most accurate.

The Slave province acted as a stable cratonic platform during the formation of the Wopmay Orogen. Hoffman and St-Onge (1981) suggest that the margin of the Slave craton was drawn into a west-dipping subduction zone, then compressed into north–south trending, west-dipping thrusts and folds in a first collisional event. Intrusion of this margin by plutons of the Hepburn (and Wentzel) Batholith metamorphosed the cover rocks from regional greenschist- to local granulite-facies. An exotic terrain along the mid-western edge of the Great Bear Batholith may represent an island arc at least

¹All ages stated as being "after" a given source have been revised according to the decay constants recommended by Steiger and Jager (1977).

²Douglas (1980) provides the most recent geochronological overview of the entire Canadian Shield.

1920±10 Ma old (van Schmus and Bowring 1980).

A shallow, east-dipping subduction zone, west of the exotic terrain, resulted in a second collision. The Great Bear Batholith represents the magmatic arc above this zone, with magmatic activity moving eastwards with time towards the Wopmay Fault. This batholith comprises granitic plutons and their extrusive equivalents. Although comparisons have been made between the Great Bear Batholith and modern Andean arcs (*e.g.* Badham 1973b), there is a fundamental difference in crustal thickness and consequent elevation between the two (Hoffman and McGlynn 1977). The Andean arcs are also considerably more basic in their chemistry. The Basin and Range Province of the USA has also been proposed as a model, since it shows crustal attenuation and floods of silicic ignimbrites (Hoffman and McGlynn 1977).

B. Great Bear Batholith

The Great Bear Batholith is exposed in a north-trending belt about 450 kilometres long and 125 kilometres wide, overlain to the north by the Helikian Hornby Bay Group (Fig. 2). Intense weathering preceded the deposition of this cover, which was of unknown original extent. Biotites in the plutons are always more or less chloritised, and much of the batholith is locally hematitic. The present surface of at least the northern half of the batholith is essentially the re-exposed Helikian surface. The batholith is composed of felsic ignimbrites, with locally abundant andesite and basalt flows, intruded by epizonal plutons consanguineous with the extrusive rocks. 90% of these plutons are more potassic than granodiorite (Hoffman and McGlynn 1977). Plutonic rocks are more abundant in the more deeply eroded southern half, and are overall the predominant lithotype.

Individual plutons have been mapped by Hoffman and McGlynn north of the 66°N parallel, the effective tree-line. They are syn- and post-volcanic, and some were unroofed to contribute boulders to the overlying sequences. One pluton intrudes Hepburn gneisses (Hoffman and Bell 1975). Four gradational varieties of pluton have been recognised (Hoffman and McGlynn 1977):

(1) The hornblende monzonite suite, the oldest group, is characterised by intense alteration haloes. It is restricted to the mineralised region around the Camsell River and Echo Bay mining camps, where it has been named the Mystery Island intrusive suite and

Figure 2: Key to Deposits

A	Coppermine River group
B	Mountain Lake
C	Bear Mountain
D	JOHN claims
E	Naga Lake
F	Leith showing
G	Raspberry Ridge
H	Echo Bay and Eldorado mines
J	Achook Island
K	Dog Island
L	JD group
M	PITCH 8-10
N	PITCH 27-28
P	Beaverlodge Lake
Q	Mazenod Lake
R	Rayrock mine
S	JACKPOT claims
T	HAM and JONES claims
U	JLD claims
V	NORI/RA claims
W	UGI/DV claims
Y	McLaren Lake

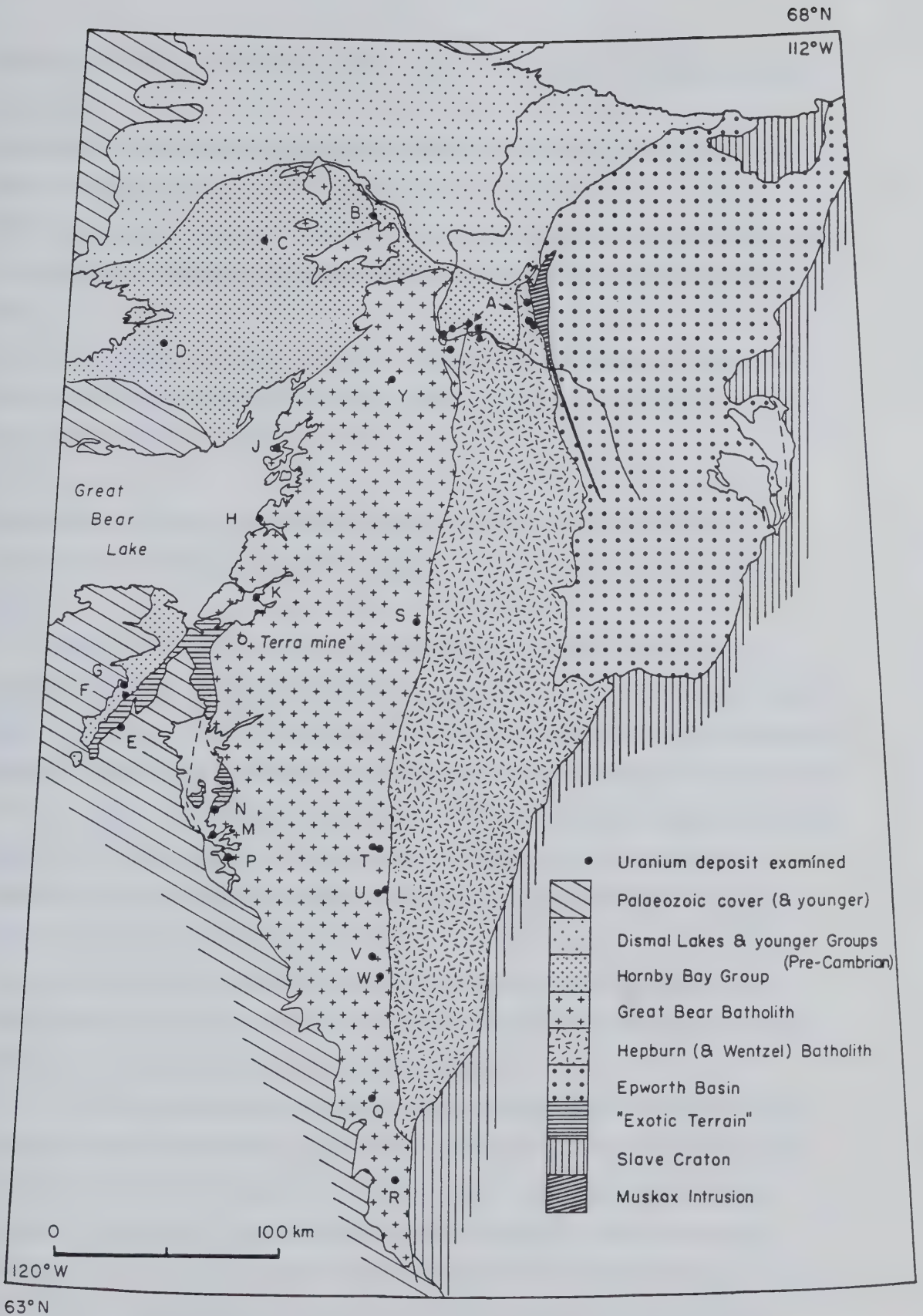


Figure 2: General geology and location map of the uranium deposits.

includes the Tut pluton at Echo Bay. There are some isolated similar plutons elsewhere in the batholith.

(2) The biotite–hornblende adameliite suite displays the largest metamorphic aureoles; one member, the Hogarth pluton, was unroofed during volcanism.

(3) The biotite granite suite has no equivalent extrusive rocks; the undifferentiated plutons are completely discordant, with steep walls and flat roofs, and postdate the episodes of folding.

(4) The hornblende tonalite suite also has no related extrusive phases; it is the youngest suite, completely discordant and apparently undifferentiated (although the plutons are only exposed in plan view, not in section).

As the batholith evolved, so the plutons became larger and more granitic, while the related extrusive activity dwindled into rhyolite dome emplacement and hydrothermal activity.

In the northern area, the volcano–sedimentary rocks, termed the *McTavish Supergroup*, outcrop in three linear belts, the western (or Labine) which is structurally the lowest, the central (or Sloan) and the eastern (or Dumas). The Labine Group is essentially bimodal, of basalt and rhyolitic ash; the other two are cycles of andesite–dacite–rhyolite extrusion, a typical calc–alkaline suite (Badham 1973b). The current nomenclature of these volcanic rocks is essentially a field classification. "Dacite" contains less than 10% combined quartz and potassium feldspar, and includes true andesites and rhyodacites, with hornblende as the dominant mafic mineral. "Rhyolite" contains more than 10%, and includes the quartz latites; biotite is the common mafic mineral. A more precise classification will be followed herein. In the south of the batholith, the minor volcanic suites have not yet been correlated with these groups.

The *Labine Group* comprises four formations, deposited on a sialic basement (Hildebrand 1980). The lowest is the *Port Radium Formation*, of thin–bedded arenites and argillites with minor carbonates and tuff, overlain by the 3000m thick *Echo Bay Formation* of porphyritic andesite flows and associated clastic rocks. These two formations comprise the *Echo Bay Group* of earlier terminology. The overlying *Cameron Bay Formation* includes ignimbrites, conglomerates and lacustrine arenites emplaced

during cauldron collapse at several centres. The fourth, *Feniak Formation* comprises tuffs and pyroclastic rocks. Plutons subsequently intruded the ash-flow magma chambers. Comparing basalts in the Echo Bay Formation with average alkali basalts, Badham (1973b) postulated extensive iron and potassium metasomatism (with a concomitant loss of calcium and sodium).

The Labine Group underwent weathering, tilting and faulting before deposition of the Sloan Group commenced (Hildebrand pers. comm. 1980). The *Sloan Group* is a vast, monotonous succession of acidic to intermediate ignimbrites.

The *Dumas Group* consists of acidic lavas and ignimbrites, and a few thin, potassic basalt flows and clastic deposits which thicken towards the Wopmay Fault. The rhyolitic flows have generally oxidised tops, and contain rare plugs and domes, one to five kilometres across, marking the old vents. Porphyritic units may be intrusive or extrusive, differentiated by the degree of crystal fracture.

Remnants of pre-volcanic sedimentary rocks are common in the east and south of the batholith. A belt of paragneiss and schist extends parallel to and just west of the Wopmay Fault for much of its length, for which no definitive map exists. This belt is up to several kilometres wide, and the closest lithological equivalent is perhaps the *Akaitcho Group* to the east (*q.v.*) (R. Hildebrand, pers. comm. 1980). Smaller pendants of much lower grade sedimentary and intercalated volcanic rocks are often correlated with the *Snare Group* (p. 12).

The McTavish Supergroup is gently folded about north-west trending axes. The folds have a wave-length of 5–10 km and are separated by homoclines up to 30 km across, which expose deeper levels in the south (Hoffman and McGlynn 1977). The folding occurred before and during the major faulting (Hildebrand pers. comm. 1980). The Supergroup totals at least 50 km of apparently superimposed ignimbrites, yet the regional metamorphism is only of sub-greenschist facies. The eruptions possibly occurred in a basin caused by crustal attenuation, forming sheets that dipped to the north-east and overlapped like tiles, but which never reached excessive thickness in any one place (Hoffman and Cecile 1974). Alternatively, the depositional basin may have been growing at a major bend in a transcurrent fault system, which removed successive strata from the site of eruption as they formed (Hoffman and McGlynn 1977). A basin is

indicated since there is no proven basement, sediment entered it from the east, and the region is depressed and undissected. Deposition was, however, generally subaerial, apart from some early pillowed basalts, while local lakes formed mudstones by the Wopmay Fault.

By analogy with modern subduction zones, these calc-alkaline suites probably formed during the subduction of oceanic lithosphere. The moderately potassium-rich basalts of the Dumas Group suggest an initial phase of continental rifting, while the trend towards more granitic plutons suggests crustal anatexis (Hoffman and McGlynn 1977). The Sloan and Dumas Groups may occupy a back-arc rift basin (Hoffman and Bell 1975).

The exotic terrain

A single zircon date of 1920 ± 10 Ma was obtained for a granodiorite from this recently-defined terrain, which includes Bell Island and parts of the adjacent east shore of Hottah Lake, and Leith Peninsula (McGlynn 1979). Its extension westwards beneath the cover rocks is unknown. There is no evidence for any original northward or eastward extensions subsequently assimilated by the Great Bear Batholith magmatism. The ancient basement of granodiorite and metamorphosed basic volcanic rocks comprising the exotic terrain on Bell Island is unconformably overlain by a sequence of lithic and arkosic sandstones, conglomerates, mudstones, basalts and rhyodacitic to rhyolitic flows and ignimbrites. These were correlated with the early batholithic development by McGlynn (*op. cit.*) but the possibility that they are somewhat older is not excluded in this thesis. Some 30 cm thick bands of quartz pebble conglomerates on Bell Island contain up to 50% detrital rutile and Fe-Ti oxides (completely oxidised), and several per cent of zircon, within the sand matrix, a significant lithology which will be referred to later.

The origin of the terrain is not known. The possibilities range from an island arc, formed above the subducted margin of the Slave craton prior to the formation of the Great Bear Batholith, to a continental fragment rafted in from the west during a plate tectonic collision.

C. Epworth Basin

The Epworth Basin or Fold Belt contains Aphebian sedimentary and minor volcanic rocks, termed the *Coronation Supergroup* (Hoffman 1981), which pre-date the batholiths (Fig. 3). Divided along the Cloos Anticline, some 10–20 km east of the present Hepburn Batholith, the western "internal zone" is eugeosynclinal (deposited upon the continental rise), while the eastern "external zone" is miogeosynclinal (deposited upon the continental shelf and craton) (Hoffman *et al.* 1978).

The lowermost unit is the *Akaitcho Group*, which has been intruded by the Hepburn Batholith and which may extend slightly into the Great Bear Batholith. A basal basaltic unit was overlain by 3–4 kilometres of arkosic turbidites, then 2 km of basalt capped by 1–1.5 km of rhyolite, pelites, basalts and volcanoclastic rocks. Rare-earth element studies suggest that this pile was deposited in an opening rift (Easton 1980). Above the Akaitcho Group lie the *Odjick* and *Rocknest Formations* of coastal marine clastics, comprising the *Epworth Group* (Hoffman 1981). The *Recluse Group* above comprises turbidites and greywackes of the *Tree River*, *Fontano* and *Asiak Formations*, with proximal and distal facies in the "external" and "internal" zones. Sedimentary sources were to the east. Orogeny capped the Recluse Group with flysch (the *Cowles Lake Formation*), molasse and red-beds (the *Takijuk Formation*) (Fraser *et al.* 1972). These had a western sediment source from the unroofing of the Hepburn Batholith.

The *Snare Group*, supracrustal rocks within the Hepburn Batholith, and perhaps including scattered pendants in the Great Bear Batholith, is generally regarded as a westward correlative of the basal Epworth strata, *i.e.* the Akaitcho Group. It was highly deformed and metamorphosed during orogeny, however, and the correlation is uncertain. It is younger than 2200 Ma (*e.g.* Frith *et al.* 1977) and older than 1890 ± 20 Ma. It is suggested later herein that some so-called Snare Group rocks adjacent to the Wopmay Fault are actually equivalent to the Cowles Lake and Takijuk Formations.

D. Great Slave and Kilohigok Basins

The Kilohigok Basin, or Bathurst Aulacogen, occupied by rocks of the Aphebian *Goulburn Group*, extends along the Bathurst Fault. The Goulburn Group correlates well with rocks from the Epworth and Great Slave Basins, and will not be considered further.

AGE	GREAT SLAVE BASIN	EPWORTH BASIN, COPPERMINE H'CLINE
65 Ma	Undivided marine clastics	
CRETACEOUS		
135 Ma		
350 Ma		
LOWER PALAEOZOIC	Dominantly Carbonates	
600 Ma		
HADRYNIAN		Rae Group (units 19-25)
1000 Ma		
NEO- HELIKIAN		Coppermine R. Group (units 17-18) Dismal Lakes Group (units 11 - 16)
1400 Ma		
PALAEO- HELIKIAN		Hornby Bay Group (units 8-11)
1800 Ma	Et-then Group	
APHEBIAN	<u>GT. SLAVE SUPERG'P</u> Christie Bay Group Pethei Group Kaihochella Group Sosan Group Union Island Group	<u>CORONATION SUPERG'P</u> Takijuk Formation Cowles Lake Fm. Recluse Group Epworth Group (= Rocknest Fm., Odjick Fm.) Akaitcho Group
	Wilson Island Group	

Figure 3: Stratigraphic columns for the Great Slave Basin, Epworth Basin and Coppermine Homocline.

The Great Slave Basin, the East Arm of Great Slave Lake, is a significant U–Ag metallogenic province, close to the Great Bear Batholith and somewhat analogous to the Echo Bay region (Badham 1978). It is also a probable aulacogen (the Athapuscow Aulacogen), between the Slave and Churchill provinces, although Walker (1977) only found evidence of a graben structure west of McDonald Lake. He proposed that, east of this point, the Churchill craton was simply uplifted along the McDonald Fault to form a wedge-shaped trough that shallowed northwards.

The oldest cover on the basin's Archaean basement is the Aphebian *Wilson Island Group* of mixed volcanic rocks, with a Rb–Sr age of 1846 ± 24 Ma and an initial $^{87}\text{Sr}/^{86}\text{Sr}$ ratio of 0.7048 (Frith 1980). This was folded and metamorphosed before the deposition of the *Great Slave Supergroup* on top, comprising the *Union Island* (oldest), *Sosan*, *Kahochella*, *Pethei* and *Christie Bay Groups* (Hoffman 1969; Badham 1981). These are volcanic, carbonate and clastic units from an easterly source, overlain by turbidites from a westerly source, and capped by red-beds and basalts of the *Et-then Group*. The *Seton Island volcanics*, spilitic basalts between the Sosan and Kahochella Groups, have a Rb/Sr age of 1832 ± 10 Ma, initial $^{87}\text{Sr}/^{86}\text{Sr} = 0.7018$ (amended from Baadsgaard *et al.* 1973). Bloy (1979) reported unpublished Rb–Sr ages by Wanless of 1800–1890 Ma for volcanic rocks ranging from the Wilson Island to the Christie Bay Groups. The Great Slave Supergroup was thus formed during the Great Bear Batholith plutonism, but some anomalously old Rb–Sr and K–Ar dates for the Wilson Island and Union Island Groups show an unexplained geological complexity beneath the Supergroup (*e.g.* Bloy 1979, p. 53; Badham 1978; Burwash and Baadsgaard 1962; Davidson 1978).

The Easter Island Dyke is a differentiated alkaline intrusion of uncertain age, cutting basement rocks in the Great Slave Basin and locally containing Ag–Co–Ni–As mineralisation (Badham 1978). K–Ar dates of 2170 and 2200 Ma (Leech *et al.* 1963; Burwash and Baadsgaard 1962) suggest affinities with the nearby Blachford Lake alkaline complex (2057 ± 56 Ma by K–Ar, Davidson 1978). However, xenoliths of Sosan Group rocks occur within it, and diatremes spatially related to the dyke contain blocks of the Christie Bay Group (Badham 1978; Hoffman 1978a). Either the K–Ar dating, or the Rb–Sr dating of the volcanics, is in error, or the dyke represents several completely distinct events. Diorite laccoliths in the Great Slave Basin have been variously dated at

1630–1845 Ma (K–Ar, Hoffman 1969), >1750 Ma (discordant Pb–Pb age of pitchblende vein, Gandhi 1978a), ~1790 Ma (Badham 1981), ~1860 Ma (Frith 1980) and 1705 ± 52 , 1758 ± 60 , 1759 ± 30 and 1811 ± 81 Ma (Rb–Sr, Wanless, reported by Bloy 1979).

E. Coppermine Homocline

The Coppermine Homocline, part of the Amundsen Basin, overlaps the north–west part of the Great Bear Batholith. The basin had a locally rugged topography before burial, and the regolith is a palaeo–talus in places. The overlying Helikian strata were divided into numbered units by Baragar and Donaldson (1973). The regolith, which may be oxidised or reduced, is overlain by the *Hornby Bay Group*, comprising a basal sandstone (unit 8) passing up into dolostone (unit 9), sandstone and shale (unit 10) and through a minor unconformity into further sandstone (unit 11). The basal unit 8 may be hematized, and the unit as a whole strongly resembles published descriptions of the coeval Athabasca Formation (Dahlkamp 1978; Hoeve and Sibbald 1978). Hassard (1975) reassigned unit 11 to the base of the unconformably overlying *Dismal Lakes Group*, which comprises sandstone and black shale (unit 12), red mudstone and dolostone which may contain halite casts (unit 13), and further dolostones (units 14–16). Conformably overlying the dolostones is the *Coppermine River Group*, of massive basalt flows some 1200 Ma old (unit 17) and red sandstones (unit 18). The Hadrynian *Rae Group* unconformably overlies these red–beds, comprising a sequence of varicoloured sandstones, siltstones, shales and dolostones (units 19–25). It is unconformably overlain by Palaeozoic sediments, and intruded by the Coronation sills and Franklin dykes, 650 Ma old (Douglas 1980). Of this sequence, the Hornby Bay Group is the only one known to host uranium mineralisation, and is the most extensive.

F. Metamorphism

Metamorphic conditions across the Bear Province were varied. The regional metamorphic grade in the Great Bear Batholith is sub–greenschist facies. The zeolites thomsonite and chabazite were formed by the reaction of andesine and hornblende with CO_2 and H_2O in the Echo Bay Formation at Echo Bay, representing a temperature below 200°C and a pressure of perhaps 0.1–0.2 kb (Robinson and Morton 1972). Contact

metamorphism, metasomatism and skarn formation occurred around some of the plutons, overprinting the regional metamorphism (Mursky 1973; Hoffman and McGlynn 1977). Badham (1973a) found hornblende–hornfels contact metamorphism around plutons in the Conjuror Bay area, and estimated conditions of 600°C and 1–3 kb, but he could not recognise any regional metamorphism. The belt of migmatised schist and gneiss by the Wopmay Fault (p. 10) reaches upper amphibolite facies, a grade more typical of the more deeply eroded Hepburn Batholith, where the Sharn Group ranges from greenschist up to granulite facies (Nielsen 1978; Easton 1981a). The eastern Epworth Basin is essentially unaltered; deformation and metamorphism increase westwards, up to cordierite amphibolite facies. All the metamorphism in the province dates to the Hudsonian Orogeny, except possibly for older metamorphism beneath the Great Slave Supergroup.

G. Non-granitic Intrusions

All the known dyke swarms appear to be parallel to fundamental structural trends, such as the Bathurst Aulacogen or the McDonald Fault. Some unfolded dykes in the Epworth Basin have not yielded consistent ages, but are probably about 1550–1600 Ma old. Similar dykes have been reported from the eastern Slave and northern Churchill Provinces. Diabase sills of the *Western Channel Diabase* (Irving *et al.* 1972) were emplaced between Hornby Bay and Echo Bay, and have been dated at 1392 ± 48 Ma (Rb–Sr, after Thorpe 1978) and 1400 ± 75 Ma (K–Ar, Wanless *et al.* 1970, anal. 67–80). The full extent of this swarm is unknown. The large Mackenzie diabase dyke swarm is about 1200–1250 Ma old (Patchett *et al.* 1978), and is coeval with the Coppermine River Group basalts (Baragar and Donaldson 1973) and the Muskox Intrusion (Hoffman 1980). The Franklin diabase dykes and the Coronation sills in the Coppermine area are about 675 Ma old (Douglas 1980).

A syenitic complex at Blachford Lake has been dated by K–Ar methods at about 2100–2200 Ma (analyses 78–124 to 78–136, Wanless *et al.* 1979) and 2057 ± 56 Ma (Davidson 1978). The alkali–carbonatite complex at Big Spruce Lake is similar, emplaced at 2140 ± 30 Ma (Rb–Sr, Martineau and Lambert 1974, amended by Lambert pers. comm., 1981). K–Ar dating of the Big Spruce Lake material gives ages of some 1800 Ma (Martineau and Lambert *op. cit.*; Lowdon 1963, analysis 62–92).

H. Folding and Faulting

A number of major faults surrounds the Bear and Slave Provinces. The *Bathurst Fault* may have a sinistral throw of 140 km (Campbell and Cecile 1979), and the *MacDonald Fault* a 60 km dextral offset (Walker 1977). They appear to have been active at the same time as the north-east faulting, *i.e.* about 1750 Ma ago (Hoffman and McGlynn 1977). The McDonald Fault system has been traced magnetically to the Rocky Mountain foothills, and mapped north-eastwards as far as the Dubawnt Group, a distance of 1300 km (Walker 1977, reporting previous studies). Movement commenced by at least some 2500 Ma ago and ceased about 1735 Ma ago (Walker *op. cit.*).

Although tight and complex folding occurs in the Epworth Basin and in the Snare Group rocks, it is generally not important in the Great Bear Batholith (*e.g.* Fraser *et al.* 1972). The dextral, strike-slip *Wopmay Fault* truncated the Wentzel Batholith and underwent continual movement, with a west-side-down normal component, until the final Dumas Group clastics overlapped upon the Hepburn Batholith, when all movement finally ceased (Hoffman and McGlynn 1977). The fault system may split into several parallel branches, splaying at the northern end, and defines the eastern margin of the Great Bear Batholith.

Ubiquitous north-east trending faults generally splay and die out at the Wopmay Fault, although they can occur throughout the Bear Province. These are steep, dextral strike-slip faults with displacements of up to 15 km, emplaced after plutonism during the waning stages of the orogeny, although at least one preceded plutonism at Echo Bay (R. Hildebrand, pers. comm. 1980). Some north-west trending sinistral faults in the Hepburn Batholith, sometimes displacing the Wopmay Fault, may form a complementary set with the north-east faults. Caused by continuing east-west compression after the second subduction event, the faults were rotated to their present 90° intersection angle, and then became the edges of thrust slices in the Hepburn Batholith, which are pointed and overlap like west-dipping tiles (Hoffman and St-Onge 1981). West dipping thrusts in the "internal" zone of the Epworth Basin were a product of the first subduction event.

Dip-slip rejuvenation of the strike-slip faults occurred before the Franklin intrusive event (675 Ma). Some are isostatic adjustments, bordering a downthrown block with a positive gravity anomaly beneath. Kidd (1933) noticed that giant quartz veins in the

north-east striking faults of the Great Bear Batholith were also rejuvenated.

1. Giant quartz veins

These structures, up to 300 m wide and 80 km long, were first studied by Kidd (1933) and Furnival (1935), and over eighty are known from the Great Bear Lake region alone, emplaced in the north-east trending dextral shears (Mursky 1973). They have a quartz core flanked by quartz stockworks, silicifying the host rocks for some metres or tens of metres. Furnival (*op. cit.*) studied the alteration in granodiorite and fine-grained porphyry host rocks, and noted that the feldspars and hornblende were altered to phyllosilicates and thence to quartz. Rocks 30 cm from the vein had lost some 60% each of Na and K, while H_2O^+ had doubled and a 564% gain in Fe^{3+} was equalled by the loss in Fe^{2+} .

The early quartz forms a massive core of broken crystals in a white chalcedony matrix, and may include 1 cm blebs of kaolin with plagioclase. Later quartz forms banded veins with fluid and solid inclusions. Minor chlorite and sericite may turn the quartz green. At least three phases of quartz deposition are usually recognisable. Subsequent fracturing of the veins allowed the local emplacement of pitchblende, specularite, siderite and iron-copper sulphides (bornite, chalcopyrite, covellite, chalcocite, pyrite and famatinite), but these are apparently unrelated genetically to the veins.

The majority are >1200 Ma old, being truncated by the Hornby Bay Group, but at least two cut this group during subsequent reactivation (Furnival 1935; Kidd 1933). Some penetrate Hornby Bay Group rocks on Leith Peninsula at approximately $118^{\circ} 45'W$, $65^{\circ} 40'N$ (Balkwill 1971). None are known to cut the Palaeozoic cover rocks, although several form inliers, and activity had thus ceased by 600 Ma ago (Fraser 1967; Lord 1942; Balkwill 1971; McGlynn 1971 p. 109, "HUMP claims").

Typical veins were seen at the JD and Rayrock mine showings and at McLaren Lake. At McLaren Lake, the vein core is 50 m wide, with a 5 m wide diabase dyke along the centre. Coarse honey-brown manganiferous dolomite forms lenses in the quartz, which also contains minor chalcopyrite in vugs and late stage quartz veins, probably pre-dating the dyke. Roed (1968) and Thorpe (1972) reported bornite, chalcopyrite, pyrite, chalcocite, hematite, siderite and minor magnetite from this vein, but no

radioactivity. Lead from a chalcopyrite sample yielded a negative model age, discussed further on page 147.

The Rayrock vein some 60 m wide occupies the Marian River Fault, a structure at least 75 km long (p. 98); Cu–U mineralisation postdating the quartz occurs in fractures. The intense sodium metasomatism around this deposit is presumably related to the uranium mineralisation, being absent in Furnival's material and at McLaren Lake. At the JD claims, a vein strikes north in a branch of the Wopmay Fault and is some 35 m wide. Pitchblende occurs adjacent to it, but the mineralisation is controlled by the immediate wall rocks, and the vein *per se* is barren. Alteration adjacent to this vein does not include alkali metasomatism. Other examples of copper–mineralised giant quartz veins include the AID, GW, FIN and RED claims (McGlynn 1971; Thorpe 1972), while the UR claims cover a uraniferous vein (Thorpe *op. cit.*).

Mursky (1973) and Badham (1973a) have suggested that uranium mineralisation occurred as a late stage of the giant quartz vein emplacement. On the contrary, pitchblende from Rayrock was dated at 5.11 ± 0.86 Ma (Miller 1982) when quartz emplacement had ceased. These fractured veins are no more than channels for subsequent hydrothermal fluids. They are likely to extend to great depth; since, as Furnival (1935) pointed out, pegmatites in the batholith are scarce, the veins may represent an equivalent plutonic stage after the batholith had been fractured during a continental collision.

J. Deep Structure

The crust of the Bear Province is generally about 30.6 kilometres thick, that of the Slave craton is about 33.9 km thick, and that of the Great Slave Basin is about 37.9 km thick (minimum values; Barr 1971). This suggests a graben or aulacogen structure for the Great Slave Basin, which is also underlain by a positive 20 milligal gravity anomaly (Fraser *et al.* 1972). The depths of erosion suggested by cover rocks and metamorphic grades range from 2.5 – 4.5 km at Echo Bay (Robinson and Ohmoto 1973) to as much as 8.5 km along the northern batholith margin (Baragar and Donaldson 1973) and 10–12 km at the HAM and JONES claims along the Wopmay Fault (p. 116). The Slave craton may also have lost up to 12 km of cover (McGlynn and Henderson 1972). By comparison, the

average crustal thickness of the Canadian, Scandinavian, Baltic and Ukrainian shields is 40 – 50 km, of the Appalachians is 50 km, of the Sierra Nevada, Rocky Mountains and Alps is 40 – 60 km and of the Andes is 70 km (Bamford and Prodehl 1977; Windley 1977). The Great Bear Batholith appears to be somewhat thin for a typical shield or continental subduction zone. Better comparisons may be the 30 km thick Basin and Range Province of California, as Hoffman and McGlynn (1977) suggested, or the 500–1100 Ma old Arabian Shield, 35 km thick, which is probably composed of back-arc basins and successive island arcs (Bamford and Prodehl *op. cit.*; Gass 1977).

Gravity highs in the Bear and Slave Provinces generally reflect ultramafic bodies, such as the Muskox Intrusion (Fraser *et al.* 1972). There is also a slight gravity high along the Hepburn Batholith, perhaps reflecting the metamorphism of the supracrustal rocks to amphibolite facies. Gravity highs tend to underlie depressed areas where supracrustal rocks are preserved, while gravity lows tend to mark exposed basement.

K. Palaeohistory

Latitude data from palaeomagnetic work by Irving (1979) are summarised graphically in Fig. 4. Irving suggests that there is no significant error (10° of latitude or 1000 km) in regarding the Bear–Slave area as a single unit, although the exotic terrain may be allochthonous.

By 2200 Ma, the Slave craton was generally stable, with the McDonald and probably the Bathurst Faults established. Between 2200 and 2100 Ma, the Blachford Lake and Big Spruce Lake alkali complexes, and possibly the Easter Island dyke too, were emplaced in the craton. By perhaps 2000 Ma, the Akaitcho Group bimodal volcanics and related sediments marked an opening rift in the Slave craton, along the Cloos Anticline. This widening basin was filled by the Epworth and Snare Groups.

Subduction of the western edge of the Slave craton then closed this basin, and 1920–1870 Ma ago, the western part of the basin was invaded by the somewhat basic Hepburn and Wentzel Batholiths during the first collisional event. Unroofing of these batholiths provided flysch and molasse sediments to the basin remnant, and the collision caused north–south trending folds and thrusts in the western Epworth Basin. To the west, the Hottah Lake exotic terrain may be the island arc over the Benioff zone, or a

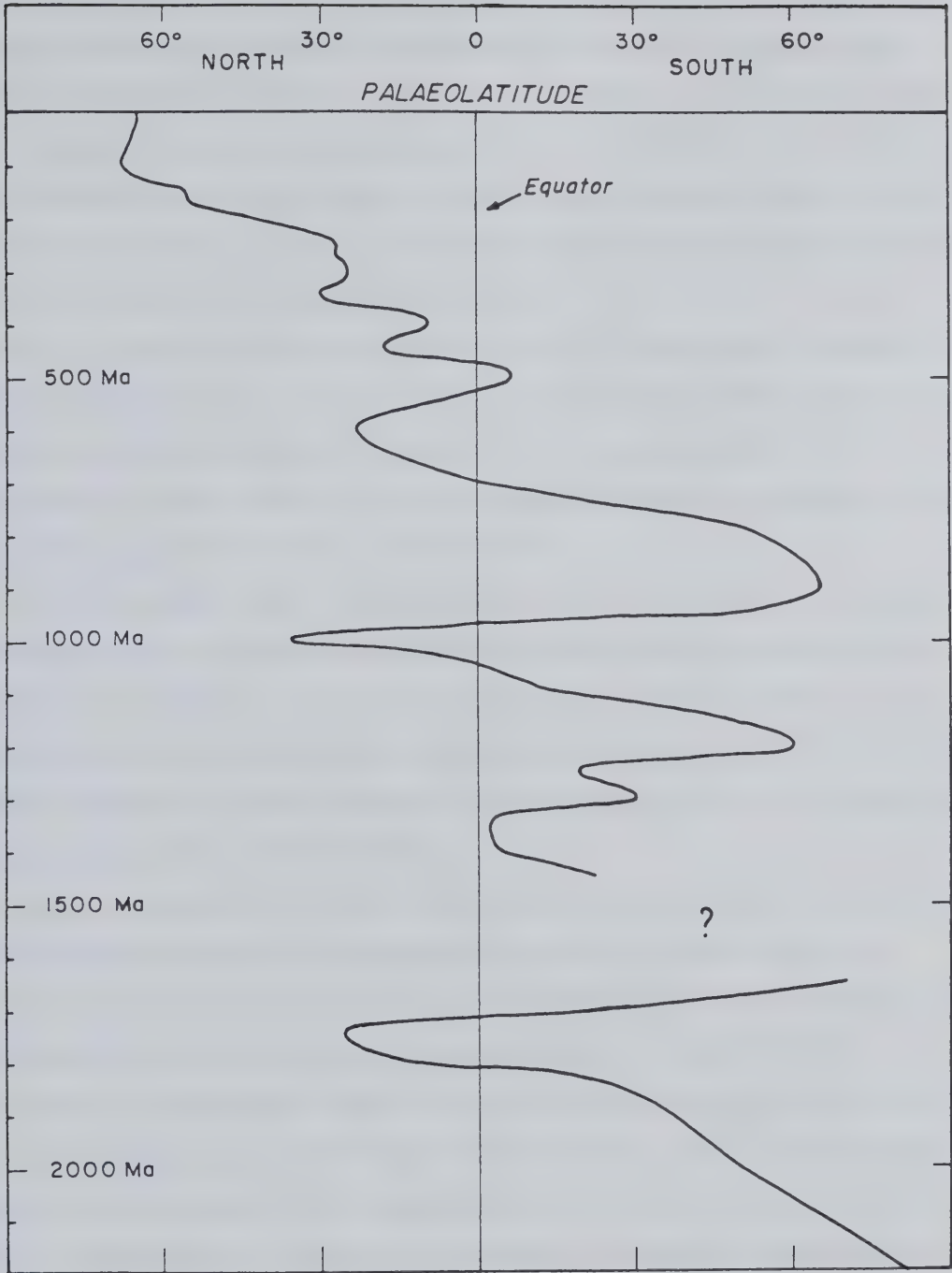


Figure 4: The palaeolatitude of the Great Bear Batholith (from the data of Irving (1979)).

fragment of the colliding block. Continuing compression opened a new subduction zone, dipping east beneath the Hepburn–Wentzel mass. Behind this zone the Great Bear Batholith was emplaced some 1875–1850 Ma ago, in a basin defined by the Wopmay Fault to the east. Activity ceased following a second collision far to the west, which induced thrusting and conjugate transcurrent faults. These periods of igneous activity were also marked in the Athapuscow aulacogen, by volcanism and final plutonism, where some of the volcanic units have an oceanic character.

By the close of the Hudsonian Orogeny, no great mountain chain had been built in this area; the low regional metamorphic grade in the Great Bear Batholith, and the thin crust there, attest to this. Giant quartz veins and stockworks, sometimes hundreds of metres wide and tens of kilometres long, marked the final stages, filling great north–east trending shear systems formed by regional stress.

Warping created the Amundsen Basin (and others, such as the Thelon, Nonacho and Athabasca Basins). Diabase intrusions had started by 1400 Ma, as sills at Echo Bay, culminating in the 1200 Ma old Coppermine River Group basalts, the Mackenzie dyke swarm and the Muskox Intrusion, which marks the suture between the Slave craton and the Hepburn Batholith. Dip–slip rejuvenation of the strike–slip faults and rejuvenation of some giant quartz veins accompanied this.

Down–warping of the batholith was initiated at about 675 Ma, marked by the Franklin diabase dykes and the Coronation sills in the north. Whether the ensuing transgression covered the batholith is uncertain, but the preserved sequence to the west, from the basal Cambrian to the upper Devonian, indicates final regression by approximately 350 Ma (Balkwill 1971). A marine Cretaceous succession (some 135–70 Ma old) to the south and west of the Bear province indicates another transgression and regression (Balkwill *op. cit.*). These transgressions may not have extended as far as the Great Slave Basin, where pitchblende U–Pb systems were apparently not reset as they were elsewhere (discussed in Chapter VI). Final erosion has stripped the cover from the batholith, to re–expose much of the Helikian palaeo–surface.

III. URANIUM: ASPECTS OF GENERAL GEOCHEMISTRY AND DEPOSITION

A. Uranium Geochemistry

Uranium is a lithophile element enriched in the upper crust, with an average crustal abundance of some 2.0–2.6 ppm (Rich *et al.* 1977; Dyck 1978). According to Wedepohl *et al.* (1969–1978), its average concentration is about 0.5 ppm in basalts, 0.85 ppm in gabbros, 2–7 ppm in "normal" granites and acidic extrusives, and 0.04–19.7 ppm in alkaline intrusives. Anomalous or "fertile" granites may average 15 ppm U (Fehn *et al.* 1978), 20–22 ppm (Leroy 1978) or even reach ore grades (Rogers *et al.* 1978), as may alkaline intrusives, possibly after metasomatic alteration (*e.g.* Robertson 1978). Sedimentary and metamorphic rocks have extremely variable uranium contents, but black shales are notably enriched (3–1244 ppm; Bell 1978), as are lignites, asphalts and other organic-rich lithologies; bauxites may also sometimes be enriched (average 11.4 ppm). Graphitic schists (metamorphosed carbonaceous shales) are associated with many unconformity-associated deposits, such as the Australian examples (Langford 1978a). Metamorphism to granulite facies may deplete uranium (Heier and Adams 1965). The Aphebian metasediments underlying some Athabasca Basin polymetallic deposits contain some 50 ppm U (Dahlkamp 1978). Seawater contains 1–4 ppb uranium, and average rivers about 1 ppb (Langmuir 1978a). Dyck (1978) tabulates other recent estimates of the uranium contents of various lithologies and natural waters.

Uranium and thorium are closely associated in primary magmatic rocks, but become separated during magmatic differentiation. Typical Th/U ratios of 2–3 in mafic rocks rise to 5–6 in the more differentiated plutons as the uranium becomes concentrated into the fluid fractions (Rogers *et al.* 1978). Anatectic granites typically have Th/U ratios of <1, and mantle-derived granitoids have ratios >1 (Rogers *et al.* 1978). During weathering or oxidative alteration, uranium becomes oxidised, mobilised and removed, raising the Th/U ratio in the residuum. Deposits formed from the mobilised uranium are consequently thorium-free (hence the low Th content of pitchblende) and sedimentary rocks formed in a reducing environment may show uranium enrichment (hence the low Th/U ratios for some anatectic granites). The Th content of weathered granitic rocks may give an indication of their original uranium content and the extent of

uranium loss.

Primary minerals are generally uranous, and secondary minerals generally uranyl, although primary uranyl minerals may be found in pegmatites. Throughout this thesis, pitchblende is regarded as the finely crystalline, non-idiomorphic form of uraninite, $\text{UO}_2\text{--U}_3\text{O}_8$, according to common usage. Pitchblende is typically hydrothermal in origin, free of Th and rare earths, formed at lower temperatures, and is often rather more oxidised, denser and with a smaller unit cell than uraninite (Rich *et al.* 1977; Steacy and Kaiman 1978; Heinrich 1958). These minerals have variable overall oxidation states, and species such as UO_2 , U_4O_9 , U_3O_8 and UO_3 (Langmuir 1978b) and tetragonal U_3O_7 (Dahlkamp 1978) are known, but this degree of precision was not sought in this study. Uranium in igneous and metamorphic rocks is sometimes held in primary uraninite, but more often in refractory minerals such as zircon, apatite, pyrochlore, davidite, brannerite, titanite, monazite, xenotime, allanite, columbite and euxenite. These minerals may form inclusions in the major silicates, which probably contain less lattice-bound uranium than analyses suggest, with the notable exception of phyllosilicates (Gavshin 1972; Cuney 1978; Snelling 1980) and perhaps garnet and hornblende (Snelling *op. cit.*). Coffinite, USiO_4 (sometimes given as hydrated), is sometimes treated as a uranous secondary mineral (Rimsaite 1979), sometimes as a primary phase (Langmuir 1978b).

Dissolved uranium may be adsorbed, particularly by organic materials, zeolites, and fine-grained ferric, Ti and Mn oxy-hydroxides; clays are less important (Langmuir 1978b). Syngenetic uranium in sedimentary rocks can therefore be held both by adsorption and in detrital primary minerals.

Uranium solubility

The following overview of uranium solution chemistry is based on Langmuir (1978a, 1978b). The hexavalent uranyl ion UO_2^{2+} forms soluble complexes with common ligands, whereas the tetravalent uranous U^{4+} ion is essentially insoluble. The pentavalent U^{5+} ion is somewhat soluble as UO_2^- complexes at $\text{pH} < 7$, but is of minor importance in solutions. In normal waters at 25°C , uraninite is essentially insoluble to U^{4+} except (1) as fluoride complexes at $\text{pH} < 4$, or (2) as hydroxyl complexes at $\text{pH} > 7$; pitchblende is rather more soluble. Uranyl ions are soluble, particularly as (1) fluoride complexes in acid

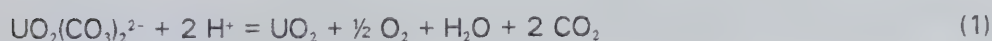
solutions, (2) phosphate complexes in neutral solutions, and (3) carbonate complexes in alkaline solutions, while silicate and sulphate complexes may be important locally. The carbonate complexes are perhaps the most important at 25°C, but by 100°C they are superseded at all pH values by hydroxy complexes if $p(\text{CO}_2)$ is $<10^{-2}$ atm. Under such conditions, the predominant dissolved uranyl species are UO_2^{2+} at low pH, UO_2OH^+ at pH = 5, and $(\text{UO}_2)_3(\text{OH})_5^+$ at high pH (a useful pH indicator in some deposits is marcasite, which is precipitated under conditions of low pressure and a pH of 3.0 – 5.5 at 150°C (Cuney 1978, citing Russian data; Kullerud 1967)). Uranium transport by carbonate complexes has often been assumed by previous workers, but unless deposited carbonates and UO_2 are demonstrably coeval, this assumption may be invalid.

Certain anions form uranyl salts under appropriate chemical conditions. The commonest are vanadate, phosphate, arsenate and silicate, and more rarely molybdate, carbonate, selenate and tellurate. These secondary uranium minerals are considered further in Chapter VIII.

Mechanisms of uranium precipitation

The deposition of U^{4+} minerals is fairly well understood for the roll-front types of deposit, where carbon "trash", natural gas or sulphides act as reducing agents. Less importance has generally been attached to precipitation mechanisms in hydrothermal or unconformity-related systems, where conversely the mechanisms are often more obscure. The efficiency of reduction and precipitation may be far more important than the concentration of U^{6+} in solution, since U^{4+} solubility (under reducing conditions with no dissolved fluoride) is only some 0.5 ppb at 25°C (Langmuir 1978a). The commonly cited reducing agents are reduced Fe-, S- and C-bearing compounds, in order of their general increasing reduction potential (Fig. 5).

The precipitation of uraninite or pitchblende from an oxidised solution requires the destruction of the uranyl complex and reduction of the uranyl ion. These two steps are intimately linked, as the general redox reaction for the uranyl dicarbonate complex shows (after Rich *et al.* 1977):



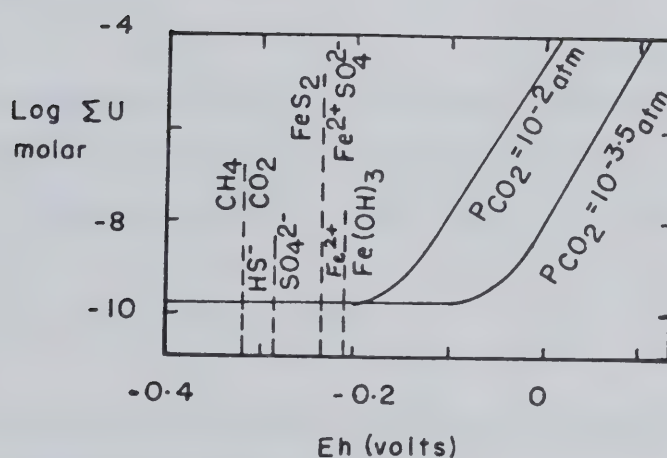
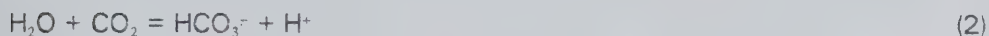
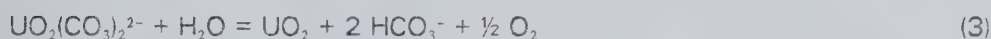


Figure 5: Uraninite solubility at $\text{pH} = 8$ and 25°C as a function of Eh and $p(\text{CO}_2)$. Eh values for important redox reactions are shown, assuming $\text{CH}_4 = \text{CO}_2$, $\text{SO}_4^{2-} = \text{HS}^-$, $\text{Fe}^{2+} = 10^{-4}\text{M}$, $\text{SO}_4^{2-} = 10^{-3}\text{M}$ (after Langmuir 1978a).

In the general case, uraninite precipitation from a uranyl carbonate solution could be induced by changes in $p(\text{CO}_2)$, pH, Eh or temperature. Loss of CO_2 following pressure release or boiling would encourage pitchblende deposition, but it also raises the pH by the reaction:



Hence CO_2 loss must be accompanied by a pH buffering reaction for pitchblende to be precipitated from uranyl carbonate solutions. Similar buffering is required to dissociate uranyl hydroxy complexes. Equations (1) and (2) can be re-written:



The HCO_3^- ion is the most abundant dissolved carbonate species at intermediate pH values, and a possible pH buffer is provided by:



Thus calcite precipitation drives reaction (2) above to the right, lowering the pH and allowing reaction (1) to proceed. The combined reduction of uranyl carbonate and hydroxide may need little pH buffering, although it will subsequently produce H^+ and HCO_3^- by reaction (2) above:



Decreases in Eh and/or pH can move uranyl carbonate solutions into the stability field of UO_2 (Fig. 6). Wall-rock alteration reactions probably control the Eh/pH conditions in most hydrothermal systems, and hematitic alteration is particularly characteristic of hydrothermal uranium deposits (Rich *et al.*, 1977). Possible pH buffers include the bicarbonate-calcite equilibrium (equation (4) above) or such reactions as:

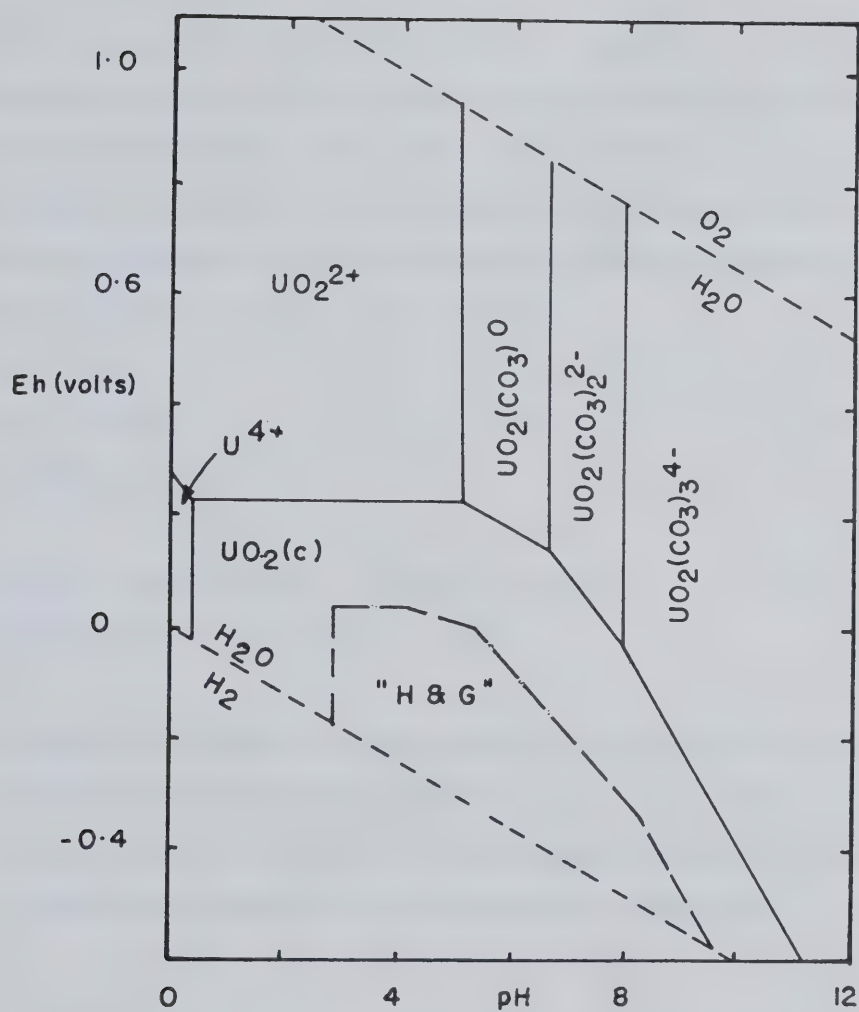
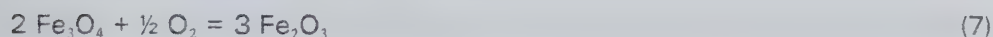


Figure 6: Eh - pH diagram for the system $\text{U}-\text{O}_2-\text{CO}_2-\text{H}_2\text{O}$ at 25°C , $p(\text{CO}_2) = 10^{-2}$ atm. "H & G" denotes the uraninite stability field calculated earlier by Hostetler and Garrels (1962). From Langmuir (1978a).



(muscovite + quartz + K⁺ = K-feldspar + H⁺)

The solution pH is probably continually buffered by such equilibria, so that precipitation of UO₂ is induced by altering the other variables. Mixing processes may introduce dissolved reductants such as Fe²⁺, ionic reduced sulphur species or H₂S, H₂ and perhaps CH₄. More frequently, solid phases in the wall rocks are the probable reductants, such as sulphides and organic carbon in the roll-front deposits, ferrous silicates (altered to partially oxidised chlorite ± hematite), or Fe-Ti oxides:



(magnetite + oxygen = hematite)



(biotite + oxygen = hematite + K-feldspar + water)

This reaction implies the diffusion of oxygen outwards into the wall rocks, or equally the diffusion of Fe²⁺ into the hydrothermal system. The typical hematitic alteration zones suggest that ferrous iron is the commonest reducing agent, although in the study area much of the observed hematisation may be due to palaeo-weathering.

The roles of chlorite

Chlorite, as the common low- to medium-temperature breakdown product of ferromagnesian minerals, probably plays a double role in uranium deposits. Firstly, it is produced during the oxidation of ferrous silicates; secondly, it may itself become a reducing agent, altering in the process to a more oxidised chlorite. The Fe³⁺ ions produced may enter the chlorite lattice or form hematite, resulting in lower total iron contents or higher Fe³⁺/Fe²⁺ ratios in the chlorite. As Fe²⁺ is lost, it may be directly replaced by Mg²⁺; the loss of 2 Fe³⁺ may be balanced by the gain of 2 Al³⁺ or Mg²⁺ + Si⁴⁺; or Fe²⁺ + Al³⁺ may be replaced by Mg²⁺ + Fe³⁺ during oxidation. The combined oxidation/substitution reactions may lead to progressively higher Si and Mg contents.

"Lost" alumina may be reconstituted as new chlorite or a sericitic white mica by the introduction of Si, Mg, H₂O and alkalis. Snelling (1980) found such a trend towards increasing Si and Mg contents in, and locally sericitisation of, the massive chlorite in the Koongarra deposit, Australia.

Dissolved reducing agents

Although Rafalskiy *et al.* (1963) have suggested that dissolved reductants can co-exist stably with uranyl complexes without reduction, reactions (1) and (3) make this seem improbable, unless the reaction kinetics lead to metastability of the uranyl complexes. The alternating deposition of pyrite and pitchblende was interpreted by Cuney (1978) as evidence that during UO₂ deposition, the activity of dissolved reduced sulphur species fell, in turn implying that such species were being oxidised to precipitate the UO₂. Figure 7 shows that under the conditions specified, hematite, pyrite and UO₂ coexist stably with SO₄²⁻ as the predominant dissolved sulphur species, so that reduced sulphur is not available to precipitate UO₂.

Figure 8 implies that UO₂ cannot co-precipitate from a uranyl carbonate solution (at 25°C) with either pyrite or hematite, since no soluble iron species are stable in the uranyl carbonate field. However, hematite in low-temperature systems is not directly precipitated, but is a recrystallisation product of ferric oxy-hydroxides (Langmuir 1978a). The stability field boundaries may also be moved by changing the assumed concentrations; for example, the Fe²⁺ field may be expanded by reducing the dissolved iron concentration, the pyrite field expanded by increasing the dissolved sulphur concentration, and the UO₂ field decreased by raising the p(CO₂). Higher temperatures will also affect the boundary positions. Without specific thermal and compositional data, it is sufficient to note that such co-precipitation *does* occur, that reduced sulphur species are probably absent if hematite is stable, and that ferrous iron is the most generally available reducing agent in uraniferous hydrothermal systems.

Unseen reducing agents

Frequently there is no visible reducing agent in the host rock. One possible reason, cited above, is the presence of a dissolved reduction agent. A second possibility is that the

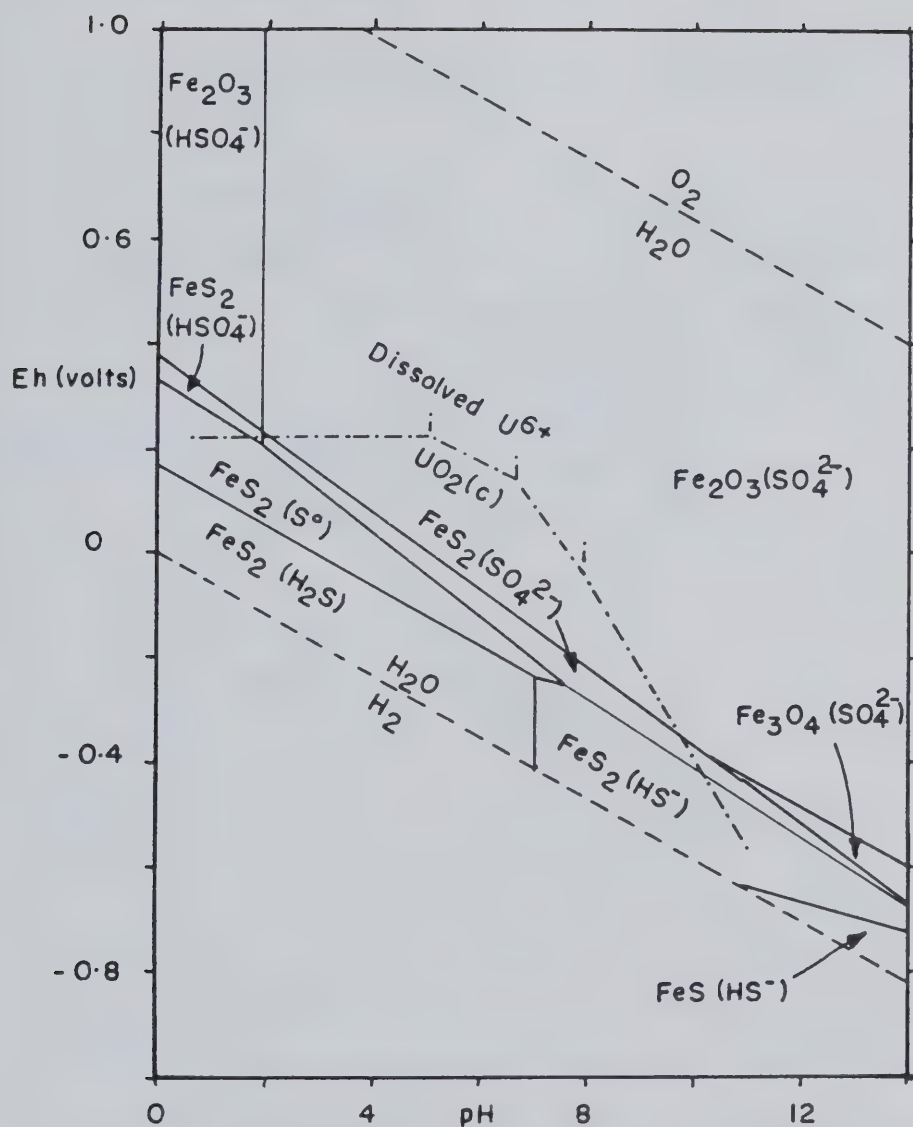


Figure 7: Eh - pH diagram of iron sulphides and oxides and dissolved sulphur species in water at 25°C, 1 atm total pressure and total dissolved sulphur = 10^{-1} (after Garrels and Christ (1965), omitting metastable boundaries). The uraninite stability field of Figure 6 is superimposed for comparison.

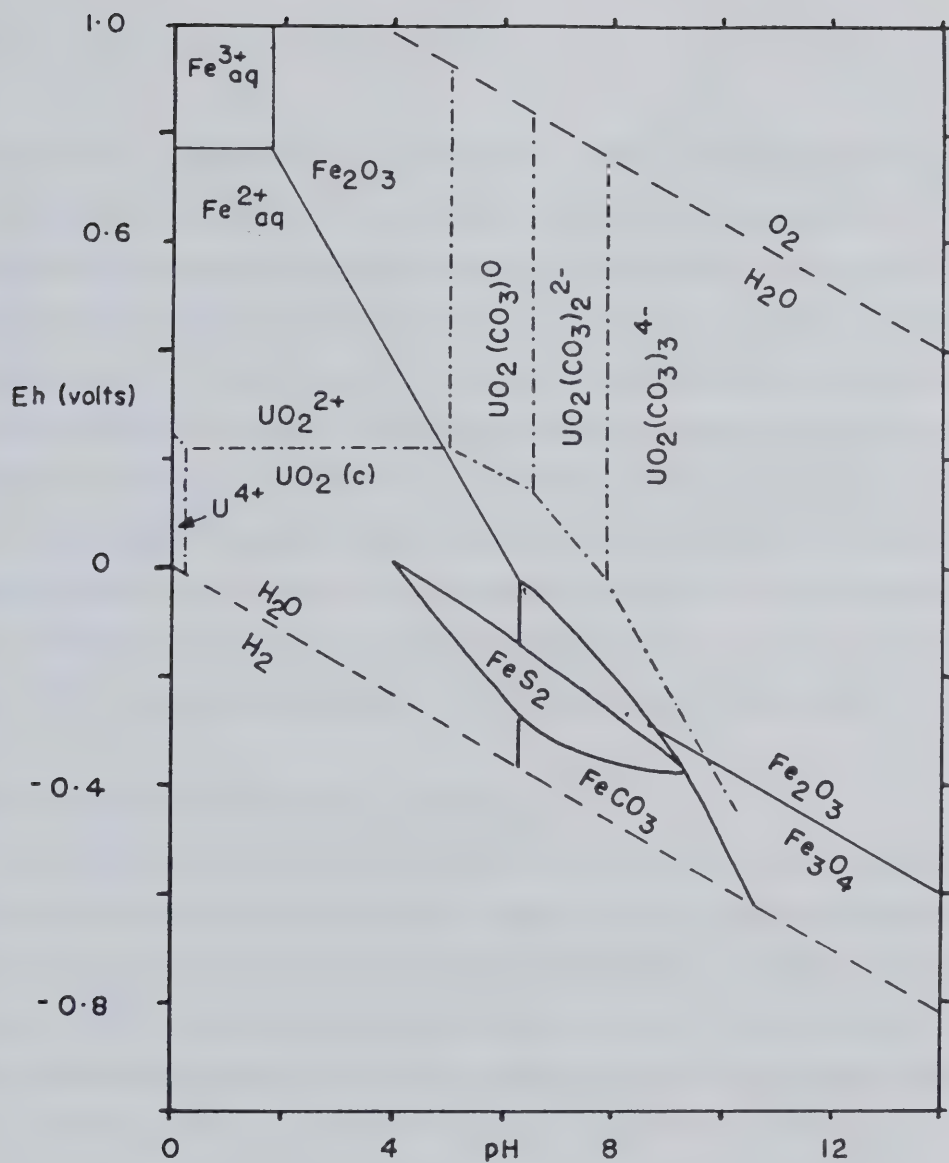
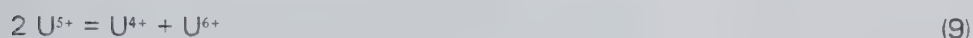


Figure 8: Eh - pH diagram of iron oxides, sulphides and carbonates and dissolved iron species in water at 25°C, 1 atm total pressure, total dissolved sulphur = 10^{-6} , total dissolved carbonate = 10^0 (after Garrels and Christ 1965). The uraninite stability field of Figure 6 is overlain, drawn for $p(\text{CO}_2) = 10^{-2}$ atm.

reductant was a minor, dispersed phase which has not been recognised (unlikely, considering the mass balance). A third possibility is the reaction:



Another possibility, suggested by Robertson *et al.* (1978), is the electrolytic deposition of pitchblende by natural electro-chemical cells, although the cell described is indistinguishable from the conventional reduction of a percolating uranyl solution in a reducing medium. However, a cell mechanism may be possible, illustrated in Figure 9. The characteristics are, (1) its geological simplicity, and hence likelihood; and (2) the fact that the uranyl solution and the reducing agent never come into physical contact, and could be perhaps tens of metres apart. Diffusion along the ionic bridge would probably be the limiting kinetic factor. Pitchblende would be deposited at the cathode, the end of the conducting feature which might be quite unnoticed in practice. An example might be where mineralisation is adjacent to, but not in, graphitic units (*e.g.* Koongarra, Australia – Snelling 1980; Athabasca Basin deposits – Hovee and Sibbald 1978, p. 1465).

B. Uranium deposits: classification and origins

The classification of uranium deposits is still as contentious as their genesis, since genetic factors such as uranium sources or methods of transport and precipitation are often used as classification criteria. Other criteria include the host lithology, age, gangue mineralogy, alteration effects and geochemical associations of the deposit. Authors have tended to adopt either genetic or descriptive subdivisions, such as the hydrothermal deposits (genetic) of Rich *et al.* (1977) or the igneous intrusive-hosted deposits (descriptive) of Rogers *et al.* (1978). Most classifications are subdivisions into sedimentary-, igneous- and metamorphic-hosted deposits. A classification scheme after Morton (in prep.) is adopted here and shown in Table 1, which uses both genetic and descriptive criteria.

Some distinction should be made between hydrothermal deposits, where uranium is transported upwards by heated, cooling water (*per ascensum* mechanisms), and those where uranium is carried downwards or laterally by cold groundwater (*per descensum*

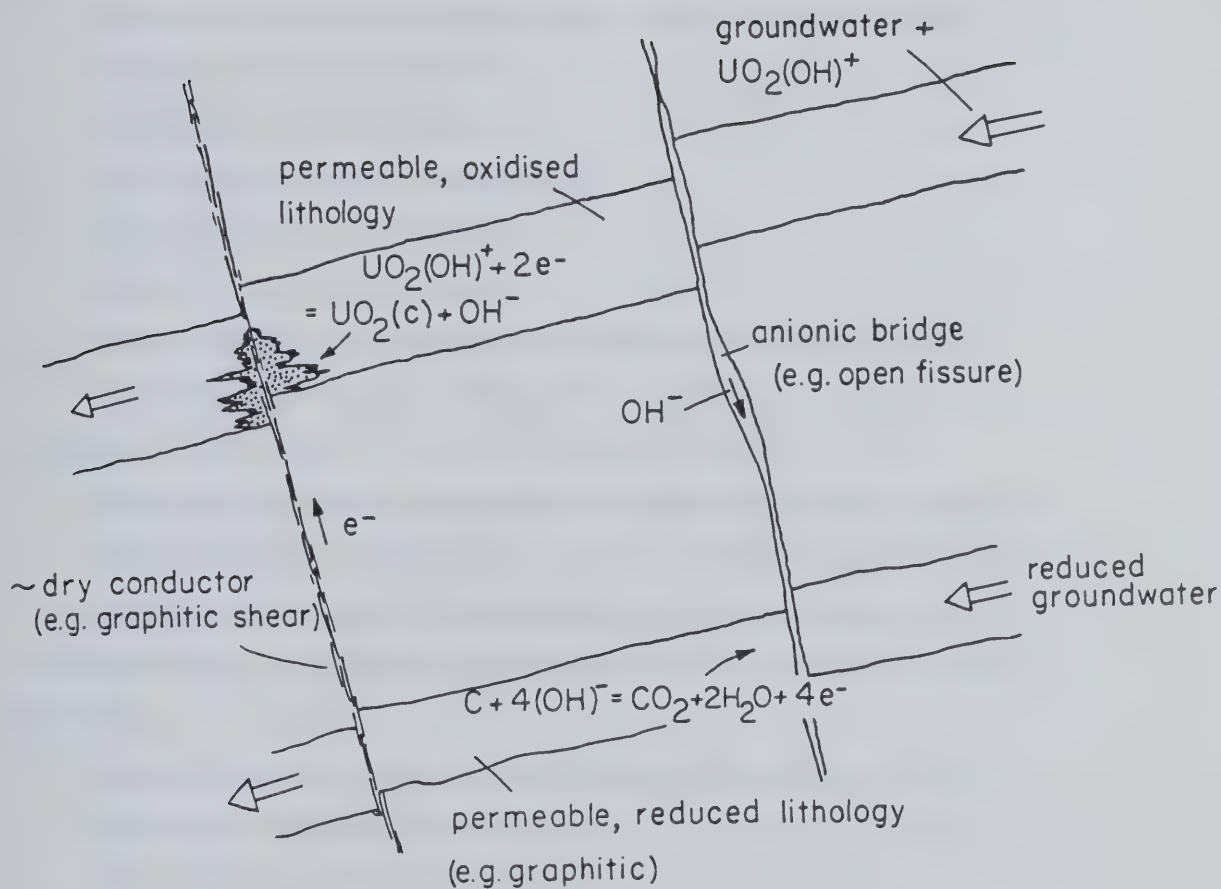


Figure 9: Proposed electrochemical cell precipitating UO_2 at a distance from a reducing agent (in this case graphite). Similar cells for other uranyl complexes and reductants are possible, and this model is not exclusive of others.

CLASSIFICATION OF THE PRINCIPAL URANIUM ASSOCIATIONS

1. SEDIMENTARY-HOSTED URANIUM DEPOSITS

- 1(i) Placer and modified-placer deposits (S,D,E,)
- 1(ii) Coarse- and medium-clastic and pyroclastic hosted deposits (D,E)
- 1(iii) Pelite-hosted deposits (S,D)
- 1(iv) Diatomite-hosted deposits (D,E)
- 1(v) Phosphorite-hosted deposits (S,D)
- 1(vi) Limestone-hosted deposits (S,D,E)
- 1(vii) Duricrust-hosted deposits (S,E)
- 1(viii) Lignite-, coal- and carbonaceous-lutite-hosted deposits (S,D,E)
- 1(ix) Diatremic and exhalative (?) deposits in sedimentary sequences (S,E)

2. IGNEOUS- AND VOLCANIC-HOSTED URANIUM DEPOSITS

- 2(i) Plutonic segregations; disseminations, pegmatites, diatremes, veins (S,E)
- 2(ii) Volcanogenic-exhalative deposits of disseminated- or vein-character (S,E)
- 2(iii) Supergene or deuterite deposits within plutonic or effusive suites (E)

3. METAMORPHIC-HOSTED, METAMORPHOSED AND METAMORPHIC URANIUM DEPOSITS

- 3(i) Disseminations or veins in regionally metamorphosed terrains (S,E)
- 3(ii) Metatect pegmatitic deposits (S,E)
- 3(iii) Anatectic granitoid deposits (S,E)
- 3(iv) Diatremic deposits in metamorphic terrains (E)
- 3(v) Contact metamorphic/metasomatic deposits (S,E)
- 3(vi) "Coincident unconformity type" (sub- and supra-unconformity) (E)

S = Syngenetic, D = Diagenetic, E = Epigenetic

Table 1: The classification of uranium deposits (after Morton, in prep.).

mechanisms). This is a somewhat subjective but helpful distinction. Quartz deposition might accompany a cooling *per ascensum* fluid rather than a warming *per descensum* one (Fehn *et al.* 1978). Hydrothermal deposits occur principally in felsic igneous host rocks (Rich *et al.* 1977), and although wall-rock reactions are important, physical effects such as boiling and temperature–pressure changes are probably equally important for uranium precipitation. Such processes as deuteritic alteration or the formation of exhalative veins could be included as hydrothermal. Fehn *et al.* (1978) found that radioactive plutons (with 15 ppm U, 57 ppm Th and 4% K) can cause groundwater convection by radioactive heating, of the same magnitude as convection due to the initial cooling of the pluton, and presumably rather longer in duration. Extrapolating further, any moderately uranium-enriched source rock with adequate permeability is probably capable of generating its own hydrothermal system without external heat sources, leading to hydrothermal systems in upwelling areas and supergene or ground-water transported deposits in intake areas.

By comparison, pitchblende precipitation from groundwaters is probably controlled almost entirely by reduction processes, producing deposits ranging from pitchblende veinlets to the roll-front (concordant) and peneconcordant types, where uranium carried in oxidised groundwater through a porous lithology is precipitated by reductants in the rock. Supergene re-deposition of uranium at a reducing water-table is probably common. Adsorbed uranium can produce sedimentary-hosted deposits in coals, lignites and black shales, where the trapped uranium is eventually reduced by the organic materials. Other sedimentary-hosted deposits include phosphorites, where tetravalent uranium substitutes for calcium in apatite; duricrusts; and the large early Proterozoic quartz-pebble conglomerate placers. Carbonates are more rarely uraniferous, but organic-rich or phosphatic carbonates can trap uranium syngenetically, or provide reductants for epigenetic deposits (*cf.* roll-front deposits or Mississippi Valley-type Pb–Zn deposits).

Igneous-hosted deposits typically include the hydrothermal and groundwater types noted above. Uranium being a fugitive element in magmatic systems, carbonatites, late-stage extrusive rocks, pegmatites and alkali complexes can all form deposits. Pervasive late-stage alkali-uranium metasomatism may create disseminated ores in acidic

extrusives (Gandhi 1978b). The process is essentially similar to the formation of uraniferous episyenites (Leroy 1978; Cuney 1978). A full discussion of uranium deposits in intrusive rocks is given by Rogers *et al.* (1978).

Metamorphic hosts may contain metamorphosed pre-existing deposits and those formed by uranium-remobilising metamorphic processes. This latter group includes hydrothermal veins and pegmatites as in igneous systems, and deposits formed by anatexis and contact metasomatism.

Cutting across such classifications are the polymetallic and polygenetic unconformity-associated, or "coincident unconformity", types (Morton, in prep.). Typically these occur at unconformities between lower Proterozoic or Archaean basement rocks and relatively unaltered Proterozoic sediments. This group is probably the result of multiple cycles of enrichment of uranium derived from the sub-unconformity metasedimentary rocks, particularly from pelitic facies. For example, in the Athabasca Basin, the overlying sandstones are not obvious uranium sources, whereas the underlying metasediments are uranium enriched (Dahlkamp 1978). The multiple-stage origins, which have been proposed for many other deposit types as well, only add to the complexities of this (and other) deposit types. An unconformity is probably important as a channel-way and site of mixing for groundwater, hydrothermal solutions and possibly gas, resulting in localised variations of oxidation state. It acts as a chemical trap for any uranium, from whatever source, in transit through it. The present surface of at least the northern part of the Great Bear Batholith is essentially the re-exposed Helikian unconformity beneath the eroded Hornby Bay Group.

Since uranium is relatively easily remobilised and reprecipitated, epigenetic deposits may be hosted by enriched source rocks such as pelites, evaporites and lateritic regolith, or igneous sources such as volcanic flows, volcanoclastic sediments and siliceous tuffs. Siliceous tuffs represent the final differentiates of a magmatic system, and should be enriched in fugitive elements. Their explosive eruption indicates that these elements have not been lost by prior outgassing of the volatile components, although outgassing itself can form mineralised breccia pipes (Tilsley 1978). Not all volcanic glasses release their uranium, depending upon the style of alteration that they undergo (Walton *et al.* 1981). Uranium can be leached out of granitoids, and a 75% uranium loss

(without thorium loss) has been demonstrated in Wyoming granites (Rosholt *et al.* 1973). Very high-grade metamorphic rocks are generally depleted in uranium, and metamorphism is a possible process for releasing uranium (Rich *et al.* 1977). However, it will be shown that uraninite has survived such metamorphism under sufficiently reducing conditions (the meta-placer deposits – p. 103 *et seq.*).

The temporal aspect of uranium deposition is perhaps the least appreciated. Lambert (1975) has suggested that during the Archaean, the chance of lithospheric slabs developing was negligible, and that "skin" or single-plate tectonics may not have commenced until about 2600 Ma ago. A comparatively large amount of uranium could have been flushed to the surface from the mantle and lower crust shortly afterwards, to accumulate as uraninite in sediments after weathering. Uranium is still being liberated from the mantle, by partial melting processes or directly into fluids (Rogers *et al.* 1978), but presumably at a lower rate. Detrital uraninite would have been stable until at least 2000 Ma ago, when atmospheric oxygenation started to form continental red-beds (Cloud 1976). Thus by 2000 Ma, the largest amount of uranium ever was present in the terrestrial weathering zone, being oxidised, dissolved and flushed into the sea. This uranium was adsorbed by suitable marine sediments, particularly the carbonaceous pelites, and formed a unique group of uranium-enriched precursor rocks of early and middle Proterozoic age. These, it is suggested, are the logical ultimate source of uranium for the classical unconformity-associated deposits, either directly or by intermediate processes and derived sediments. For chemical reasons, then, the age of Witwatersrand-type placer uranium deposits was succeeded by the age of protore formation for several hundred million years, from which protore uranium has been remobilised ever since.

IV. THE DEPOSITS

Foreword

During two summers of field work, over forty separate sites and areas were visited, of which about thirty had some level of uranium mineralisation. Some were selected as they were under active exploration, the remainder by searching the records of the Department of Indian Affairs and Northern Development (DIAND or DINAG), Yellowknife, where exploration records must be filed and made public after two years. Understandably, not all companies were prepared to share their current data. As far as is known, this selection is fully representative, but only outcrops and sometimes trenches were generally available for sampling. A few areas were sketch-mapped, but pre-existing maps were used wherever available. The deposits are identified by a letter corresponding to their location on Figure 2, page 8.

250 thin sections and 150 polished mounts were studied from these deposits. A minority of sites, where only country rock samples were collected, will not be described. The identifications of most opaque minerals were confirmed by qualitative electron microprobe analysis after optical identification, while all secondary minerals were identified by X-ray powder diffraction analysis, confirmed where necessary by qualitative SEM-EDS chemical analysis. One suite of opaque minerals was exhaustively analysed by quantitative electron microprobe techniques (Miller 1981), and certain other samples were also analysed quantitatively.

Computer files were compiled as aids in mineral identification, being, (1) ELEMINE, a listing of all opaque minerals from standard references and new mineral lists, arranged by order of increasing atomic number of their components, and used for selecting possible mineral species from electron microprobe data; (2) URAMINE, a similar file for all uranium-bearing minerals, but not arranged in order and thus only useable by computer scanning; (3) ORDD2, a listing of the four principal X-ray diffraction d-spacings of all uranium minerals (revised from Morton 1978), synthetic uranium and uranium-lead oxides and hydroxides, clay minerals, carbonates, common supergene minerals and a few common rock-forming silicates, used for identifying X-ray diffraction patterns, again by

computer scanning. Appendix I, p. 220, is an explanation of the sample numbering system employed, to enable the reader to approximately locate any sample or analysis of interest.

The isotopic age determinations which are part of this study are to be published separately (Miller 1982) (Appendix III) and are summarised in Chapter VI. The age, mineralogy, genesis and possible uranium sources are discussed with the descriptions, for ease of reference, and some inter-deposit comparisons are also made. These topics are discussed from a regional perspective in the succeeding chapters. The deposits are listed in the sequence, (a) supergene, (b) sandstone hosted, (c) hydrothermal, and (d) metamorphosed palaeoplacer (= meta-placer) or "xerogenic" deposits.

A. The Coppermine River deposits

(A)

Figure 10 shows the location of a number of small uranium deposits along the Coppermine River, and the names assigned to them by B.P. Minerals geologists. The area straddles the splayed, indeterminate end of the Wopmay Fault, and rocks east of the main fault zone are herein assigned to the Akaitcho Group for convenience, although as Figure 10 shows, some of the units have not been assigned by the B.P. personnel. Seven or eight deposits in the Akaitcho Group and Hepburn Batholith, and three or four in the Dumas Group and plutons of the Great Bear Batholith, were visited. The present land surface represents the re-exposed Helikian land surface, and most of the deposits are within 2 km of the Hornby Bay Group outcrop. The genesis of the group is discussed on page 46.

The MAC U-Fe-Cu-S-(Co-As-carbonate) showing

(116°13'W, 66°49'N)

Minor pitchblende mineralisation occurs here in a sheared diabase dyke, composed of chlorite, undetermined brownish phyllosilicates, plagioclase and leucoxene, cutting albitised, rhyolitic Dumas Group tuff. The dyke appears to be truncated by an indurated, hematitic regolith or palaeo-talus of angular rhyolite cobbles. The mineralisation has altered the plagioclase to white mica, the unidentified mafic phenocrysts into brownish green micas, and has impregnated the dyke with hematite dust and blebs. Yellow uranium silicates, not identified but probably uranophane or beta-uranophane, coat fractures and mineralised veinlets.

One veinlet examined is 1 millimetre thick, composed of a layer of quartz on the host rock, followed by layers of hematite rosettes with chalcopyrite, massive or granular pitchblende with pyrite, earthy hematite, and the yellow uranyl minerals. The immediate wall-rock is diabase containing minor carbonate and traces of Co-arsenide (probably skutterudite) and amoeboid pyrite. Staining suggests that the carbonate is ferroan dolomite or ankerite. There are also veinlets of what appears to be uraniferous chlorite.

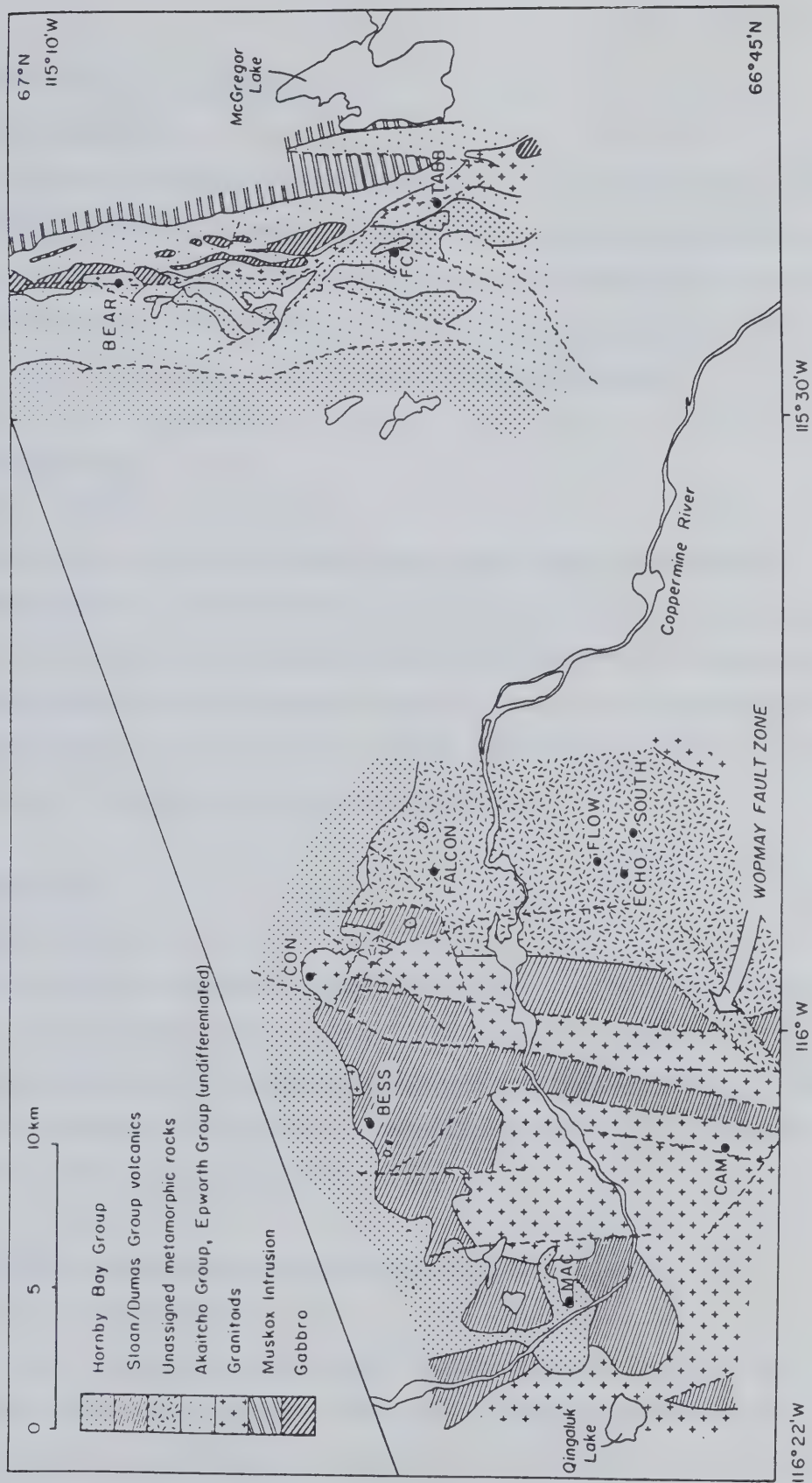


Figure 10: Geology and location of the Coppermine River pitchblende deposits (from unpublished data of B.P. Minerals Ltd.).

The BESS U-Co-Cu-As showing

(116°05'W, 66°53'N)

This showing occurs in the Dumas Group rhyolite, beneath a rhyolitic palaeo-talus regolith filling a small palaeo-valley. The regolith has a friable yellowish grey clay-like matrix, and is slightly radioactive in places. Erythrite coats some fractures in the regolith, and B.P. Minerals personnel have reported secondary copper minerals, but no uranium mineralisation was visible. The rhyolite is possibly zeolitised in parts.

The CAM showing

(116°06'W, 66°46'N)

Minor yellow secondary uranium mineralisation was found in a gossany, brecciated adamellite, where B.P. Minerals geologists have reported radioactivity in the margin of one of two dykes. These are stated to trend north in the St. Germain pluton of the Great Bear Batholith, but could not be located. A sample from the gossany material shows 85% granular hematite replacing magnetite, with rare magnetite cores surviving in places, and also contains traces of pyrite and chalcopyrite.

The CON showing

(115°58'W, 66°54'15"N)

Although no mineralisation was found here, there is an interesting recessive schist with up to 10% graphite, cutting a sheared biotite granite at the contact of the Hepburn and Great Bear Batholiths, and immediately beneath the Hornby Bay Group. The schist is probably a graphitised shear zone, and is the type of unit required for reduction-cell uranium deposition as proposed earlier (p. 33).

The FALCON U-Si-Cu-Fe-Pb-(carbonate) showing

(115°52'30"W, 66°51'45"N)

Uranium mineralisation here is hosted by steeply dipping, Akaitcho Group paragneiss, in which radioactivity and yellow uranyl minerals are confined to a diatreme-like breccia, containing disseminated sulphides and numerous quartz and carbonate veins. The breccia is composed of red, radioactive, microcrystalline quartz

clasts ("chert") and the grey, fine-grained host paragneiss. The faintly laminated, radioactive "chert" contains sub-micrometre flecks of hematite and what is either pitchblende or coffinite in similar-sized grains. Apart from small grains of chalcopyrite and pyrite-galena intergrowths and some replacive carbonate patches, the "chert" contains only Si, Fe, U and Pb. Some unidentified material resembling chlorite is also locally present in the laminae. The paragneiss is a laminated quartz-chlorite rock, with pyrite sometimes replacing the chlorite, and it is slightly radioactive in parts. Cementing the breccia are grains of pulverised quartz, which are unsorted and unoriented, and quartz veins.

The stages of mineralisation were:

- (1) Formation of the uraniferous "chert", and deposition of pyrite, galena and chalcopyrite in small vugs within it.
- (2) Tectonic brecciation; deposition of chalcopyrite in fractures.
- (3) Cementation by the quartz veins.
- (4) Deposition of pyrite, chalcopyrite, galena and sphalerite; of hematite; of marcasite; of calcite and pyrite (the relative ages of these minerals are not established).

This deposit is evidently associated with a tectonic-hydrothermal event in the area. The isotopic analysis of a single galena sample suggests that it is also considerably older than the others of the group (Miller 1982). The "chert" may be metasedimentary in origin, but it closely resembles recrystallised uraniferous opal described from Thailand (Gocht and Pluhar 1981), which is opalised tuff containing chalcopyrite, coffinite, V-bearing minerals and rare earth elements. Other possible interpretations include a brecciated hydrothermal chalcedony or an exhalative siliceous sinter.

The ECHO, FLOW and SOUTH U-carbonate-(Cu-Fe-S-Ag) showings

(115°52'30"W, 66°48'N; 115°52'W, 66°48'30"N; 115°50'30"W, 66°48'N)

These are all within 2 km of each other, in amphibolite and gneiss of the Akaitcho Group.

At ECHO, patches of diffuse, botryoidal pitchblende in a carbonate matrix impregnate an intensely carbonated, fine-grained paragneiss composed of quartz, chloritised biotite, oligoclase, potassium feldspar and up to 29% carbonate. The

pitchblende, which contains pyrite, marcasite and a little chalcopyrite, was only found in porous and friable parts of the rock. Up to 10 oz/t Ag has been reported by B.P. Minerals personnel (pers. comm. 1979). Three pitchblende samples were dated at 415 ± 29 Ma.

At FLOW, a locally garnet-bearing amphibolite contains breccia veins > 10 cm thick which are radioactive, although the precise uraniferous phase could not be isolated. The uranium may be adsorbed on fine-grained TiO_2 which rims most of the comminuted clasts. Carbonate veinlets also cut the amphibolite.

At SOUTH, beta-uranophane occurs in a fractured gneiss of granitic and granodioritic composition, adjacent to the amphibolite just described. The gneiss breccia is cemented with calcite containing clots of fine-grained hematite. Pitchblende grains isolated from a crushed sample yielded a single Pb/Pb age of 420 Ma, with extreme negative discordance.

This group is interesting for the diversity of mineralisation styles it shows. They are essentially monomineralic deposits; ECHO and SOUTH are also supergene deposits similar to the MAC occurrence previously described, while FLOW reflects a tectonic-hydrothermal event similar to that seen at the FALCON showing, perhaps due to some form of violent gas escape.

The BEAR showing

(115°23'30"W, 66°58'N)

This showing lies within gneiss and foliated monzonite or granite of the Hepburn Batholith, described as "protomylonitic granite" by Hoffman *et al.* (1980). One fine-grained monzonitic sample contains 6% pyrite in veinlets up to 3 mm wide, and is slightly radioactive, but no other mineralisation was found, nor was the radioactive source identified. A little calcite occurs along joints.

The FC U-Fe-Cu-S showing

(115°22'W, 66°52'30"N)

This showing is hosted by altered, tuffaceous rocks and quartz-chlorite-muscovite schists of the Akaitcho group, which reportedly includes basalts in this area. Silicification has destroyed the textures in the tuffaceous country rock. Minor pyrite and

chalcopyrite occurs in the rhyolitic regolith above. One pitchblende veinlet about 1 mm thick was found, in a brecciated, hematitic schist, which also carried traces of pyrite and chalcopyrite. The veinlet was unfortunately destroyed during sample preparation, but pitchblende grains yielded a single discordant $^{207}\text{Pb}/^{206}\text{Pb}$ age of 660 Ma.

The TABB U-Si-Fe-S-(Co-As) showing

(115°20'W, 66°51'40"N)

This showing occurs in Akaitcho Group biotite-, chlorite- and graphite-schists, which are faulted against a hematitic dioritic gneiss. Some of the material shows signs of anatexis and migmatization. There is a local high radiometric anomaly (some 50x background), and uranophane and unidentifiable yellow secondary uranium minerals (possibly kasolite in part) are common. Radioactivity reportedly extends up into a large area of the overlying Hornby Bay Group rocks (B.P. Minerals personnel, pers. comm. 1979). The regolith is hematitic and cemented with white calcite, which occurs in veins elsewhere. The graphitic schists contain up to 10% graphite.

1 mm veins of pitchblende occur in a fine-grained granodioritic gneiss, and contain a little quartz, probable coffinite and pyrite; the age relationships of these phases are unclear, and there are two optically-distinguishable varieties of pitchblende. Small euhedral cobaltite grains flank one veinlet. The deposit is probably supergene in origin, despite containing more quartz than might be expected in such deposits. Four pitchblende samples gave an isotopic age of 536 ± 66 Ma.

Discussion of the Coppermine River deposits

Except for the FLOW and FALCON showings, the deposits of the Coppermine River area are regarded as supergene in origin, by the criteria listed elsewhere (p. 155). The uranium was perhaps transported as uranyl carbonate complexes, and precipitated with carbonate after reduction by unidentified reducing agents. The precise source of the uranium and the reductant is not known. Concentration by adsorption to the ferric oxy-hydroxides and fine-grained phyllosilicates may also have been important. Alkali metasomatism, characteristic of many of the obviously hydrothermal uranium deposits elsewhere in the batholith, was not found in this group. Their age of some 400–660 Ma

corresponds to a period of marine transgression and regression along the south west edge of the Great Bear Batholith, and corresponding fluctuations in the water table and ground-water regimes might account for the uranium remobilisation (Chapter VI). FLOW and FALCON hint at an older phase of tectonic activity and the formation of breccia pipes, perhaps due to catastrophic outgassing. One possible cause is the emplacement of the Muskox Intrusion at about 1200 Ma; another is the original igneous activity of the batholith.

Nearly all these deposits are intimately associated with carbonate. However, Rich *et al.* (1977, p.60), discussing calcite precipitation as one mechanism for precipitating pitchblende from uranyl carbonate solution, state:

"However, pitchblende is not usually deposited simultaneously with calcite or other carbonates in hydrothermal uranium deposits..."

(Other deposits, as at Beaverlodge Lake, Saskatchewan (Smith 1974) also controvert this principle). The thick dolostones in the once overlying Hornby Bay and Dismal Lakes Groups are an obvious source for groundwater-leached carbonate. Uranium precipitation is favoured by the destabilisation of uranyl carbonate complexes with rising temperature (Langmuir 1978b), but this mechanism is difficult to reconcile with formation during a marine transgression. One may also speculate that the uranium was derived from upfaulted basement blocks (granitoids, tuffs and metapelites) or upwelling groundwaters, from older FALCON/FLOW types of deposits, or from sandstone-hosted uranium deposits in the Hornby Bay Group such as the Mountain Lake occurrence, and the sources proposed for that deposit (*q.v.*).

Cobalt is associated with three deposits, and pyrite, chalcopyrite and usually hematite with those containing pitchblende. At the low temperatures likely for supergene deposits, equilibrium was probably not attained, and the observed oxide-sulphide mineral assemblages do not help to define the conditions of deposition.

B. The Mountain Lake U-(Cu-Co-Ni-Fe-Ag-S-As-Ba) deposit

(B) (116°57'30"W, 67°18'N)

Minor stratabound mineralisation was first discovered here in the PEC claims in sandstones of unit 10 (Moss and Marten 1975) or unit 11 (Gandhi 1980) (Fig. 11). Further exploration revealed sub-surface mineralisation in unit 11 in the PEC and YUK properties,

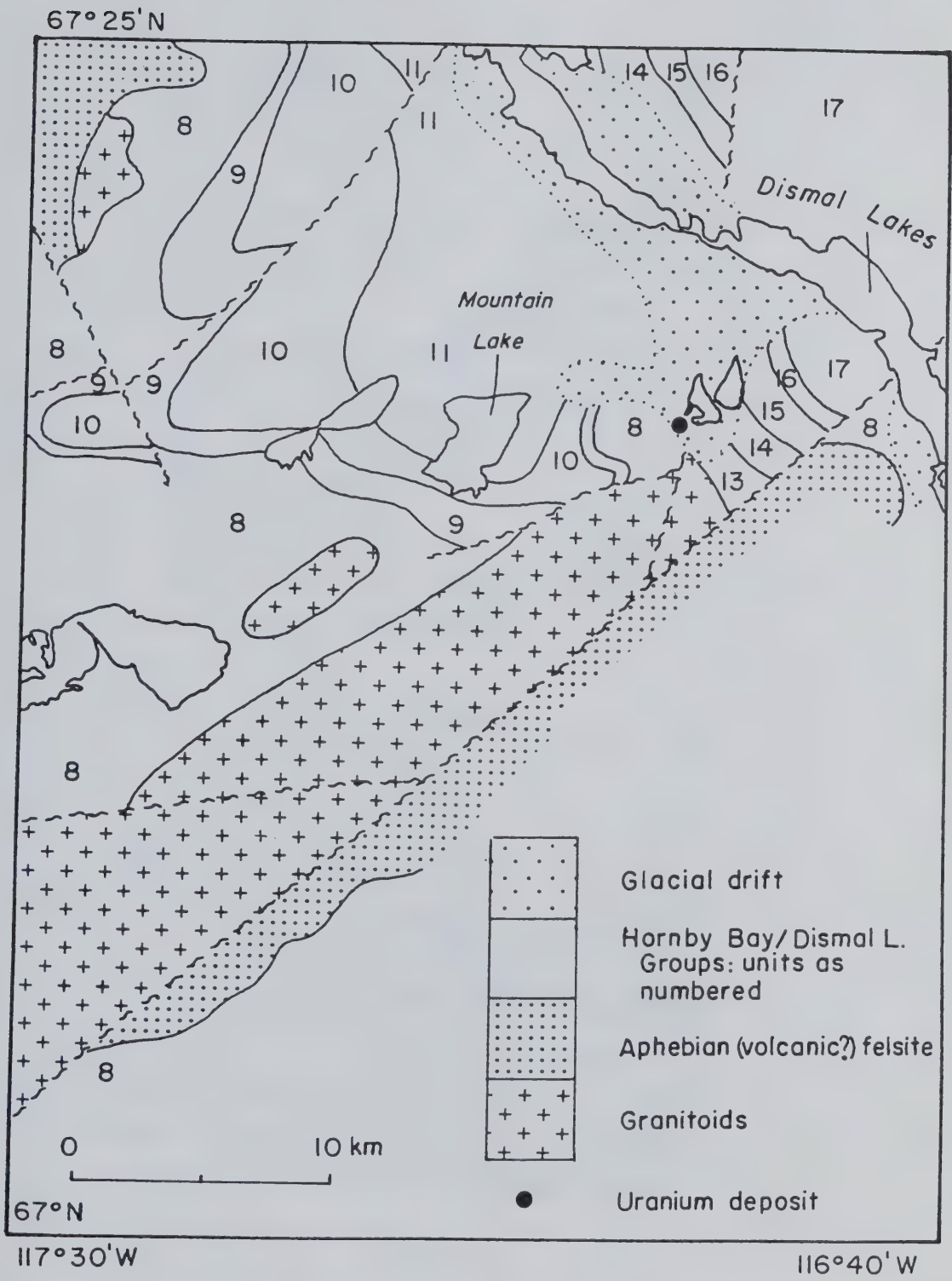


Figure 11: Regional geology of the Mountain Lake area (after Baragar and Donaldson 1973).

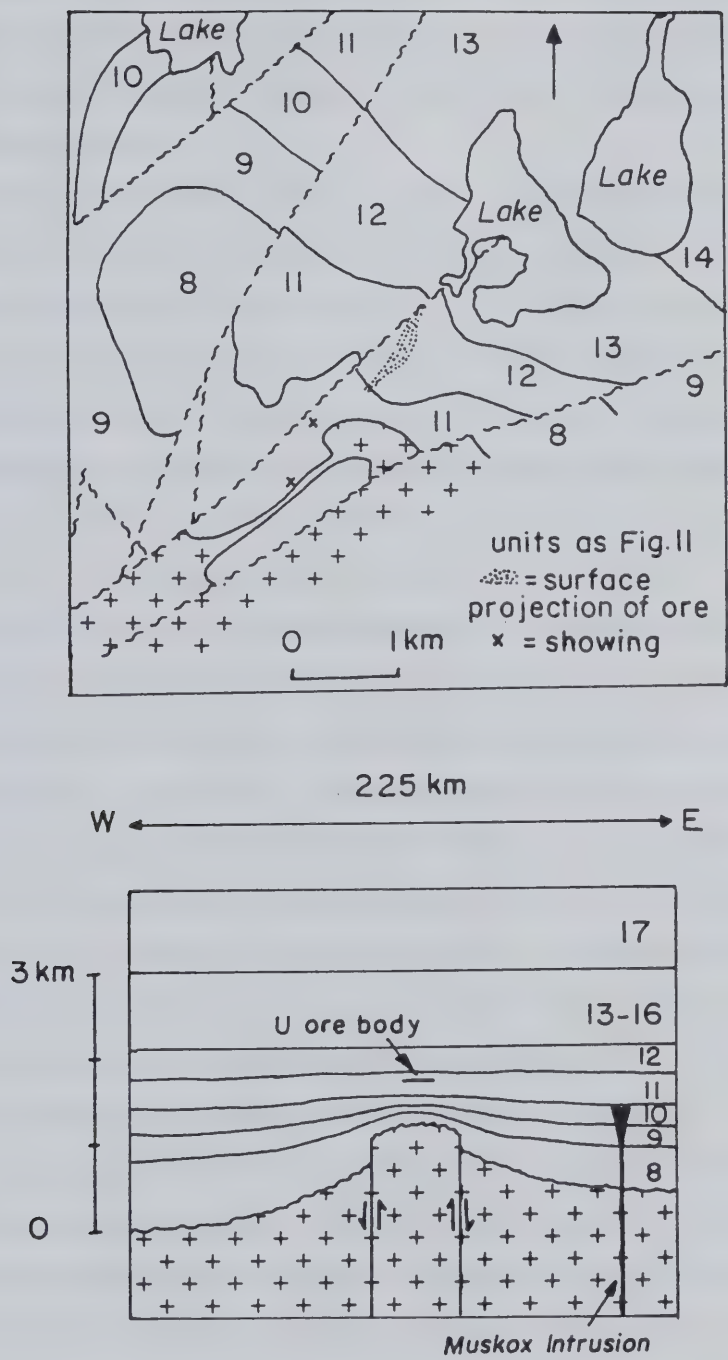


Figure 12: Geology of the Mountain Lake pitchblende deposit and its regional stratigraphic position (after Gandhi 1980).

and the latter claims were visited by the author. Exposure is poor, with up to 60 m of glacial overburden. The property has also been briefly described by Ruzicka (1979), and S. Gandhi of the Geological Survey is currently preparing a paper on the deposit. Isotopic analysis of the pitchblende gave an age of 1076 ± 96 Ma, with some possible remobilisation at 450 Ma.

The uraniferous mineralisation occurs above a basement horst (Gandhi 1980), a ridge of which originally formed a Helikian cape or island of granodiorite 1–2 km south of the deposit until it was submerged by upper unit 11, a shallow off-shore marine sandstone (Fig. 12). At the YUK property, unit 11 rests directly upon a strongly hematitic regolith of basement rocks, or upon unit 8. Basement faults were probably reactivated during sedimentation and again after mineralisation (Gandhi 1980). Outside the claims, unit 11 is a massive, buff, pink or white sandstone, composed of well- to moderately-sorted quartz sand with minor conglomeratic intercalations. Sandy members of the unit 9 dolostones have a high detrital zircon content, but unit 11 contains only up to 5% of detrital feldspar with the quartz. Attempts to analyse lead from these dolostones are discussed in Chapter V. Although now cemented by syntaxial quartz overgrowths, some sericitic clay matrix remains in unit 11 samples. Barite occurs in small vugs lined with terminated quartz crystals, reaching 22.0% by volume in unit 11 and 1.5% in sandy dolostone of unit 9, and perhaps occurring in other units as well. Dust and fluid inclusions suggest that (1) barite deposition occurred between two stages of silicification, and (2) an original carbonate or sulphate cement may have been silicified. Unit 11 in the YUK drill cores is often quite porous. A poikilitic barite cement occurs in mineralised core samples from the YUK claims (Trigg Woollett personnel, pers. comm. 1979).

The mineralised block lies between intersecting faults (Fig. 12) and has been offset by the more northerly (Gandhi 1980). The mineralisation being lenticular, grade and size estimates vary. One estimate suggests that three major and several minor lenses are up to 400m x 200m x 2m, and contain 0.3–0.5% U_3O_8 , <1 oz/t Ag and minor chalcopyrite, pyrite and Co–Ni arsenides (Gandhi *op. cit.*), *i.e.* approximately 1600 t of U_3O_8 . A second estimate suggests that the mineralisation is 900m x 350m x 1–2m, containing 0.15–0.25% U_3O_8 , 0.53% Cu, 0.24% Ni and minor Co and Ag (anon. Gulf Canada in-house reports, pers. comm. 1979), *i.e.* 2400 t of U_3O_8 . Higher grades reportedly occur

along subsidiary faults, and may indicate a later remobilisation of U, Co, Ni and As.

The YUK boreholes show that unit 11 comprises some 50–175 m of pink sandstones, locally green or gray and pyritic, with rare shale partings. Several radioactive horizons occur some 10 m apart, picked out by pitchblende and/or green platy secondary uranium minerals, and sometimes by a distinct hematitic redox interface. Polished mineralised core samples from the YUK claims (provided by Messrs. Trigg Woollett Consulting Ltd.) show the following mineral paragenesis:

- (1) Deposition of pyrite and chalcopyrite.
- (2) Cementation of the sandstone with carbonate or sulphate; recrystallisation of the pyrite and silicification of this cement, deposition of barite in vugs, and a second stage of silica deposition.
- (3) Brecciation, forming micro-fractures (a continuous process); emplacement of marcasite.
- (4) Emplacement of pyrite, bravoite (?), primary covellite, "chalcocite"³ and an anisotropic Cu–As–S mineral; the pyrite sometimes rimming marcasite.
- (5) Emplacement of pitchblende ± pyrite, sometimes replacing marcasite, "chalcocite", covellite and chalcopyrite. Two types of pitchblende are visible, of uncertain relative age. Gersdorffite–cobaltite is intergrown with the pitchblende in one instance, and cemented by it elsewhere. The "chalcocite" may be an optically similar phase such as digenite or djurleite.
- (6) Late silicification, altering pitchblende to minor coffinite replacing quartz, and cementing arsenides into syntaxial quartz overgrowths.

Several small euhedral grains of electron microprobe-identified TiO₂ were found, but could not be ordered paragenetically. Both primary and secondary covellite exist, sometimes with peculiar optical properties. The pitchblende and coffinite both have low but persistent levels of phosphorus, and the pitchblende is siliceous; neither mineral contains exsolved galena. The interlayered pitchblende–arsenide mineralisation could be an effect of remobilisation, since the sample showing this paragenesis yielded a

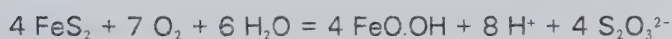
²⁰⁷Pb/²⁰⁶Pb age of 450 Ma.

³"Chalcocite" is used here to refer to any of the optically-indistinguishable minerals chalcocite, djurleite, digenite and anilite (Craig and Scott 1974).

A radioactive boulder of pink, rusty sandstone collected by the author outside the claims is 82% quartz, 17% pinkish barite and 1% malachite and cobaltite–gersdorffite. The Co–Ni minerals, which occur within or adjacent to barite, are partly replaced by botryoidal “chalcocite” and minor covellite. Some small pyrite cubes are occluded in the syntaxial quartz overgrowths.

The deposit has characteristics of both the Zambia/Zaire U–Cu deposits and of the “stack” type of peneconcordant, clastic–hosted uranium deposits. “Stack” deposits are typically hosted by bi–facies fluvial sands, and often contain V and/or Mo in addition to Cu, Ni, As, P and other elements. In contrast, the Mountain Lake deposit is hosted by generally oxidised marine sands, and lacks known Mo and V. The deposit has a mineralogy and possible paragenesis similar to that of the Benavides, Texas, roll–front deposit (Goldhaber *et al.*, 1978), despite its apparent “stack” morphology. For Benavides, these authors propose:

- (1) Initial sulphidisation of a channel sand by H_2S and HS^- introduced through a fault, altering detrital Fe–Ti oxides to pyrite and anatase.
- (2) Entry of oxidised, uraniferous water, the uranium being derived from indigenous tuffs and reduced by the oxidation of pyrite (the Benavides deposit is free of organic carbon). Pyrite oxidation produced metastable anions such as thiosulphate ($\text{S}_2\text{O}_3^{2-}$), and sulphite (SO_3^{2-}), in an acid solution, *e.g.*:



The reduced solution moved on into reduced rock, to precipitate ferrous ions as marcasite by a disproportionation reaction such as:



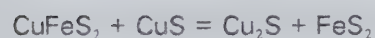
Marcasite would be superseded by pyrite if the pH was gradually raised by reaction with the host rock.

Applying this model to Mountain Lake, the initial sulphidisation stage may be the precipitation of syngenetic sulphides, as seen in this unit at Leith Peninsula (*q.v.*). Such

sulphides were possibly the original reducing agents. Potential sources of uraniferous solutions include the granodiorite basement (faulted against units 10 and 11 at the PEC occurrence), the black shales of unit 12 and the evaporites of unit 13, the latter also capable of supplying Ba (Fuchs 1980). Evaporites have been suggested as a source of uranium in some Nova Scotian deposits (Dunsmore 1977). The granodiorite has almost the lowest U content of the granitoids analysed, 2.1–2.2 ppm, but the Th : U ratio is 18.6, and uranium has clearly been leached out at some stage (p. 176). Metastable marcasite was preferentially replaced and possibly partly reprecipitated with pitchblende as pyrite; H₂S may also have been introduced via the faults during mineralisation. The silicification and barite deposition may not be directly related to the uranium mineralisation.

Uranium mineralisation at 1076±96 Ma would have coincided with late stage hydrothermal activity in the overlying Coppermine River Group basalts (Douglas 1980), and the uraniferous solutions may have been introduced by way of the boundary faults and trapped beneath the unit 12 shales. The uranium mineralisation took place beneath at least 5 km of Helikian cover, mostly flood basalts, and probably another 1 km of the Hadrynian Rae Group, compared with the 40 m of cover implied by Ruzicka (1979). This militates against the downward percolation of uraniferous solutions, and at present a basement source is indicated. The boundary faults subsequently dropped the PEC mineralised block, perhaps beneath every subsequent water table, which thus preserved it from oxidation. The Dease Lake showings (*q.v.*) are probably the oxidised remnants of similar deposits.

The mineral assemblages imply a low temperature origin, although not unexpectedly the deposit is out of equilibrium. For example, the following reaction should occur, all four species being present:



Free energy calculations indicate that chalcopyrite and covellite should be the stable pair when $T > 15^\circ\text{C}$, but pyrite is particularly slow to react, and covellite + chalcopyrite is a common metastable assemblage (Barton and Skinner 1979). At 25°C the assemblages in the Cu–Fe–S system should be covellite–pyrite–“chalcocite”, bornite–pyrite–“chalcocite”

or bornite–chalcopyrite–pyrite (Barton and Skinner *op. cit.*, p.375). However, Runnels (1969) observed that bornite is unstable, and that the stable low–temperature assemblages for the Cu–Fe–S system are covellite + chalcopyrite + pyrite and covellite + chalcopyrite + "chalcocite".

Models of Zambia/Zaire copper–belt Cu–U mineralisation are discussed further in connection with the Leith Peninsula deposits (p. 59). Mountain Lake is an unusually ancient "stack" or "roll–front" deposit, types usually confined to the Phanerozoic, although even older examples occur in the Great Slave Basin (Robertson *et al.* 1978; Morton 1974; Bloy 1979).

C. The Dease Lake U–Cu–Fe–As–S deposits

(C) (Bear Mountain, 118°00'W, 67°10'30"N; (D), JOHN claims, 119°05'W, 66°46'N)

Two minor showings in the Hornby Bay Group were visited in this area, at Bear Mountain and the JOHN claims. The exposure is poor to fair; trenches have been cut, but the drill cores seen did not intersect any mineralisation. Maps were not available for these deposits, shown on Figure 2.

The Bear Mountain occurrence lies within cross–bedded red, buff and white quartzite of unit 11 (Plate 1). Five parallel horizons, spaced up to some tens of metres apart vertically, are mineralised over known strikes of 15–20 m. As at Mountain Lake, the cement is syntaxial quartz overgrowths, and a trace of zircon and barite in rounded grains occurs in an otherwise clean quartz sand. Interstitial hematite and a yellowish clay–like material (possibly goethite) colour the rock, while bleached spots contain traces of chlorite instead of hematite. Green metazeunerite, $\text{Cu}(\text{UO}_2)_2(\text{AsO}_4)_2 \cdot 8\text{H}_2\text{O}$, resembling malachite, was the only mineralisation found in outcrop, usually confined to the cores of the bleached spots.

The JOHN claims extend over hard, white or pale grey quartzite of unit 8, containing rare heavy–mineral laminae and occasional green shale clasts. Chalcopyrite occurs in small clots replacing quartz grains, following small–scale cross–beds picked out by zircons, and some minor malachite staining is present. Individual sulphide grains some 200 micrometres in diameter are slightly radioactive, while a veinlet of a secondary uranyl phosphate containing K, Ca, Fe, Mg, Al and Si was the only other mineralisation

found.

Lead from two chalcopyrite samples was isotopically analysed, and suggests either a Palaeozoic or a late Helikian age (see Chapter V). It is difficult to reconcile this with the apparently syngenetic origin of the sulphides unless they have been recrystallised.

These minor occurrences are regarded as the oxidised remnants of a Mountain Lake type of "stack" deposit, and show a similar suite of elements. It is not known whether the meta-zeunerite is replacing the primary mineralisation *in situ*, or whether the components were introduced, but the multiple mineralised horizons are consistent with a "stack" morphology. Although the chalcopyrite is replacing quartz, it is also stratabound down to very small scales, and it is probably a recrystallised syngenetic sulphide (in this regard, see also the description of the Leith Peninsula deposits).

D. Leith Peninsula

Leith Peninsula is a spine of granitic rocks, recently correlated with the exotic terrain at Hottah Lake, overlain to the west by the Hornby Bay Group (Hoffman and St-Onge 1981; McGlynn 1976) (Fig. 13). Unconformably overlying both units is a Cambro-Ordovician marine sequence (including evaporites), in turn unconformably overlain by grey marine Cretaceous rocks with minor lignite (Balkwill 1971). With three unconformities, organic-rich reduced sandstones and a late Aphebian granitic basement, the Peninsula is a classic exploration target for unconformity-associated and roll-front uranium deposits, and three sites were visited. The isotopic analyses of lead extracted from some Hornby Bay Group dolomite are discussed in Chapter V.

Naga Lake

(E) (119°15'W, 65°13'N)

An aerial radiometric anomaly is centred over a grassy, sandy swamp in Palaeozoic sediments west of Naga Lake, into which drains water from the surrounding basement and Palaeozoic rocks (Plate 2). More than twenty bore-holes reportedly intersected unmineralised arenites beneath the swamp, the best intersection being some 470 ppm uranium over 3 m (M. Male, pers. comm. 1980). Since neighbouring swamps are



Plate 1 (top): Hornby Bay Group sandstone at the Bear Mountain occurrence. The sandstones are maroon and white and contain small amounts of metazeunerite.
Plate 2: General view of the Naga Lake radioactive swamp.

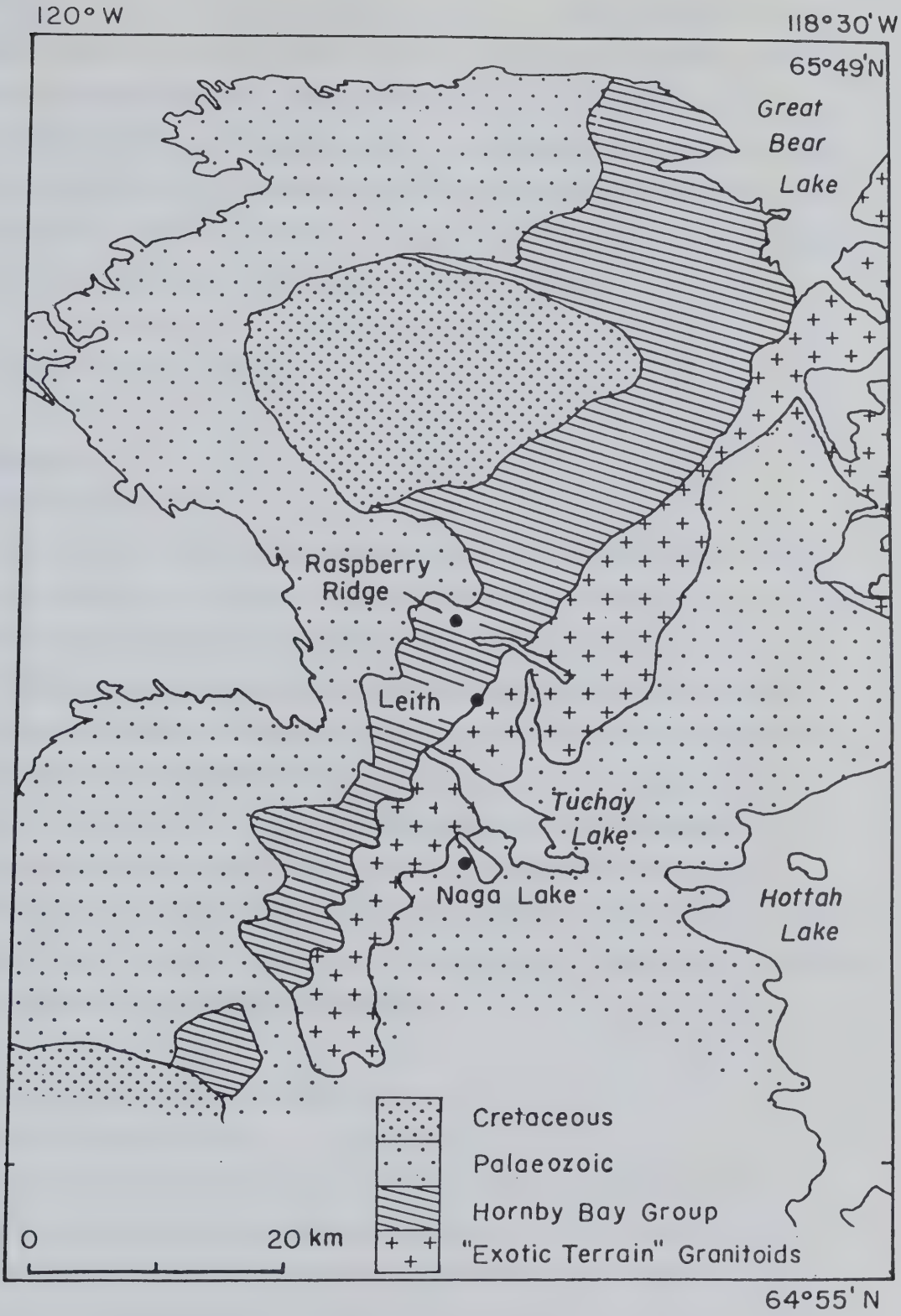
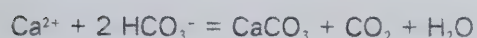


Figure 13: Geology of the Leith Peninsula showings (after Balkwill 1971).

not radioactive, the radio-isotopes probably come from a uranium deposit or a very restricted uraniferous lithology, rather than from a dispersed, bedrock source. This deposit may underlie the swamp or lie upstream. No attempt was made to ascertain whether the radioactivity is ultimately due to U or to unsupported ^{226}Ra ; ^{222}Rn , ^{234}Th and ^{230}Th are not thought likely to be ultimate sources. A whiteish precipitate covers some of the sand flats and forms crusts around some boreholes; it could be sulphate, or calcium carbonate (with which Ra co-precipitates) deposited by CO_2 loss:



Leith Showing

(F) (119°13'W, 65°20'N)

This informally-named area, south of Fenwick Lake, covers arenites where the Helikian and Palaeozoic unconformities virtually coincide (not evident from Figure 13 but apparent from confidential company data). The basement granodiorite is overlain by red or buff Helikian conglomerate, overlain in turn by micaceous, thin-bedded grey and purple (hematitic) sandstones. These sandstones could not be positively identified as unit 8, and although they resemble this unit as seen at Hornby Bay, they differ from the description by Balkwill (1971). The grey-purple redox interface is approximately conformable, but unconformable in detail, and thus an epigenetic feature. The radioactivity at the redox interfaces is occasionally up to 7x background, but no uraniferous phases could be located. The occurrence is neither significant nor unusual for redox boundaries in groundwater flow regimes.

The Raspberry Ridge Cu-Fe-S showing

(G) (119°15'30"W, 65°23'30"N)

The ridge is an informally named escarpment, west of Fenwick Lake, of unassigned Hornby Bay Group sandstones which are white, buff or pink. The basal sandstone is clean, well-sorted and cemented by syntaxial quartz overgrowths, and shows ripples, cross-beds and desiccation cracks in rare silty horizons. It is overlain by softer dolomite-cemented sandstones, sandy dolostones, shales and stromatolitic

dolostones. Two malachitic beds occur 8 m apart in the dolomitic sandstones. Up to 30 cm thick (average 10 cm) and traced for two kilometres along strike, they are medium to fine-grained quartz sandstone, with occasional zones of green shale clasts. Similar beds above and below these are not cupriferous. A coarse poikilitic dolomite cement is restricted to these two horizons, texturally resembling the barite seen in some cores from the Mountain Lake deposit. They are precisely stratiform and stratabound, as defined by dolostone and shale marker horizons. Zones of up to 50% porosity occur in and near these Cu-bearing horizons, the voids being spherical, up to 2 mm in diameter, and sometimes filled with malachite or limonite with relict pyrite; the adjacent quartz grains may be slightly corroded. The voids could be subsequently-infilled gas bubbles, the casts of syngenetic sulphide nodules or preferentially dissolved calcite oolites. Fresh examples of the cupriferous bands contain several per cent of interstitial chalcopyrite clots up to 2 mm across, partially replacing quartz and perhaps coeval with the dolomitic cement.

Raspberry Ridge is not uraniferous, but similar copper deposits may have pre-dated the uranium mineralisation at Mountain Lake. This copper mineralisation, and probably that at the Dease Lake deposits (*q.v.*), resembles some "red-bed" syngenetic deposits, formed by the reduction of copper-rich brines by rotting organic (algal?) matter. Similar deposits at Mountain Lake may have been the reducing agents necessary for subsequent uranium mineralisation. Mountain Lake may even resemble the African copper-belt U-Cu-Co-Ni deposits more closely than it does the "stack" peneconcordant deposits, particularly in terms of age if not in size.

Briefly, the Zambian deposits are hosted by sandstones and shales, often highly metamorphosed and 1000–1300 Ma old (Meneghel 1981). The deposits in Shaba Province, Zaire, contain U-Cu-Co-Ni mineralisation in a siliceous dolostone, while the north west Zambian deposits contain copper sulphides, gold, uranium arsenates and vanadates, and minor Ni, Co, Pb, Cr and Mo (Meneghel *op. cit.*). The Cu-Fe-Co sulphides precipitated syngenetically on the sea floor after the reduction of cupriferous brines by a reducing bottom water layer (Fleischer *et al.* 1976). Meneghel (*op. cit.*) has suggested that the uranium is syngenetic in origin, being restricted to the base of the copper sulphide zones, but it could also have been precipitated by the sulphides after concentration and

remobilisation by metamorphism. The uranium, occurring as veins and disseminations, is 706–520 Ma old in Zaire and 520–235 Ma old in Zambia, while orogenic pulses have been dated at 840 ± 40 –710 Ma, 670 ± 20 Ma and 620 ± 20 Ma (Meneghel *op. cit.*).

Red-bed copper deposits are sometimes more diagenetic than syngenetic in origin, the copper sulphides replacing pre-existing pyrite (*e.g.* Ripley *et al.* 1980). No indication of pyrite replacement by chalcopyrite was seen in this material. Palaeomagnetic data show that tropical and desert conditions prevailed from 1450 to 1250 Ma ago, the likely depositional interval, within latitudes of 0° to 25° (Irving 1979). Interestingly, "chalcocite" also occurs in Palaeozoic shales just to the south (Thorpe 1972, p. 57).

E. The Echo Bay Ag-U-Bi-Cu-Co-Ni-Fe-Pb-As-S-Si-carbonate (-Te-Se-Mn-Zn-Ba) deposits

(H) ($118^\circ 02'W$, $66^\circ 05'N$)

The hydrothermal, polymetallic vein deposits of the Echo Bay area have been so thoroughly documented by previous researchers that only some additional pitchblende isotopic dating was undertaken. The veins are mineralised principally with Ag, U, Bi, Cu, Co, Ni, As and S in a gangue of quartz and carbonate. Similar deposits occur in the Camsell River/Rainy Lake area, 50 km to the south, indicating a comparatively widespread event (Fig. 14). Access to the underground workings at Echo Bay was denied, and the Camsell River area was not visited. Literature sources used for this account include Rich *et al.* (1977) for a brief summary; Hoffman *et al.* (1976), Mursky (1973), Badham (1973a and b), Robinson (1971), Jory (1964), Lang *et al.* (1959) and Campbell (1955) for the general geology; Robinson and Morton (1972) for the geology and geochronology; Thorpe (1974, 1971) for the common lead isotope systematics; Jory (1964) for the early pitchblende U-Pb study (although Jory's zircon U-Pb study has been challenged by van Schmus and Bowring, who suggest a zircon age of some 1855 Ma for the Hogarth pluton (S. Bowring, pers. comm. 1981)); Kieller (1962) for the ore mineralogy at the Eldorado mine; and Robinson and Ohmoto (1973) for mineralogy, fluid inclusion and stable isotope studies. Thorpe (1972) lists many minor showings in the area. Nomenclature follows that of Hildebrand (1980).

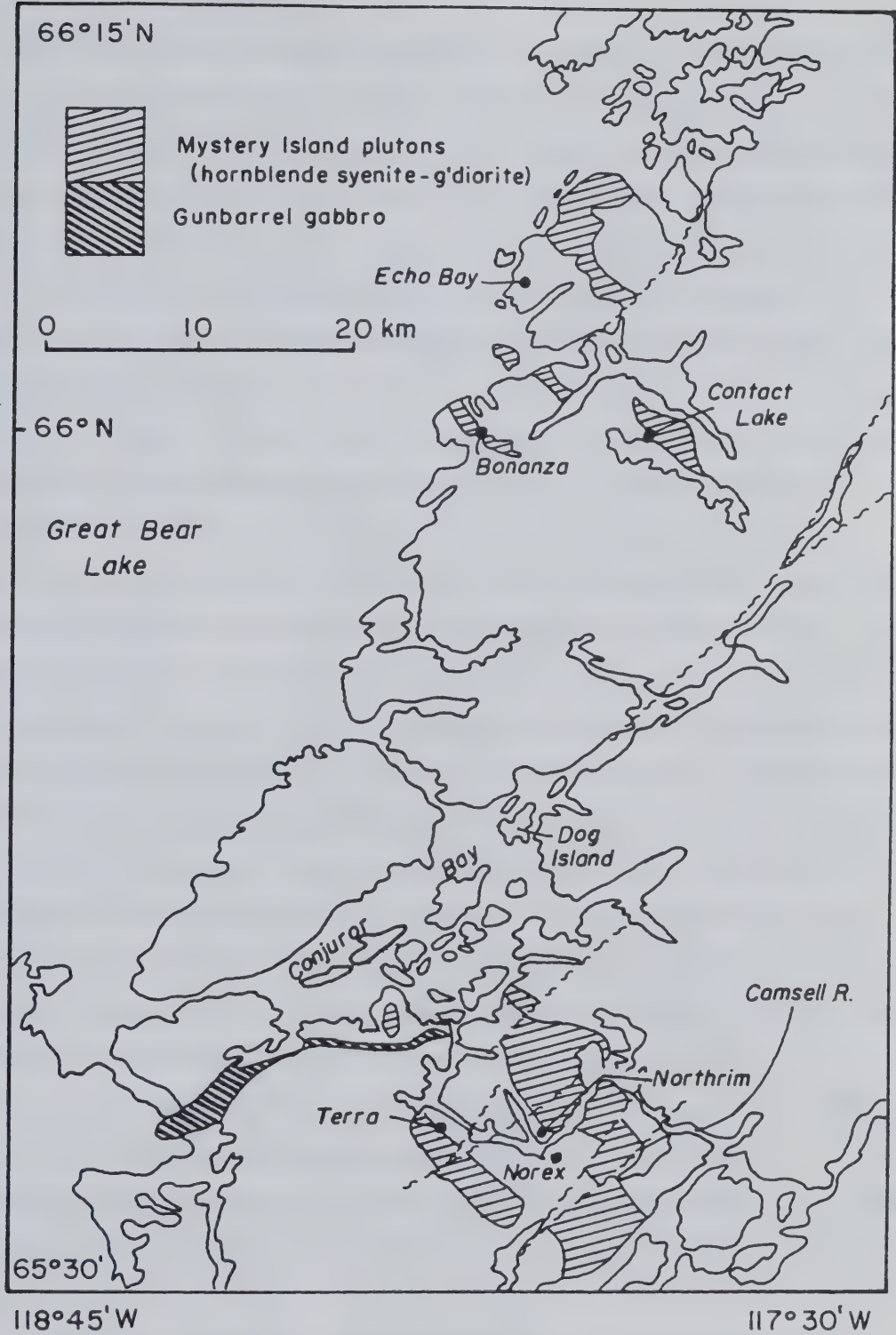


Figure 14: Echo Bay/Camsell River area, showing the location of the principal Ag ± U deposits, Dog Island, and the total known outcrop of the Mystery Island plutonic suite (after Hoffman *et al.*, 1976).

Echo Bay and Eldorado mines

The Eldorado Mine produced at least 6300t of uranium metal from 1933 until its closure in 1960 (McGlynn 1971; Jory 1964), while the Echo Bay mine, 1–2 km to the north-east, produced silver and copper until 1981, each mine working different veins up to 500 m long within the same quartz–carbonate vein system (Fig. 15). Numerous smaller deposits nearby include those mined at Contact Lake (in monzonite of the Mystery Island suite) and at Dowdell Point (the Bonanza and El Bonanza mines). The economic mineralisation occurs in a north-east trending, north dipping, cymoid loop fault system, principally where it cuts tuffs of the upper Port Radium Formation of the Labine Group (Robinson and Morton 1972; Jory 1964). The Eldorado mine ore shoots were confined to areas with volcano–sedimentary wall-rocks (Lang *et al.* 1959, fig. 20). The mineralisation is structurally controlled by dilatant zones on steeper sections of the fractures, and only where these are concave to the north (Campbell 1955; Jory 1964). Reported secondary minerals include pyrolusite, psilomelane, polianite, malachite, azurite, gummite, uranophane, zippeite, erythrite and annabergite (Mursky 1973), becquerelite, curite and liebigite (Lang *et al.* 1959), and uranophane, zippeite and possibly becquerelite and curite (Palache and Berman 1933). This study identified zeunerite, cuprosklodowskite, uranophane and possibly metanovacekite, and further unidentified species are present.

Zeolites in the country rocks indicate regional metamorphism to <200°C and 0.2kb (Robinson and Morton 1972). The Tut granodiorite pluton, one of the Mystery Island monzonite–syenite intrusive suite (p. 6), is just east of the mineralised area and coeval with the Labine Group volcanics. It possesses an alteration halo of inner bleached and albitised rocks and outer gossan-forming zones containing chlorite, actinolite–apatite–magnetite pods, epidote, pyrite and chalcopyrite (Hildebrand 1980; Mursky 1973). The slightly younger Hogarth granodiorite pluton has a minor hornblende–hornfels aureole, and cuts the Labine Group just west of the mineralised belt (Robinson and Morton 1972). All these units have been pervasively dusted with hematite (Mursky 1973).

A sheet of the Western Channel quartz diabase, 30–60 m thick, outcrops between the Echo Bay and Eldorado mines, with a Rb–Sr age of 1392 ± 48 Ma (after Thorpe 1978), and is cut by the final stages of mineralisation (Jory 1964). The extent of

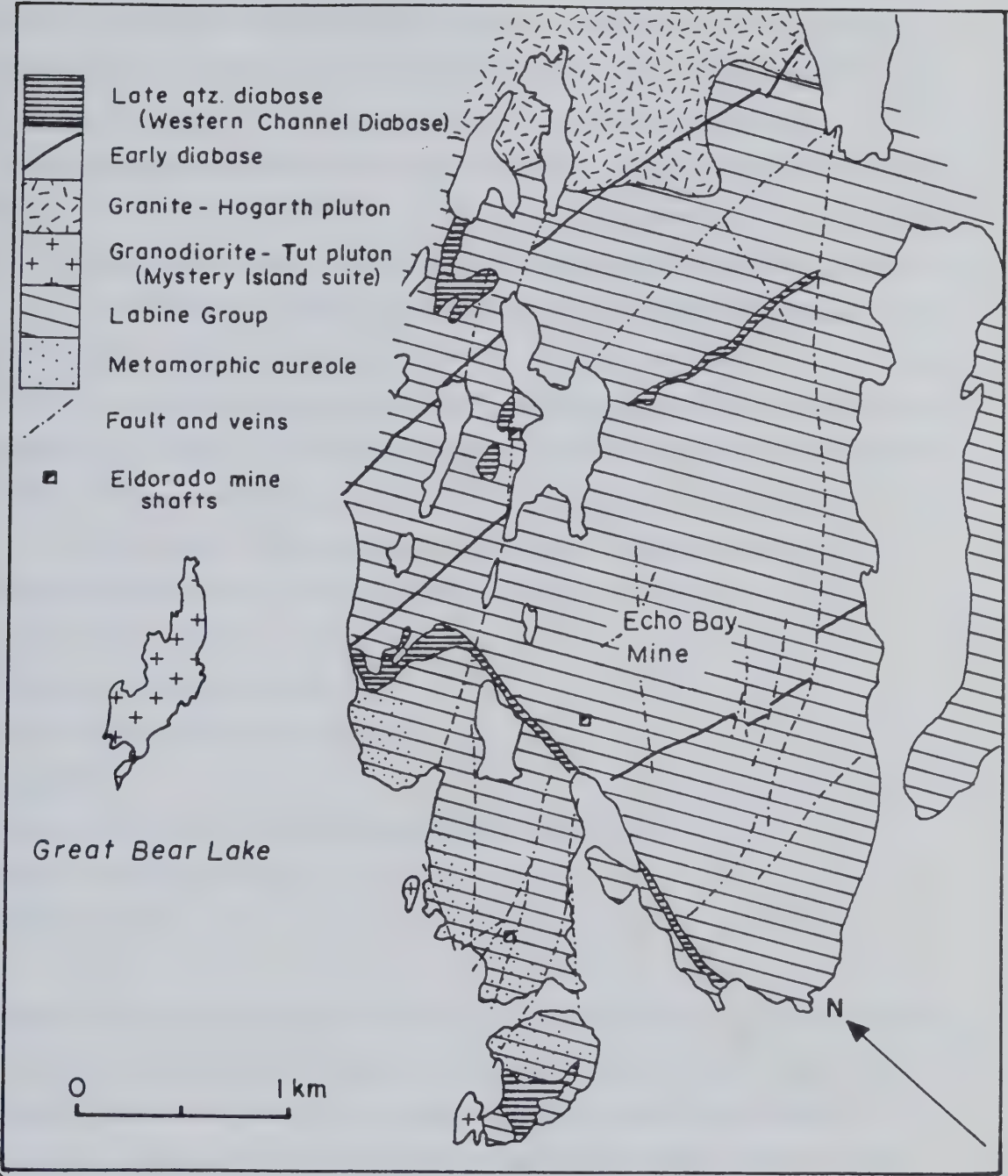


Figure 15: Geology of the Echo Bay and Eldorado mines area (after Robinson and Morton 1972).

its alteration is not recorded, but it is not markedly hematitic, and contains secondary hornblende, chlorite, carbonate, sericite, leucoxene, magnetite and hematite (Mursky 1973; Lang *et al.* 1959). The main pitchblende mineralisation is 1424 ± 29 Ma old, and there is some suggestion of an earlier phase 1500 ± 10 Ma old (Miller 1982).

Actinolite–magnetite pods in the Port Radium Formation at Echo Bay mine are 1408 ± 60 Ma old (K–Ar, Robinson and Morton 1972), although similar material in the Camsell River area is cut by a quartz–porphyry dyke (Badham 1973a) and is presumably > 1800 Ma old.

The complex structure is controlled by the intrusions, and includes small tight folds and brecciation, superimposed on a north trending, east dipping homocline (Mursky 1973). Major fractures trend north–east in five groups, and may contain quartz veins or diabase dykes (Mursky 1973). Diabase dykes striking east were emplaced between the initial fracturing and the final economic vein mineralisation (Robinson and Morton 1972).

Seven stages of mineralisation are recognised at Echo Bay (Mursky 1973; Robinson and Ohmoto 1973). From oldest to youngest, these are:

- (1) quartz and hematite.
- (2) rhythmic quartz and pitchblende.
- (3) Co–Ni arsenides, native Ag, native Bi.
- (4) acanthite
- (5) Cu and Ag sulphides, dolomite, chlorite and white mica.
- (6) quartz and late native Ag.
- (7) mckinstryite.

Stages 1–4 are fracture filling, the later stages generally replacive (Jory 1964). Other minor sulphides and hessite (Ag_2Te) have also been recorded (Mursky 1973). The economic pitchblende and silver do not extend below some 600 m and 250 m respectively (Mursky 1973). The pitchblende occurs in botryoidal, colloform, cellular, dendritic, brecciated and vein forms, and a softer, sooty variety is apparently related to ground–water circulation (Jory 1964). No sulphides pre–date the pitchblende, which was extensively brecciated during stage 5 (Jory 1964).

The wall–rock tuffs are now composed of 80% pink albite or oligoclase with hornblende, magnetite and rare diopside, garnet and scapolite (Jory 1964). The wall–rock

alteration comprises zones of apatite–microcline–quartz–hematite and argillic and chloritic hydrothermal alteration, passing outwards into intensely carbonatised zones; the hematitic alteration is directly related to mineralisation (Mursky 1973; Jory 1964; Lang *et al.* 1959). A degree of potassium metasomatism evidently occurred during mineralisation.

From studies of fluid inclusions, mineral stability and stable isotopes, Robinson and Ohmoto (1973) concluded:

- (1) That the hydrothermal water was uniform and not magmatic;
- (2) That the total sulphur in the fluid, with $\delta^{34}\text{S} = 25 \pm 3$ per mil, was probably marine in origin.
- (3) That temperatures varied from about 100–150°C for stages 1 to 4, rising to 175–225°C for stages 5 and 6, and finally falling to <100°C for stage 7.
- (4) That emplacement occurred at some 2.5–4.5 km depth.

Sea–water concentrated by circulation through the hot diabase is the most likely hydrothermal mechanism in view of the pressure, temperature and timing of the events.

Camsell River

The Terra, Norex and Silver Bay (= Northrim or Federated) mines, which were not visited, are 5 to 10 km south east of the Gunbarrel quartz gabbro, perhaps one of the Western Channel diabases (Fig. 14). The host rocks are andesitic tuffs and sulphide–rich "skarns" at Terra, basalts and tuffs at Silver Bay and andesitic flows and tuffs at Norex (Badham 1973a), approximately equivalent to the Port Radium and Echo Bay Formations. The Terra mine sulphide–rich rocks were interpreted as a metasomatised calc–argillite and tuff sequence by Badham, but were regarded as a volcanogenic exhalative sulphide body by Thorpe (1974). This unit contains no appreciable silver, nor any indication of isotopic or trace–element changes when it was recrystallised during the main silver mineralisation (Badham 1973a). There are no known volcanogenic exhalative sulphides at Echo Bay. All the deposits are evidently close to the plutons of the Mystery Island suite (Fig. 14).

The mineral paragenesis at the Terra mine is similar to that at Echo Bay, but there is also notable fluorite, and up to 3% mercury in the native silver (Badham 1973a). Badham

confirmed similar mineralisation temperatures at Terra to those given above for Echo Bay, using mineral assemblage stability criteria. The Silver Bay and Norex properties contain similar mineralisation, but with some paragenetic stages omitted; uranium is absent at Norex, and only a minor constituent at Silver Bay. Minor, unidentified uranium mineralisation in giant quartz veins has been noted from this district (Badham *op. cit.*).

F. The Achook Island U-Cu-S-Si(-Fe-Co-Ni-Zn-As) deposits

(J) (RHY, 117°52'W, 66°21'40"N; SHORE, 117°53'W, 66°20'50"N)

Two showings were seen on Achook Island, 40 km north of Echo Bay in Western Channel, Great Bear Lake, both showings being hosted by well-exposed rhyolite and tuff of the Cameron Bay Formation (Fig. 16). The island has been prospected for copper mineralisation (Thorpe 1972).

The RHY showing is some 50 m east of a steep, north-east striking fault between a coarse hematitic arenite to the west and red rhyolite to the east, the fault containing a stockwork of agate-like quartz. The rhyolite has been altered to a hematitic, quartz and white mica assemblage with local chlorite and carbonate patches, and contains quartz-hematite veinlets. Copper sulphide and pitchblende mineralisation occurs as blebs and a vein in bleached rhyolite, the vein being up to 3 cm thick and traceable for 10 m. Traces of green and yellow copper and uranium secondary minerals locally stain the outcrop, and brochantite was identified in small vugs.

Two chalcocite-like phases occur, identified by X-ray powder diffraction as djurleite and digenite; the phases could be distinguished optically but not identified. They occur as discrete, intergrown blebs and as fine parallel laminae, resembling twinning, presumably an exsolution feature. Polished sections indicate the following paragenesis:

- (1) Deposition of quartz; impregnation of wall rocks with fine-grained chalcopyrite, bornite, "chalcocite", euhedral cobaltite and possibly tennantite.
- (2) Deposition of intergrowths of "chalcocite" with a Fe-Mg-Al silicate, perhaps chlorite.
- (3) Deposition of layered botryoids some 200 micrometres in diameter, of alternating pitchblende and 2 "chalcocite" laminae.

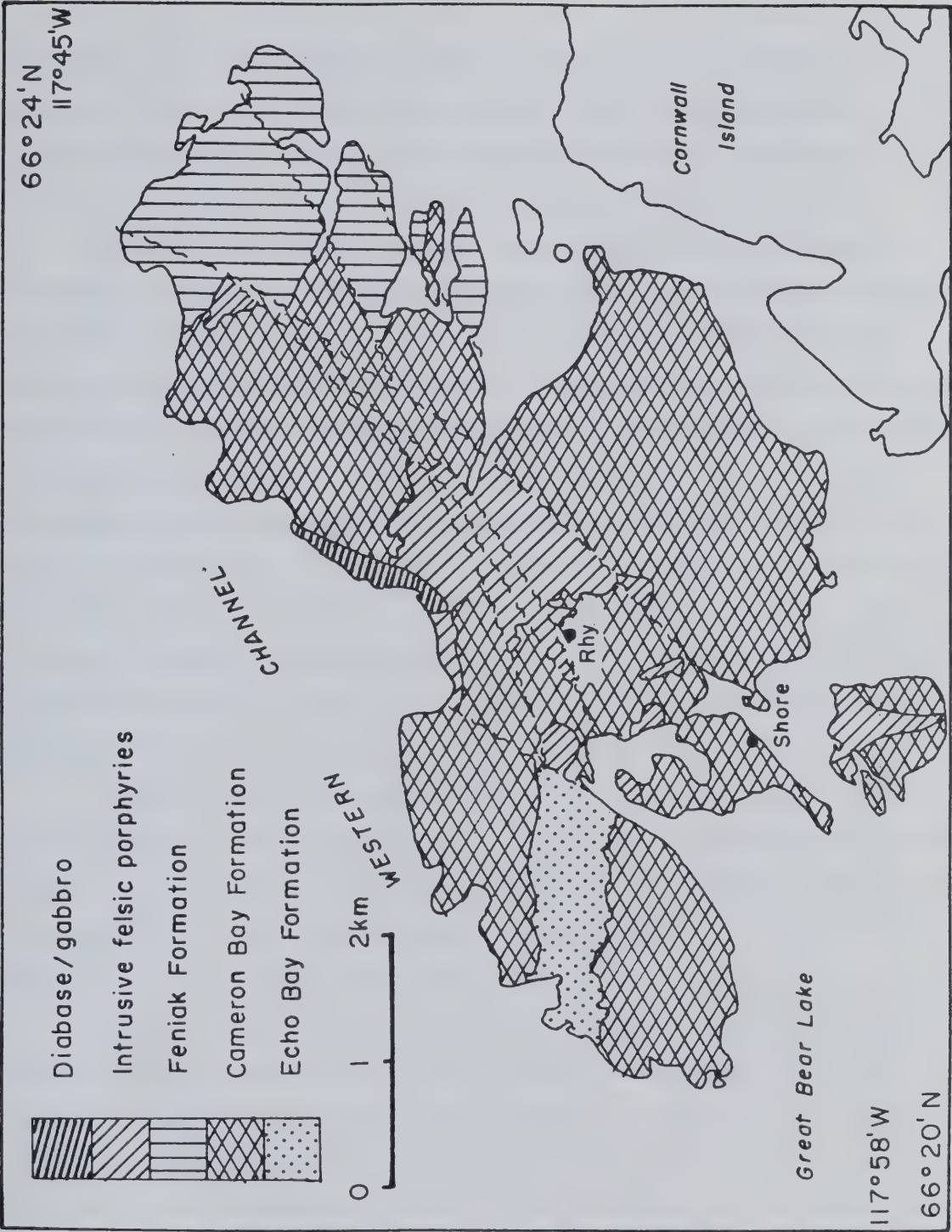


Figure 16: Geology of the RHY and SHORE pitchblende occurrences, Achook Island (much simplified after Hildebrand 1980).

(4) Brecciation; deposition of coarse "chalcocite" and minor bornite.

The "chalcocite" has partly altered to covellite, while the bornite is rimmed with secondary "chalcocite" and covellite and contains a mesh of chalcopyrite plates. The cobaltite has extremely variable Co : Ni : Fe and As : S ratios. Rare grains of a U-Ti mineral with minor Si, probably brannerite, were found in the rhyolite wall rocks.

The SHORE occurrence is hosted by a dark green, brecciated tuff, altered to white mica, quartz, chlorite and leucoxene. This is cut by a vein 10 cm thick, striking 080° and composed of quartz-cemented breccia containing veinlets of pitchblende up to 5 mm wide. The vein is locally coated with an orange mixture of goethite and uranophane. The pitchblende contains chlorite in syneresis cracks, and is intergrown with up to 5% chalcopyrite and minor pyrite. An earlier phase of pitchblende botryoids up to 600 micrometres in diameter, the pitchblende laminated with a Fe-Mg-Al silicate (perhaps chlorite), has been slightly brecciated and recemented with a more massive phase. There are traces of skeletal or euhedral cobalt sulpharsenide, ranging in composition from cobaltite to arsenopyrite, together with traces of chalcopyrite, sphalerite, bornite and covellite, impregnating the wall rocks. The paragenesis is essentially the same as that described for the RHY occurrence, except that "chalcocite" is absent.

Pitchblende from the SHORE showing was used for isotopic dating. It is coeval with the Echo Bay pitchblende mineralisation, *i.e.* 1424 ± 29 Ma, and also defines an earlier stage at 1500 ± 10 Ma. Lead extracted from "chalcocite" from the RHY showing was also analysed, and the single analysis suggested a maximum mineralisation age of some 400 Ma, from a source of maximum age 730 Ma (Miller 1982).

These pitchblende veins are a hydrothermal response to the same period of Western Channel diabase intrusion noted at Echo Bay; a diabase sheet from Hogarth Island to the south has been dated at 1400 ± 75 Ma (K-Ar, Wanless *et al.* 1970, anal. 67-80), and numerous sheets outcrop on Doghead Peninsula, 5 km to the north. The chemistry of the deposits differs widely from that at Echo Bay, but they do not occupy the same strata, nor occur within the aureoles of the Mystery Island plutons, suggesting that the Ag-Bi-Co-Ni-As suite at Echo Bay was derived from the country rocks, independently of the U and perhaps Cu. The primary Cu-Fe-S phases at Achook Island

were djurleite, digenite, chalcopyrite, bornite and a "chalcocite" phase which has subsequently unmixed. Chalcopyrite tended to occur when "chalcocite" phases were absent. These assemblages place little restriction upon the temperatures of formation.

G. The Dog Island U-Si-Fe-carbonate deposit

(K) (118°01'W, 65°46'N)

The BERNI claims on Dog Island, 40 km south of Echo Bay in Conjuror Bay (Fig. 14) are underlain by red-weathering purple siliceous extrusive and intrusive rocks of the Labine Group (Hoffman *et al.* 1976), immediately south of a small fault-bounded stock of hornblende monzonite or granite resembling the Mystery Island intrusive suite (Fig. 17). A high radiometric anomaly within the claims was investigated by Paterson (1976d), who reported:

"It appears that the radioactive zone is a high background volcanic porphyry and no high concentrations of uranium mineralization are present."

Grab samples returned generally <200 ppm uranium (Paterson, *op. cit.*).

The volcanic rocks contain phenocrysts of quartz, plagioclase, orthoclase and chloritised ferromagnesian minerals in a hematitic matrix of equigranular quartz and orthoclase with minor plagioclase. Some samples have intensely developed micrographic textures, and contain trellises of TiO₂ (probably rutile) after ilmenite or titaniferous magnetite. Irregular areas have a radiometric anomaly up to 20x background (140 cps), Paterson (*op. cit.*) recording one such area to be 130m x 5m.

A glacially polished, vertical rock face at the lake shore, several metres square, was studied in detail with a scintillometer. Count rates were measured over a ten-centimetre grid and contoured *in situ* with a marking pen (Plate 3). Count rates ranged from 800 to 2100 cps over the selected face, which was sufficiently flat and uniform to discount mass effects. The resulting contours showed that high count rates are associated with reddened fracture systems or "crackle zones", a few centimetres wide, although not all such zones were radioactive. The mineralisation is therefore epigenetic, and isotopic studies indicate a similar age to the 1424±29 Ma old deposits at Echo Bay.

The fractures contain fine-grained coeval carbonate, hematite, minor quartz, indeterminate silicates and rutile, and although minute veinlets of pitchblende or coffinite less than 1 micrometre in width were found in one sample, the uranium is probably

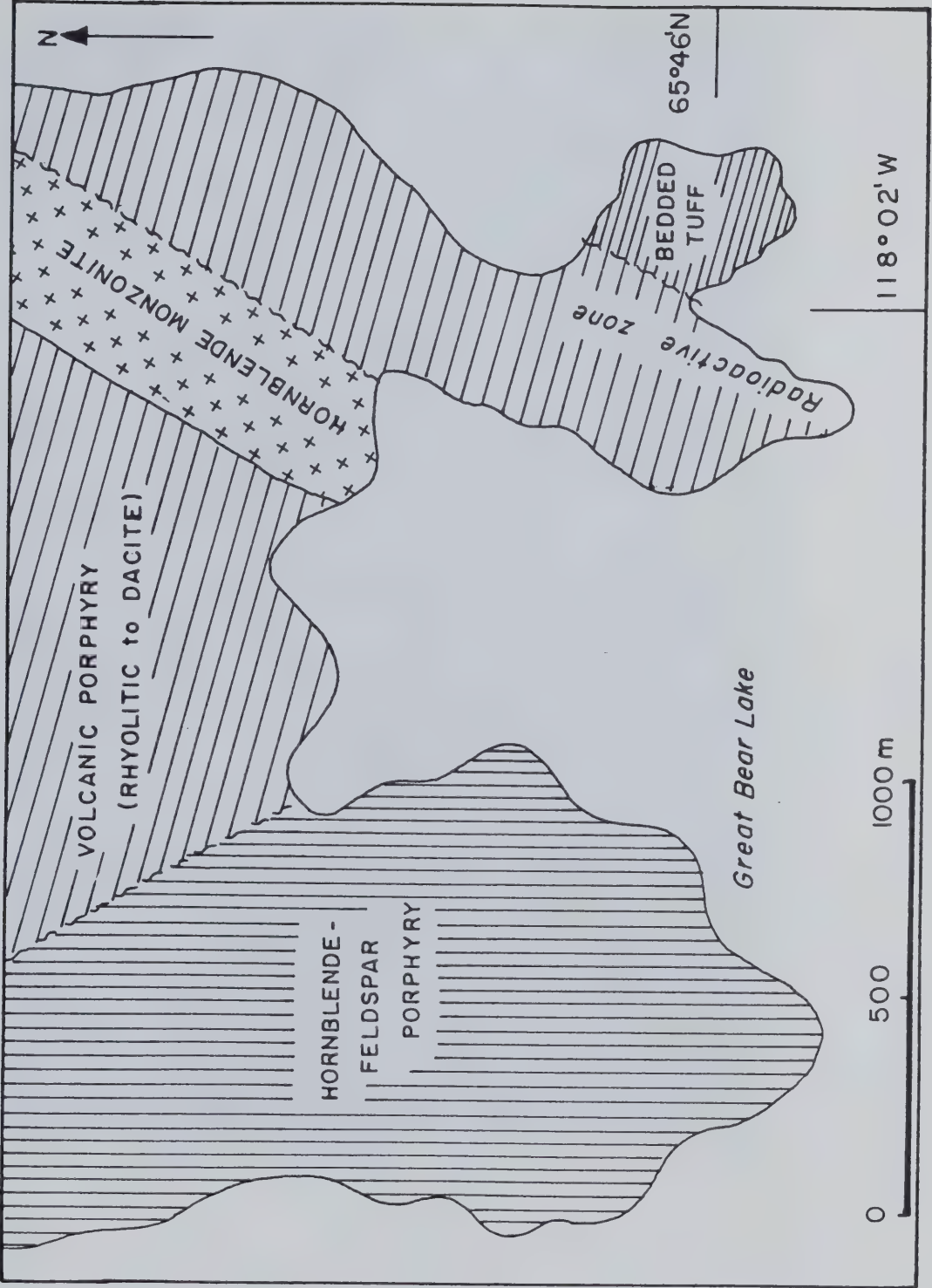


Figure 17: Geology of the BERNI uranium occurrence, Dog Island, Conjuror Bay (after Paterson 1976d).

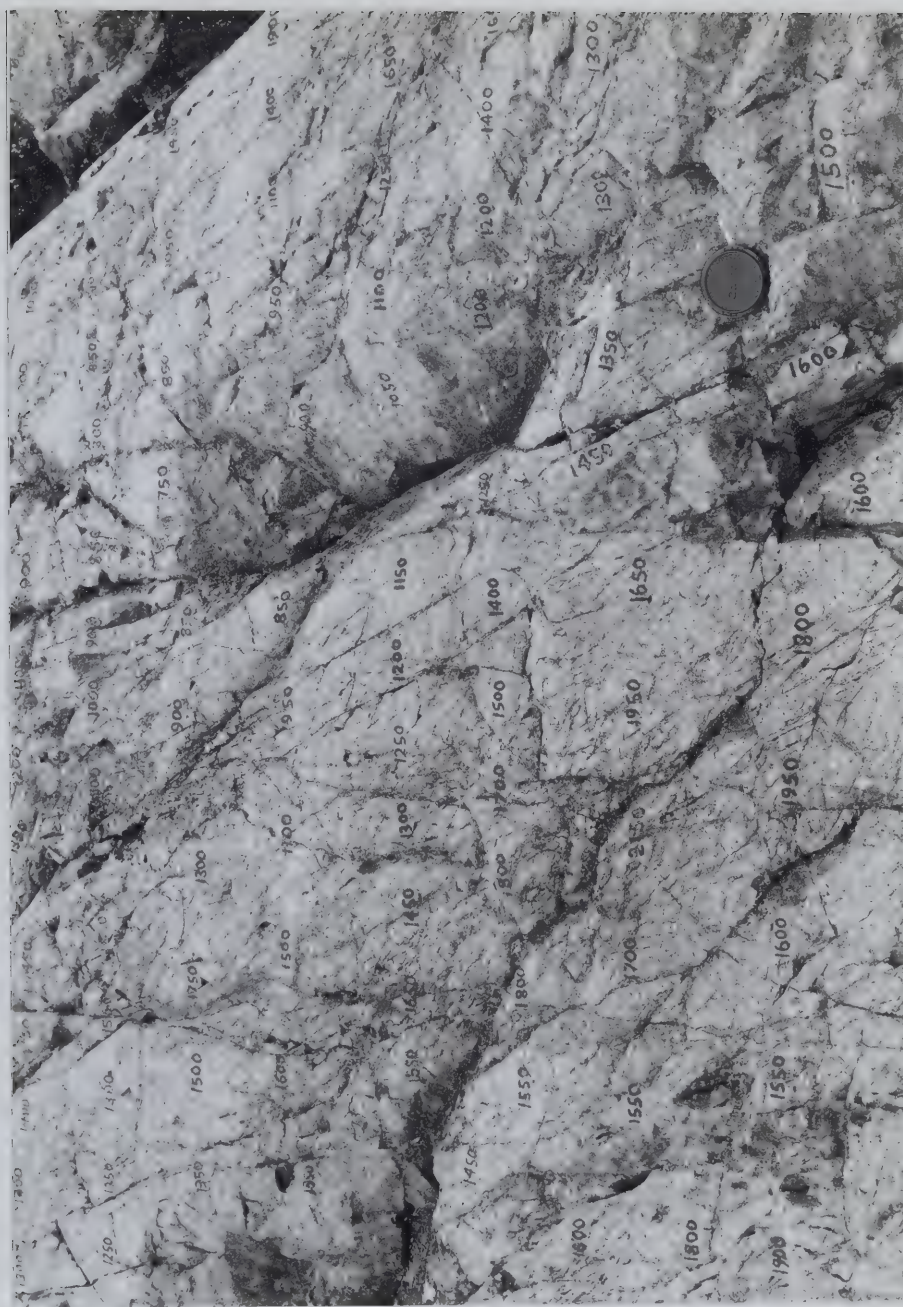
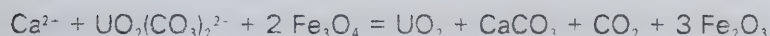


Plate 3: Polished face of radioactive tuff at the BERNI occurrence, Dog Island, showing part of the scintillometer survey. Numbers on the outcrop are total radioactivity c.p.s., and can be seen to show radioactivity generally following weathered-out fractures.

primarily adsorbed on to the rutile. Radioluxograph studies also showed that some rutile clots probably replacing magnetite in the host rocks are similarly uraniferous. The mineralisation occurs in both the intrusive and extrusive lithologies, and is not directly related to the degree of fracturing. A non-radioactive ignimbrite 400 m to the east does not contain these "crackle zones", but it does host some carbonate veins several centimetres wide.

It is difficult to assign a paragenesis to the deposit based on these data. Being coeval with the known diabase magmatism in the area (*cf.* Echo Bay), it is in some sense hydrothermal, the brecciation perhaps being caused by high-pressure gas release. The mineralogy suggests that pitchblende was precipitated by CO₂ loss and the reduction of uranyl carbonate complexes by host-rock ferrous minerals, for example magnetite, by a reaction such as:



(See also p.25 *et seq.* for similar reactions).

H. Models of mineralisation for the Echo Bay, Achook Island and Dog Island deposits

Robinson and Ohmoto (1973) proposed that the Echo Bay ore metals were leached out of the country rocks. Assuming that 720 t of silver were produced from Echo Bay, and assuming the Western Channel diabase to be 60 m thick and to contain 0.1 ppm Ag (Wedepohl 1969–1978), a diabase slab 5 x 10 km would have to be totally depleted to yield the mined silver alone (although Badham (1973a) reported up to 1.6 ppm Ag in diabase and basalt at Camsell River, and approximately 1 ppm in intermediate and felsic igneous rocks). Similar calculations for the 6300 t of known mined uranium yield a slab 4 x 10 km (assuming 1 ppm uranium in the diabase; Badham (1973a) and Robinson (1971) give average values of 0.6 ppm). This diabase is evidently the source of heat but not of the metals, outcropping at Echo Bay, Achook Island and probably Camsell River (the geology around Dog Island is not well documented).

Badham (1973a), ignoring the diabase as a mineralisation mechanism, proposed a continuum of events from pluton emplacement to metamorphism, metasomatism (producing skarns), barren quartz veins and mineralised veins, after finding somewhat high background levels of Co, Ni, Cu and Ag in the Echo Bay intrusive and extrusive rocks. There was, however, a 400 Ma interval between magmatism and mineralisation, and the mineralisation temperature data indicate a short heating event synchronous with the diabase intrusion. Badham (*op. cit.*) compared the deposits to those around the Cornish Hercynian granites, where he implied that mineralisation spanned 230 Ma. In fact these 290–300 Ma old granites host polymetallic veins emplaced some 270 Ma ago at temperatures of about 300°C (Halliday 1980); the Cornish uranium minerals have unreliable Pb/Pb ages which range from negative to 371 Ma (revised after Darnley *et al.* 1965). Subsequent hydrothermal events were quite distinct, probably related to early Atlantic rifting (Halliday and Mitchell 1976), while the 50–55 Ma old Lundy Island granite nearby is the southern extremity of a Tertiary igneous province equally capable of rejuvenating the hydrothermal activity (Darnley *et al.* 1965; Bennison and Wright 1969).

Although all the deposits are coeval, some are Ag-free pitchblende deposits and others are U-free silver deposits. The source of U, and possibly some Cu, is probably different from that of the Ag–Co–Ni–Bi–As suite, since the two suites behave semi-independently.

Essentially identical processes formed the Echo Bay and Camsell River deposits. Since the silver deposits, (1) all occur in the same general volcanic horizon; and (2) all occur within the metasomatic aureoles around the Mystery Island intrusives (Hoffman *et al.* 1976), one of these lithologies is the likely source of silver; the plutonic aureoles may have concentrated fugitive elements, to be remobilised during the diabase intrusion.

The possible uranyl complexes involved include carbonates, stable at $f\text{CO}_2 = 10^{-2} - 10^2$ atm and 100–150°C, although hydroxy complexes may be more likely at elevated temperatures (Langmuir 1978a; Robinson and Ohmoto 1973). Apatitic wall-rock alteration at Echo Bay also suggests the involvement of phosphate complexes. The reducing agent in all the deposits may have been ferrous minerals in the wall-rock tuffs, now altered to hematite or (rarely) chlorite.

I. The JD claims group

(L) (116°43'W, 64°37'N)

These claims contain uraniferous veins hosted by basalts and sediments and the altered granite pluton which intrudes them (Fig. 18). The overall metamorphic grade is low greenschist facies, since argillite has not been altered beyond fine-grained chlorite and white mica. The rocks are all cut by a north-trending, barren giant quartz vein 35 m wide, which is intermittently exposed for 15 km and occupies a branch of the 6 km wide Wopmay Fault zone. The showings were investigated by Gill (1969b) and in more detail by Armstrong (1969a, 1969b) following extensive trenching and drilling.

The volcano-sedimentary rocks were correlated with the Snare Group by Wilson and Lord (1942), being their unit 5. Unit 5 includes members of the paragneiss belt along the Wopmay Fault (p. 10); the volcano-sedimentary suite at the JD showings is possibly not stratigraphically equivalent, although small gneissic patches have been reported (Armstrong 1969a). The term Snare Group will be retained for convenience.

On the property, a north-trending ridge of red-weathering granite is flanked by quartzite, arkose, conglomerate, siltstones with graded bedding (tops to the west where determined), a minor feldspar porphyry and greenstones, showing no contact metamorphism. The contacts are frequently faulted and recessive, while the west edge of the granite is partly defined by the giant quartz vein. Four showings are known, named the JD, T1, Main and DB3 zones (Armstrong 1969a), the last of which could not be located. The isotopic study showed that the T1 and Main Zone mineralisation is 1092 ± 115 Ma old, while the JD mineralisation is probably 535 ± 164 Ma old. The age difference is reflected by marked geological differences and several stages of pitchblende deposition.

The JD Zone U-Cu-Fe-Pb-S-Si-carbonate deposit

The JD showings comprise pitchblende in quartz and calcite veins in a well exposed, trenched and drilled zone some 180 m long and 15 m broad along the east side of the giant quartz vein (Armstrong 1969b). The veins are generally <5 cm thick and trend at approximately 160° and 225°, but are somewhat variable and discontinuous.

The showings are mostly in an unpillowed, locally pyritic, basaltic greenstone unit 14 m wide, faulted against the giant quartz vein to the west, but two trenches were

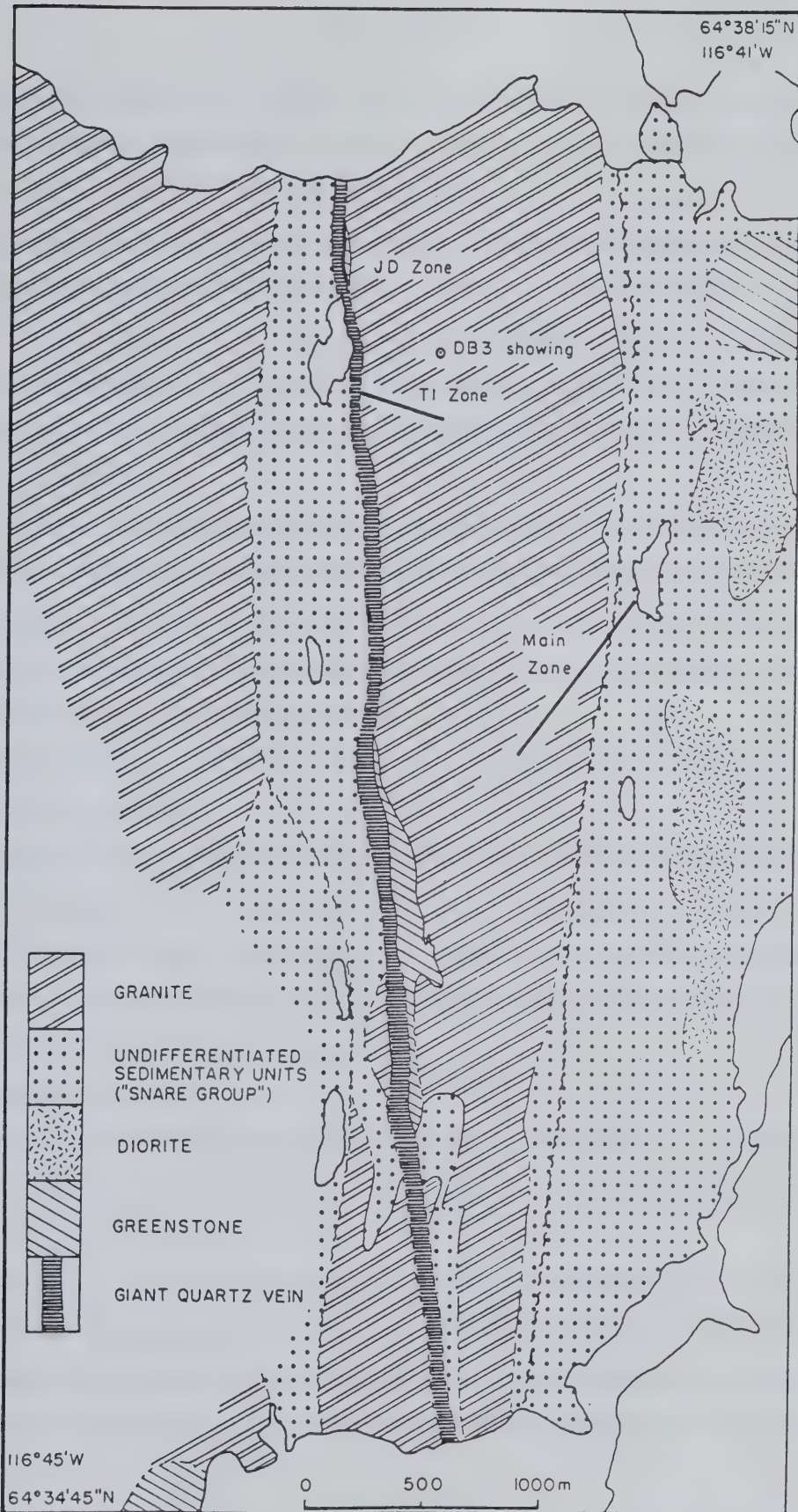


Figure 18: Geology of the JD group of occurrences, extrapolated from the outcrop map of Armstrong (1969a).

blasted into an adjacent red and brown arkose unit, which is 12 m thick and truncated by granite to the east. The greenstone has locally been shattered, reddened and cemented by dark red calcite. Secondary minerals include yellow and brown uranophane, lime green cuprosklodowskite ($\text{Cu}(\text{UO}_2)_2\text{Si}_2\text{O}_7 \cdot 6\text{H}_2\text{O}$), mats of intergrown malachite, brochantite and posnjakite ($\text{Cu}_4\text{SO}_4(\text{OH})_6 \cdot \text{H}_2\text{O}$), and probably azurite (not checked by XRD methods) and possibly billietite ($\text{BaU}_6\text{O}_{19} \cdot 11\text{H}_2\text{O}$) (inconclusive XRD pattern, not checked chemically). Veinlets and impregnations of pyrite, chalcopyrite, fluorite and quartz with up to 1% chalcopyrite occur in the country rocks, and minor fluorite is widely distributed (Armstrong 1969a).

Veins of pitchblende up to 1 cm wide occur within quartz–carbonate veins up to 5 cm thick in the greenstone. Pitchblende also occurs as veinlets in the greenstone, in the calcite cement of brecciated greenstone, and as brecciated fragments within quartz veins. The paragenetic sequence involves two similar cycles of quartz, calcite and pitchblende deposition, the second including sulphides:

- (1) Deposition of low reflectance pitchblende. Brecciated carbonate recemented with quartz may be of this age.
- (2) Brecciation of early pitchblende. Deposition of high reflectance pitchblende containing up to 25% isolated quartz euhedra, up to 25% chalcopyrite, up to 10% galena, and calcite and minor bornite. This UO_2 may form rare subhedral uraninite rhombs. Quartz veins containing chalcopyrite, pyrite, galena and traces of bornite may be of this age.
- (3) Deposition of calcite, chalcopyrite, galena.
- (4) Deposition of calcite.
- (5) Red and white quartz veins emplaced, containing calcite in vugs. Possible coffinite rims locally formed around pitchblende. Veining of pitchblende with remobilised galena.

The wall rocks are hematized and strongly silicified, and contain traces of fine-grained chalcopyrite and aggregates of TiO_2 . The early pitchblende phase, and possibly the later, also impregnated the wall rocks. The bornite contains exsolved plates of chalcopyrite and is rimmed with secondary covellite. The calcite was identified by staining methods.

The T1 Zone U-Fe-Pb-S-Si deposit

The T1 Zone is a breccia-vein system in the granite east of the JD occurrence, with orientations ranging from 122°/66°S to 098°/68°S (strike and dip). Radioactivity is not continuous along the moderately exposed 90 m strike, and Armstrong (1969a) described the zone as a group of en echelon veins up to 20 m long. Despite being highly radioactive, most trenches showed no pitchblende and only traces of yellow secondary uranium minerals, including boltwoodite ($K_2(UO_2)_2(SiO_3)_2(OH)_2 \cdot 5H_2O$). Grades nevertheless reached 1.44% U_3O_8 over 30 cm (Armstrong 1969a). The zone consists of some 30 cm of brecciated granite cemented by a fine-grained black mosaic of untwinned alkali feldspar; staining tests to identify this feldspar were inconclusive. Minor fine-grained chlorite, muscovite, leucoxene, pyrite and uraninite occur in the feldspar mosaic, which is also cut by white quartz veins up to 20 cm thick. Coarse euhedral pyrite occurs within the feldspar mosaic and the quartz veins. The zone may have a 50 cm halo of minor chloritic alteration and pyritic impregnation of the granite, and episyenitic patches are common in the nearby granite (discussed later).

The uranium mineralisation is confined to the black vein matrix. Up to 5% euhedral pyrite, often with euhedral but unoriented pyrite overgrowths, is accompanied in the feldspar mosaic by up to 3% uraninite forming aggregates of rhombic crystals, 10–20 micrometres in diameter. Very rarely, the pyrite is corroded and replaced by uraninite, which in turn has low-reflectivity rims ascribed to coffinite. Pyrite also forms a later generation of much smaller grains, <10 micrometres in diameter, and a sulphide (perhaps pyrite or galena) occurs as barely resolved plates in the uraninite, 0.1 to 4.0 micrometres long. Some patches of galena up to 70 micrometres across were noted. All the brecciation and mineralisation appears to have been essentially synchronous, and chips of the black matrix were used for the U-Pb isotopic analyses.

The Main Zone U-Fe-Cu-Pb-S-Si deposit

The Main Zone is a fracture some 500 m long, oriented 041°/66°–79° N (strike and dip) and flanked by radioactive zones of altered, sometimes greyish, granite. The north end of the zone is the most radioactive, where the best trench assay was 0.42% U_3O_8 over 40 cm, and drilling intersected up to 0.174% U_3O_8 over 60 cm (Armstrong

1969a). This deposit was not studied in detail; the exposure is only fair, except in pits and trenches. A cross section shows:

25 cm of grey-brown cherty quartz, radioactivity = 3400 cps.

5 cm of silicified breccia, radioactivity = 7700 cps.

30 cm of reddish silicified granite, radioactivity = 7500 cps (one chip used for U-Pb isotopic analysis).

50 cm of red and black altered granite, radioactivity = 1600 cps.

Fresh granite, radioactivity = 1000 cps.

The scintillometer readings were taken *in situ*, and thus the stated radioactivity is only a guide. The exact source of radioactivity was unclear in this case, although some conspicuous yellow uranium secondary minerals occur in cracks in parts of the zone. Some dark granitic breccias were noted, similar to those of the T1 Zone. Accessory chalcopyrite, pyrite, galena and fluorite have been reported (Armstrong 1969a).

The episyenite

This is a brick-red variety of the granite, ranging from diffuse patches to sharp-edged, dyke-like masses, well exposed in the vicinity of the unlocated DB3 occurrence (Plates 4, 5). It is not obviously directly related to uranium mineralisation. The unaltered granite is composed of approximately 53% microperthitic orthoclase, 35% quartz, 9% albite/oligoclase (optically determined), 3% chlorite (after biotite) and a trace of zircon. The feldspars are dusted with hematite, and the plagioclase is slightly sericitised. The quartz has several fine fracture cleavages, crossing grain boundaries, and conspicuous Bohm lamellae. The episyenite is similar but darker red due to hematitic microfractures, finer grained, and contains only some 10% quartz, as veinlets and recrystallised mosaics. There is no visible sign of alkali metasomatism. The episyenite also has small cataclastic patches containing fine-grained muscovite and chlorite, and minor muscovite occurs interstitially. The episyenite contains 62 ppm Th and 9.2 ppm U, compared to the granite, which contains 47 ppm Th and 4 ppm U.

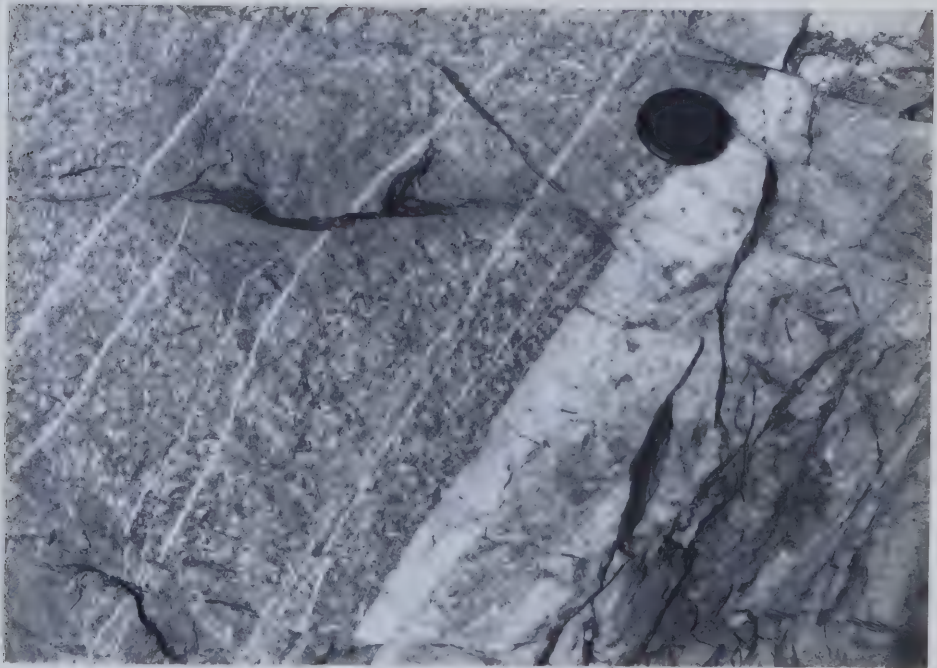
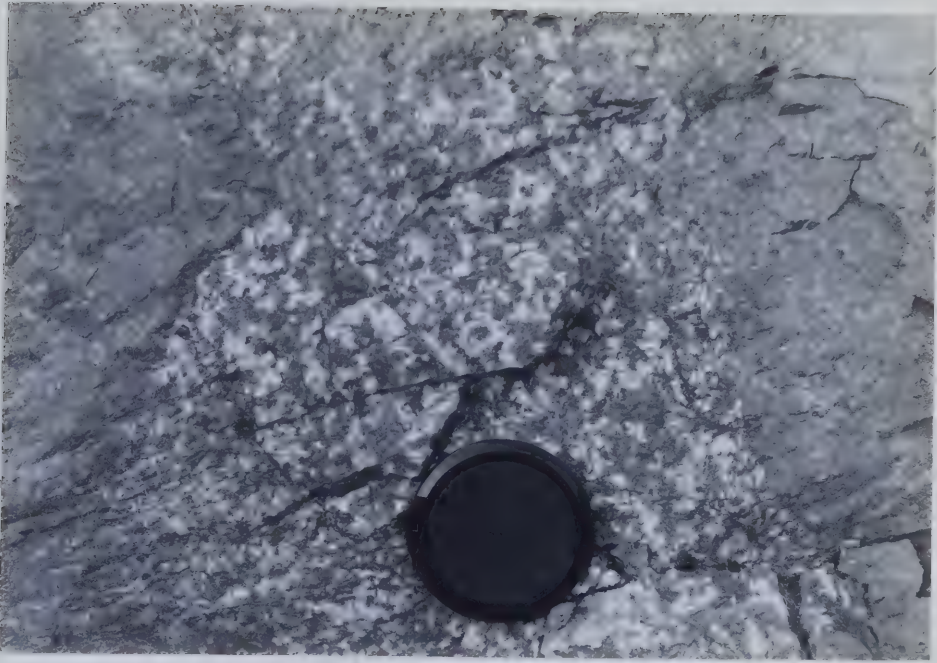


Plate 4 (top): Fine-grained red episyenite, produced from the desilicification of coarse red granite, T1 Zone deposit.

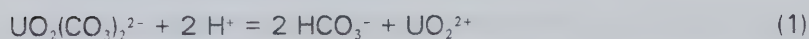
Plate 5: Fine-grained red episyenite patch in the coarse red granite at the T1 Zone deposit.

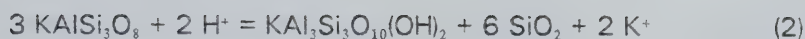
Discussion of the JD deposit group

Episyenites are associated with vein uranium deposits in some French granites of the Massif Central. Cuney (1978) described a vuggy episyenitic assemblage of microcline-perthite, albite, chlorite, calcite, zircon and apatite from the Bois Noirs biotite granite, and a fine-grained, late-stage granite similar to the JD episyenite except for the replacement of orthoclase by microcline. The Bois Noirs-Limouzat veins contain quartz, pitchblende, hematite, pyrite, marcasite, carbonates, minor sulphides and arsenides and late fluorite. The fine-grained granite at Bois Noirs is the most uraniferous variety (8–11 ppm), but contains the least thorium (27–32 ppm). Cuney suggested that:

- (1) Deuteric alteration of the granite released uranium from biotite and accessory minerals and concentrated it as uraninite in the silicates.
- (2) Later hydrothermal activity dissolved the uraninite as the uranyl monocarbonate complex, $\text{UO}_2(\text{CO}_3)^0$, and re-precipitated it as pitchblende in porous breccia zones, using reduced sulphur species in the solution as reductants at a temperature of 77°–100°C. As discussed (p. 30), this reduction mechanism is regarded as improbable.

Leroy (1978), describing deposits from the biotite-muscovite St-Sylvestre granite, suggested that mica-episyenitisation (= muscovitisation and desilicification), lamprophyre intrusion and pitchblende deposition occurred simultaneously, some 60 Ma after the emplacement of the granite. This granite contains 20–22 ppm uranium and 23–31 ppm Th. Earlier feldspar episyenites of chloritised biotite, perthitic orthoclase and new microcline, albite and adularia were produced from the granite along shear zones. The mineralised veins are breccias containing spherulitic pitchblende, pyrite and hematitic quartz as the earliest phases, cemented by fine-grained phyllosilicates and "black oxides" (Leroy *op. cit.*). Fluorite, barite, carbonate, sphalerite, galena, marcasite and hematite were subsequently deposited. Similar mineralisation also occurs as disseminations within the mica episyenites. Leroy suggested that mica episyenitisation is a simple hydrothermal alteration caused by circulating, heated ground-water, and that mineralisation involved the reactions:





(K-feldspar + H⁺ = muscovite + quartz + K⁺)

No pH buffer was suggested for these reactions, which took place at about 345°C during CO₂ loss by boiling. After cooling to below 135°C, pitchblende was altered to coffinite, and fluorite, barite and calcite were deposited.

The following points should be noted in comparing the JD and the Massif Central deposits:

- (1) Muscovite was not generally produced in the JD claims area.
- (2) The Main and T1 Zone deposits were formed at least 700 Ma after the granite was emplaced, and the JD Zone deposits even later.
- (3) The T1 Zone contains euhedral uraninite, not pitchblende.

A speculative history of the JD group can be suggested, albeit based on insufficient data. Note that stages 2–4 may have been essentially synchronous:

- (1) The original granite possibly assimilated meta-arkoses and uraniferous meta-placers of the paragneiss belt (p. 10, p. 103 *et seq.*). The granite contains 47 ppm Th but only 4 ppm U, with Th/U = 11.7, suggesting that uranium has been lost since emplacement.
- (2) Late-stage episyenitisation either released and reconcentrated the uranium, or involved uraniferous late-stage fluids. The episyenite contains 9.2 ppm uranium and 62 ppm Th, Th/U = 6.7.
- (3) Movement along the Wopmay Fault induced splay faults by some 1850 Ma.
- (4) The Mackenzie diabase event hydrothermally remobilised uranium, perhaps as fluoride or carbonate complexes, into splay faults of the T1 and Main Zones, locally remobilising thorogenic ²⁰⁸Pb from the paragneiss meta-placers (Miller 1982). Traces of wall-rock ferrous silicates may have acted as reductants, although hematite is now insignificant. The pH may have been buffered if required by the reverse of reaction (2) above, *i.e.* the feldspathisation of micas, and the episyenitisation and uranium mineralisation may have been coeval.
- (5) During a marine transgression and regression in at least the western part of the batholith, uranium (as uranyl carbonate) and considerable radiogenic lead were again remobilised at least twice, the uranium being precipitated in the JD Zone by ferrous iron

in the fractured greenstones, now hematized. The carbonate ligands were precipitated as calcite.

Somewhat different examples of alkali metasomatism associated with uranium mineralisation are the Rayrock mine and the Mazenod Lake deposits (*q.v.*).

J. Hottah Lake

The south-east shore of Hottah Lake was intensively prospected between 1950 and 1955. It is underlain by granite (units 5c and 5d) and intrusive dacite to rhyodacite porphyry (unit 4) of the Great Bear Batholith, and in the north by granodiorite (unit 1) of the "exotic terrain" (p. 11; McGlynn 1979). Faults and diabase dykes define a strong north-easterly grain to the area (Fig. 19).

The JB, LOIS, PITCH 8–10 and PITCH 27–28 claim groups were seen. The JB group was reported to be mineralised by radioactive quartz–carbonate stringers with pyrite, chalcopyrite and hematite, along the contact of diabase in granite, according to press reports (*News of the North*, 10 October 1952). No sign of radioactivity now remains along the contact or in the trenches. The LOIS group also appeared to be barren after a brief inspection, although Day (1950) stated that quartz–hematite–pitchblende mineralisation occurred at the sheared contacts of a giant quartz vein and unit 4 porphyry. Quite probably both sites contained isolated pockets of mineralisation that were completely removed during trenching and bulk sampling operations, a frequent occurrence in the area (R. Folinsbee, pers. comm.).

The PITCH 8-10 U-Cu-Fe-Bi-Pb-Ag-S-Se-Si-carbonate deposits

(M) (118°23'W, 64°48'20"N)

An unsuccessful mine was operated on these claims by Indore Gold Mines Ltd. from 1950 to 1956 (McGlynn 1971). The adit and first level were accessible in 1980, but the shaft and second level were choked with ice. Pitchblende mineralisation occurs along both contacts of a diabase dyke, 5 m wide and striking approximately north through unit 5c granite for 200 m (Lang 1951). Two smaller parallel dykes to the east in the adit portal are not mineralised, while a fourth dyke some 50 m to the west, stated by press reports to be mineralised, was not examined. Traces of yellow uranium secondary

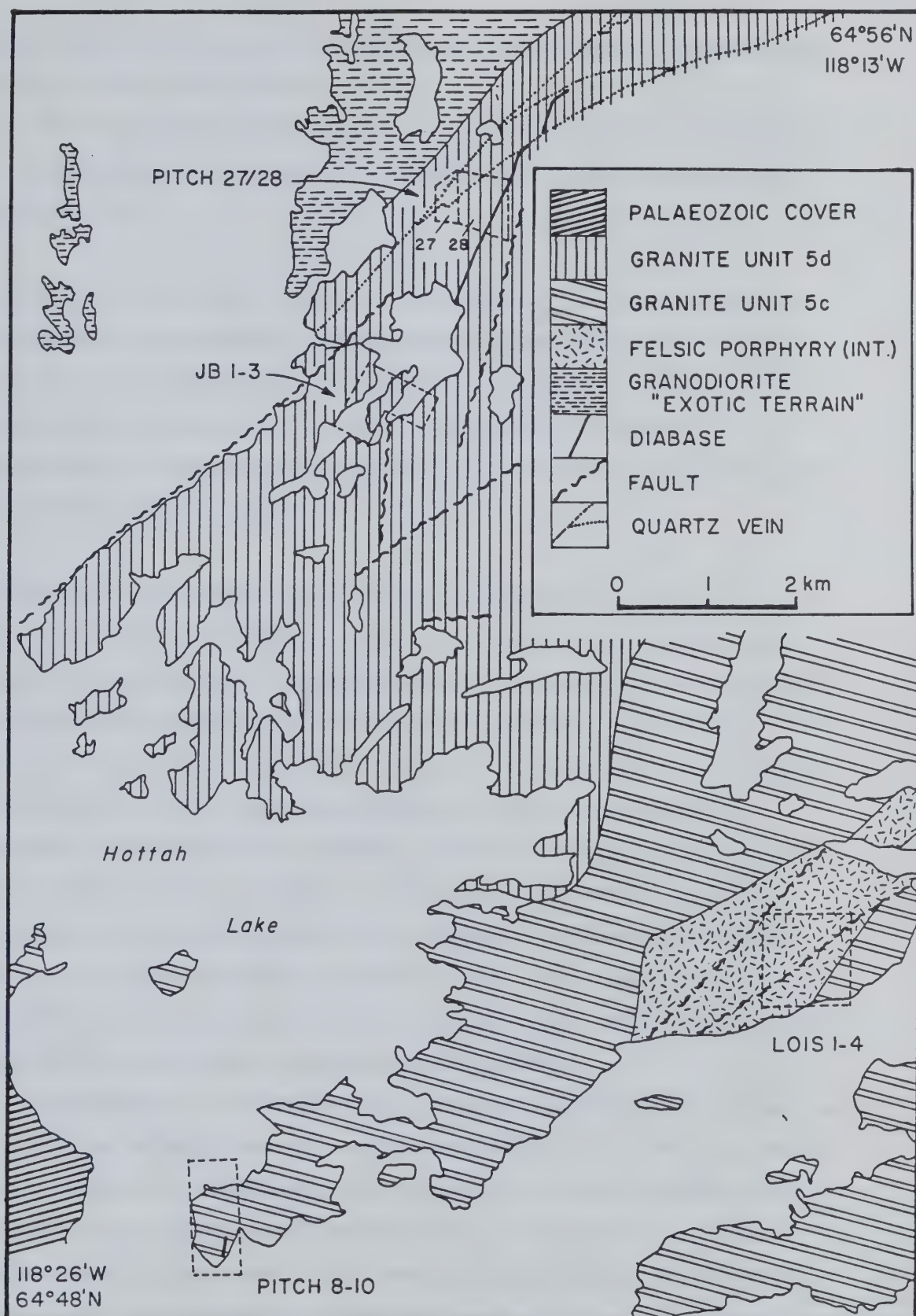


Figure 19: Location and geology of the PITCH 8-10, PITCH 27-28, JB and LOIS claims, Hottah Lake. Many of the faults have quartz stockworks in them. Geology after Smith (1955) and McGlynn (1979), nomenclature after McGlynn (*op. cit.*).

minerals occur in the adjacent granite, which also contains numerous barren quartz veins striking 016° , 025° , 036° and 045° .

The pitchblende is hosted by quartz–carbonate veins up to 30 cm thick along the dyke contacts and in fractures peeling into the dyke. The paragenetic sequence of mineralisation is:

- (1) Deposition of coarse white quartz and minor specularite, followed by cherty quartz.
- (2) Veining and slight replacement of the quartz with dolomite; deposition of dolomite, pitchblende, minor hematite, Cu–Fe–S minerals and minor Bi–Pb–Ag–S–Se minerals.
- (3) Minor late-stage deposition of Cu–Pb–Bi–S minerals and carbonate.
- (4) Emplacement of blebs and veins of marcasite, up to 1 mm thick. Possibly late quartz veins and hematitic red carbonate.

The pitchblende, which contains minor Fe and Si, was deposited variously as veins of botryoids some 10 micrometres in diameter, as subhedral uraninite, in small massive lenses, or along crystal planes in the dolomite (Plate 6). Chalcopyrite was coprecipitated with the pitchblende in blebs some 10 micrometres in diameter, locally with minor galena, bornite, pyrite and primary covellite. Syneresis cracks in the pitchblende contain dolomite and the stage (3) minerals, which include bornite, chalcopyrite and at least three unidentified Cu–Pb–Bi and Cu–Bi sulphosalts. Within the dolomite are traces of several minerals in grains up to 5 micrometres in diameter; qualitative electron microprobe analyses showed phases containing Pb + Se (clausthalite?), Bi + S (bismuthinite?) and Ag + Bi + Se (+ S?) (bohdanowiczite, AgBiSe_2 ?), and others are probably present. Repeated movement during mineralisation brecciated the veins, and post-mineralisation movement has produced minor gouge and chloritic fractures.

The plagioclase in the diabase has been strongly carbonatised and sericitised, and the original ferromagnesian minerals are altered to chlorite, fibrous tremolite–actinolite, hematite and rutile; minor apatite is unaltered. Veinlets of carbonate + epidote cut the dyke. This was the most intense hydrothermal wall–rock alteration found in diabases during the field work, and is similar to that described from the Echo Bay sheet (p. 62). The greenschist–type assemblage suggests a temperature of some 300°C or more

(Winkler 1979). The deposition of dolomite indicates that uranyl carbonate complexes transported the uranium, and that magnesium was available for chloritisation reactions. Barton and Skinner (1979, p. 351) indicate that hematite + pyrite is a univariant assemblage at 250° and $p\text{H}_2\text{O} = 40$ bars, buffering the fluid chemistry within the ranges:

$$\log a\text{S}_2 = -8.5 \text{ to } -11.5$$

$$\log a\text{O}_2 = -31.0 \text{ to } -34.5$$

$$\text{pH} = 3 \text{ to } 6.5$$

These conditions are confirmed by the presence of chalcopyrite rather than pyrite + bornite (Barton and Skinner, *op. cit.*). The pitchblende was probably precipitated by the general mechanism:



Isotopic studies show the age of pitchblende mineralisation to be 440 ± 57 Ma. There is no evidence for igneous activity younger than the Franklin event some 650 Ma ago, nor for significant depths of burial, so that the temperatures indicated are somewhat surprising. The age of the dykes is not known.

The PITCH 27-28 U-Mo-Bi-Pb-Cu-Zn-REE-S-Te-Si deposit

(N) (118°19'30"W, 64°54'50"N)

The claims overlie granite of unit 5d, immediately south of unit 1 of the exotic terrain as mapped by McGlynn (1979). The local geology is complex, with north-east trending quartz veins and diabase dykes cutting units of "massive granite and pegmatite", "older granite and migmatite" and "metamorphic rocks, mostly volcanic" (Smith 1955; McGlynn 1971), a description similar to that of unit 1 (McGlynn 1979). The immediate host rock in claim PITCH 27 is a slightly foliated, micrographic leucogranite with chlorite clots about 1 cm in diameter.

Pitchblende mineralisation in the PITCH 27 claim occurs for some 200 m along a quartz vein, oriented 034°/65°E (strike and dip). The vein is one of a large group, but the complex lacks the great widths and intense silicification associated with giant quartz veins. The vein typically comprises 150 cm of chloritised granite, 15 cm of grey-brown

cherty quartz with pitchblende, 10 cm of sheared granite and 10 cm of white vein quartz containing chlorite and epidote. The chloritisation ranges from heavy veining to either total replacement of the granite or cavity infilling, but hematite is notably lacking.

Uranophane and beta-uranophane occur along fractures.

The grey-brown cherty quartz has been brecciated, and the fragments coated with botryoidal pitchblende, which may cement the breccia into veins several centimetres thick. The pitchblende comprises two intergrown optical varieties, too fine-grained for adequate resolution by the electron microprobe, although qualitative analyses suggest that one phase is rich in Y, together with other rare earths. Some pitchblende patches contain up to 20% fine-grained, coeval molybdenite, while others without molybdenite contain traces of fine-grained Te metal containing minor S, a Bi + Te phase (possibly with minor Pb and/or S), galena, chalcopyrite and coarser grains of sphalerite (Plate 7). Minor chlorite and uranyl minerals developed around the clasts before being cut by late stage white quartz veinlets.

This deposit is hydrothermal, but the nature of the uranyl complex and the reducing agent is not known. The chloritised zone adjacent to the pitchblende-quartz vein is probably either a reactant or a product of the pitchblende deposition mechanism. Only two samples were analysed isotopically; they yield a two-datum $^{207}\text{Pb}/^{206}\text{Pb}$ "isochron" age of 1444 Ma, and a two-datum U-Pb discordia age of 1546 Ma, and a value of 1450 ± 150 Ma probably brackets the true age.

K. The Beaverlodge Lake U-Fe-Si(-Bi-S) deposits

(P) (118°10'W, 64°44'N)

Beaverlodge Lake is a southern extension of Hottah Lake, the two being separated by a north-east trending ridge of volcano-sedimentary rocks 200 m high (Fig. 20). The ridge is a roof pendant, some 16 km long, intruded by granite unit 5c to the north and granite unit 5e to the south, and it will be referred to herein as part of the Snare Group, although McGlynn (1979) could not correlate this sequence with any other. The central sector of the belt contains uranium mineralisation and was the target of unsuccessful mining ventures in 1956 and the early 1930s (Baykal 1967a; McGlynn 1971; Thorpe 1972). Henderson (1949) thoroughly mapped and surveyed the ridge, and his

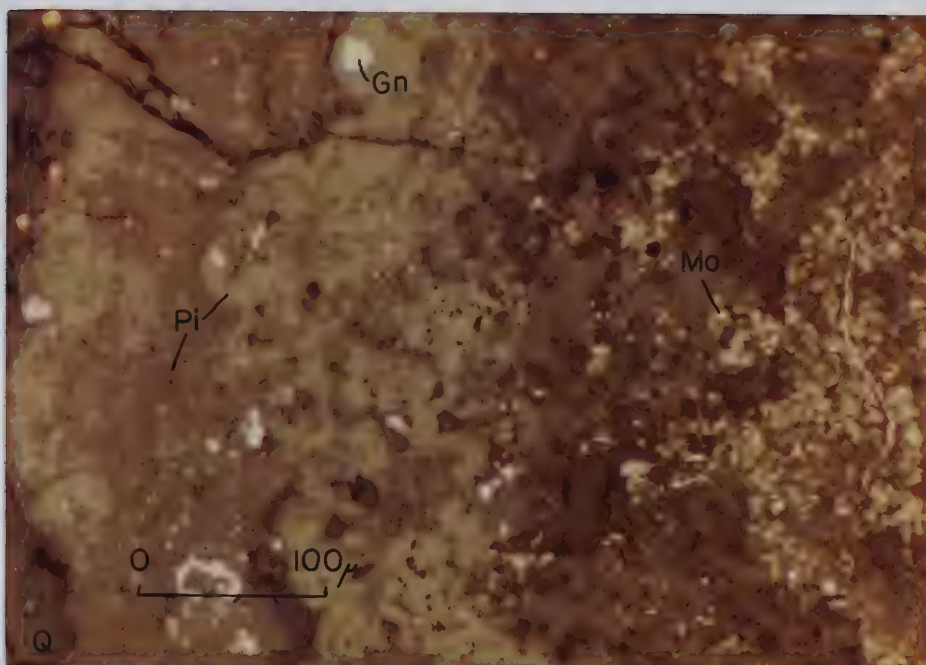
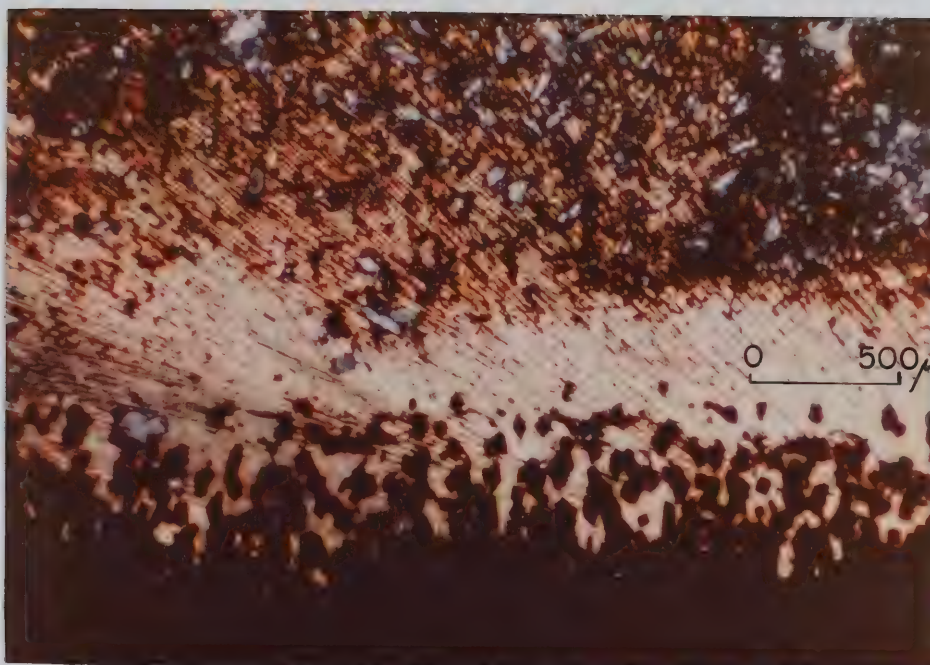


Plate 6 (top): Pitchblende (bottom, black) in a dolomite matrix from the veins at the PITCH 8–10 occurrence, transmitted light, X-polars. The material following crystal planes in the dolomite is pitchblende \pm hematite, but in detail in reflected light appears to be somewhat replacive or intrusive. Some quartz is present.

Plate 7: Molybdenite flakes (white, right) in botryoidal pitchblende (pale grey) hosted by quartz (brown), PITCH 27–28 deposit; reflected plane polarised light, x16 objective, in air. A few larger grains of galena (white) are present.

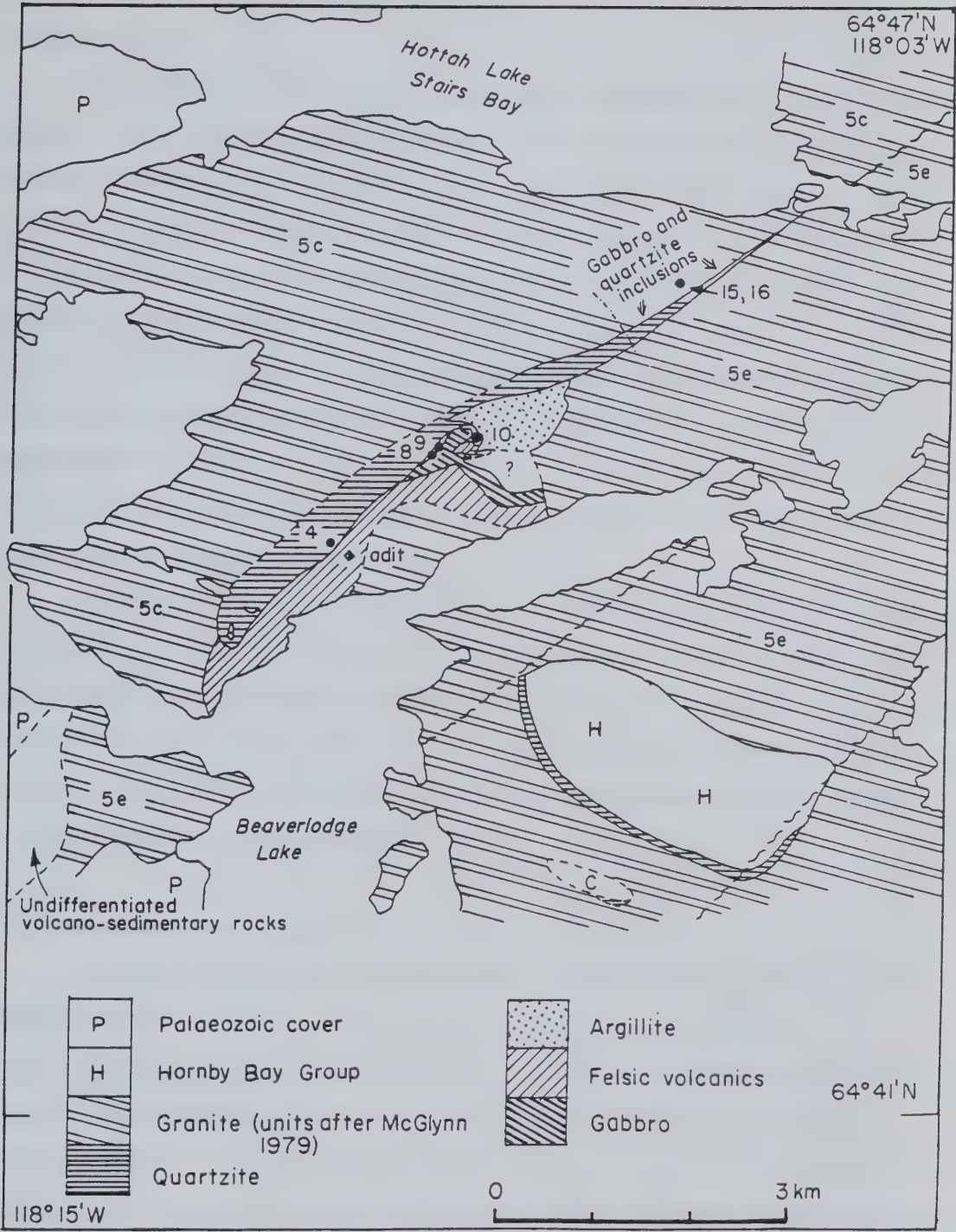


Figure 20: Geology of the Beaverlodge Lake pitchblende occurrences, numbered after Henderson (1949). Geology after Henderson (1949), Baykal (1967a) and McGlynn (1979).

nomenclature will be followed. Some 2 km to the south east is a small quartzite outlier, correlated with the Hornby Bay Group, which also contains uranium mineralisation (McGlynn 1979).

The belt of Snare Group rocks has an upper resistant unit of at least 130 m of quartzite, white or pink in outcrop but green in the mine dumps, divided by a central green argillite which may represent a lateral facies change. The quartzite has a mosaic texture, with minor white mica outlining the grains. These units unconformably overlie locally absent dacitic flows and ignimbrites, which in turn overlie at least 150 m of feldspar and quartz-feldspar porphyry, extrusive at least in part (Henderson 1949); these units are not distinguished on Figure 20. Rusty-weathering, dark green gabbros occur in the Snare Group, and as probable xenoliths in the northern granites. Baykal (1967a) interpreted the quartzite-dacite unconformity as a thrust, but this is clearly not the case (Plate 8). Some folding is evident in the belt, particularly as chevron folds in the argillite unit, the axes plunging 40° towards 055°.

Henderson (1949) described 38 uranium occurrences in the belt, in two distinct geological environments. Showings #2-#10 occur within the quartzite, usually at its lower contact, and showings #1 and #11-#36 are hosted within gabbro xenolithic sheets in the northern granite, too small to show on Figure 20. Showings #37-#38, which are radioactive veinlets in the granite, are assigned to the second group. Baykal (1967a) located several more minor showings.

The quartzite-hosted deposits

Showings #2-#4 and #8-#10 were seen, while #5-#7 could not be located. Showings #2-#4 cover the vertical shaft and four adjacent pits, where pitchblende-hematite blast debris was found but no *in situ* mineralisation apart from traces of green metatorbernite in one pit. Showing #8 is particularly interesting, occurring at the unconformity where a pinnacle of porphyry, 5 m wide at the base, projects upwards 10 m into the quartzite. Showing #9 is insignificant, although possibly misidentified. Showing #10 comprises three trenches and a pit in argillite, quartzite and conglomerate, cut by a quartz stockwork and a decomposed limonitic band, some 70 m stratigraphically above the unconformity.

The host quartzite in these showings is typically a hematized grit. In mineralized samples, the quartz grains have been intensely brecciated and healed, the secondary fluid inclusions containing some 20% vapour but no visible liquid CO_2 , and strain lamellae are strongly developed. Recrystallisation occurred after the emplacement of quartz veinlets, followed by partial to complete replacement by chlorite and minor muscovite. The quartz veining and silicification has completely destroyed the original textures in most cases. In the mineralisation from showings #2–#4 and #8, the chlorite is replaced by massive fine-grained hematite and pitchblende, either simultaneously in laminated botryoids, or alternately. Some blebs of pitchblende occur between the quartz grains, and hematite selectively replaces quartz grain boundaries (Plate 9). A trace of marcasite and bismuthinite occurred in the mineralisation at showing #10, where the pitchblende forms gangue-free veinlets of pitchblende some 3 mm thick: the paragenetic sequence at #10 is not clear. A trace of barite was tentatively identified in a thin section from slightly radioactive quartzite (Baykal's showing #4).

The gabbro-hosted deposits

Showings #15 and #16 were examined, and several adjacent occurrences appeared to be essentially similar in nature. The #15 site is marked by a 12 m long trench along a quartz vein, 5–20 cm thick, cutting a large irregular body of gabbro. The quartz vein is locally cherty, cut by coarser quartz veins with specularite, then partly replaced by hematite and finally cut by fine pitchblende–hematite veinlets. The host gabbro contains some 7% specularite, and resembles the altered dyke at the PITCH 8–10 mine in hand specimen (p. 84). This specularite does not have the skeletal or trellis form typical of oxidised ilmenite or magnetite. The #16 site is more typical of the group, comprising traces of secondary uranyl minerals in fractures in a quartz veinlet in the gabbro.

The adit

The adit is completely choked with ice, but samples were collected from the dump. Vuggy chloritic and silicified quartzite containing small pitchblende blebs is similar to the quartzite-hosted deposits in the outcrops, but the pitchblende has lost most of its lead and yields extremely discordant U–Pb ages (the B5 samples in Miller 1982). Vugs in

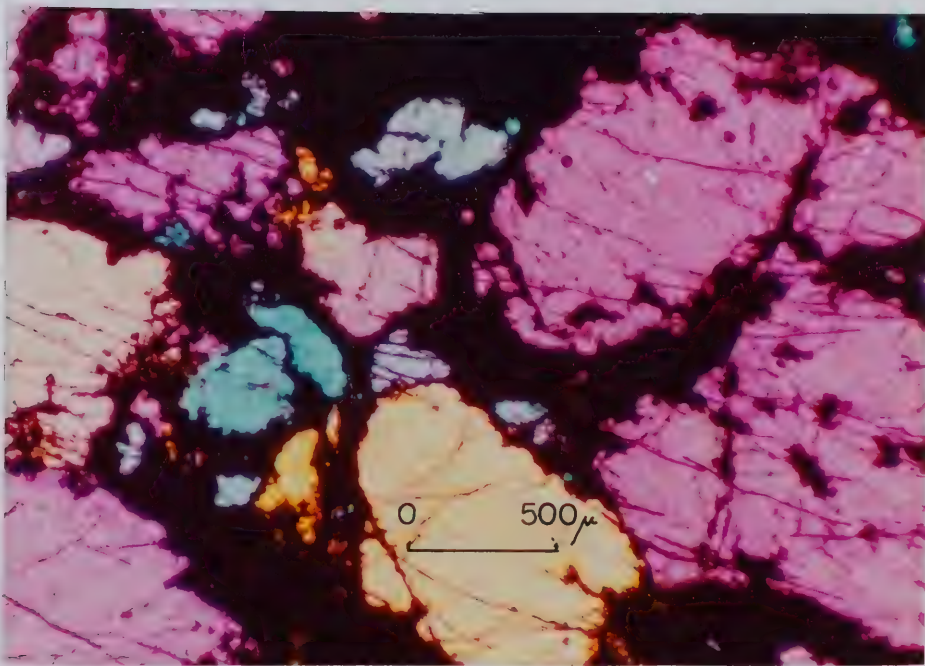
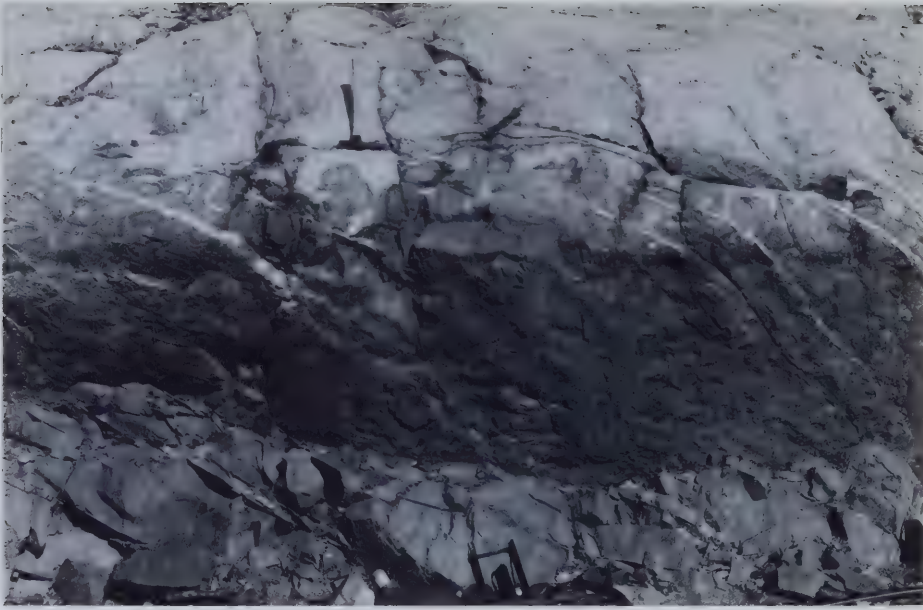


Plate 8 (top): The unconformity beneath the quartzite at Beaverlodge Lake, general stratigraphic position of many of the showings. Baykal (1967a) places a thrust fault here, with the quartzite *o/der* than the underlying volcanic porphyry, but note the basal conglomerate of porphyry boulders. Photograph from 5m west of shaft.

Plate 9: Pitchblende-hematite mineralisation in quartzite from Beaverlodge Lake, transmitted light, x2.5 objective, X-polars; sensitive-tint plate used to enhance contrast of opaque phases. Hematite + pitchblende occurs interstitially, and also forms sub-parallel veinlets cutting the quartz grains.

pieces of coarse quartz veins have interstitial blebs of framboidal and cubic pyrite, a yellowish clay of muscovite and an unidentifiable component, and spectacular doubly-terminated quartz crystals. Another mineralised sample is composed of friable earthy hematite, calcite and minor quartz, containing blebs of marcasite, pyrite and galena, some diffuse and unidentifiable uranium mineralisation, and some grains, possibly allanite, composed of U, Ca, Si, Fe and Al, and hosted by the calcite. One piece of slickensided coarse vein calcite was observed.

Discussion of the Beaverlodge Lake deposits

All of these deposits are hydrothermal, and there is sufficient similarity between them to imply a common origin; only the vein pitchblende at showing #10 was significantly different mineralogically. The bimineralic pitchblende + hematite assemblage, together with the almost complete absence of carbonate, distinguishes this group of deposits. The hematite indicates that ferrous iron was the probable reducing agent; the gabbro is the obvious source of ferrous iron for some deposits, and probably chlorite or a precursor ferrous silicate was the source in the quartzite-hosted occurrences. There is no evidence for the species of uranyl complexes involved.

All the hematite-pitchblende mineralisation had crusts of secondary uranyl minerals, which were similar throughout the area. The identified minerals were dark yellow schoepite (common), yellow billietite and becquerelite, yellow rutherfordine and yellow to brownish uranophane, in addition to the metatorbernite at showings #2-#4.

The pitchblende-hematite mineralisation, or "pitchblende-hematite fels", gives isotopic data open to two interpretations, but indicating a date of 2058 ± 34 Ma. This may be either its true age, and thus the minimum age of the Snare Group, or the age of a precursor source of radiogenic lead (and, by inference, of uranium). The material also records a much younger event some 440 ± 57 Ma old. This may either be the mineralisation age or a time of remobilisation and lead loss for the material. 440 Ma is the mineralisation age defined by all the vein pitchblende samples from the PITCH 8-10 claims and showing #10, and the pitchblende from the adit dump. The high, variable levels of ^{208}Pb in the isotopically analysed samples could have been derived from materials such as the Th-rich heavy-mineral concentrations in sedimentary strata on Bell Island, Hottah

Lake (p. 11, 178; McGlynn (1979) correlated these with the Great Bear Batholith; they are younger than the exotic terrain granodiorite basement, and could be older than the batholith, but are unlikely to be as much as 2058 Ma old).

L. The Mazenod Lake Cu-U-Bi-Cu-Pb-Fe-S-Se-Te(-Ag) deposits

(Q) (116°55'W, 63°45'N)

The SUE and DIANNE claims at Mazenod Lake have some potential as a small copper ore-body, but were originally staked over a strong aerial radiometric anomaly (Geological Survey of Canada, Open File 188, 1974). The claims overlie extensively faulted rhyolitic to dacitic ignimbrites (McGlynn 1979; Climie 1975) (Fig. 21). Some ten groups of so-called "breccia pipes" have been located, reportedly coinciding with major aeromagnetic anomalies (Noranda Mines Ltd. personnel, pers. comm. 1979; GSC aeromagnetic anomaly map 7197 "Marian River", 1969). These pipes exhibit intense brecciation and hematisation and minor silicification, and are well defined by radiometric anomalies of some 2x background, with mineralised sectors reaching 20x background (Climie *op. cit.*). Two pipes on an island in Mazenod Lake were also briefly examined, where tuffs and quartz siltstone with carbonate have been locally brecciated and veined with magnetite (now oxidised to hematite) and schorl, although uranium and copper are apparently absent. One pipe at the Dianne claims was sampled; it is marked by a surrounding quartz stockwork and intense hematisation and brecciation of the ignimbrite.

Fresher samples of the purplish ignimbrite contain devitrified glass shards and fragmental phenocrysts of albite (An_6 , optically determined), untwinned alkali feldspar (probably orthoclase), minor perthitic orthoclase and quartz. The matrix comprises trachytic plagioclase laths in a groundmass of fine-grained albite, white mica and minor chlorite and hematite. Clots of rutile and hematite occur pseudomorphous after magnetite crystals, and the rocks are often magnetic. The albite phenocrysts may be completely altered to white mica. Within the pipes, the ignimbrites are red and contain veins and impregnations of massive hematite, replacing magnetite. The plagioclase phenocrysts are progressively replaced by microcline and minor quartz, or are completely absent; one or two are altered to chess-board albite (Plates 10, 11). The potassium feldspars are turbid but otherwise unaltered. The matrix is altered to fine-grained microcline, probably with a

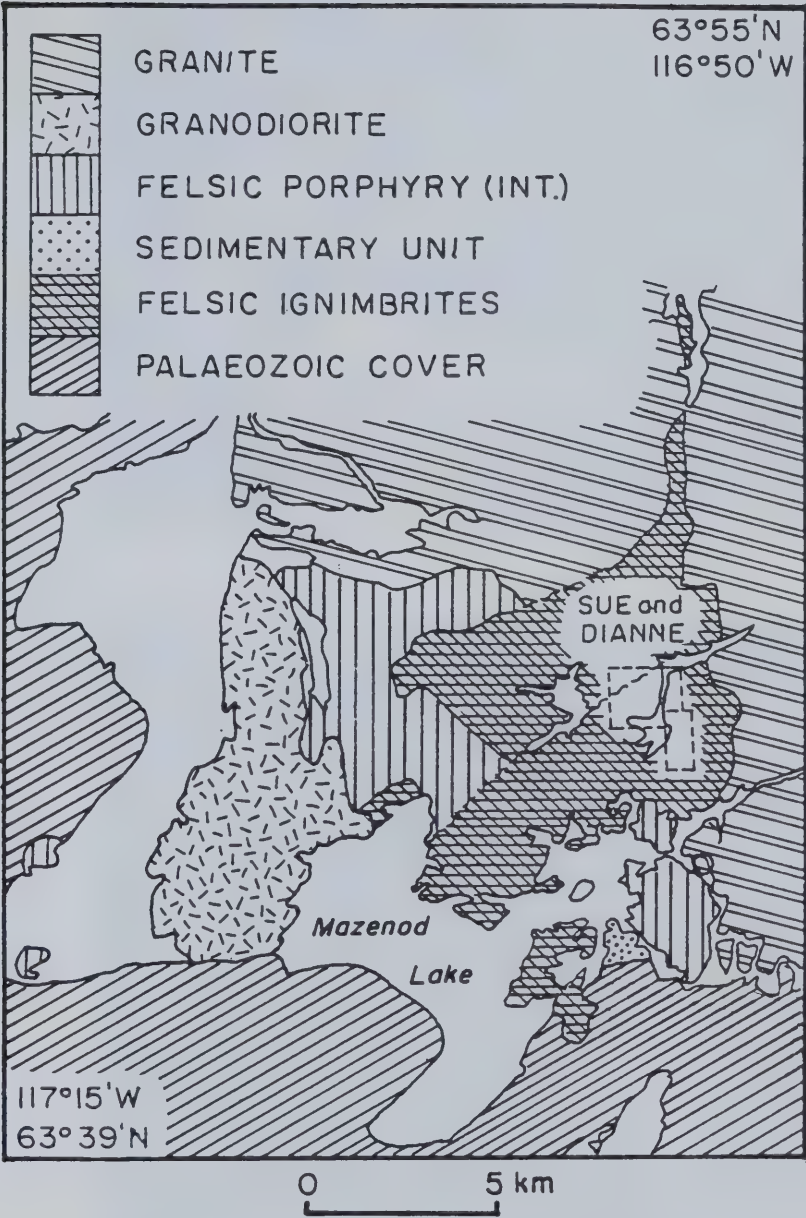


Figure 21: Geology of the Mazenod Lake area (simplified after McGlynn 1979).

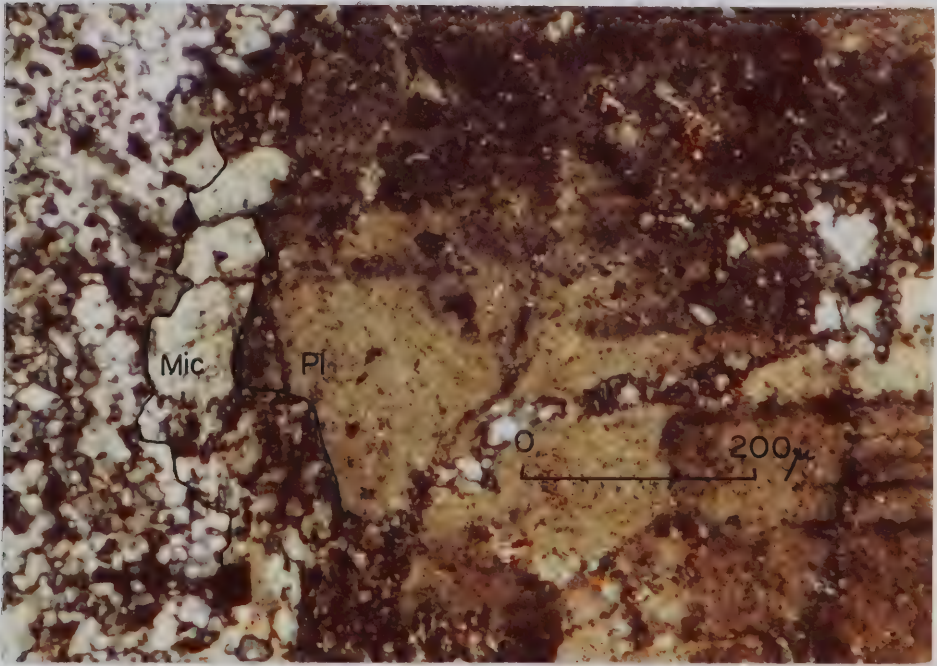
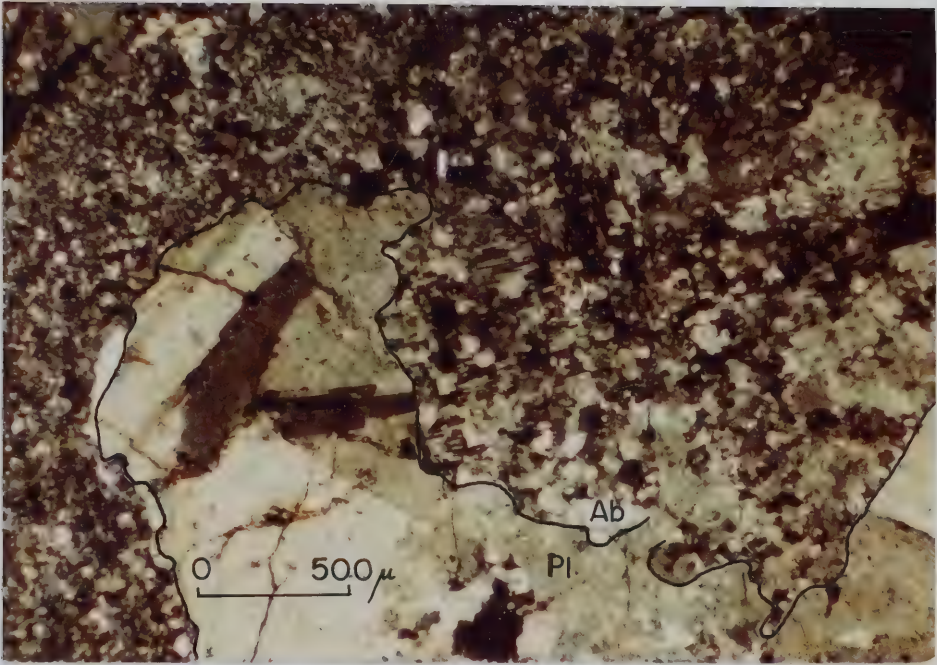


Plate 10 (top): Chess-board albite replacing large polycrystalline plagioclase phenocryst at Mazenod Lake deposit. Transmitted light, x2.5 objective, X-polars.
Plate 11: Plagioclase phenocryst altering around margin to indistinct microcline, Mazenod Lake deposit. Sample matrix is fine-grained microcline. Transmitted light, X10 objective, X-polars.

little albite, or in some cases is partially or completely silicified. This potassium metasomatism was confirmed by staining with sodium cobaltinitrite. White mica is absent, and hematite impregnates and rims each feldspar grain. A few samples contained clinopyroxene grains which have been recrystallised, partially resorbed or formed into veinlets, and which have partially altered to epidote or amphibole + titanite. These samples contain some 10% epidote in the matrix. Carbonate may occur as small patches and veinlets in all the samples, identified qualitatively as ankerite or ferroan dolomite.

Within the sampled pipe, small areas contain green secondary minerals, including brochantite and probably langite ($\text{Cu}(\text{SO}_4)(\text{OH})_6 \cdot 2\text{H}_2\text{O}$) and metatorbernite. Primary uranium mineralisation was found in veinlets up to 7 mm thick, containing brecciated wall rock, pitchblende, hematite and a suite of Bi–Cu–Pb–S–Se–Te minerals. This suite includes tellurobismuthite, kawazulite ($\text{Bi}_2\text{Te}_2\text{Se}$), some unidentified and possibly new Bi minerals, selenian *blaubleibender* covellite, bornite, chalcopyrite and digenite, and was extensively studied. The results have been published separately and form appendix IV (Miller 1981). Traces of silver occur in some of the Bi phases, which have the general formula $\text{Bi}_2(\text{Se}, \text{Te})_3$, where Bi may be replaced by $0.75(\text{Pb} + 2\text{Cu})$. The pitchblende mineralisation was dated at 457 ± 26 Ma.

The paragenetic sequence is:

- (1) Brecciation of pipes; cementation and impregnation with magnetite, locally with tourmaline, hematisation and alkali metasomatism of host rocks. Magnetite oxidised to hematite + rutile; impregnation with hematite, bornite and chalcopyrite \pm covellite.
- (2) Fracturing; breccia coated with hematite; deposition of pitchblende with up to 50% hematite in breccia veins. Deposition of Bi–Cu–Pb–S–Se–Te phases, coeval with and later than pitchblende + hematite, forming up to 20% of the vein, \pm bornite, selenian covellite, digenite, chalcopyrite.
- (3) Emplacement of hematite in fractures.
- (4) Minor calcite deposited.
- (5) Emplacement of quartz veins and stockworks? (based on one observation).

Quartz veins and stockworks surround the pipe (Noranda Mines Ltd. personnel, pers. comm. 1979), but their paragenetic position is not clear. The altered magnetite forms

equidimensional grains of hematite with occasional relict magnetite cores, as compared to lath-like primary hematite, and some samples contained 30% iron oxide. In one instance, the UO_2 occurred as uraninite crystals some 40 micrometres in diameter. The bornite has altered to covellite and exsolved chalcopyrite lamellae. Occasionally the bismuth phases occur interstitially between hematite laths without pitchblende. Minute flecks of native copper occur within the wall rock silicates, where the matrix potassium feldspar grains have also been rimmed with hematite.

It appears that the coeval alkali metasomatism and mineralisation with copper sulphides and iron oxide are not directly related to the subsequent polymetallic veinlets, which follow independent fractures. The possible relationships are either, (1) that alkali metasomatism and the tourmaline, magnetite and copper mineralisation are a metasomatic aureole around unexposed intrusive stocks, and that the polymetallic mineralisation was emplaced later, utilising the brecciated pipes and perhaps involving the magnetite in pitchblende-precipitating reactions; or (2) that the polymetallic veinlets are a late stage of the metasomatism event, which must therefore be younger than, and unrelated to, the original igneous activity. Potassic wall-rock alteration is also a feature of the Echo Bay deposits (p. 64–65). No precise depositional mechanism can be suggested. Alkali metasomatism, altering white mica to feldspar, provides a possible pH buffering reaction (p. 27); a very similar situation occurs at the Rayrock mine deposit, where sodium metasomatism has taken place. The ubiquitous hematite suggests that reduction was probably performed by the magnetite and/or ferrous silicates in the wall-rocks. There is no obvious source of uranium except the ignimbritic host rocks themselves.

M. The Rayrock mine U-Cu-Ni-S-As-Si(-Co-Bi) deposits

(R) (116°32'18"W, 63°26'54"N)

The Rayrock mine was operated in a branch of a giant quartz vein or stockwork in the Marian River Fault from 1957 to 1959 (Lang *et al.* 1959; McGlynn 1968) (Fig. 22). The mine produced approximately 150 tons of uranium from 70,000 tons of ore (Gandhi 1978a; McGlynn 1971). The fault strikes north-east and dips steeply to the south-east with perhaps 10 km of dextral offset, and has short parallel or east-striking subsidiary faults (McGlynn 1971). It cuts granodiorites of the Great Bear Batholith, locally gneissic and porphyroblastic, and roof pendants of Snare Group dolostones, skarns and quartzites (McGlynn *op. cit.*). Pitchblende showings in the stockwork and the silicified wall rocks occur for at least 20 km along strike, while the stockwork extends for at least 30 km and the structure extends geomagnetically for at least 75 km southwest of the Wopmay Fault (GSC aeromagnetic anomaly map 7197 "Marian River", 1969). Numerous claim groups have been staked for uranium, one for cobaltite (the TT group – McGlynn 1971) and one for Co-Bi (the CAB group – Thorpe 1972).

A north-west trending belt of Snare Group metasedimentary rocks and gneissic granodiorite north of the fault is juxtaposed against gneissic granodiorite to the south at the mine (McGlynn 1971). The quartz stockwork weathers white or red and hosts a breccia of red-weathering country rocks, whose fresh colours depend on the hematite : epidote ratio (Lang *et al.* 1959). Drilling records of Rayrock Mines Ltd. (from DIAND records) describe radioactive, reddened fractures in "the injected quartz-ferromagnesian zone". These records also refer to fine-grained diorite intrusions, which were sometimes chloritised or contained "granitic remnants", and were variably hematized. A blueish hydrothermal chlorite in vuggy quartz from the mine waste was identified as probable clinocllore by X-ray diffraction and optical study.

The "gneissic granodiorite" unit was granitic where sampled, containing plagioclase, microcline, quartz and chloritised biotite and minor hematite. The plagioclase is strongly altered to white mica and was not determined. Veinlets of carbonate and epidote cut the rock, which has a recrystallised cataclastic texture. The Snare Group rocks are pink, grey or green, poorly-foliated metasediments, with grains some 50 to 200 micrometres in diameter, and occur as xenoliths in the granodiorite. The lithologies

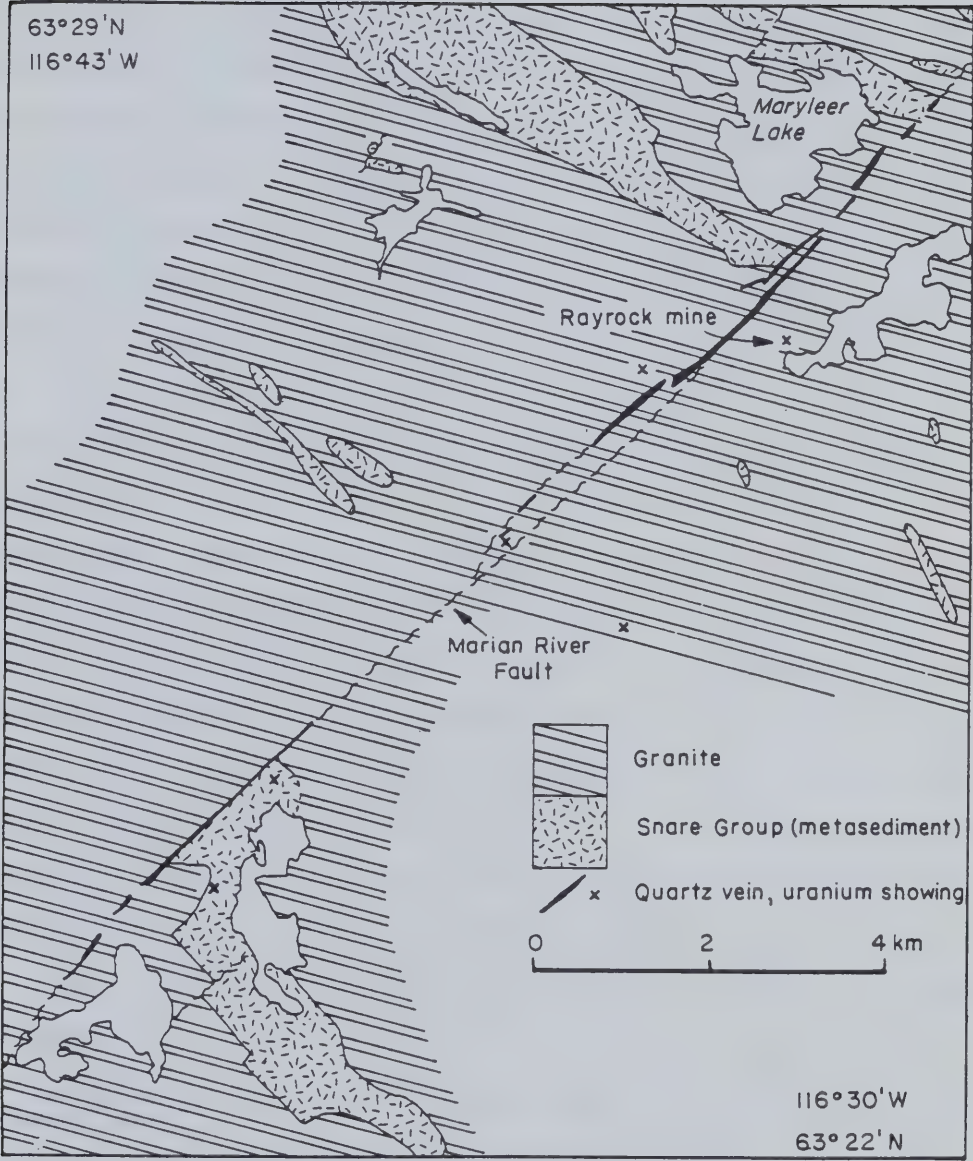


Figure 22: Geology of the Marian River Fault and Rayrock mine area (after McGlynn 1968).

include, (i) quartz–diopside–plagioclase schist with minor carbonate, garnet and microcline; (ii) plagioclase–quartz–microcline–actinolite schist with zircon, apatite and late chlorite and epidote; and (iii) diopside–actinolite schist with muscovite, phlogopite, altered plagioclase, epidote and carbonate. A temperature of 500°–600°C (500 bars, $p_{H_2O} = p_{CO_2}$) or 580°–650°C (1500 bars) is suggested by the absence of tremolite–actinolite + quartz + carbonate assemblages and the presence of tremolite–actinolite + carbonate (Turner 1968). Some units may have been porphyritic felsic volcanics, altered to quartz–feldspar–biotite schist with phenocrysts of quartz and epidotised plagioclase. One magnetic pod, some 100cm x 0–7cm, composed of hematite, blueish maghemite, epidote and minor bornite, was found at a contact between granodiorite and Snare Group rocks.

At the showings, the host granodiorite has developed an uneven texture and may resemble a porphyry, due to intense sodium metasomatism and probable cataclasis. The microcline has been altered to chess-board albite, large turbid feldspars with rare albite twinning probably represent albitisation of the original sericitised plagioclase, and quartz is heavily corroded or completely absent; most of the rock is composed of fine-grained, hematized albite, apparently not previously reported (Gandhi 1978a) (Plate 12). The quartz veins contain small rectangular albite crystals and prominent fluid inclusions, typically containing a daughter salt and a small vapour bubble or a vapour bubble some 80% of the inclusion volume. Thin sections show that pitchblende, accompanied by chlorite and hematite, selectively replaces the albitised host rock rather than the quartz (Plate 13).

The giant quartz vein *per se* is essentially barren at the outcrop, but as McGlynn (1971) stated:

"Pitchblende occurs in veins in fractures in the stockwork and bounding siliceous rocks."

and Lang *et al.* (1959, plate IX) confirmed that pitchblende postdates the quartz. Pits and trenches show veins of pitchblende, hematite and chlorite up to 1 cm thick in the granodiorite, stained with malachite, yellow uranophane, betauranophane and becquerelite, yellow–orange schoepite, bright green cuprosklodowskite and pinkish grey sklodowskite.

At the showings, the crystals of vein quartz are typically outlined by hematite, and more rarely by seams of pitchblende some 5 micrometres thick. Pitchblende fills some quartz–crystal interstices, followed by later bornite, "chalcocite", covellite and hematite

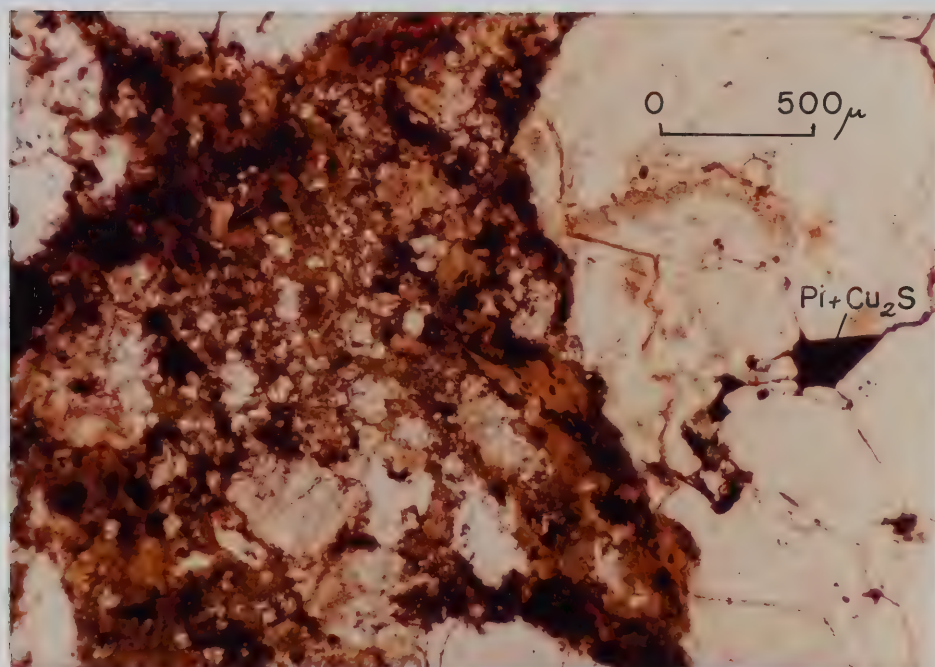
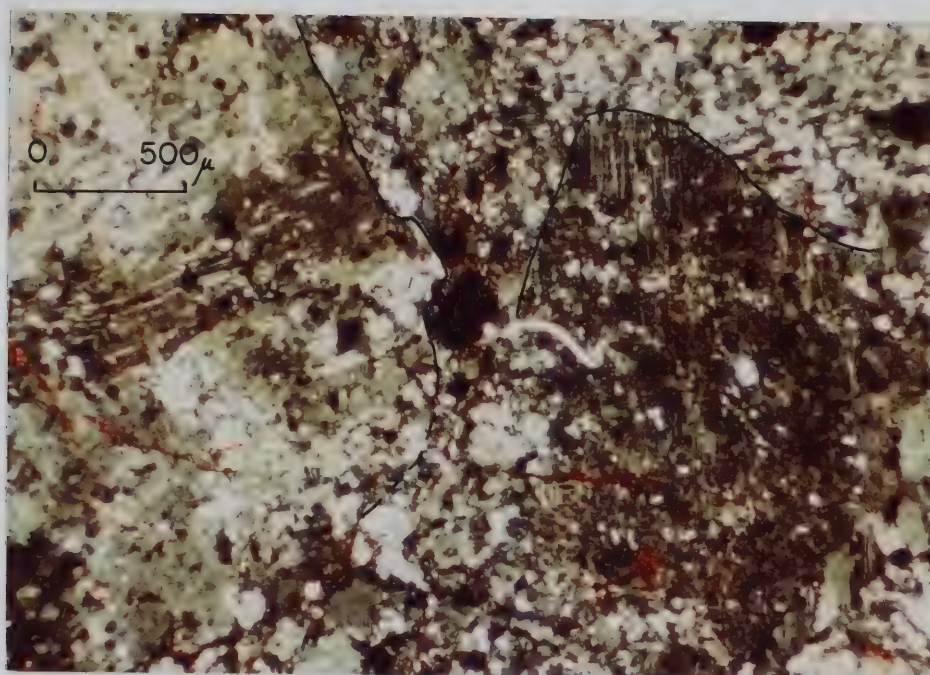


Plate 12 (top): Large grains of plagioclase (l) and microcline (r) altering to chess-board albite; Rayrock mine, transmitted light, X-polars, x2.5 objective. Retouched for clarity.
 Plate 13: Pitchblende-chlorite-hematite mineralisation selectively replacing a clast of albitised granitic wall-rock, Rayrock mine. Note that some pitchblende (black) does also occur in the vein quartz at right. Transmitted plane polarised light, x2.5 objective.

intergrowths. The country rock contains hematite sheafs and botryoidal or diffuse pitchblende, with covellite and "chalcocite" subsequently emplaced in syneresis cracks in the pitchblende. The pitchblende and hematite usually occupy separate micro-domains, but the close association suggests that they are at least partly coeval. Botryoidal pitchblende and hematite plates are sometimes intergrown with chalcopyrite or an unidentified Cu-Fe sulphide, which resembles a high-reflectance orange bornite (R at 591 nm = 29.2%, $VHN_{100} = 120$). This sulphide has exsolved a few chalcopyrite lamellae and has partially altered to covellite and "chalcocite". Normal bornite, specks of native copper and traces of niccolite were also found. Pitchblende occupies the cleavage traces of chlorite in one veinlet. Qualitative electron microprobe analyses indicated an impurity in the pitchblende, which was either yttrium or phosphorus.

Adjacent deposits

Many similar deposits occur along the Marian River Fault, but some are sufficiently different to merit a brief discussion based on old records. Disseminated pitchblende occurs in pore spaces between pyroxene grains in Snare Group skarns adjacent to a syenite at the HONK claims (Bond 1976). The DEL, GS, GAMMA and CA claims all show pitchblende-hematite mineralisation in faults subsidiary to the Marian River Fault where they cut Snare Group metasediments and paragneisses (various DIAND internal reports). The ME and PB claims contain pitchblende in fractures cutting a skarn (Mylrea 1953). All of the uranium showings in the area are closely associated with Snare Group rocks; conversely the PAL claims, some 10 km from the nearest known Snare outcrop, are barren (Baykál 1967b).

The proposed paragenesis

Pitchblende, copper sulphides and at least some hematite were deposited contemporaneously around the stockwork. The isotopic study showed an age of 511 ± 86 Ma, which is within error of the Mazenod Lake copper-uranium mineralisation (457 ± 26 Ma), some 40 km to the north, where potassium metasomatism rather than sodium metasomatism has occurred. The giant quartz veins were dormant by 600 Ma ago (p. 18), and the Marian River stockwork was only a passive channelway for hydrothermal

solutions. The age of albitisation is not known, but alkali metasomatism did not accompany the giant quartz veins studied by Furnival (1935), and it may be related to the uranium mineralisation.

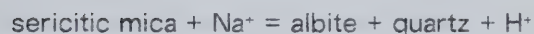
As at Mazenod Lake, the mineralisation does not include carbonates, and a somewhat similar mechanism of pitchblende deposition is proposed:

(1) Deep tropical weathering released uranium from Snare Group rocks; the palaeolatitude was within 25° of the equator 400–600 Ma ago (Irving 1979).

(2) Hydrothermal circulation commenced from an unknown heat source. Fluids acquired high sodium levels and unidentified uranyl complexes from oxidising metamorphic rocks of the Snare Group.

(3) Boiling or CO₂ loss induced breakdown of the uranyl complexes, and reduction caused the precipitation of UO₂.

The pH was maintained by the general reaction:



A low Eh was maintained by wall-rock reactions or by mixing with reducing solutions. The precise reducing agent may have been a ferrous silicate (now altered to hematite or a low-iron chlorite such as clinocllore), or magnetite, both of which could be present in the Snare Group rocks. Alternatively a reduced solution, equilibrated with unoxidised Snare Group rocks and carrying dissolved Fe²⁺, may have mixed with the uranyl carbonate solution. In all of these models, the Snare rocks provide the uranium and subsequently reduce it, explaining the close association noted.

N. The metamorphosed palaeo-placer deposits

Introduction

These deposits lie within a narrow, north-trending belt of discontinuous schists, paragneisses and migmatites up to 10 km wide, just west of the Wopmay Fault. Lord and Parsons (1952), Wilson and Lord (1942) and Lord (1942) correlated these rocks with the Snare Group, and they resemble the possibly Snare-equivalent Akaitcho Group to the east of the fault (R. Hildebrand, pers. comm. 1980). Although they will be referred to

herein as the Snare Group, they may not be stratigraphically equivalent to certain unmetamorphosed volcano-sedimentary sequences which are also termed Snare Group, as at Beaverlodge Lake and the JD claims. The metamorphic rocks at the Rayrock mine are also part of the belt, which probably extends for 400 km, the entire length of the batholith (McGlynn 1977). The belt coincides with positive aeromagnetic anomalies, according to the relevant Geological Survey of Canada aeromagnetic survey maps.

The host rocks are all high-grade metamorphic lithologies intruded by granitoids. The showings seen, from north to south, are on the JACKPOT claims, the HAM and JONES claims at Hailstone Lake, the JLD claims and the NORI/RA and UGI/DV claims at De Vries Lake. Numerous other lapsed claims, including the TAN and NAN claims further south (McGlynn 1971; Thorpe 1972) and the HONK claims near the Rayrock mine (p. 102), are probably similar. The deposits are characterised by magnetite, uraninite and high rare-earth contents, and often by hydroxyapatite⁴ and massive fine-grained tourmaline. A sample of uraninite from each locality was quantitatively analysed with the electron microprobe (Table 2). The magnetite-rich zones are well under 100 m wide, although multiple zones are present and continuity has not been proven beyond a few hundred metres in any example. The isotopic study showed a general uraninite U-Pb age of 1860 ± 20 Ma, the same age as the granites which intrude them. In more detail, two age trends were established at 1849 ± 12 Ma (the JACKPOT and JLD showings) and 1872 ± 8 Ma (the HAM, UGI/DV and NORI/RA showings).

The JACKPOT claims

(S) (116°30'W, 65°42'N)

Although JACKPOT was the name current during test mining, these claims were last staked as the JEN group (Fig. 23). Granite and Snare Group paragneiss at the claims are cut by an inclined and locally horizontal sheet of quartz gabbro, similar to a major sheet 140 km to the south which is one of the Franklin swarm, with a K-Ar age of 619 ± 85 Ma (Wanless et al. 1965, anal. 64-64). A 10 m horizontal adit has been driven under the sheet into a uraniferous paragneiss, probably in 1956-1957 (McGlynn 1971),

⁴ Qualitative electron microprobe analyses showed no F or Cl in the apatites tested (from the HAM, JONES, NORI/RA and UGI/DV deposits) except for a trace of Cl in one sample from the NORI/RA claims. They are assumed to be hydroxyapatite, but could also be oxyapatite, and a carbonate content is also possible.

ELECTRON MICROPROBE ANALYSES OF MINERALS FROM META-PLACER DEPOSITS

A: URANINITE

Sample	O	Fe	Y	La	Ce	Nd	Sm	Pb	Th	Total		Source
										U	Wt. %	
A28Gi	13.40	nd	2.15	0.004	0.640	0.576	0.257	17.32	1.27	56.29	94.29	UGI/DV
B24Ai	14.08	2.12	7.69	nd	0.048	0.466	0.391	14.84	0.24	50.85	92.34	HAM
B25G	13.40	1.76	3.00	0.048	0.302	0.364	0.363	16.61	0.00	57.21	94.34	JONES
B29A	13.99	3.69	0.29	0.058	0.053	0.117	0.220	17.78	3.40	57.08	97.96	JLD
B39A	13.41	1.29	1.03	nd	0.064	0.258	0.331	17.86	4.50	57.78	97.86	JACKPOT
C1B	13.56	0.88	6.50	0.065	0.686	0.698	0.495	14.46	0.00	52.69	91.72	NORI/RA

Notes: Other elements found in traces, particularly Si.

Low totals partly due to poor background-fitting by data-reduction programme EDATA2 (Smith and Gold 1979) (visible on reduced spectrum plots).

All uranium assumed as U_3O_8 and iron as ferrous, and oxygen calculated accordingly.
nd = not determined

B: PSEUDOBROOKITE

Sample	O	Ti	Fe	Nb	Pb	U	Total wt. %	Fe Ti O (atomic ratios)		
								Fe	Ti	O
B38Ei	39.83*	31.26	25.15	1.51	0.25	0.16	-*	1.08	1.57	5.00
B38Ei	40.54*	30.47	20.99	0.77	0.85	1.50	-*	0.90	1.52	5.00
B39A	33.74#	30.12	27.69#	0.70	0.27	0.46	94.55	1.18	1.49	5.00
B39A	33.16#	30.80	22.92#	0.68	0.60	2.14	92.77	0.99	1.55	5.00

Notes: Other elements found in traces.

* = oxygen calculated to give 100% totals

= oxygen calculated to give all Fe as ferric

Table 2: Electron microprobe analyses of pseudobrookite from the JACKPOT occurrence and of uraninite from all the xerogenic, meta-placer deposits.

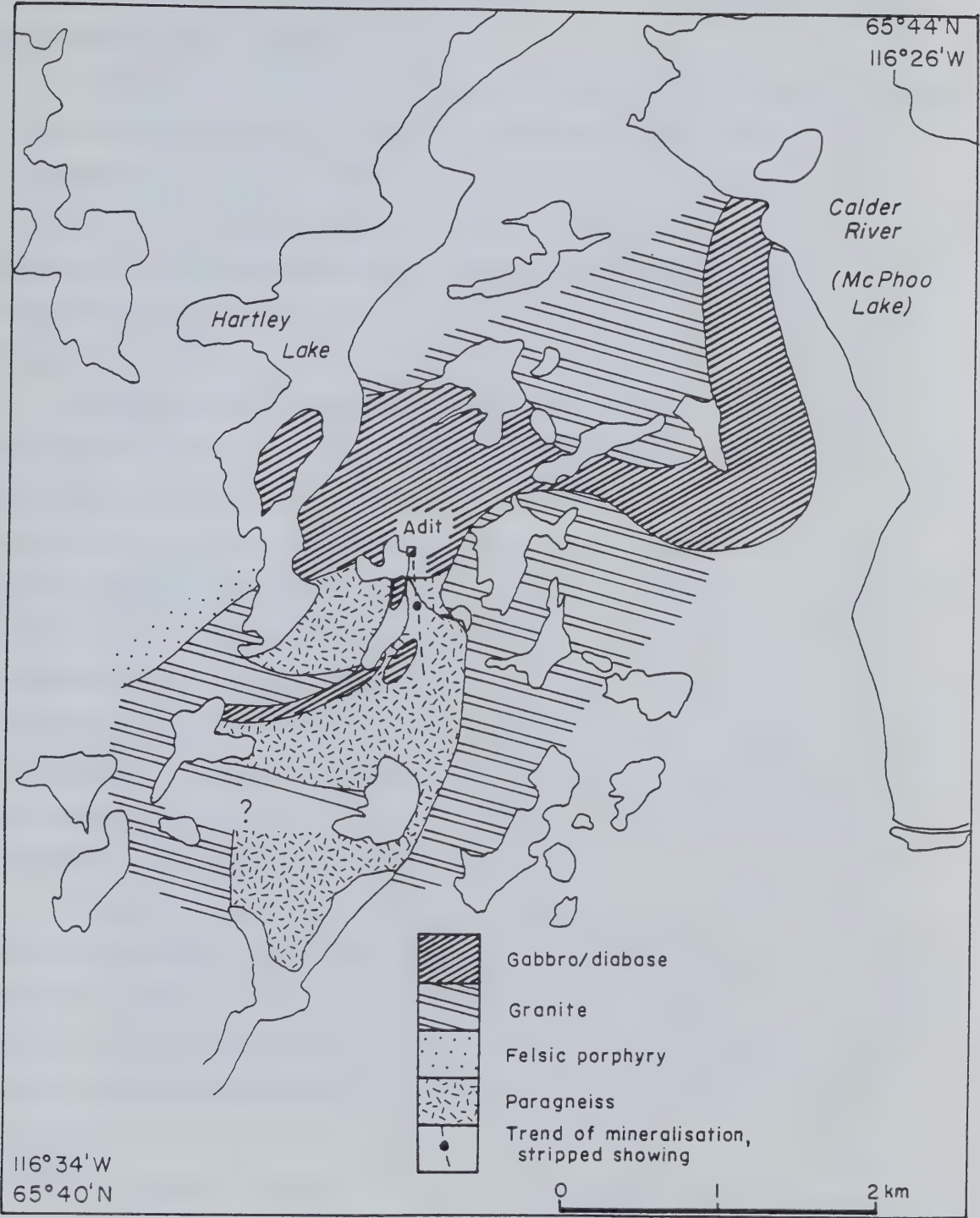


Figure 23: Field sketch-map of the JACKPOT uranium occurrence (additions after Lord and Parsons 1952).

and between sixteen and twenty-four boreholes were drilled (data from DIAND records). Stripped, trenched and drilled showings extend for at least 1 km southwards from the adit but their continuity cannot be proven.

Perthitic microcline phenocrysts distinguish the granite from granitised paragneiss in the migmatitic contact zone. The granite is composed of approximately 38% recrystallised quartz, 35% microcline, 20% plagioclase, 5% green biotite and minor amounts of opaque minerals, subhedral titanite and apatite. The plagioclase is strongly altered to white mica and minor epidote, the biotite is locally chloritised, and granophyric textures have developed along some grain contacts. The variable grain size suggests a degree of cataclasis.

The Snare Group paragneisses are somewhat foliated and locally crenulated. Isoclinal folds, ptygmatic granite veins and boudins obscure the original bedding, although sedimentary laminations can still be seen in thin sections. Some slightly sheared pegmatitic veins of quartz, microcline, sericitised plagioclase, biotite, muscovite, tourmaline and minor magnetite, pyrite and chalcopyrite occur at one radioactive zone, grading into quartz veins. The pink or grey leucogneisses are composed of very fine-grained, equigranular quartz, microcline, plagioclase (somewhat altered to white mica), minor biotite, muscovite and magnetite. The melanocratic varieties have a complex mineralogy including quartz, mangiferous almandine, altered cordierite, slightly chloritised biotite and magnetite, and grade into tourmalinised and radioactive lithologies; one sample is probably a quartz-hedenbergite schist.

Radioactivity occurs within conformable magnetite-rich lenses up to several metres long and tens of centimetres wide, in a belt of mafic paragneiss up to 15 m wide, dipping some 60°W and striking north west. These pods have been broken into boudins, locally with ptygmatically folded tips (Plates 14, 15). Traces of lamination are rare but exist as variations in the grain size. All the samples taken from these lenses were radioactive. The adjacent mafic paragneiss was altered to 50–100% blue and brown massive, fine-grained schorl tourmaline, after metamorphism. The alteration front is evident in thin sections, where the quartz-hedenbergite lithology has been converted into a coarser assemblage of quartz, tourmaline, biotite, anthophyllite, zoisite and opaque minerals. The tourmaline schist weathers indistinguishably from the unaltered mafic



Plate 14 (top): View of stripped showing at the JACKPOT occurrence. Hammer lies on partly tourmalinised mafic paragneiss veined with pale pegmatite; left of hammer are two darker discordant magnetite veins, right of hammer are boudins and blocks of conformable magnetite (partly trenched).

Plate 15: Magnetite boudins in paragneiss from Plate 14.

paragneiss and was apparently not previously recognised; its full extent is not known, nor whether it is restricted to the uraniferous zones, but it is at least some tens of centimetres thick around magnetite lenses, and need not be accompanied by the tourmaline pegmatite. The magnetite- and tourmaline-rich samples collected usually contain disseminated uraninite; uraninite was not found elsewhere, but this may not be a consistent relationship.

Some slightly discordant, non-radioactive veins of coarse magnetite 5–10 cm thick host a brecciated quartz-tourmaline schist and are clearly a later generation of material with a distinctly different mineralogy (Plates 16, 17). Up to 20% of unoriented quartz, muscovite, tourmaline and biotite occurs with this magnetite, which may have been remobilised from the conformable magnetite bodies. Late cracks in these veins are filled with unoriented biotite and minor quartz. Some rare late-stage quartz-fluorite veins occur near the adit.

The uraniferous, magnetite-bearing paragneiss contains 55–70% schorl, 20% chloritised biotite, 5–10% opaque minerals and minor quartz, garnet, xenotime (up to 1%) and purple fluorite. The fluorite and some quartz occur as "eyes" along biotite cleavages, a feature of similar deposits in Labrador (Kerswill and McConnell 1979) (Plate 18). The fluorite has a blue-purple pleochroism resembling dumortierite, ascribed to intergrown biotite flakes. The xenotime (Plate 19) occurs as loose polycrystalline aggregates of rounded grains, and was qualitatively identified with the electron microprobe (Overstreet (1967) suggests that monazite, and thus perhaps xenotime, is initially unstable during metamorphism but may be reformed at higher metamorphic grades).

The opaque phases include magnetite, ilmenite, pseudobrookite, minor hematite replacing magnetite, an unidentified TiO_2 phase, uraninite, minor sulphides (galena, chalcopyrite and skeletal pyrite) and unidentified breakdown products. Quantitative analyses of the magnetite showed traces of Al, Si and Mg, sometimes V, Cr, Mn and Zn, sometimes major Ti, and an unidentified, fine-grained exsolved phase containing Mg, Al and Si. No consistent compositional difference between the conformable and vein magnetite was found. The pseudobrookite has replaced ilmenite laths with polycrystalline aggregates that contain up to 25% uraninite in 20 micrometre diameter blebs, and traces of fine-grained galena, chalcopyrite, a TiO_2 phase and other unidentified oxides

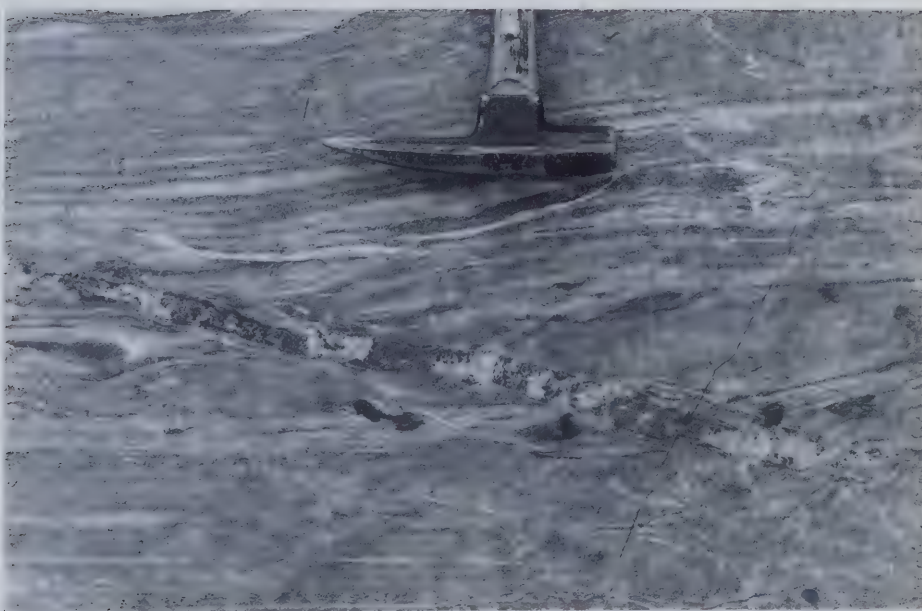


Plate 16 (top): Magnetite vein containing brecciated tourmalinised paragneiss, JACKPOT occurrence.
Plate 17: Discordant magnetite vein, JACKPOT occurrence.

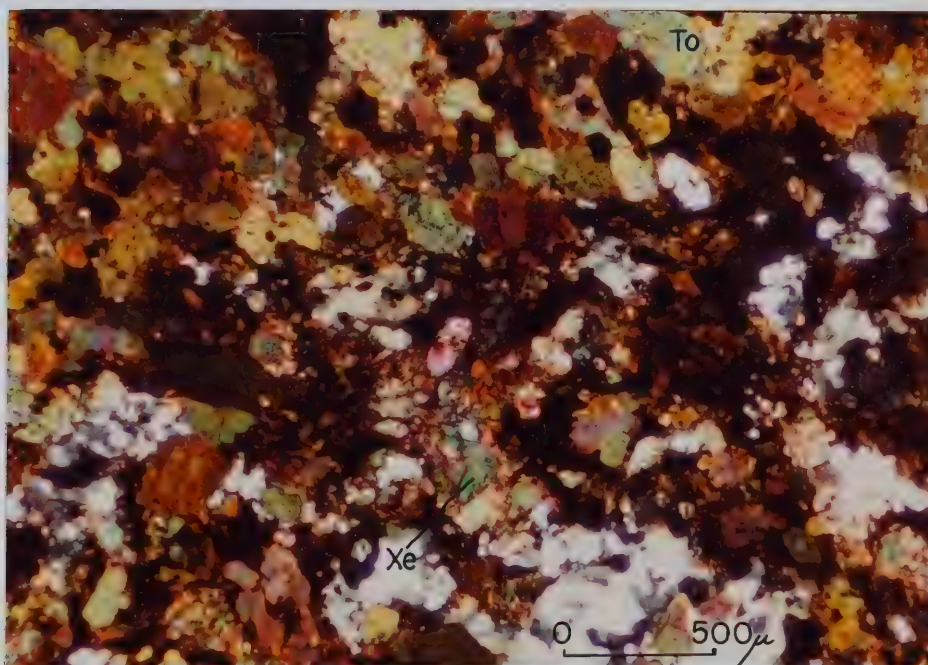
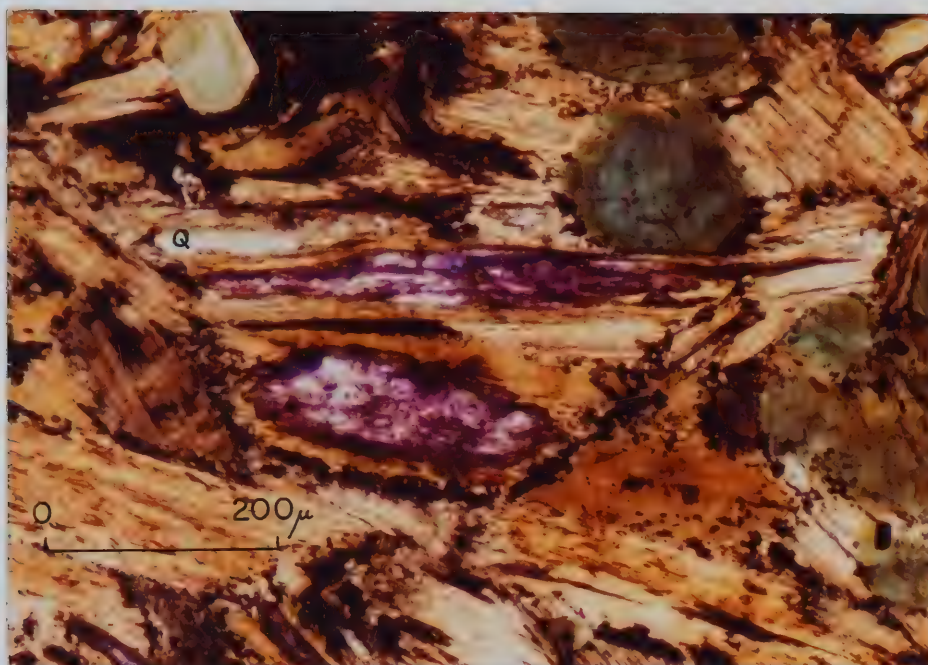


Plate 18 (top): Two "eyes" of purple fluorite and one of white quartz in biotite, JACKPOT occurrence. With tourmaline and opaque minerals. Transmitted plane polarised light, x10 objective.

Plate 19: Xenotime (with high birefringence) occurring with quartz, tourmaline, opaque minerals and altered biotite, JACKPOT occurrence. Transmitted light, X-polars, x2.5 objective.

(Plates 20, 21). Quantitative electron microprobe analyses of the pseudobrookite gave atomic Fe/Fe+Ti ratios of 0.39 and 0.44, rather than the ideal value of 0.67 in Fe_2TiO_5 . The pseudobrookite also contains up to 1% by weight Nb and 2% U (Table 2). Ilmenite replaced by pseudobrookite was described by Smith (1965), who also found excess Ti in the analyses, although not to the extent found in this study.

Isolated blebs of yttrian uraninite also occur enclosed within tourmaline and biotite. Rare earths including La and Ce were detected in the alteration haloes around uraninite and uraninite-bearing pseudobrookite in the host tourmaline. These haloes have an outer rim of a uraniferous TiO_2 phase in grains about one micrometre in diameter. McGlynn (1971) reported a Th/U ratio in the mineralisation of about 1, confirmed herein by a whole-rock sample analysed by neutron activation which contained 2800 ppm U and 2400 ppm Th. Electron microprobe analyses showed the uraninite to be thorian (Table 2). McGlynn also reported significant "cesium", probably a misprint for cerium.

Pyrite and minor chalcopyrite locally constitute some 10% of the magnetite-rich samples collected, forming interstitial grains or occurring along the cleavages of biotite grains, and sampling of the JEN claims returned an assay of 1.42% Cu and 0.17 oz/t Ag (from DIAND records).

Boron, fluorine and water have apparently been introduced into magnetite-rich metasedimentary rocks, remobilising some of the magnetite into veins, but there is no evidence that any other elements were introduced during the metasomatism. The adjacent granite is not tourmaline-bearing, but might still be the source of boron. The uraninite may pre-date the tourmaline which surrounds it, and by inference, so may the alteration of ilmenite to uraniferous pseudobrookite, so that the following sequence of events is indicated:

- (1) Metamorphism of heavy-mineral sands in a sedimentary sequence; deformation into boudins and lenses.
- (2) Alteration of ilmenite to pseudobrookite; redistribution of uraninite and xenotime.
- (3) Introduction of a volatile phase; alteration of schistose mafic silicates to non-schistose tourmaline and hydrous ferromagnesian minerals; intrusion of pegmatites.
- (4) Final minor shearing and slight deformation.

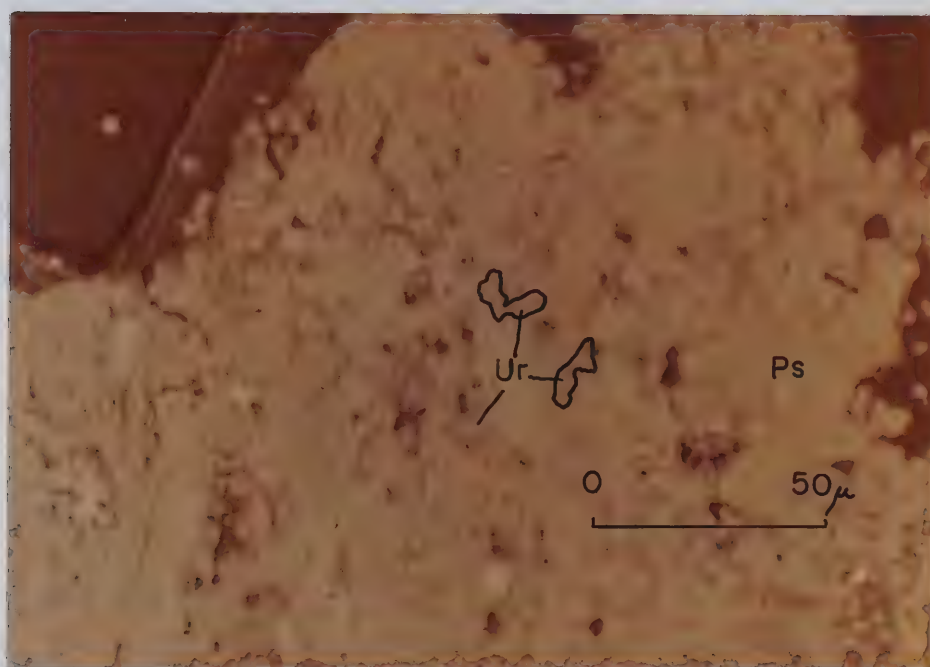
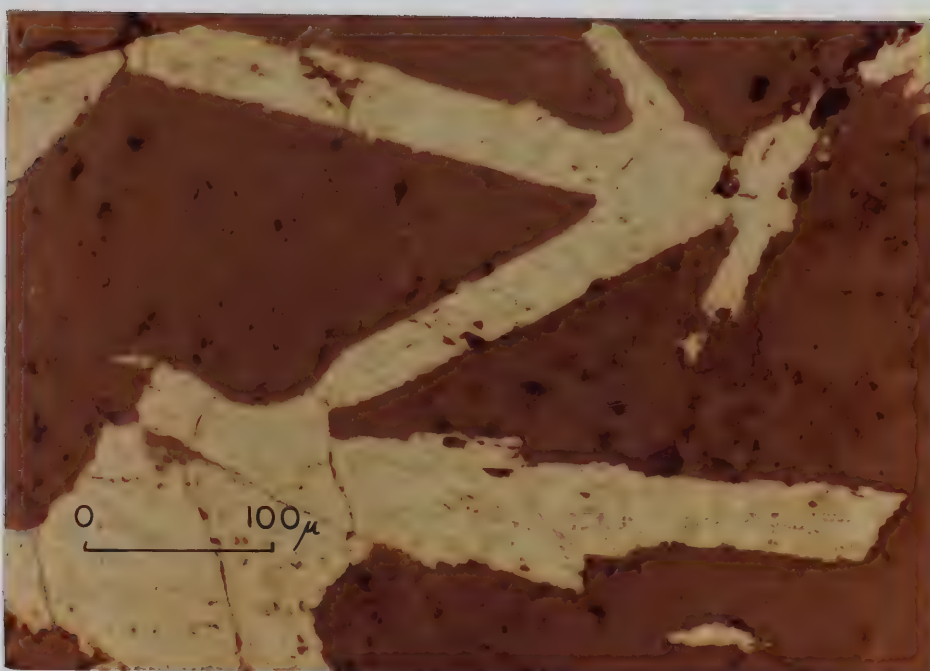


Plate 20 (top): Ilmenite laths in silicate matrix, altering to pseudobrookite and possibly other unidentified Fe-Ti-O phases, JACKPOT occurrence. Reflected plane polarised light, x16 objective, in air.

Plate 21: Uraninite grains within the pseudobrookite, JACKPOT occurrence. Some have been retouched for clarity. Reflected plane polarised light, x40 objective, in air.

The HAM and JONES claims

(T) (116°48'W, 64°47'N)

The JONES claims on the west shore of Hailstone Lake lie 2 km east of the HAM claims and 100 km south of the JACKPOT claims (Fig. 24). Granite, migmatite and Snare Group paragneiss underlie the showings, locally well exposed; the Snare Group here is far more extensive than was shown by Wilson and Lord (1942). Paterson (1976c) and Ahuja (1974) investigated these showings, dividing the paragneisses into gradational units which have not been adopted herein. A major north–east fault, visible as a photolineament, crosses the south end of Hailstone Lake, and causes a dextral offset in two parallel magnetic anomalies which trend 130°–160° (Paterson *op. cit.*). Two small ground radiometric anomalies, one on each side of the fault, overlie the smaller magnetic anomaly. The northern radiometric anomaly, in claims JONES 16 and 30, was examined, together with all the showings depicted on the HAM claims by Ahuja (*op. cit.*). In both areas the magnetite bands trend east rather than south–east.

The somewhat cataclastic granite is composed of 60% perthitic microcline, 30% recrystallised quartz, 6% chlorite, 4% sericitised plagioclase and traces of apatite, but zircon was not found. Paterson (*op. cit.*) found 5% quartz and 30% mafic minerals in samples of this unit. Veins of granite and granitic pegmatite cut all the units, including a chilled plagioclase–hornblende gabbro plug at the JONES occurrence.

Paterson (1976c) described foliated, porphyritic quartz–feldspar rhyolite containing radioactive magnetite lenses, which are probably units of the Snare Group, and foliated, andesitic or basaltic dykes and sills, cut by aplites. One aplitic vein was found cutting a dark green amphibolite dyke in the paragneisses on the HAM claims. This amphibolite contains 52% altered plagioclase (An_{44}), 22% ferrohastingsite (confirmed by qualitative electron microprobe analyses), 15% biotite and minor quartz, ilmenite, Cr-bearing magnetite, apatite and muscovite. A second amphibolite containing 25% quartz and numerous rounded or fractured zircons some 50 micrometres in diameter is probably metasedimentary in origin.

The Snare Group paragneisses range from pink leucogneiss to grey or black biotite–magnetite schist and gneiss. The leucogneisses may contain 40–50% quartz, 20–35% microcline (sometimes perthitic), 15–25% plagioclase, 5% partially chloritised

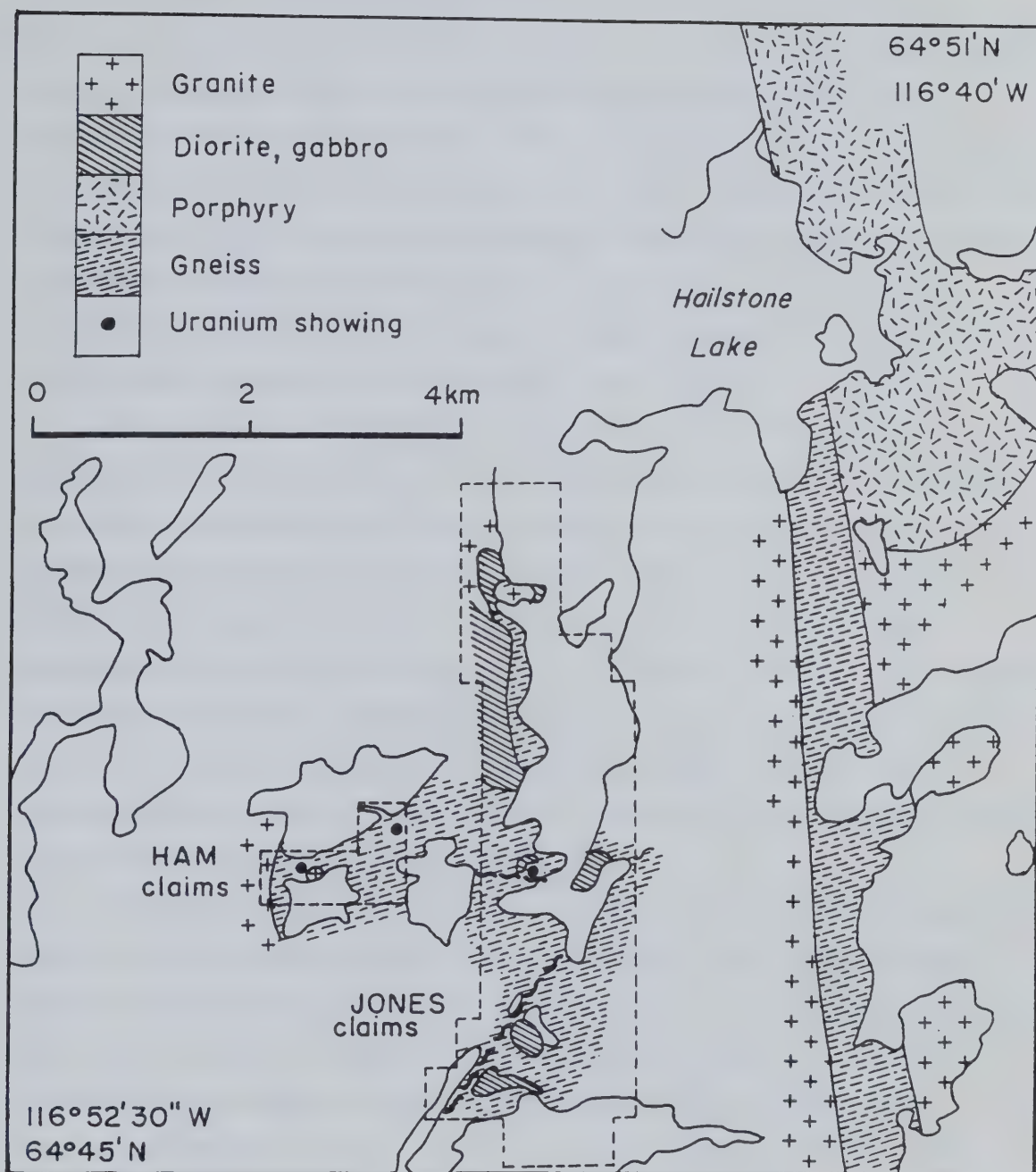


Figure 24: Geology of the HAM and JONES uranium occurrences (compiled from Wilson and Lord (1942), Paterson (1976c) and Ahuja (1974)).

biotite and 5% magnetite with traces of muscovite. Microcline and polycrystalline quartz form occasional aggregates up to 1 cm in diameter in a matrix of grains between 0.1 and 4 mm in diameter, which may be a relict sedimentary texture. Zircon, allanite and monazite/xenotime are common accessories; up to thirty zircons were commonly found in some thin sections (Plate 22). The plagioclase ranges from An_{34} to An_{47} , but is commonly altered to coarse white mica. The biotite is partially chloritised and interleaved with muscovite laminae and leucoxene aggregates. All the paragneisses contain magnetite, ranging from disseminated grains in the leucogneiss to almost pure magnetite lenses and pods. Most of them also contain infilled "eyes" in the biotite or chlorite up to 200 micrometres long, containing pistacite epidote, quartz, rarely calcite, or (usually in the mafic varieties) anomalously pleochroic purple fluorite (*cf.* p. 109).

The melanocratic paragneisses are scarce in the HAM claims, and grade into pure magnetite at the JONES showing, where one sample contains garnet, biotite, muscovite, cordierite, sillimanite, plagioclase, quartz, and magnetite with hercynite or pleonaste rims, suggesting metamorphic conditions of 625°–675°C and 3–4 kb (Winkler 1979). This sample contains large numbers of radioactive inclusions in the biotite, the larger tentatively identified as zircon but ranging down to the limits of resolution. Other samples contain, (1) 67% variably sericitised plagioclase, 27% chloritised biotite, 3% magnetite, 2% quartz and 1% apatite; (2) 59% quartz, 26% untwinned feldspar, 7% garnet and minor biotite, muscovite and opaque minerals. Epidote is a common anhedral accessory mineral and sometimes an alteration product of plagioclase.

The massive magnetite is not uniformly radioactive. The anhedral magnetite grains are 0.1 to >1 mm in diameter, and may be accompanied by minor ilmenite. Anhedral apatite is often present, particularly at the JONES showing, constituting from a trace to 50% of the rock within or adjacent to the magnetite bands, in grains up to 1 mm in diameter. Crenulated layers of silicates or apatite define a poor lamination in the magnetitic bands, assumed to be sedimentary in origin. Radioactive orthite or brown clinozoisite occurs in late quartz veinlets.

At the HAM showings, the magnetite rocks are weakly- to non-radioactive, hosted by leucocratic paragneiss but also forming xenoliths, emplaced either tectonically or during magmatism, in the granite and the amphibolitic dyke. The magnetite originally

formed irregular layers which have been tectonically disrupted into boudins and cut by granitic veins. One such pod measures 14m x 1.5m, and Ahuja (1974) recorded one nearly 5 m thick (Plate 23). Anhedra uraninite grains some 20 micrometres in diameter were found adjacent to, and sometimes enclosed by, magnetite grains in a sample containing 68% magnetite, 30% actinolite, 2% apatite and rare fluorite (Plate 24). The magnetite adjacent to uraninite has been oxidised to hematite along radiating cracks, perhaps by the auto-oxidative decay of U^{4+} to Pb^{2+} . Minor amounts of pyrite and chalcopyrite occur in some samples, interstitially or enclosed within magnetite.

At the trenched JONES showing, the magnetite-rich unit is at least 4 m thick and grades into mafic paragneisses. The magnetite may be disseminated or concentrated into pods, which may be porous and not always radioactive. Veinlets of paragenetically late pyrite and minor chalcopyrite comprise 5–10%, and locally 50%, of the magnetite-rich rocks; a flake of molybdenite was found in one such veinlet. The paragneiss here retains evidence of its sedimentary origin, seen for example in an isolated, stretched quartz pebble 2 cm long (Plate 25) and in a layer 5 mm wide which is approximately 20% zircon (identified by fluorescence in ultra-violet light). One sample contains two adjacent lamellae of anhedra magnetite each some 2 mm thick, one being barren with grains 500 micrometres in diameter, the other having grains 100 micrometres in diameter and carrying some 2% (and locally 10%) of Y-bearing uraninite. The host paragneiss around these lamellae is composed of approximately 60% quartz, 30% biotite and 10% magnetite, locally with 5% plagioclase and significant amounts of monazite (with $Ce > La$), orthite (containing both Ce and La) and rare zircon and Yb-bearing xenotime, identified by qualitative electron microprobe analyses. Another sample contains thin bands of, (1) 37% quartz, 40% sericitised plagioclase, 15% biotite, 8% magnetite and numerous zircons; (2) 60% hydroxyapatite, 40% magnetite; (3) 50% apatite, 20% magnetite, 30% chloritised biotite; (4) quartz, biotite, chlorite and magnetite schist with clots of zircon (locally up to 30% in micro-domains).

The HAM and JONES showings demonstrate the original sedimentary nature of the uranium deposits. The magnetite forms laminae or lenses on all scales, and uraninite and zircon are also distributed in presumably sedimentary bands. Magnetite is also widely disseminated throughout the paragneiss, however, or may enclose presumably detrital

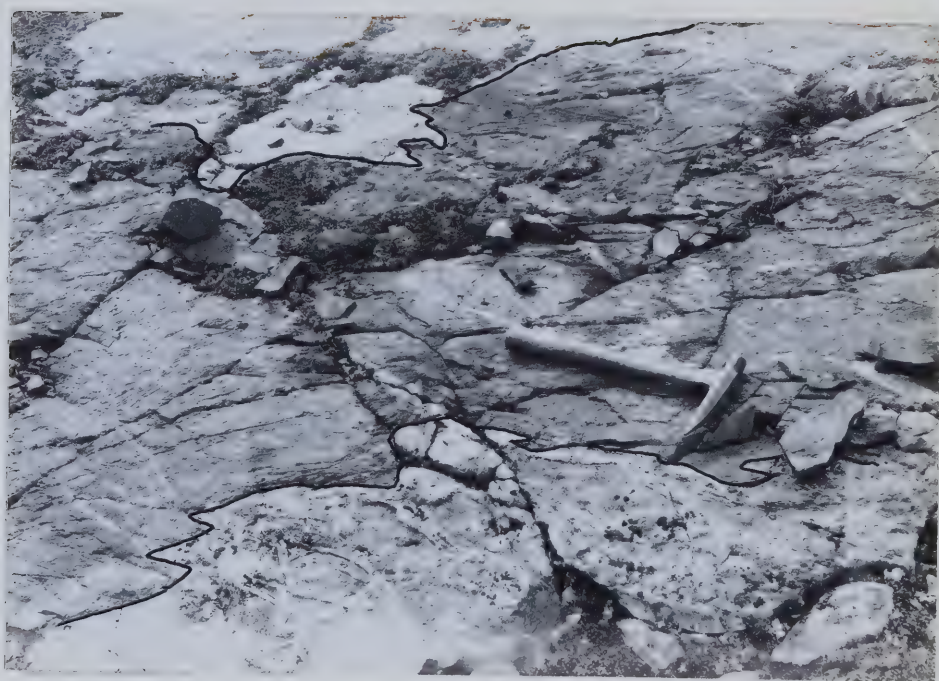
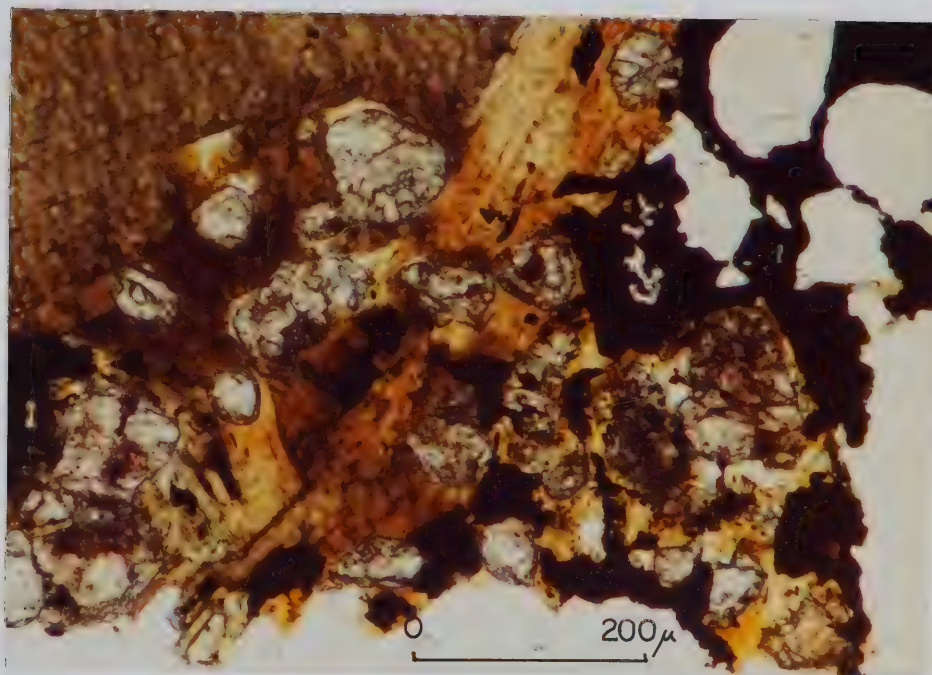


Plate 22 (top): Zircon-rich paragneiss from the JONES occurrence, with biotite, quartz and opaque minerals. Transmitted plane polarised light, x2.5 objective.
 Plate 23: Massive outcrop of magnetite on the HAM claims. Hammer tip points to contact with amphibolite (paler), hammer shaft lies on the magnetite, which is 3m x 2m in area. Retouched for clarity.

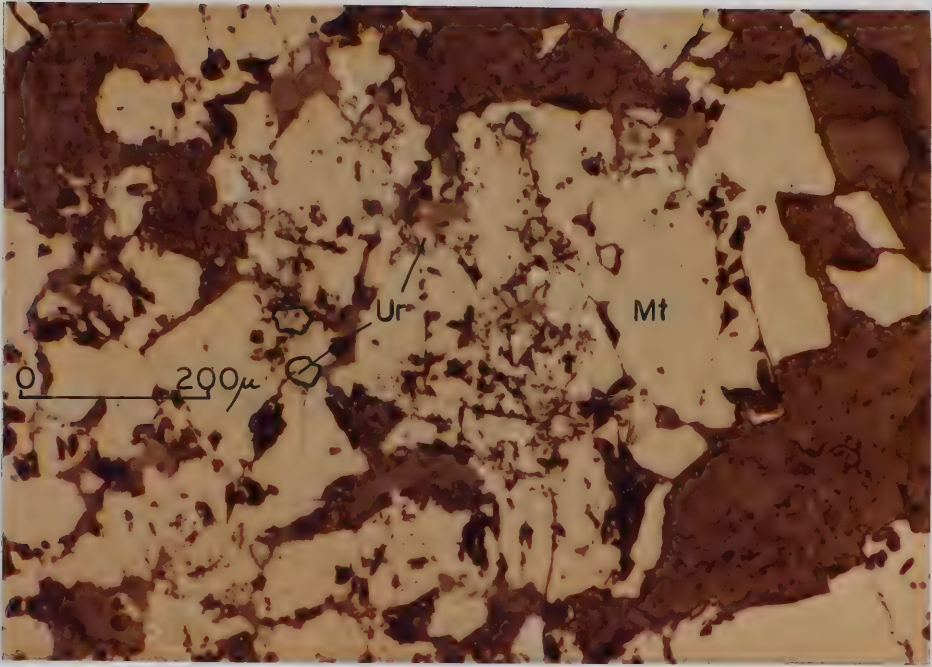


Plate 24 (top): Magnetite (slightly pinkish) with uraninite (slightly darker grey) and minor hematite (white) from the JONES occurrence. Retouched for clarity. Reflected plane polarised light, x8 objective, in air.
 Plate 25: Banded radioactive paragneiss from the JONES occurrence, showing a quartz pebble. This sample also contains a lamina of zircons.

uraninite, which suggests a partially metamorphic origin and a degree of recrystallisation. Zircon also appears to be exsolving from some biotites. The large non-radioactive magnetic anomaly, and the non-radioactive magnetite lenses found, show that the uranium distribution is not directly controlled by the magnetite, and the relationships can be explained by a sedimentary origin for the magnetite, uraninite, apatite and zircon, modified on a scale of millimetres by metamorphism.

The JLD claims

(U) (116°50'W, 64°37'N)

First staked as the VU group (Gill 1969a), these claims lie 17 km south of the HAM and JONES claims; 4 km to the east are the JD claims (*q.v.*), hosting a much younger group of deposits (Fig. 25). The area is underlain by Snare Group paragneisses as well as the granodiorite shown by Wilson and Lord (1942). At the claims, a 400 m wide block of paragneiss is faulted against a red-weathering hill of granodiorite to the west and a pink feldspar-biotite porphyry to the east; the exposure is variable. North-east of the area, the porphyry appears to be gradational into the paragneiss.

The granodiorite contains approximately 59% saussuritised andesine, 17% chloritised hornblende, accessory titanite, and interstitial or poikilitic quartz (17%) and microcline (7%). The paragneiss is typically white or pink with chloritic green flecks, containing up to 60% quartz and up to 60% microcline (confirmed by staining) with accessory green or chloritised biotite, muscovite, magnetite, Mn-almandine and cordierite; fluorite and epidote may form 'eyes' along the biotite cleavages, and rare zircon was found. Some of the microcline poikilitically encloses quartz grains, and may be locally replaced by chess-board albite. More mafic varieties occur adjacent to the magnetite units, containing greater amounts of garnet and biotite, and sometimes very little primary feldspar, although fine-grained, untwinned secondary feldspar (probably albite) occurs along grain boundaries.

Radioactive magnetite bands and pods occur in the paragneiss. At zone "A" (Gill 1969a), one discontinuous layer 20–100 cm thick was traced for 50 m, and numerous other pods occur within 100 m of this band, striking 080°–150°. One trench was located on the exposed hillside to the west, probably zone "B" of Gill (*op. cit.*). It covers a small

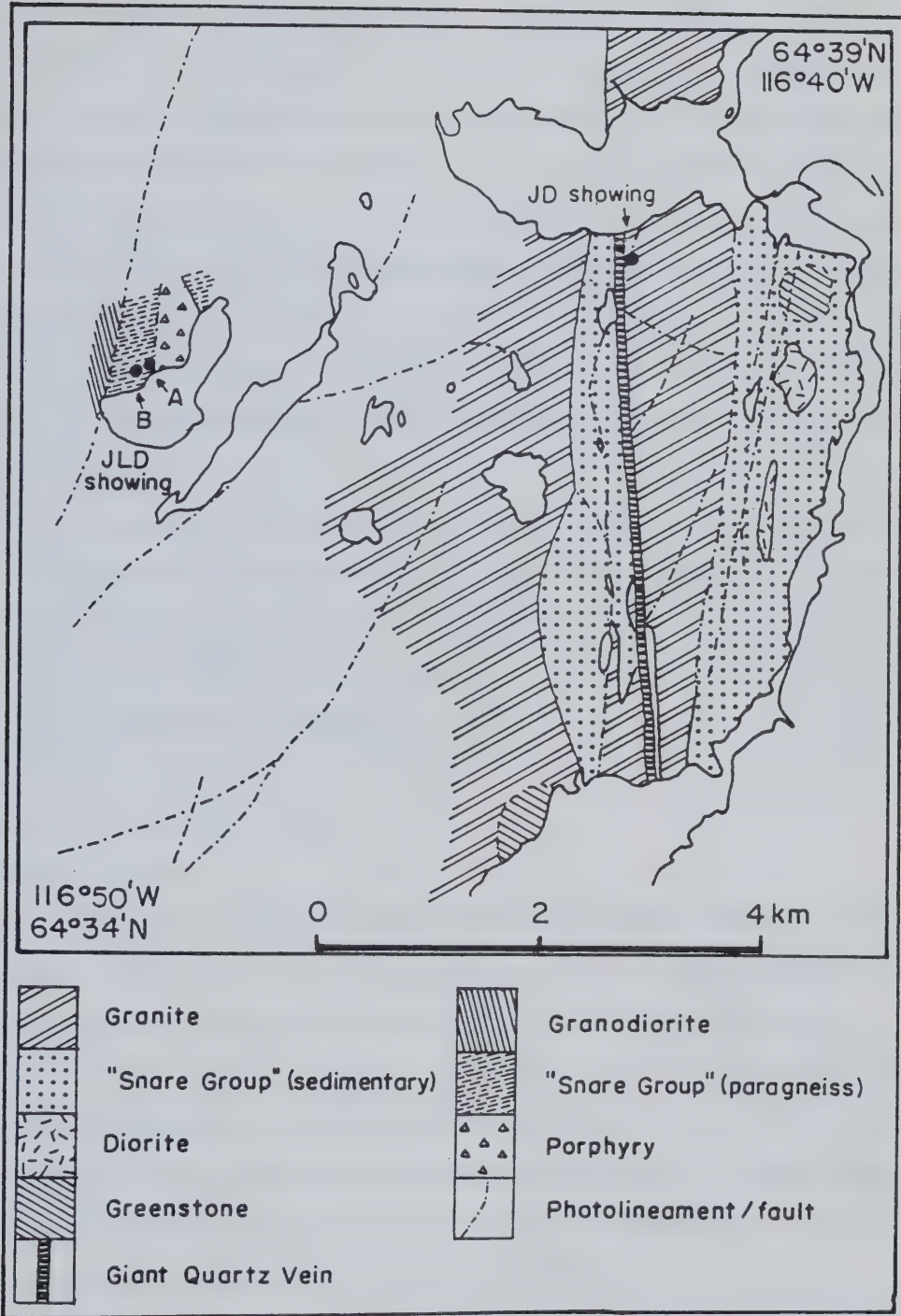


Figure 25: Field sketch-map of the JLD uranium occurrence; eastern half as per Figure 18, after Armstrong (1969a).

magnetite pod striking 170° , a few centimetres thick and one or two metres long, which has been slightly remobilised into small veinlets (Plate 26).

Uraninite occurs as small blebs some 20 micrometres in diameter, adjacent to and within magnetite grains in the magnetite rocks. Some fifty grains in a polished section from zone "A" form a straight line 1 cm long, interpreted as a single sedimentary lamina. The adjacent magnetite grains are cracked and partly altered to hematite, perhaps by auto-oxidation processes (*cf* p. 117). Late coarse pyrite and minor chalcopyrite also occur in zone "A", and some of the magnetite grains contain ilmenite laths. The magnetite is intergrown with up to 50% quartz and minor biotite. At zone "B", the magnetite grains are intergrown with epidote and minor fluorite, and up to 30% apatite in one 3 mm lamina. The apatite and magnetite have been locally remobilised into veinlets. A few zircons were also noted in zone "B" material.

The JLD deposit is similar to the others of this group, containing apatite and magnetite with apparently detrital uraninite, but it is much poorer generally in uraninite, magnetite and zircons. The zone "A" band is a particularly extensive, tectonically disrupted unit. Contrary to Gill (1969a), shearing along these bands was not observed, and they are unlikely to be vein deposits of any type.

De Vries Lake: the NORI/RA claims

(V) ($116^{\circ}50'W$, $64^{\circ}21'N$)

First staked as the NORI group (McMorland 1955; McGlynn 1971) and restaked as the RA group in 1967 (Thorpe 1972), these claims lie 30 km south of the JLD group on the north shore of De Vries Lake (originally Culbert Lake) (Fig. 26). McMorland's nomenclature for the mineralised zones will be followed herein. The area is underlain by granite and Snare Group rocks, less regular in form than the circular outlier shown by Wilson and Lord (1942). Five trenched radioactive showings occur in a broad tongue of variably exposed Snare Group paragneiss that projects northwards for 2 km into a porphyritic granite between two north-east trending faults.

The granite contains microcline phenocrysts up to 7 cm in diameter and has a strong metamorphic aureole, marked by the appearance of cordierite in the Snare Group paragneiss 500 m from the contact. This contact varies from almost vertical to almost



Plate 26: Specimen from zone "B", JLD occurrence. Paragneiss containing a 3 cm band of magnetite on the right, clearly remobilised into veinlets extending out to the left.

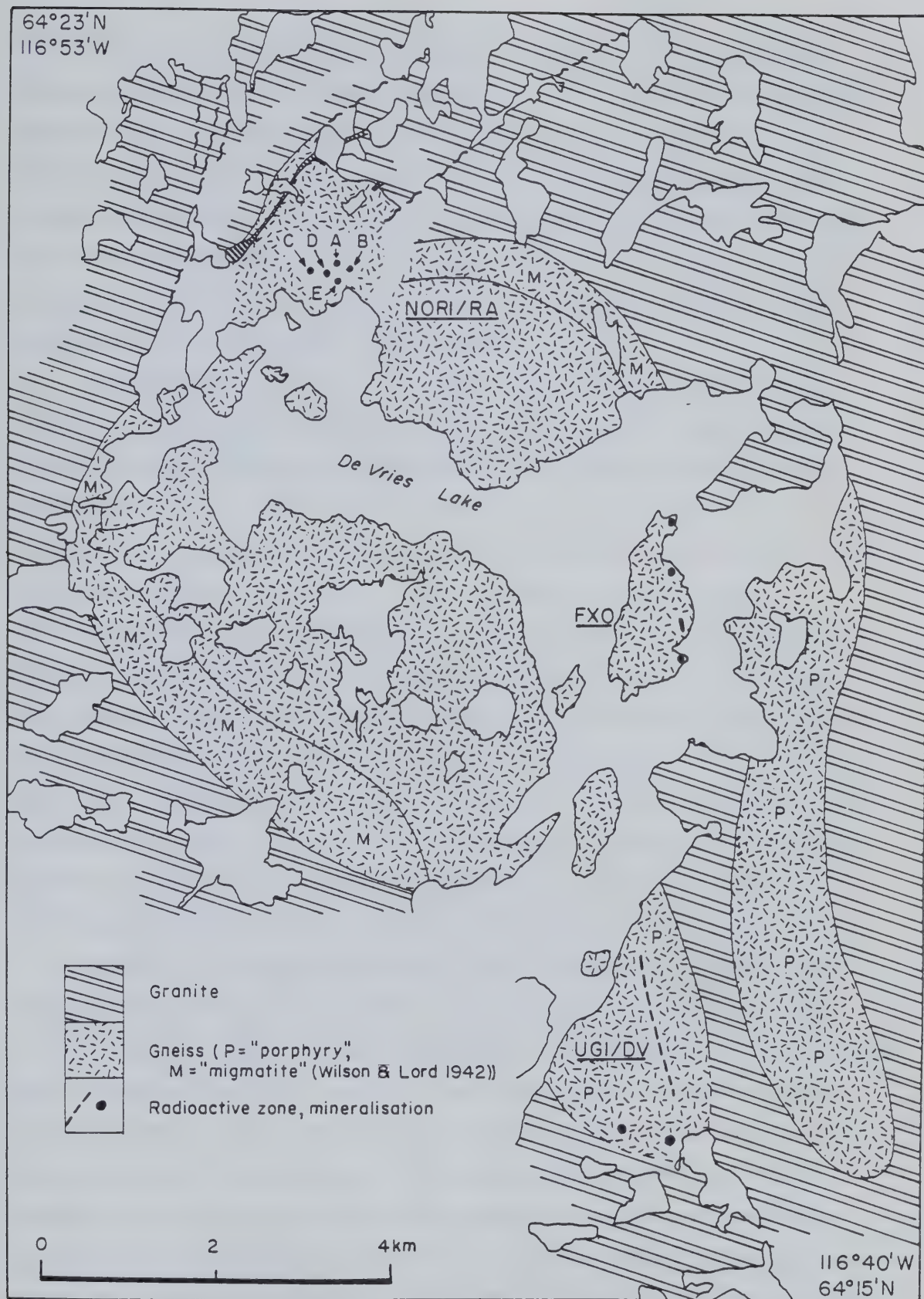


Figure 26: Geology of the NORI/RA and UGI/DV uranium occurrences, De Vries Lake. NORI/RA area from field sketch-map, the remainder after Wilson and Lord (1942), Legagneur (1969) and Paterson (1976a, b).

horizontal, with the granite overlying the paragneiss. Within 1 km of the contact, the paragneisses become brecciated and veined with an unfoliated biotite felsite, emplaced after the regional metamorphism. The intensity of brecciation increases towards the contact, and xenoliths of the felsite and breccia occur within the granite, which has probably engulfed its own volcanic vent. A white-weathering biotite-feldspar porphyry dyke cuts the granite, and a late tourmaline pegmatite forms veins and pods up to several metres wide in the Snare Group rocks. Pods of quartz or quartz and feldspar in the metamorphic rocks are probably "sweat" pegmatites.

The Snare Group has been strongly deformed, but bedding is still preserved as thick arenite units and as compositional and grain-size variations on a millimetric scale. Granitic veinlets form boudins orptygmatic folds, and all units including the pegmatite have been folded. The regional strike is north or north-west, but the dip is variable on all scales. The leucogneisses contain magnetite ranging from tiny augen, to plastically folded magnetite-rich streaks, up to beds of brittle, non-radioactive magnetite up to 3m x 10cm, broken into boudins (Plates 27, 28). The magnetite has been locally remobilised into the augen and along some pegmatite veins, and has occasionally been recrystallised into euhedral grains. Beyond the showings, the paragneiss is typically pink, composed of 44% microcline, 22% quartz, 15% magnetite, 13% chloritised biotite and 6% muscovite, in interlocking grains up to 0.5 mm in diameter. Staining tests showed virtually no plagioclase in these rocks. A quartz-muscovite-magnetite rock from zone E contains andalusite breaking down to muscovite, suggesting retrogression from peak metamorphism at 550°–675°C and <2.5 kb ($p_{H_2O} = p_{total}$) (Winkler 1979).

At the uranium occurrences, which lie 1000–1500 m from the granite contact, the paragneisses are usually more mafic, composed of biotite (20–60%), microcline (5–75%), magnetite, epidote and quartz (up to 6%). It is not clear whether the epidote is of detrital or metamorphic origin, or possibly both. Hydroxyapatite was not recognised in the field, and has not been previously reported, but is prominent in zones A, C and D. It is pale greenish grey in hand specimen, forming anhedral single crystals up to 1 cm in diameter at zone A, giving the paragneiss the appearance of a grit or conglomerate containing up to 87% apatite with minor biotite and magnetite (Plate 29). The apatite grains do not show signs of recrystallisation, and are often rimmed with biotite; a small amount



Plate 27 (top): Augen of magnetite in the paragneiss country rocks from the NORI/RA occurrence.

Plate 28: Magnetite-rich laminae in the paragneiss, a few metres from Plate 27. These are assumed to be sedimentary in origin, and clearly pre-date the folding.

was remobilised with biotite into late-stage veinlets at zone C. One apatite sample contained a trace of Cl.

One other lithotype occurs, being a friable, jarosite-stained arenite at zone C and a pale green pyritic arenite at zone E. The E zone material varies from 100% microcline to 95% quartz, with accessory muscovite and andalusite as previously mentioned. Up to 20% pyrite is accompanied by traces of chalcopyrite, sphalerite and molybdenite. The C zone material may be stratigraphically equivalent but more strongly weathered, with up to 20% porosity in some material. It may contain large pyrite cubes, modified by (h,k,0) faces, and a trace of molybdenite. One coarse sample contains 65% pyrite with minor veinlets of late chalcopyrite, 15% biotite, 8% tourmaline, 5% apatite, 5% quartz and traces of microcline and plagioclase. The pyrite both contains and is contained within quartz and biotite grains, and extends into an adjacent mafic paragneiss.

Uraninite is restricted to the mafic paragneiss, although not necessarily to magnetite-rich material, and some radioactive showings also contain tourmaline and molybdenite. The uraninite grains are typically 40 micrometres in diameter, occurring only in the melanocratic units, and in all such units seen except for the isolated magnetite beds in leucocratic paragneiss. Only a trace of tourmaline occurs at the magnetite-rich A zone, where paragneisses composed of biotite, magnetite, Ce-La allanite and microcline contain euhedral uraninite. This uraninite forms zoned and broken cubes of apparently detrital origin up to 40 micrometres in diameter, completely occluded at times within biotite crystals (this texture occurs in a somewhat similar deposit in Labrador (Kerswill and McConnell 1979)) (Plates 30, 31). A little pyrite and chalcopyrite occurs in this material, and the magnetite is sometimes euhedral, which is unusual. Zone D is almost magnetite-free, and the magnetite reported by previous workers may have been fine-grained tourmaline rock, which has not been previously reported from these claims. Radioactivity in this zone is highest in the alteration haloes around pegmatite veins, and the uraninite has apparently been remobilised, occurring as a row of spherical grains up to 200 micrometres in diameter along the contact between biotite schist and a pegmatoid lens in one sample. Other samples show very diffuse uraninite grains, or subhedral uraninite co-existing with small clusters of a few uraninite grains.

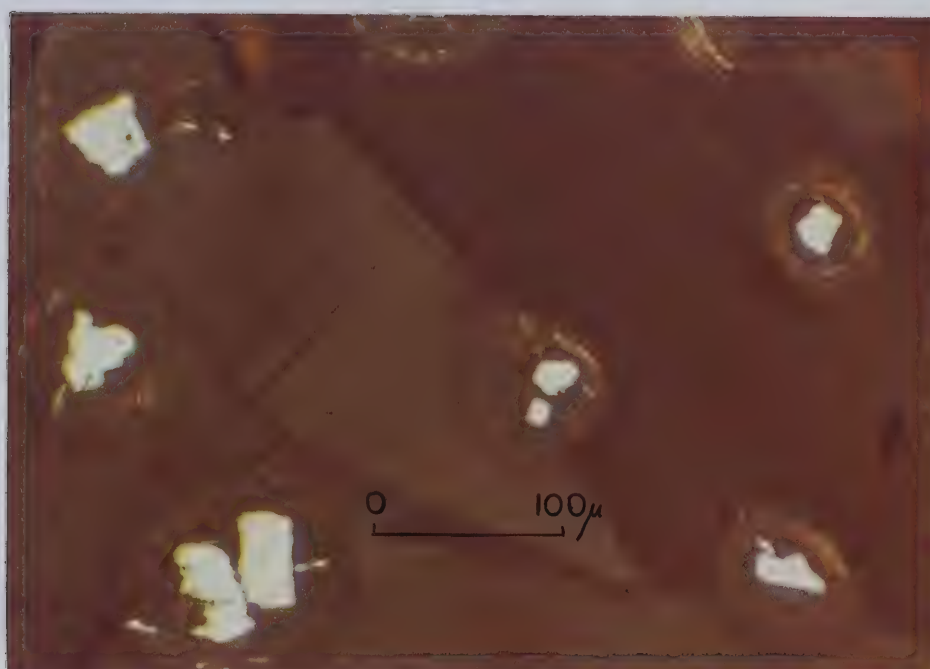
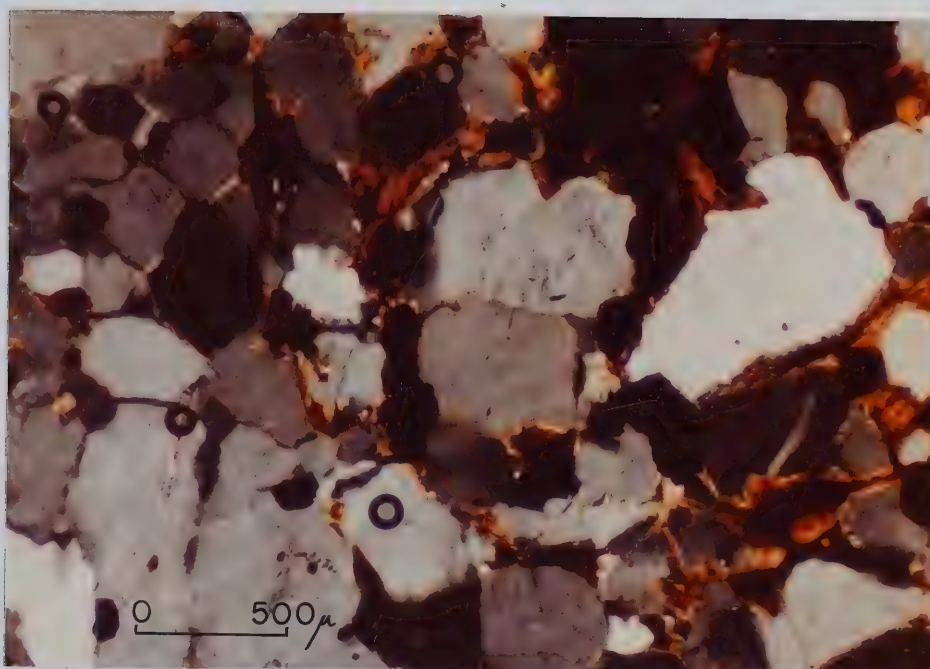


Plate 29 (top): Apatite rock from the NORI/RA occurrence, "zone A". Transmitted light, X-polars, x2.5 objective. Note that each apatite grain is rounded, a single crystal, and surrounded by biotite.

Plate 30: Uraninite grains from the NORI/RA occurrence, "zone A", showing their often zoned, euhedral form. Reflected plane polarised light, x16 objective, under oil.



Plate 31: A selection of uraninite grains from the "zone A" material, NORI/RA claims, showing their zoned euhedral nature. Some have apparently been broken across the zones prior to emplacement within the surrounding coarsely crystalline biotite. Others appear essentially unbroken, some are somewhat rounded, and some could be interpreted as having a core of detrital uraninite with an authigenic overgrowth. All samples in reflected plane polarised light, x100 objective, under oil.

Although traces of tourmaline and molybdenite were found in some showings without pegmatites, the major occurrences are where pegmatites cut biotite-rich rocks. Such tourmalinisation of wall-rock biotite by pegmatite is not uncommon (*e.g.* Kretz 1968, p.87). Coarse tourmaline occurs in the pegmatites throughout the area, and at the showings the pegmatite veins form tourmalinite fringes as thick as the veins themselves, transecting the original schistosity. Zone D is particularly rich in molybdenite, which occurs as tiny hexagonal flakes in the schists within some 30 cm of a pegmatite vein, or more commonly in the tourmalinite fringes, in fractures and sparingly in the pegmatite itself. Assays returned 2.4% MoS₂ (and 0.5% U₃O₈) from zone D (DIAND assessment records). No molybdenite was found outside the uranium showings. Somewhat similar U–Mo mineralisation occurs at Cape Makkovik, Labrador, in metamorphosed rhyolite (Gandhi 1978b).

The original uraninite was apparently deposited here in heavy-mineral lenses in a sequence of microcline-rich arkoses. There is, however, a marked lack of the zircon that might be expected from such material, and which occurs in some other deposits of the group. The distinctive "eyes" of fluorite, pistacite and quartz are also absent. The showings might all be stratigraphically equivalent, and the pyritic arenite might provide a marker horizon to test this hypothesis. After metamorphism, and during the final stages of granite emplacement, tourmaline pegmatite veins caused intense tourmaline alteration of the biotitic wall-rocks. Molybdenite was simultaneously precipitated, presumably due to reactions with suitable wall-rocks, and uraninite within this alteration zone was apparently remobilised and reprecipitated.

De Vries Lake: the UGI/DV claims

(W) (116°44'W, 64°17'N)

The UGI (previously DV) claims lie on the east shore of De Vries Lake, 9 km south-east of the NORI/RA claims (Legagneur 1969; Thorpe 1972; Paterson 1975b, 1976b) (Fig. 26). Similar mineralisation on a nearby island was also once staked, as the FXO claims (Paterson 1975a, 1976a). These claims overlie Snare Group metasedimentary and metavolcanic rocks mapped by Wilson and Lord (1942) as feldspar and quartz–feldspar porphyries, hosted within granite. The bedding and foliation trend

northwards, generally with a moderate easterly but variable dip.

The Snare Group complex is difficult to classify and subdivide consistently. The overall succession comprises a basal pink quartz–feldspar porphyry, overlain by white paragneiss, melanocratic porphyry, melanocratic paragneiss and a white or pale green quartzite. All these lithologies appear to be gradational into each other, even some apparently volcanic and obviously sedimentary types, and differences are more obvious in hand specimen than under the microscope. One reason for this is the intense metamorphism and scapolitisation; another possibility is that rocks which resemble porphyritic extrusives in hand specimen might have been crystal tuffs, which grade into adjacent sedimentary units. The plagioclase in the matrix of these rocks is usually fresh, despite co-existing with scapolite, while plagioclase phenocrysts or clasts are usually completely altered to scapolite, or to saussurite, or in rare cases show signs of alteration to microcline or microcline + titanite. A few zircons were observed in samples throughout the pile, and minor hydroxyapatite is widely distributed.

The mafic paragneisses have grains some 100–200 micrometres in diameter, and are more or less foliated. They are composed of 20–30% quartz, up to 45% plagioclase, up to 30% microcline, up to 55% scapolite, up to 20% opaque minerals, up to 5% biotite, up to 2% apatite, and minor hornblende, epidote, carbonate and titanite. The scapolite was optically identified as Cl-rich dipyre, or approximately marialite 80%, meionite 20% (Deer *et al.* 1963, Vol. 4, p. 329). The opaque phases include magnetite, maghemite, a blueish isotropic non-magnetic iron oxide (R at 591 nm in air = 19%, VHN_{100} = 600), and locally uraninite. Dark purple fluorite is an accessory mineral, and fluorite and pistacite form rare "eyes" in the cleavages of biotite. Patches of recrystallised quartz or scapolite (replacing plagioclase) may represent sedimentary clasts or augen. The mafic porphyry contains anhedral phenocrysts or porphyroblasts of altered plagioclase, perthitic microcline (the exsolved plagioclase being altered), and recrystallised quartz in a fine-grained matrix of plagioclase, microcline, quartz, opaque minerals and up to 30% biotite. Xenoliths of similar material are evident in weathered surfaces, and fragments of microcline–chlorite paragneiss were found in thin sections (Plate 32). The hematite previously reported (Paterson 1976b) was not found. The leucogneiss ranges from pink quartz–feldspar porphyry to white, fine-grained paragneiss, and may not be foliated. It has a granitic

composition of microcline, quartz and plagioclase, but lacks ferromagnesian minerals and has a very variable grain size. The phenocryst phases are 4 mm (quartz) to 1 cm (feldspar) in diameter. The distinctive upper white quartzite unit contains minor biotite and muscovite, and has a linear rather than planar texture in hand specimen.

Several lithologies resembling pegmatites are coarse-grained apatite- or scapolite-bearing rocks. In one lens measuring 5m x 30cm, anhedral apatite grains or plates several centimetres in diameter are accompanied by subordinate hornblende and minor biotite, plagioclase, scapolite and quartz (Plates 33, 34). A second sample contains 90% hornblende, 5% fine-grained quartz, 5% coarse apatite plates and minor uraninite, and a third sample contains coarse scapolite, quartz, hornblende and euhedral titanite, with minor biotite and magnetite. These lithologies can occur within the so-called "porphyries", but may be palaeo-placer concentrations.

Minor metamorphosed and folded mafic and aplitic dykes a few centimetres thick cut the paragneiss. The mafic type is composed of hornblende, plagioclase and titanite, the aplitic type of plagioclase, microcline, quartz, scapolite, biotite and opaque minerals. An appinite-like sill or dyke, several metres thick with a chilled margin, contains euhedral hornblende phenocrysts 5 to 10 mm in diameter, in a matrix of granular diopside or augite, plagioclase and quartz, and minor potassium feldspar, titanite, biotite, carbonate, epidote and opaque minerals. It intrudes the hornblende-apatite rocks described previously, and possibly the dyke could be interpreted as a metamorphosed sediment, or the palaeo-placer as an altered, metasomatised wall-rock.

Uraninite is not concentrated in any particular lithology, and the massive tourmaline or magnetite host rocks typical of the other deposits of this type are absent. Instead, irregular radioactive zones up to 100m x 5m occur parallel to the foliation in the mafic paragneisses and porphyries, containing up to several per cent of Si- and Y-bearing uraninite (Plate 35). Traces of yellow and orange uranophane and beta-uranophane mark the more uraniferous areas. Uraninite also occurs as small anhedral grains in the hornblende-apatite rock previously described, strongly altered to unidentified minerals. The iron oxides are abundant but widely disseminated, and are probably metamorphic in origin. The scapolitisation is ascribed to the reaction of plagioclase (directly or indirectly) with carbonate in the original Snare Group sediments.



Plate 32 (top): Wispy xenoliths within the gneissic "porphyry" at the UGI/DV occurrence.
Plate 33: Pod of apatite-hornblende rock (containing microscopic anhedral blebs of uraninite) from the UGI/DV occurrence. White blebs below lens cap are pure apatite.

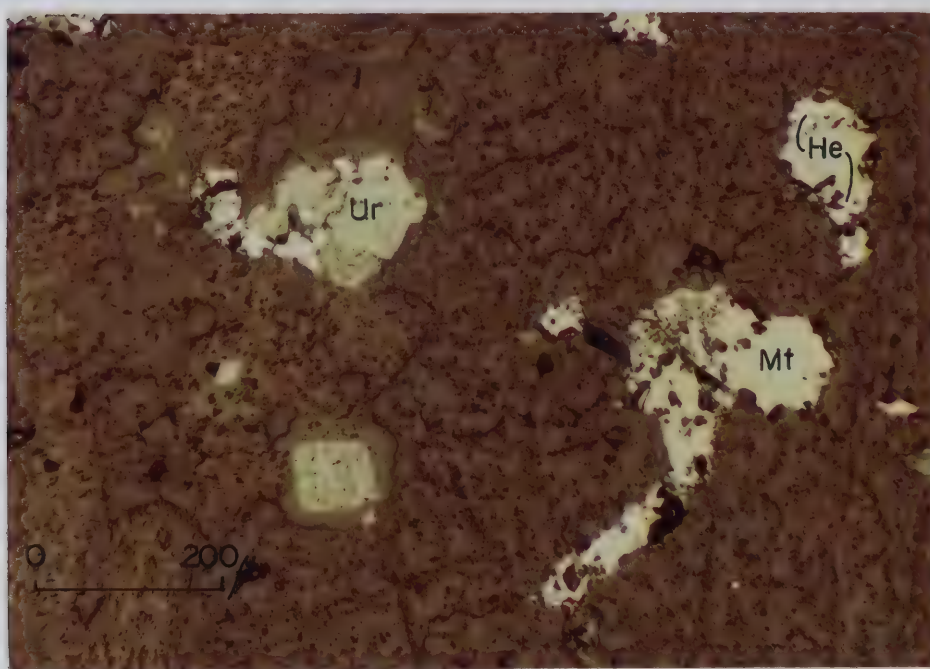
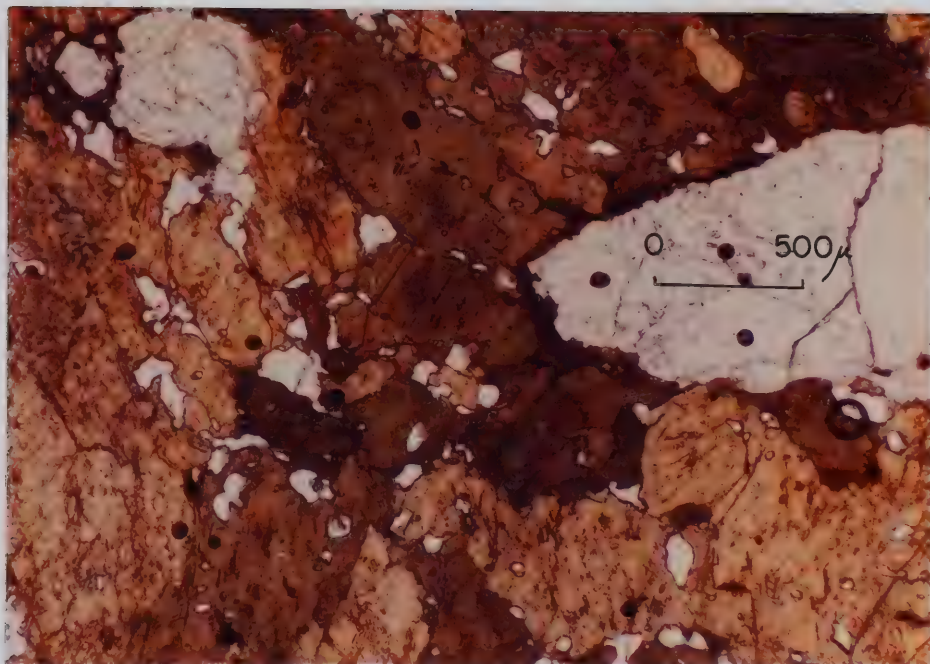


Plate 34 (top): Fine-grained sample of the hornblende-apatite rock in plate 33, UGI/DV occurrence. Note the texture of the apatite, which resembles immiscible textures. (The black blebs are air bubbles in the thin section). Other parts of the section contain significant amounts of uraninite and a minor phase (probably zircon). Transmitted plane polarised light, x2.5 objective.

Plate 35: Uraninite in mafic porphyritic paragneiss from the UGI/DV occurrence. Reflected plane polarised light, x8 objective, in air. Silicate matrix contains uraninite (poor polish; note one euhedral grain), magnetite and hematite.

The genesis of the metamorphosed palaeo-placer deposits

Allowing for the effects of metamorphism, the meta-placer deposits are mineralogically and chemically similar, occurring in the same stratigraphic unit at similar metamorphic grades, and confined to the single narrow belt 5–15 km west of the Wopmay Fault. The Akaitcho and Snare Group rocks elsewhere are apparently not uraniferous although they have a similar aeromagnetic anomaly pattern. The belt pre-dates the 1850–1875 Ma old Great Bear Batholith, and it is probably a molasse deposit at the foot of the 1890 ± 20 Ma old Hepburn Batholith, equivalent to the Cowles Lake and Takijuk Formations (p. 12). It might also be an older remnant equivalent to the Akaitcho Group turbidites, crushed between the two batholiths, but turbidites are unlikely to have formed placer concentrations; moreover, modern volcanic arc sediments are predominantly lithic with abundant plagioclase, and no marine plate tectonic setting is known which produces potassium feldspar sands (Breyer and Ehlmann 1981; Valloni and Maynard 1981). The important difference between the "molasse" and "Akaitcho" models is the provenance of the sediments, being the Slave craton or the Hepburn Batholith respectively. Uraninite has rarely been reported from the Slave craton, strengthening the argument for its derivation from the Hepburn Batholith. Approximately coeval sedimentary rocks from the Coronation Supergroup (Epworth Basin) are known to have higher contents of U, Th and REE than the underlying Archaean metasedimentary rocks (Easton 1981b). Besides the evident similarities, each deposit does have unique mineralogical features, discounting the subsequent tourmaline–molybdenite mineralisation. Such variations both within and between deposits are simply explained by sedimentary models of deposition.

Qualitative electron microprobe analyses of several apatite samples from each of the HAM, JONES, NORI/RA and UGI/DV deposits showed no F or Cl, except for a trace of Cl in one NORI/RA sample, and they are assumed to be hydroxyapatites. Sedimentary phosphorites are usually F-bearing francolite, while fluorapatite is typical of igneous associations, and hydroxyapatite of metamorphic rocks (McConnell 1973).

Any genetic model for these deposits must take into account the following features:

(1) Strata-bound magnetite apparently occurs in a single chrono–lithological unit.

- (2) The occurrences are accompanied by iron-rich, aluminous paragneisses within K-feldspar-rich leucogneisses.
- (3) The tourmaline, apatite, scapolite and minor fluorite indicate enrichment in boron, phosphorus and halides.
- (4) The deposits may exhibit suites of typical heavy detrital minerals.
- (5) Some of the uraninite has a detrital morphology.
- (6) Some of the occurrences are enriched in such elements as Mo, Cu, Zn, Ag, Y, Nb and the rare earths (REE).

The palaeogeography of these deposits is fundamental to their interpretation. The emerging Hepburn Batholith of some 1900 Ma ago formed a north-east trending mountain range at about 35°S (Irving 1979) which may be termed the "Hepburn highlands" (Fig. 4). Western Australia and southwest Africa provide modern latitude analogues, although the Hepburn highlands were probably flanked by the sea on both sides. Nevertheless, the highlands were part of the xerochore, the desert region, without soil or vegetation. The rapid run-off from the low rainfall would produce piedmont fans, flash-flood plains, playa lakes and transient salt pans, much as in the Australian and African analogues. Conglomerates are surprisingly scarce in the paragneiss belt, although rare pebbles do occur, and a sandy terrain is indicated. The emplacement of the Great Bear Batholith followed so closely upon the volcanism of the Hepburn highlands that fumarolic and late-stage activity probably continued while these deposits formed.

The western Hepburn highlands were composed of volcanic and high-level, "S-type" anatectic plutonic suites (p. 167), and metamorphosed pre-existing cover rocks of the lower Epworth (or lower Snare) groups, from which a suite of quartz, feldspar and heavy detrital minerals would have been derived. The original sediment was clearly arkosic, although plagioclase is almost completely absent in one case. Although the newly-oxygenated atmosphere and the lack of a biota would have distinguished late Aphebian weathering processes from modern, plagioclase and ferromagnesian minerals were probably the first major phases to be destroyed. Plagioclase in semi-arid and humid granitic terrains weathers more rapidly to limonite, kaolinite and smectite than does potassium feldspar, although not to the complete exclusion of plagioclase (James *et al.*

1981). Potassium metasomatism during metamorphism or granite intrusion might be required to account for the local predominance of microcline.

Within the palaeo-xerochore, xerogenic uranium deposits could be formed, that is, deposits which owe their formation to a dry climate. These can be broadly divided into placers and duricrusts, both of which are probably present, but difficult to distinguish after metamorphism. The term "meta-placer" is used because some detrital characteristics have survived, such as the form of the uraninite grains, the presence of zirconiferous laminae and the shape of some magnetite bodies. Placers could be formed by aeolian winnowing of desert sands, or in the transient rivers, or by the marine reworking of sands along a possible shoreline. A shoreline environment would permit sabkhas as a source of carbonate for the meta-calcareous rocks. Such placers would contain typical "felsic" mineral suites of tourmaline, apatite, magnetite, ilmenite, xenotime, monazite, zircon, allanite-epidote and thorium uraninite, precisely those minerals found in the deposits. For comparison, the time-equivalent red-beds 1800 ± 160 Ma old at Richmond Gulf, Hudson Bay, are braided fluvial conglomerates and arkoses, with heavy-mineral lenses which contain magnetite, titanomagnetite, zircon, apatite, thorite and monazite (Miller and Kerswill 1980); as stated, conglomerates were not found in the meta-placer deposits. The recent placer deposits derived from the Archaean Slave craton described by Folinsbee (1955) have been concentrated from eskers overlying Archaean schists, migmatites and granitoids; lake shore beach sands washed from the eskers form heavy-mineral lenses 15–30 m long, 1–3 m wide and 15 cm thick, containing less than 1% combined quartz and feldspar. These are well-sorted, pebble-free, medium- to fine-grained sands. Apatite, andalusite, garnet, kyanite, sillimanite, staurolite, epidote and magnetite (at one lake) are "abundant", biotite, pyroxene and tourmaline are "minor", scheelite and olivine are "rare", rutile, brookite and zircon are present but were not assessed quantitatively, and monazite forms 1% of one sample. Allowing for a paucity of metamorphic minerals, similar but uraniferous placer lenses could have been derived from the Hepburn highlands, and no special source of sedimentary apatite or magnetite is required.

Modern duricrust deposits are perhaps best known from Yeelirrie in Western Australia, 27°S of the equator, where carnotite, $\text{K}_2(\text{UO}_2)_2(\text{VO}_4)_2 \cdot 3\text{H}_2\text{O}$, has been deposited

by evapotranspiration processes in a dolomitic calcrete (Mann and Deutscher 1978; Langford 1978b). Ferricretes and laterites have also been extensively developed, and the total lithology is a reasonable precursor for the paragneiss belt. Carnotite is the only uranium mineral present at Yeelirrie, however, and vanadium is conspicuously absent from the paragneiss deposits (and indeed apparently from all uranium deposits throughout the entire batholithic complex – p. 191). A phosphate such as autunite, $\text{Ca}(\text{UO}_2)_2(\text{PO}_4)_2 \cdot 10\text{--}12\text{H}_2\text{O}$, might be similarly precipitated from phosphatic solutions in the absence of vanadium; a possible mechanism would be the precipitation of calcrete, a reduction in the dissolved carbonate content of the groundwater, and breakdown of dissolved uranyl carbonate complexes. If this was the case, the hydroxyapatite might be either the original source of phosphate or a product of the metamorphic breakdown of autunite. The high volcanic activity of the palaeo-environment also suggests high levels of metalliferous brines in the groundwaters, containing U, Cu, Mo, Pb, Zn, Ag, B, F, Cl, C and S. Concentrated in salt pans and lakes and reacting with the host rocks during metamorphism, these could produce the tourmaline, scapolite, apatite and various sulphides found. Significant original boron could only have been present in detrital minerals (considered unlikely) or as evaporites and brines, since Fleet (1965) showed that boron is adsorbed by clays, preferentially illite, to a maximum of only 100 ppm (although montmorillonite containing 2160 ppm boron has been synthesized from 5 ppm boron solutions (Brockamp 1973)).

This is not to deny a role to the Great Bear Batholith granitoid plutons, which may have remobilised and assimilated these elements. Tourmaline, molybdenite and possibly some uraninite at the NORI/RA claims, for example, was emplaced by pegmatites of this batholith. Whether the necessary elements were introduced by the pegmatite, or simply remobilised from the country rocks, is not known. If the granitoids are anatectic, they may have assimilated and recycled xerogenic concentrations of these elements. Apatite commonly accompanies the tourmalinisation around some pegmatites (Kretz 1968).

Other genetic models

Both placer and duricrust formation can account for the paragneiss-hosted deposits, and both should be expected in xerogenic uranium deposits, although

metamorphism has destroyed much of the textural evidence except for the detrital form of some uraninites. Further remobilisation by granitic intrusions has resulted in deposits which, individually, are open to several different interpretations. The magnetite has been previously regarded as metavolcanic ironstone (Paterson 1976c), veins or intrusions (Ahuja 1974; Gill 1969a), and the uraninite as metamorphic segregations or hydrothermal impregnations (Gandhi 1978a). They are clearly not volcanic ironstones, veins or magmatic intrusions, although remobilisation into veins has occurred. Relict sedimentary textures argue against the metamorphic segregation of magnetite beyond the scale of the ubiquitous augen, but much of the uraninite could have been formed in this way. Nash (pers. comm. 1982) has suggested that this chemical association, here and elsewhere (as in the Mary Kathleen area of Australia or the Highlands of New York) is better explained by chemical sedimentation in a marginal marine setting.

Iron-phosphorus associations are well known elsewhere, and a few may be reviewed.

(1) Phosphorites can be associated with marine ironstones; phosphorite deposits of late Aphebian age exist elsewhere, and between 1900 Ma and 1800 Ma ago, the regional palaeolatitude was suitable for phosphorite deposition (Christie 1980; Cook and McElhinny 1979).

(2) Magnetite-apatite-actinolite pods such as at the Terra mine, Echo Bay, were both replacive and intruded as a crystal mush at $<600^{\circ}\text{C}$, probably derived as immiscible fractions from monzonitic plutons (Badham 1973a).

(3) Magnetite-apatite-actinolite veins with K-feldspar, quartz, uraninite, pyrite, chalcopyrite, calcite, fluorite and rare earth element minerals occur within monzonitic laccoliths in the Great Slave Basin (Badham 1978; Bloy 1979).

(4) Magnetite, apatite and Zr, U, Th and rare earth elements commonly occur in carbonatites (Notholt 1979; Erdosh 1979; Erickson and Blade 1963), and alkaline complexes such as the Big Spruce Lake and Blachford Lake suites (p. 16) (Martineau 1970; Davidson 1978).

(5) The Kiruna-type magnetite + apatite \pm amphibole ores display wall-rock alteration and late apatitic veins containing quartz, muscovite, chlorite, tourmaline, monazite, titanite, allanite, zircon, fluorite, albite, calcite, barite, talc and skarn minerals (Frietsch 1978; Parak

1975). These nelsonite ores are probably intrusions of an immiscible liquid containing 30–40% apatite and 60–70% magnetite, emplaced at 850°–1000°C (Philpotts 1967), although sedimentary origins have also been proposed (Parak *op. cit.*). Volatiles such as B, F and H₂O might lower the eutectic melting point to some 650°C, the probable temperature of the JACKPOT deposit magnetite veins. The Kiruna deposits may have acquired Zr, Ba and rare earths from an original magma of alkaline/carbonatite affinity.

Magnetitic uraniferous rocks are not uncommon. The Miles Standish mine, New York, contains a magnetite ore-body hosted by amphibolite in quartz–feldspar gneiss and alaskite of late Grenville age; the augitic wall-rocks contain quartz, allanite, apatite (10%), sulphides, monazite/bastnaesite intergrowths (5%), minor uraninite and a uranium–rare earth phosphosilicate (Baillieul and Indelicato 1981). Baillieul and Indelicato propose that the magnetite acted as a geochemical trap for U, P and REE derived from a fluid phase separated from the alaskite magma. The Th/U ratios were 0.15 and 5–7 in the two walls, and up to 60 in similar nearby deposits. Baie Johan Beetz, in Quebec, is a Grenville age migmatitic complex of quartz–plagioclase paragneisses, autometasomatised to granite, where zircon, uraninite and uraniferous magnetite occur in the granite adjacent to the more mafic paragneisses; the mineralisation has been ascribed to metamorphic remobilisation from U–Zr-bearing sediments (Hauseux 1977). At Pilot Lake, south of Great Slave Lake, U- and Th-bearing lenses of biotite, monazite, zircon, ilmenite and hematite ± apatite, plagioclase and quartz, formed in Kenoran or Hudsonian paragneisses, have been interpreted as metamorphosed placers (Burwash and Cape 1981; Cape 1977). Other examples occur in Labrador (Kerswill and McConnell 1979), where a two-stage sedimentary and metamorphic origin was proposed; possibly in the vicinity of Rabbit Lake and Key Lake, Saskatchewan (Hoeve and Sibbald 1978, p.1456; Dahlkamp 1978, p.1444); at Karpinka Lake, Saskatchewan, where they have been interpreted as meta-rol front deposits (Sawiuk and Williams–Jones, 1981); and in the unmetamorphosed basal Helikian Athabasca Formation, Saskatchewan (Munday 1979).

It becomes apparent that this type of lithology is not particularly age-dependent, nor controlled by the atmospheric oxidation state, and that it is associated with much higher-grade, better-known uranium ore deposits. This may be one of the commoner protores of uranium deposits.

The source-rock potential of the meta-placer deposits

Conventional wisdom has been that uraninite is not stable during metamorphism, certainly at granulite facies (Heier and Adams 1965). It has nevertheless survived metamorphism to at least 600°C in these deposits, despite volatile fluxing (albeit with apparent lead loss, reducing its isotopic age to that of the granite), perhaps due to particularly reducing conditions. The assimilation of such deposits could provide uraniferous or magnetite-rich igneous rocks, as at Mazenod Lake (p. 93) and possibly the CAM showing (p. 43). Similarly, the belt itself is an obvious source material for later hydrothermal deposits, such as the adjacent Rayrock mine, JD and Coppermine River occurrences. It is not suggested as a source material for the Echo Bay and Hottah Lake deposits, due to its apparently limited distribution. A corollary is that Snare Group rocks with a strong aeromagnetic response are good exploration targets for Rayrock-type vein deposits, as well as for possible multi-element deposits in their own right.

V. ISOTOPIC ANALYSES

A major program of isotopic dating was undertaken, and 106 samples of pitchblende and uraninite and 5 samples of uranophane and beta-uranophane were analysed, while lead from 11 sulphide and 5 carbonate samples was also analysed. No corrections for mass fractionation were made. The results from the pitchblende/uraninite and some sulphides were presented in Miller (1982) (Appendix III), and are summarised in chapter VI, while the secondary minerals are covered in chapter VIII. The remaining data and some comments on techniques and interpretation are presented here.

A. Uranium-lead dating

The sample preparation, analytical techniques and precision have been described elsewhere (Miller 1982), and of more concern here is the interpretation of the data. Two problems are unique to pitchblende/uraninite analyses as compared to studies on zircon and other refractory minerals: (1) the mobility of the major elements; (2) the inheritance of radiogenic lead.

Because uranium is mobile, a pitchblende sample may represent a significant time-span of initial crystallisation, or may have been partially dissolved, re-precipitated or augmented after formation. Even detrital uraninite from the meta-placer deposits may have occasional authigenic uraninite overgrowths, and Cumming and Rimsaite (1979) have demonstrated the presence of extremely small micro-domains within pitchblende. Most of the samples used here did not show obvious multiple stages of growth, and the risk of mixing generations was minimised by careful optical study and by using as few grains as possible, preferably one, for analysis. 300 micrograms of UO_2 was adequate for analytical purposes. The opposite technique of analysing bulk samples has the advantage that there may be no overall gain or loss of lead or other mobile daughters, but episodes of gain or loss cannot then be identified.

Two mixed generations of pitchblende may still yield useful concordia-plot information if subsequent lead loss has been minimal, plotting on a mixing-line discordia between the two events. Nevertheless, possible continual remobilisation and

reconstitution of pitchblende, coupled with diffusive \pm episodic lead loss and possible ^{222}Rn migration, induces a scatter in the data which results in discordia and isochrons which are not statistically valid lines within measurement error. The migration of ^{222}Rn was convincingly demonstrated by Ludwig *et al.* (1981). The errors assigned to ages from such lines were therefore multiplied by the square root of the mean square weighted deviates (MSWD) when MSWD was greater than 2, a technique suggested by Dr. G.L. Cumming (pers. comm 1982). This additional error factor makes allowance for the scatter caused by unavoidable geological factors.

Lead may be as mobile as uranium; for example, lead minerals were co-precipitated with pitchblende at Mazonod Lake (Miller 1981), and shortly after the pitchblende at Echo Bay. When uranium is remobilised from its source, the accumulated radiogenic lead may follow it in significant amounts, and enter the new generation of pitchblende or form accessory minerals. This may be termed the uranogenic lead contaminant, to distinguish it from the rest of the common lead.

If the common lead is isotopically homogeneous, a $^{207}\text{Pb}/^{206}\text{Pb}$ isochron of the pitchblende analyses avoids the problem of uranogenic lead contamination, and such contamination is seen as an isochron which passes above the assumed "ordinary" mantle lead growth curve (a topic discussed further on). Such isochrons are only valid when any parent or daughter loss or gain has occurred relatively recently, but in this study they gave generally good results. In contrast, the U-Pb concordia plot can cope with single events of parent or daughter loss at any time ("episodic loss"), but the common lead must first be corrected out. Herein lies the problem: what is its composition? If it is assumed that the common lead was derived entirely from country rocks of a known age, an ordinary lead composition of that age may be used as a first approximation, but there is no way of knowing *a priori* whether a significant uranogenic lead contaminant is present.

$^{235}\text{U}/^{207}\text{Pb}$ isochrons, not used in this study, will indicate initial $^{207}\text{Pb}/^{204}\text{Pb}$ ratios, but $^{238}\text{U}/^{206}\text{Pb}$ isochrons can give erroneous results due to the loss of ^{222}Rn from the system (Ludwig *et al.* 1981). U-Pb isochrons are not reliable when major episodic lead losses have occurred (*e.g.* Rosholt *et al.* 1973).

Large amounts of uncorrected uranogenic contaminant lead will move data points on a concordia plot. Assuming at this stage that subsequent lead loss has not occurred,

the points define a mixing line between their true position on the concordia (x Ma) and a position representing samples containing only uranium and the inherited uranogenic contaminant lead (Fig. 27); if this contaminant lead comes from a single source, the mixing line intersects the concordia at the age of that source (y Ma). In effect, a discordia is produced; mathematically, a pitchblende sample x Ma old which has acquired uranogenic lead y Ma old is identical to a pitchblende sample y Ma old which lost some of its lead x Ma ago. Thus a discordia is produced with the true mineralisation age at the lower intersection and a "precursor" age at the upper, the age of the precursor uranium source (disseminated or forming an older deposit).

Two further considerations apply. Firstly, the uranogenic contaminant may be a mixture, for example from old country rocks and a later hydrothermal uranium deposit, in which case the upper discordia intersection falls between their ages, and is the maximum age of the younger source and the minimum age of the older. Secondly, subsequent lead loss will move the data points. This movement of all points towards the origin lowers the lower discordia intersection and raises the upper (see, for example, the Mazenod Lake plots, p. 251 *et seq.*). Depending upon the proportionality of losses, the discordia may also be somewhat rotated in either sense, but if all samples lose the same proportion of all their lead, the new discordia is parallel to the old.

The approach taken was to assume that the common lead was an ordinary lead of the $^{207}\text{Pb}/^{206}\text{Pb}$ age of the sample, using the mantle lead model of Stacey and Kramers (1975); similar results are obtained with the model of Cumming and Richards (1975). Any contaminant radiogenic lead would then be seen as an upper discordia intersection age markedly greater than the age obtained from a $^{207}\text{Pb}/^{206}\text{Pb}$ isochron. The Mazenod Lake material provides a classic example of this effect. Other indications of contaminant uranogenic leads are Pb–Pb isochrons which pass above the assumed ordinary lead growth curve, and a discordia where samples with progressively more common lead, and hence lower $^{206}\text{Pb}/^{204}\text{Pb}$ ratios, plot progressively higher up the discordia. High $^{206}\text{Pb}/^{204}\text{Pb}$ ratios suggest, but do not prove, that there is little common lead present, and thus that the radiogenic contamination is probably insignificant. From the isochron, it is possible to construct models for the actual, non-ordinary common lead, which was attempted for the Mazenod Lake suite and resulted in a revised discordia age within reasonable error of

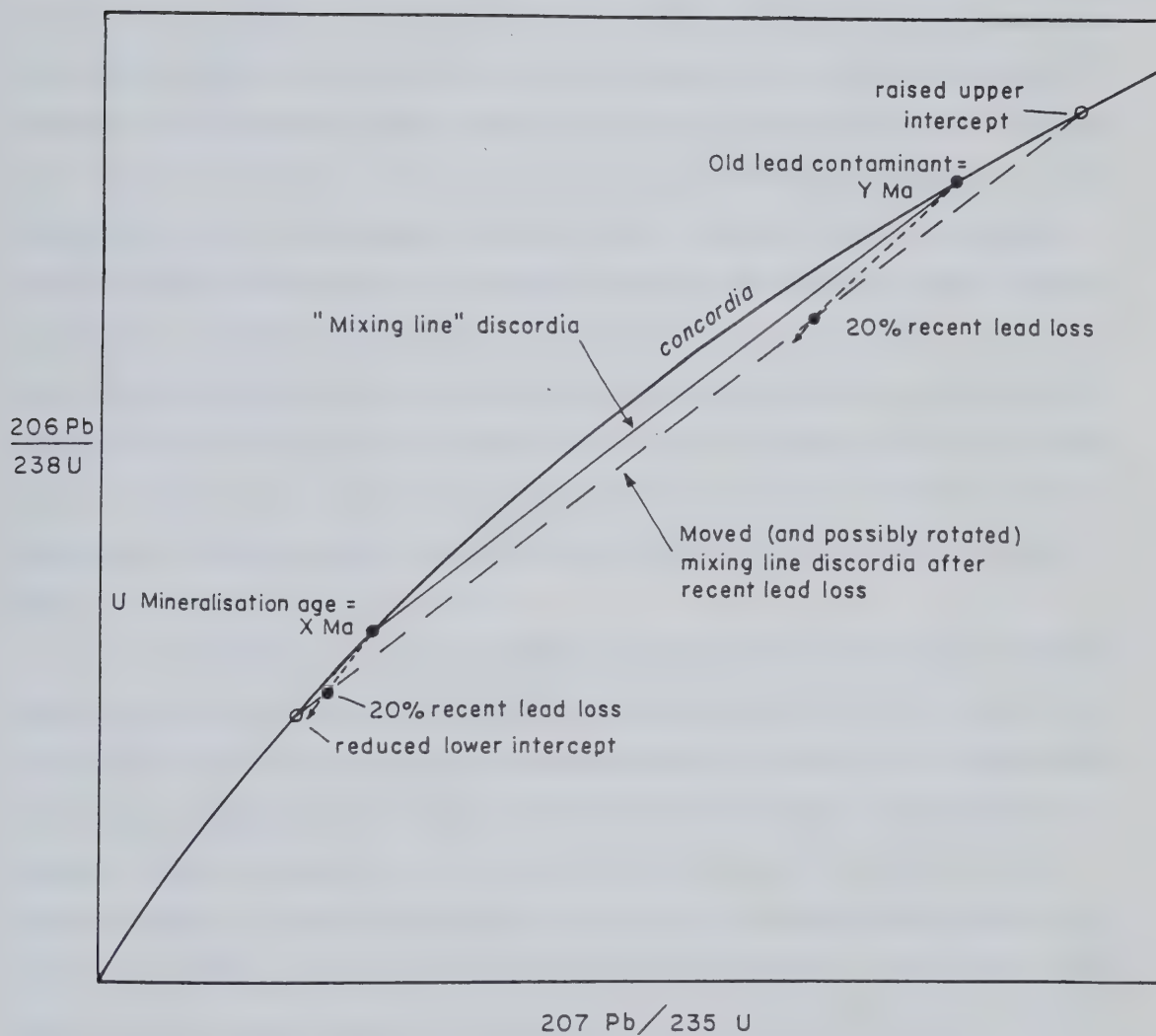


Figure 27: Generalised U/Pb concordia plot, showing the effect of contaminant older radiogenic lead and subsequent lead loss.

the isochron age (Miller 1982).

The models used for the ordinary, mantle-type lead assume a μ value ($^{238}\text{U}/^{204}\text{Pb}$) of about 9 in its source. Difficulties are numerous: (1) the source material of the Great Bear Batholith has not been identified; (2) the μ value of the underlying mantle is not known; (3) the μ value of the igneous suites is not known, and some can be shown to be probably contaminated by crustal anatexis; (4) changes in μ values have a greater effect on younger deposits, having been in force longer; (5) ordinary and radiogenic lead may not be extracted from a source rock such as a granite in their true proportion. The only salvation is to note that gaitena from a probably volcanogenic-exhalative sulphide body in the Echo Bay area gives a reasonable, slightly young, model age, using a value of approximately 9 (Miller 1982, after Thorpe 1974). Some workers have used the lead in co-existing lead minerals as a suitable common lead composition, but enough studies have shown, and this study showed again at the JD group of deposits, that lead minerals may be created from or augmented by accumulated radiogenic lead from trace uranium contents or from the adjacent uranium minerals, and need not represent the common lead.

It is remarkable how such possibilities of contamination with radiogenic lead from precursor deposits are often unconsidered. Many authors tend either not to specify, or not to justify, their choice of common lead composition. For example, in a regional study of uranium mineralisation in the Alligator Rivers region of northern Australia, Hills and Richards (1976) used lead from Mt. Isa, over 1000 km away, for all corrections, lead with a considerably younger model age than the lower Proterozoic rocks hosting the mineralisation (although to be fair, the common lead in their material was very low, and the correction probably insignificant). Cahen *et al.* (1971) used concordia plots and concordant pitchblende analyses to subdivide the Zairean uranium mineralisation into eight stages between 235 Ma and 706 Ma without specifying the correction, although again the internal consistency of their results suggests no great error despite the high precision such a tight subdivision requires. In dating very young material, such as the 51 Ma pitchblende studied by Ludwig *et al.* (1981), extreme care in the choice of common lead would be required if concordia plots were attempted (although these are not useful for young material); as these authors demonstrate, the lead within associated

sulphides may have a wide range of isotopic composition.

B. Sulphide lead analyses

Pyrite and chalcopyrite from the meta-placer deposits, a djurleite sample from Achook Island and a galena sample from the FALCON occurrence were analysed, and are described in Miller (1981) (Appendix III). Three other chalcopyrite samples were also analysed, using the same techniques (Table 3).

McLaren Lake

Described previously on page 18, chalcopyrite sample A2K from the giant quartz vein at McLaren Lake had lead isotope ratios which yield a negative model age (Table 3).

Assuming an 1850 Ma old common lead according to the model of Stacey and Kramers (1975), a radiogenic $^{207}\text{Pb}/^{206}\text{Pb}$ ratio of 0.1025 is obtained, with a maximum source age of some 1670 Ma and a maximum mineralisation age of some 960 Ma. No reliability is placed on these numbers, which are strongly influenced by the model chosen and are given only for the sake of completeness.

Dease Lake

Two chalcopyrite samples from the JOHN claims were analysed, samples A26F and A26G, to see if any indication of a syngenetic or epigenetic origin can be deduced. The lead is strongly radiogenic, either due to traces of uranium in the sulphide or to the incorporation of radiogenic lead. Considered as a 2-point $^{207}\text{Pb}/^{206}\text{Pb}$ isochron, they yield a slope of 0.0705, representing a maximum source age of some 940 Ma and a maximum mineralisation age of 510 Ma. They may represent either, (1) recrystallisation, incorporating radiogenic lead shortly after uranium mineralisation during the Palaeozoic transgression; or, (2) more probably, recrystallisation as uraniferous chalcopyrite during the Mountain Lake depositional event at 1076 ± 96 Ma. Although no great weight is laid upon these dates, the sulphide is not an original syngenetic sulphide, but has probably recrystallised from one, and incorporated traces of uranium in the process.

<u>Sample</u>	<u>Composition</u>	<u>$^{206}\text{Pb}/^{204}\text{Pb}$</u>	<u>$^{207}\text{Pb}/^{204}\text{Pb}$</u>	<u>$^{208}\text{Pb}/^{204}\text{Pb}$</u>	<u>$\pm\%$ error</u>
A2K	Chalcopyrite	21.13	15.84	39.19	0.03%
A26F	Chalcopyrite	113.39	21.91	44.50	0.56%
A26G	Chalcopyrite	831.39	72.54	42.73	1.98%
A38E	Algal dolostone	21.99	16.76	42.75	~5%
A38F	Algal dolostone	22.44	16.04	40.60	~5%
A38Giii	Algal dolostone	18.29	15.65	38.16	0.4%
B21E	Dolomite cement	24.85	16.24	42.84	0.8%
B21F	Sandy dolostone	17.96	15.71	37.43	0.6%

Table 3: Lead isotope analyses of sulphide and carbonate samples (excluding those of Miller 1982 (Appendix III)).

C. Carbonate lead analyses

Five samples of algal dolostone and dolomite-cemented sandstone from the Hornby Bay Group were analysed, to see if either their absolute age or the relative age of the cement and the uranium mineralisation can be determined (Table 3). The lead in oceanic waters should correspond to a zero model age, although it has not been directly measured (Doe, in Wedepohl *et al.* 1969–1978). Lead could be expected to co-precipitate with calcite or dolomite, and 5 ppm Pb is the mean content for sedimentary carbonates (Wedepohl, *op. cit.*).

The samples analysed were free of visible sulphide and detrital heavy minerals:

A38E, grey stromatolitic dolostone, unit 9, Mountain Lake.

A38F, white oolitic dolostone, unit 9, Mountain Lake.

A38Giii, white pisolitic dolostone, unit 9, Mountain Lake.

B2 1E and B2 1F, dolomite-cemented quartz sandstone, Hornby Bay Group, Raspberry Ridge, Leith Peninsula.

The analytical data are presented in Table 3. The samples were dissolved overnight in HCl, centrifuged and evaporated to dryness, then re-dissolved and passed three times through ion exchange columns. This treatment did not remove all organic matter, and the final loads on the rhenium filaments appeared grey and tarry; the mass spectrometer runs were highly unstable. Although the blank would have been comparatively large, enough sample lead appeared to be present for the results to be moderately significant. Probably less than 10 g of carbonate was dissolved from each sample.

Most of the results yield negative model ages, and are far too imprecise to date the carbonates. Traces of zircon or sulphides, both present in adjacent strata, would be sufficient to cause the negative ages. The results show no significant difference between the two types of carbonate, and neither contains a significant amount of radiogenic lead. Two conclusions are drawn:

- (1) The carbonate cement predates any uranium mobilisation, at least in the Leith Peninsula area; it is probably derived from the surrounding dolostones, and it probably represents the original cement which was subsequently silicified in the Mountain Lake deposit.
- (2) The dolostones of unit 9 were not precipitated in a closed evaporitic basin, which would probably have had a high input of radiogenic lead from the uraniferous hinterland

(see the discussion of the dispersed uranium content of the batholith – p. 179). An evaporitic source of uranium within unit 9 for the Mountain Lake deposit is therefore unlikely.

VI. DEPOSITIONAL CORRELATIONS AND CONTROLS

A. Foreword: the isotopic ages

The most fundamental correlation is the timing of mineralisation, and a summary of the isotopic dating results is a necessary prelude to this chapter. The concept of "contaminant lead / precursor uranium deposit" ages was detailed in Chapter V; suffice it to state here that the upper intersections of certain U–Pb discordia are controlled by a lead contaminant, and may represent the minimum age of that contaminant; they may or may not be meaningful.

The oldest mineralisation event is indicated by an upper U–Pb discordia intersection from some of the pitchblende–hematite fels of Beaverlodge Lake, yielding a date of 2058 ± 34 Ma. This age may be a true mineralisation age, or the minimum age of a uranogenic lead contaminant (and, by inference, of a precursor uranium deposit). The lower intersection reflects a 440 ± 57 Ma mineralisation event which is better defined by pitchblende from the PITCH 8–10 claims. The 2058 Ma age may be related to the exotic terrain, which outcrops at Hottah Lake and might form the "Snare Group" roof pendants at Beaverlodge Lake.

The next oldest deposits are the meta–placers, with a mean age of 1860 ± 20 Ma. Two separate ages are in fact defined, at 1849 ± 12 Ma and 1872 ± 8 Ma, but since the deposits involved (JACKPOT + JLD and HAM + UGI/DV + NORI/RA respectively) do not form obvious geographical groups, the significance of the two ages is uncertain; they may reflect two widespread pulses of granite intrusion and updating of the uraninite. None of this uraninite shows any isotopic trace of an earlier history, probably because (1) its presumed source, the Hepburn Batholith, is only 1890 ± 20 Ma old; and (2) it has been metamorphosed to at least 650°C . The zircons may perhaps yield a greater age, although some may be metamorphic in origin (*e.g.* HAM and JONES occurrences).

Major uranium mineralisation occurred some 1500–1400 Ma ago; two pitchblende samples from the SHORE deposit and one from Echo Bay suggest an early event at 1500 ± 10 Ma, prior to a main mineralisation event at 1424 ± 29 Ma. The 1424 Ma event extended southwards from Achook Island to Echo Bay, Dog Island, probably to the PITCH 27–28 deposit (1450 ± 150 Ma), and possibly to the PITCH 8–10 deposit, where it

is seen as a possible age for a contaminant uranogenic lead. It may also have extended south-eastwards to the JD claims, where a contaminant lead is at least 1428 ± 18 Ma old. As stated (p. 72), the mineralisation at Echo Bay was probably emplaced by hydrothermal activity associated with the intrusion of a sheet of the Western Channel diabase. The full extent of this group of sheets is unknown, but they extend from at least Hornby Bay to Echo Bay, and quite possibly accompany all the 1400–1500 Ma mineralisation events.

The Mountain Lake deposit (1076 ± 96 Ma old) and the T1 and Main zone deposits (1092 ± 115 Ma old) reflect in some manner the final stages of the Mackenzie diabase event (p. 16). Contaminant uranogenic lead in the Mazenod Lake mineralisation also has a minimum age of 1201 ± 62 Ma.

The remaining deposits are all Palaeozoic in age. The Coppermine River supergene pitchblende yields ages of 415 ± 29 Ma (from ECHO), 536 ± 66 Ma (from TABB), and 420 and 660 Ma (single $^{207}\text{Pb}/^{206}\text{Pb}$ ages from the SOUTH and FC deposits); the JD pitchblende is 535 ± 164 Ma old; the Mazenod Lake pitchblende is 457 ± 26 Ma old; the PITCH 8–10 and some Beaverlodge Lake pitchblende is 440 ± 57 Ma old (the date of possible lead loss at Beaverlodge Lake); and the Rayrock mine pitchblende is 511 ± 86 Ma old. The study also showed possible lead-loss events in all the older deposits, dated at 395–450 Ma, and some essentially recent lead loss from all the deposits.

These data lead to some general, tentative conclusions:

- (1) The exotic terrain has contained uranium sources, either concentrated in uranium deposits or dispersed in the country rocks, older than the Great Bear Batholith.
- (2) Major mineralisation events extended across at least the central third of the batholith at 1400–1500 Ma, and across the entire batholith during the Mackenzie diabase event and again during the Palaeozoic era.
- (3) Uranium has not been significantly remobilised in the batholith since the Palaeozoic era.

Bloy (1979) dated seven groups of uranium deposits from the Great Slave Basin, which might be expected to reflect similar trends. Mineralisation at the REX, FAIR and CC claims is hosted by, and probably derived from, monzonitic laccoliths, the remainder by sedimentary suites; the regional geology is described by Badham (1978). The ages

obtained are:

Simpson Islands: 1510 ± 9 Ma and approximately 0 Ma by U–Pb discordia, and 1405 Ma by a poor Pb–Pb isochron.

Toopon Lake: 2130 ± 25 Ma and 37 ± 1 Ma by U–Pb discordia⁵, and 1715 Ma by Pb–Pb isochron. (This discrepancy cannot be satisfactorily explained by a uranogenic lead contaminant from a precursor deposit, in the manner detailed by Miller 1982).

Meridian Lake (Reliance) and *Union Island (MDM/DM claims)*: 1671 ± 22 Ma and 91 ± 12 Ma by U–Pb discordia, 1575 Ma by Pb–Pb isochron.

Stark Lake (REX and FAIR claims) and *Labelle Peninsula (C.C. claims)*: 1755 Ma and approximately 0 Ma by U–Pb discordia (no errors stated), 1785 Ma by Pb–Pb isochron.

These deposits appear to correlate primarily with local magmatic intrusions (the laccoliths and the Easter Island Dyke, p. 14), except for the 1405–1510 Ma age from Simpson Island, which correlates with the major 1400–1500 Ma event described in this study. None of the Great Slave deposits shows the Palaeozoic event.

B. Genetic, geological, geographical and structural comparisons

Four categories of deposits can be defined and considered separately:

(1) *Helikian sandstone-hosted deposits*: The Mountain Lake, Dease Lake and Leith Peninsula groups.

(2) *Metamorphosed palaeo-placers*: The JACKPOT, HAM, JONES, JLD, NORI/RA and UGI/DV deposits.

(3) *Supergene deposits*: Most of the Coppermine River group: the term is used here for uranous mineralisation as opposed to concentrations of secondary uranyl minerals.

(4) *Hydrothermal deposits*: Possibly FALCON and FLOW of the Coppermine River group, the Echo Bay group, Achook Island, Dog Island, the JD group, Hottah Lake, Beaverlodge Lake, Mazenod Lake and the Rayrock mine.

The Helikian sandstone-hosted deposits

The genesis of these deposits was discussed with their descriptions, and they are all essentially similar in type, genesis, mineralogy and (as far as is known) age. The

⁵These ages are this author's interpretation of three of Bloy's four data points.

controls upon their distribution within the Hornby Bay or Dismal Lakes Groups are uncertain. The position of the Mountain Lake deposit upon an apparently isolated basement horst (Fig. 12) suggests that a syngenetic factor was an important control upon the epigenetic mineralisation. Whether such horsts are common or underlie other deposits, or precisely how they affected epigenetic mineralisation, is not known, but their identification might prove to be an exploration guide. Sandstones of units 8, 11, 12 and the Rae Group appear to have similar uranium–mineralisation potentials, although only the sulphidic or carbonaceous members need be considered if syngenetic minerals were the primary reducing agents during uranium mineralisation. The Cretaceous sandstones were also pointed out earlier as potential host rocks, although the palaeoclimatic correlation does not favour post–Cretaceous mineralisation (p. 161).

The late Aphebian palaeo-placer deposits

These deposits, some of which may also have been duricrust–hosted deposits prior to their metamorphism, form the xerogenic group of Morton and Miller (in prep.), and owe their creation to a unique combination of climate, topography and source materials. The palaeotopography would have controlled the original distribution of the deposits, which probably formed upon and around piedmont fans (aeolian placers), in transient braided river valleys or on coastal beaches (fluvial and beach placers) and in dry valleys or playa lakes (duricrusts). The Hepburn Batholith appears to have had an equal source potential all along the western flank, although parts of the eastern flank are remobilised Archaean crust rather than "S-type" granitoid plutons. There does not seem to be any way of predicting the present–day distribution of these deposits, although they have a distinctive aerial geophysical signature of combined magnetic and radiometric anomalies. Equivalent deposits east of the northern Hepburn Batholith in the Cowles Lake and Takijuk Formations (p. 12) might be expected. However, the effect of the (then) north–east trending Hepburn highlands upon the prevailing winds and precipitation could have had a significant effect upon the formation of surficial deposits.

The hydrothermal and supergene deposits

These groups cannot be clearly distinguished (Gandhi 1978a), and supergene pitchblende concentrations probably occur throughout the batholith, not only at the Coppermine River. It must be emphasized that isotopic dating did not show any deposits younger than some 400 Ma, and "supergene" refers to a process not necessarily restricted to the recent past. It will be shown later that supergene pitchblende has probably not been deposited in this area in the past 100 Ma (p. 198). There is a complete continuity of process between hydrothermal and supergene deposits, but from the fieldwork and published literature, some generalisations may be made:

- (1) Supergene deposits generally form between the land surface and the water-table, ancient or modern.
- (2) Supergene deposits are more likely to have a carbonate gangue, derived from uranyl carbonate complexes, and a simple mineralogy.
- (3) Hydrothermal uranium deposits are more likely to have a quartz gangue, a complex mineralogy, and pitchblende formed in the early stages of mineralisation (Rich *et al.*, 1977).
- (4) Hydrothermal deposits are likely to have extensive wall-rock alteration.
- (5) Hydrothermal deposits are likely to be larger.

These are in no sense diagnostic criteria. Supergene deposits are also gradational into unconformity-associated types of deposit, and the position of the Coppermine River deposits, demonstrably at the sub-Helikian unconformity, may be significant. The present erosional level of the rest of the Great Bear Batholith with respect to this unconformity is one of the major unknown factors in this study.

The hydrothermal and supergene deposits are structurally and lithologically controlled. In terms of structural correlation, a changing regional stress pattern could result in a correlation of the orientation of mineralised fractures with time. This is a difficult concept to test as the majority of the hydrothermal and supergene deposits do not follow single, well-defined fractures. Furthermore the batholith has been anisotropic since its creation due to the intense development of north-east trending faults, which

channelled subsequent movement. Finally, local lithological contacts, dykes and subsidiary fractures seem to be the most important structural controls; for example, pitchblende veinlets at the Rayrock mine and JD zone deposits occupy irregular fractures inclined to the adjacent giant quartz veins. Some data are listed in Table 4, and include the strikes of both major veins and minor veinlets. The only correlation found is that most of the deposits strike trend between 035° and 110° , and the 1400–1500 Ma old deposits strike 045° – 080° . This cannot be regarded as significant without more data.

The lithological controls are the requirements for sources of uranium and reducing agents; the role of uraniferous source rocks is discussed later. Even though solutions may be introduced from outside the immediate system, they are controlled by their original source rock and the final wall-rock chemistry, and correlations between mineralised veins and their host rocks might be expected. The JD Zone, the PITCH 8–10, and some of the Beaverlodge Lake and supergene occurrences, are all hosted by mafic rocks, which partly reflects the permeability of lithological contacts, but also the role of mafic rocks as reducing agents. Reductants appear to be generally available, although ferrous silicates seem to be the principal species involved, hence the disproportionate association of pitchblende veins with diabase, here and around the world (Smith 1974). Diabases therefore play two roles, by remobilising uranium during their emplacement and by acting as chemical traps afterwards (it is again unfortunate that the age of the dyke at the PITCH 8–10 deposit is uncertain; the possibility that it is as young as the pitchblende cannot be ignored). The requirement for a pH buffer in uranyl carbonate- or hydroxyl-bearing, pitchblende-depositing systems has been discussed (p. 25 *et seq.*), and wall-rock alkali metasomatism involving the conversion of original and secondary micas to feldspar, as well as alteration of the original feldspars, may not just reflect the coincidental introduction of alkalis with uranium, but may be a necessary part of the precipitation mechanism as a pH buffer (*e.g.* p. 80–81). The frequency of alkali metasomatism in unmineralised parts of the batholith is not known.

Uraniferous vein mineralisation does not seem to select between plutonic or volcanic host rocks. Data on the mineralogy of the plutons are insufficient to determine whether specific igneous suites are favoured, except possibly in the Echo Bay area, discussed previously (p. 72–73) and again on p. 167–169. Felsic volcanic rocks host the

<u>Deposit</u>	<u>Orientation of mineralised veins (strike, strike/dip)</u>
Echo Bay	045°–070°/North, steep
Achook Island	080°/Irregular
JD Zone	045°/74°W, 163°/80°W
T1 Zone	098°/68°S, 117°, 122°/66°S
DB3 showing	109°
Main Zone	041°/79°N, 041°–074°/66°N
PITCH 8–10	016°/62°E, 029°/75°E (major direction)
PITCH 27–28	034°/65°E
Beaverlodge Lake	057°/57°S, 075°/76°N, 096°/71°N
Rayrock mine	Giant quartz vein: 040° Pitchblende veinlets: 90°–100°/60°N–60°S

Table 4: Orientations of pitchblende–mineralised veins from the Great Bear Batholith. (The majority of veins seen are irregular in orientation).

veins at Echo Bay, Achook Island, Dog Island and Mazenod Lake; granitic rocks are the hosts of the T1 and Main zone deposits, the PITCH 8–10 and 27–28 deposits, and the Rayrock deposit. Basaltic greenstone, quartzite, gabbro and a giant quartz vein host mineralisation at the JD, Beaverlodge Lake and Rayrock deposits. No deposits are known within the exotic terrain.

C. The mineralogical and geochemical correlations

Multi-element whole-rock analyses were not performed, and this discussion is based upon the observed and reported mineralogy and the electron microprobe analyses performed; the meta-placer deposits are not included.

Table 5 shows the observed elemental associations of each deposit. Na and K indicate host-rock metasomatism, Si represents quartz gangue, and Fe and S are given as pyrite/marcasite, hematite and magnetite. Hematite refers only to hematite in the mineralisation, not in the wall-rocks (where it may be produced by weathering). A "?" indicates doubtful assignation to the paragenesis, although the entire paragenesis is considered, not just the uranium-precipitating stage. Although quartz and carbonate are given, they may not always be associated directly with the uranium mineralisation. Graphite (restricted to the Akaitcho Group schists), chlorite (ubiquitous but usually minor) and fluorite (easily overlooked at low concentrations) are not included. The Echo Bay area has the largest element list, being the most intensively studied, but even allowing for errors of omission amongst the other deposits, several points of interest arise:

- (1) Alkali metasomatism is restricted to the obviously hydrothermal deposits.
- (2) Virtually all the hydrothermal deposits contain quartz.
- (3) Most of the probably supergene deposits contain carbonate.
- (4) Cu, Co and As are ubiquitous, but Ni is apparently absent from the supergene deposits (although Ni accompanies numerous unconformity-associated deposits elsewhere, e.g. Key Lake).
- (5) Elements unique to the hydrothermal deposits include Pb, Zn and Ti (if the FALCON and FLOW showings are hydrothermal), Se, REE, Mo, Te and Bi.
- (6) Se, Te, Bi and perhaps hydrothermal Ag are restricted to the south-western part of

THE ELEMENTAL CHEMISTRY OF THE URANIUM DEPOSITS

Deposit	Na	Si	P	K	Ti	Mn	Co	Ni	Cu	Zn	As	Se	REE	Mo	Ag	Te	Ba	Pb	Bi	FeS ₂	Fe ₂ O ₃	CO ₃ ²⁻
MAC	✓						✓		✓		✓									✓	✓	✓
BESS							✓		?		✓											
FALCON	✓							✓	✓	✓								✓		✓	✓	✓
ECHO								✓							?				✓	✓	✓	✓
FLOW					✓																	✓
SOUTH																					✓	✓
FC									✓										✓			✓
TABB	✓						✓				✓								✓	✓	✓	✓
Mountain Lake	✓				?		✓	✓	✓	✓	✓				?		✓		✓	✓	✓	
Dease Lake								✓	✓	✓	✓						✓				✓	
Raspberry Ridge								✓	✓	✓	✓											✓
Echo Bay/Eldorado	✓		?	✓		✓	✓	✓	✓	✓	✓	✓			✓	✓	✓	✓	✓	✓	✓	✓
Achook Island	✓				?		✓	✓	✓	✓	✓										✓	✓
Dog Island	✓				✓																✓	✓
JD Zone	✓							✓	✓									✓				✓
T1 Zone	?	✓		?	✓														✓	✓		✓
Main Zone	?	✓		?				✓	✓								✓	✓	✓	✓		
PITCH 8-10	✓							✓	✓			✓			✓			✓	✓	✓	✓	✓
PITCH 27-28	✓							✓	✓	✓			✓	✓		✓		✓	✓	✓	✓	
Beaverlodge Lake	✓								✓								?		✓	✓	✓	
Mazenod Lake	?			✓					✓						✓	✓		✓	✓	✓	✓	?
Rayrock mine	✓						?	✓	✓		✓								?		✓	

Notes: 1 = reported by Kieller (1962).

? = reported (unpublished), dubious assignation in paragenesis or uncertain identification.

Elements are those involved in primary mineralisation and metasomatism, not secondary mineralisation.

Table 5: The chemistry of the accessory mineralogy of all the uranium deposits studied.

the batholith; as far as is known, this is true of the non-uraniferous deposits as well.

(7) The PITCH 27–28 deposit has a unique metallic mineralogy, perhaps due to the neighbouring exotic terrain.

(8) The Beaverlodge Lake deposits have the most chlorite and the simplest mineralogy, being essentially quartz, chlorite, hematite and pitchblende.

Chlorite is not a particularly common accessory or gangue mineral; it occurs, in decreasing amounts, in the Beaverlodge Lake, PITCH 27–28, T1 and Rayrock mine mineralisation. Although chlorite + pitchblende is a common paragenesis in other parts of the world (*e.g.* Koongarra, Australia; Snelling 1980), much of the chlorite found in the study area simply occurs as chloritic shears or by the alteration of biotite.

The simple quartz–hematite–pitchblende paragenesis typifies most of the approximately twenty vein pitchblende deposits within 50 km of the Rayrock mine which are described by McGlynn (1971). These are probably all the same age as the Rayrock and PITCH 8–10 deposits, which they resemble, and the mineralogically distinct but nearby Mazenod Lake deposit, *i.e.* some 440–520 Ma old. Hematite, a common accessory in hydrothermal uranium deposits (Rich *et al.* 1977), often apparently reflects the oxidation of ferrous silicates, and as Table 5 shows, it more commonly occurs in hydrothermal veins than in supergene veins. Other reductants such as sulphides may be more common in supergene deposits.

No strong correlation can be drawn between age and mineralogy among the non-placer deposits. If, as the isotopic study suggested, many of these deposits are remobilisations of older ones, this is not surprising. Factors such as the source mineralogy, the host rock lithology and the physico-chemical conditions of deposition probably over-ride any temporal trends. With the exception of the Mazenod Lake deposit, the Palaeozoic occurrences may have a slightly simpler mineralogy, and the two selenide occurrences are both Palaeozoic. All the supergene, sub-unconformity pitchblende from the Coppermine River area is Palaeozoic, although a galena sample suggested that the FALCON showing there is considerably older (Miller 1982).

A digression on copper mineralisation

Virtually all the deposits studied contain copper, from traces to major and possibly economic concentrations, as at Echo Bay and Mazenod Lake. A major conclusion of this study is that uranium was originally concentrated before and during the formation of the Great Bear Batholith, and has subsequently been repeatedly remobilised. Copper may be showing a similar effect, occurring with uranium or forming its own unique suites of deposits. Copper mineralisation of porphyry type is rumoured to have been located on Great Bear Lake, although Hoffman and Cecile (1974) found no such indications; it is abundant in the Coppermine River Group basalts as indigenous native copper and in hydrothermal veins; it occurs as stratiform syngenetic bodies in the Hornby Bay Group sandstones and dolomites; it has been recorded from shales in the Rae Group and from Palaeozoic shales near Leith Peninsula; and it commonly occurs in the giant quartz veins. Copper, like uranium, is mobilised as oxidised species, although it requires a stronger reducing agent for its precipitation as sulphides. Copper in the batholith probably has a history of remobilisation and precipitation parallel to that of uranium.

D. The tectonic and climatic correlations

Apparently, certain episodes of mafic magmatism (the Western Channel and Mackenzie diabbases) caused the hydrothermal or groundwater remobilisation of uranium in the Great Bear Batholith, and might act as guides to exploration. The Coronation–Franklin diabbases (about 675 Ma old) appear to have had less effect, apart from the single 660 Ma date from the FC deposit, although this could be a result of sampling too few deposits. The Palaeozoic deposits coincide with the Palaeozoic transgression and regression 600–350 Ma ago, and could be caused by major changes in the groundwater chemistry and flow regimes and the height of the water-table, coupled with heat sources such as diabbases or deep crustal fractures. If this is the case, why were no deposits apparently formed by the Cretaceous transgression? Perhaps, (1) this in fact caused some of the recent lead loss observed; (2) it was less extensive; (3) in the absence of magmatic or tectonic activity, heat sources were not available for hydrothermal circulation cells; (4) the palaeoclimate was unfavourable.

Figure 28 is derived from Irving (1979), and shows the palaeolatitude of a reference point at De Vries Lake, as calculated from palaeomagnetic studies. Defining a "tropical latitude" as being within 0° – 20° of the equator, tropical latitudes prevailed at approximately 1830–1700 Ma, perhaps 1440–1310 Ma, 1100–960 Ma, 740–630 Ma and 580–370 Ma; there is a data gap for the period 1450–1650 Ma. All the dated uranium deposits fall into these periods with only a small margin of error, except for the "precursor" 1201 Ma date from Mazenod Lake. (The 2058 Ma date from Beaverlodge Lake is assumed to reflect a uranium or lead source in the exotic terrain, for which the palaeolatitude curve need not apply before about 1850 Ma). These tropical periods approximately coincide with tectonic activity, namely the emplacement of the batholith, the Western Channel, Mackenzie and Franklin diabase events, and the Palaeozoic transgression. *No* cause and effect relationship is inferred! However, uranium would have been extensively oxidised and moved into groundwater systems under deeply penetrative tropical weathering conditions. Such solutions could then have entered any available hydrothermal system, perhaps with intermediate stages of concentration by processes such as supergene enrichment. The Cretaceous climate, similar to today's, may have inhibited uranium mobilisation and consequently explains the lack of deposits created during the Cretaceous transgression, compared to the Palaeozoic transgression.

Palaeoclimate may prove to be one of the most important controlling factors in uranium mineralisation, and this relationship would bear further study. For example, Jonasson and Dunsmore (1979) found minor uranium mineralisation in Pennsylvanian-age limestone breccias on Ellef Ringnes Island (approximately 78°N , 100°W), but apparently not in adjacent Mesozoic rocks containing lignites, coals and other potential reductants and precipitants of dissolved uranium. Perhaps this reflects uranium mobility during warm climates (the island was 31°N of the equator during Pennsylvanian times) rather than recent mineralisation under cold conditions. Similarly Dunsmore (1971) suggested a lower Carboniferous evaporite, originally deposited 5° from the equator, as the source of some northern Nova Scotia uranium deposits in upper Carboniferous rocks. The data of Bloy (1979) (p. 153) neither confirm nor refute such a climatic correlation.

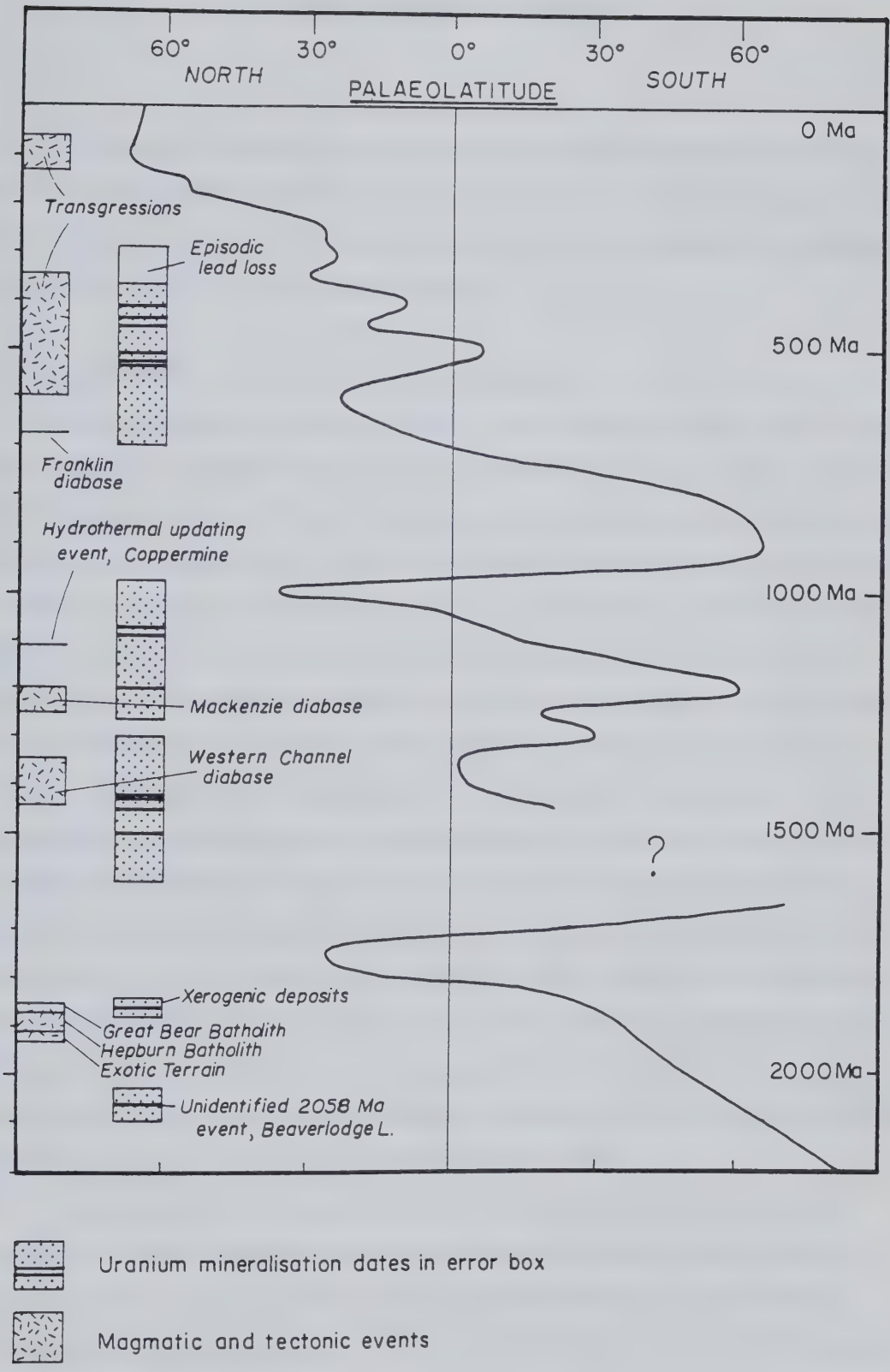


Figure 28: The correlation of uranium mineralisation with tectonic and magmatic activity and palaeolatitude.

VII. THE SOURCES OF URANIUM

The possible sources of uranium for the vein deposits include host rocks with dispersed uranium, placer concentrations, and other pre-existing uranium deposits. These may be considered from the aspects of isotopic factors, their geographical locations and their present and inferred past uranium contents.

A. The limitations of $^{208}\text{Pb}/^{204}\text{Pb}$ and $^{208}\text{Pb}/^{206}\text{Pb}$ ratios

As the daughter of ^{232}Th decay, the ^{208}Pb content of an epigenetic mineral is partly controlled by the Th content of the source, and the $^{208}\text{Pb}/^{206}\text{Pb}$ ratio is partly controlled by the Th/U ratio of this source. Assuming a sub-crustal origin for the batholith at 1850 Ma (data are scarce, but see Robinson and Morton 1972), its common lead would have been the ordinary mantle lead at that time, or approximately $^{206}\text{Pb}/^{204}\text{Pb} = 15.47$, $^{207}\text{Pb}/^{204}\text{Pb} = 15.26$ and $^{208}\text{Pb}/^{204}\text{Pb} = 35.10$ (Stacey and Kramers 1975). Any addition of lead from sources beyond the batholith at later dates is assumed to be negligible, so that the ^{204}Pb now in a pitchblende sample came from this original common lead. Common and radiogenic leads need not be released equally from the source rock, depending upon the phases hosting them and the degree of metamictisation, so that lead of any $^{208}\text{Pb}/^{204}\text{Pb}$ ratio >35.1 is theoretically extractable from the batholithic rocks. The $^{208}\text{Pb}/^{204}\text{Pb}$ ratio measured in a uraniferous epigenetic mineral cannot therefore prove anything about the source rocks. The only certain use of the $^{208}\text{Pb}/^{204}\text{Pb}$ ratio in thorium-free uraniferous samples is to ascertain the homogeneity of the common lead, and to suggest cogenetic sample groups. A constant $^{208}\text{Pb}/^{204}\text{Pb}$ ratio suggests thorium-free pitchblende with a uniform common lead, while a linear relationship between $^{208}\text{Pb}/^{204}\text{Pb}$ and $^{206}\text{Pb}/^{204}\text{Pb}$ ratios suggests a uniform common lead in uniformly thorian material.

The Th : U ratio of source rocks may be calculated for certain lead-bearing minerals, such as the J-type anomalous galena at Echo Bay (Miller 1982). From the general radioactive decay equations, it may be calculated that the radiogenic lead extracted *at any time* from a rock or mineral up to 1850 Ma old has a $^{208}\text{Pb}/^{206}\text{Pb}$ ratio of approximately its present Th/U ratio X 0.33; this assumes that ^{208}Pb and ^{206}Pb are released

proportionately from the source, which may not be the case if Th and U are hosted by different minerals. Hydrothermal pitchblende generally contains <0.25% ThO₂ (Heinrich 1958), which is perhaps 3X the electron microprobe detection limit by energy-dispersive techniques. Such pitchblende with a $^{206}\text{Pb}/^{204}\text{Pb}$ ratio of 10,000 may therefore have a $^{208}\text{Pb}/^{204}\text{Pb}$ ratio of up to $35.1 + 8.3$, or 43.4, due to an inherent Th content. All but eleven of the vein pitchblende samples have $^{206}\text{Pb}/^{204}\text{Pb}$ ratios <10,000, and $^{208}\text{Pb}/^{204}\text{Pb}$ ratios greater than about 43 in these samples are therefore caused by a radiogenic component from the source rocks entering the pitchblende. The Th/U ratio of the source cannot be calculated without knowing the $^{208}\text{Pb}/^{206}\text{Pb}$ ratio of the lead extracted from it which entered the pitchblende as the common lead. This in turn cannot be measured due to the subsequent generation of ^{206}Pb in the pitchblende.

Despite their unprovability, certain inferences may still be drawn. The highest $^{208}\text{Pb}/^{204}\text{Pb}$ ratios measured, up to 1094, were from meta-placer uraninite samples, known to contain thorium in some instances. If lead was transported with the uranium, deposits created by the remobilisation of the meta-placers could have unusually high $^{208}\text{Pb}/^{204}\text{Pb}$ ratios, such as the Mazenod Lake, Rayrock mine and T1 zone deposits, which have mean $^{208}\text{Pb}/^{204}\text{Pb}$ ratios of 55.9, 52.7 and 56.7. By comparison, most of the other vein deposits have $^{208}\text{Pb}/^{204}\text{Pb}$ values of 36 to 46. Note, however, that the JD and Main zone deposits are also adjacent to the meta-placer deposits, with $^{208}\text{Pb}/^{204}\text{Pb}$ ratios of only 36–39, while the Beaverlodge Lake/Hottah Lake pitchblende has highly variable $^{208}\text{Pb}/^{204}\text{Pb}$ ratios of 37 to 73, and is about 70 km from the meta-placer deposits. However, small, comparatively unmetamorphosed placers in the exotic terrain on Bell Island contain local Th concentrations which might explain the high $^{208}\text{Pb}/^{204}\text{Pb}$ ratios of the Beaverlodge and Hottah Lakes material (p. 178).

Uranogenic lead contamination and precursor uranium deposits

The isotopic study proved that the common lead incorporated during the formation of some pitchblende samples contained a radiogenic, contaminant component in addition to 1850 Ma old ordinary lead. Indicated sometimes by high $^{208}\text{Pb}/^{204}\text{Pb}$ ratios as discussed above, it was also shown by certain anomalous upper intersections on U–Pb discordia plots which gave ages different from those of the $^{207}\text{Pb}/^{206}\text{Pb}$ isochron plots;

the topic was discussed in Chapter V. Such intersection ages were always less than 1850 Ma with the possible exception of the Beaverlodge Lake material, and they therefore represent uraniferous sources *younger* than the batholithic rocks. Although sources of contamination such as the diabase dyke swarms may be invoked, the simplest explanation is that the present uranium deposit is composed of uranium remobilised from an older one, and has inherited some of its precursor's radiogenic lead. This is regarded as very strong evidence for the recycling of uranium deposits, an inherently probable and frequently suggested process but one which has rarely been proven before (see, *e.g.* Smith 1974). Merely finding several generations of pitchblende in one deposit does not constitute proof, contrary to Cohen *et al.* (1971).

B. The geographical location of the sources and deposits

The distance between a uranium source and a host rock in hydrothermal or ground-water systems is a completely unknown factor. Obviously a closer lithological unit is a more likely source than a similar, more distant one, and older deposits, such as the JLD occurrence, are logical sources for adjacent younger deposits, such as the JD group (Fig. 25). In this respect, the general perimetric distribution of uranium deposits around the Great Bear Batholith margin may be significant; although it may reflect such factors as stratigraphical proximity to the sub-Helikian unconformity, it is suggested that the principal, often pre-batholithic sources of uranium had this distribution, and the younger deposits were formed by their remobilisation over short distances. Thus, the meta-placer deposits form the eastern perimeter along the foot of the Hepburn Batholith, the exotic terrain with its unidentified uranium source (p. 92, 151) forms the mid-western margin, and the unidentified batholithic uranium source of the Echo Bay and Camsell River area occurs at the northwestern margin.

C. The dispersed uranium content of the batholith: local enrichment

Even when the uranium content of a rock is known, its role as a potential uranium source is not. Possible sources may now be depleted, their uranium leached and transported away to form deposits; conversely they may be the anomalously uraniferous rocks.

Although pre-batholithic uranium deposits may have supplied uranium for many of the younger deposits, this is apparently not the case for the largest known deposit, at Echo Bay, where a specific suite of plutons may have been the source of Ag and possibly U. Do "fertile" plutons exist, and can they be identified geochemically? And, on a larger scale, is the entire batholith anomalously uraniferous?

"S-type" and "I-type" granitoids

The French usage of "fertile" refers to granitoids with relatively high and significantly leachable uranium contents (*e.g.* Leroy 1978). Such granitoids are frequently the so-called "two mica", biotite-muscovite granites, where episyenitisation frequently accompanies uranium deposition (Morton, in prep.). The distinction of "S-type" and "I-type" granitoids may also be helpful, "I-types" being derived from the partial melting of pre-existing igneous rocks, or perhaps from the mantle, and "S-types" being formed by the partial melting of sedimentary rocks (Chappell and White 1974; Hine *et al.* 1978). Uraniferous sedimentary rocks, such as Archaean or Proterozoic meta-pelites and meta-placers, could produce relatively uraniferous "S-type" granitoids, although "I-types" may also become uranium-enriched by extreme differentiation processes, and should not be ignored. Table 6, from Morton (in prep.), lists some identification criteria for the two types. The only field criteria which apply to the Great Bear Batholith are the presence or absence of meta-pelitic xenoliths, amphiboles and biotite. None of the other diagnostic minerals for either type were seen, and the chemical and isotopic criteria were not tested. Meta-pelitic xenoliths are abundant in the granitoids along the Wopmay Fault paragneiss belt, and also in some of the exotic terrain granitoids at Bell Island, Hottah Lake (McGlynn 1979).

Field and published data were compiled to discover the distribution of biotite-, biotite-amphibole- and amphibole-granitoids in the batholith. No patterns are evident for the biotite-bearing varieties, and the data do not cover much of the batholith. The amphibole-granitoids are restricted to the very earliest (the Mystery Island suite - Fig. 14) and the very latest (the hornblende-tonalites - p. 9). The latter are insignificantly rare and small, and essentially random in their known distribution (Hoffman 1978b). The association of the Mystery Island suite with the silver-bearing deposits in the Echo

"S-type Granites"

- (a) These are generally aluminous and often carry large amounts of metapelite xenoliths.
- (b) They can carry aluminous minerals such as cordierite, garnets (almandine–spessartite–pyrope) and sillimanite.
- (c) Their biotites are aluminous (Al in the octahedral sites)
- (d) Their $^{87}\text{Sr}/^{86}\text{Sr}$ ratios are >0.709 .
- (e) Their $\delta^{18}\text{O}$ values are >10 per mil.
- (f) They carry ilmenite and/or pyrrhotite (reflecting an exceptionally low $f\text{H}_2\text{O}$ and thus a concomitantly high $p\text{CO}_2$, $p\text{CH}_4$ etc.
- (g) They may carry minor quantities of graphite.

"I-type Granites"

- (a) They have low-Al biotites.
- (b) They carry magnetite and pyrite.
- (c) Their ferromagnesian minerals are often pyroxenes or amphiboles.
- (d) If garnets are present, they are Mn-rich.
- (e) Their $^{87}\text{Sr}/^{86}\text{Sr}$ ratios are <0.709 .
- (f) Their $\delta^{18}\text{O}$ values are <10 per mil.
- (g) They have high Na/K and high Na, K, Ca : Al ratios.
- (h) Their xenoliths are hornblende-rich.

Table 6: Criteria for distinguishing "S-type" and "I-type" granites (after Morton, in prep.).

Bay/Camsell River area has been discussed previously (p. 73). Notably, the coeval Achook Island Cu–U deposits are silver–free and at some distance from these plutons, while the Dog Island uranium mineralisation is adjacent to a small hornblende–granite stock. The JD Zone and Hottah Lake deposits, which show some evidence of the same 1400–1500 Ma old event, are neither significantly silver–bearing nor close to these plutons. Since uranium–free silver deposits are also known from the Echo Bay area, as at Camsell River (Badham 1973a), it was suggested that Ag, Bi, Co, Ni and As were derived from these plutons, perhaps from their aureoles, and the U and perhaps the Cu from a different, but unidentified, source. As Badham (1973a) pointed out, similar silver mineralisation is frequently associated with calc–alkaline magmas along continental margin subduction zones. A similar conclusion of separate U and Ag sources may apply to the deposits of the Great Slave Basin, where Ag–Co–Ni–As mineralisation is derived from a suite of alkaline intrusions, and U–apatite–actinolite veins are associated with younger calc–alkaline diorites (Badham 1978).

The plutons of the Hepburn and Wentzel Batholiths north of 66°N have been well documented, and have some of the "S-type" granitoid characteristics; they are biotitic, and:

"Although accessory garnet occurs in nearly all the more felsic plutons, it is extraordinarily abundant (more than 5%) in certain plutons of Wentzel Batholith" (Hoffman *et al.* 1980).

The nature of the Hepburn Batholith south of 66°N is not well documented, but as far as is known it is probably similar along the western side; the south–eastern flank is known to consist of remobilised Archaean basement (p. 5). As such, this batholith is a reasonable and logical source for the uranium in the xerogenic, meta–placer deposits to the west.

Whole-rock sampling and analysis for U and Th

Country–rock samples were collected from all the sites visited during fieldwork, and to some extent they have a natural bias, since the fieldwork was usually conducted in mineralised areas. The samples all come from surface exposures, and were usually about 1 kg in size. It is not suggested that such small samples are representative of their units, but the results for the sample groups probably have some statistical significance.

Samples were prepared by sawing off all weathered faces and grinding down all other surfaces, in case of contamination with pitchblende during sample collection and transport. These were conventionally crushed by a jaw-crusher, disc mill and swing mill. The disc mill contributes large amounts of tramp iron to the sample. This can be removed from normal silicate rocks but not from magnetite-rich paragneisses, for which the disc mill step had to be omitted. The iron does not contribute uranium or thorium, but dilutes the sample by several per cent.

139 samples were analysed for U and 66 for Th by Dr. E. Hoffman of Nuclear Activation Services, McMaster University, Ontario, by neutron activation (Appendix II). The detection limits cited are 0.1 ppm U by delayed neutron counting and 1.0 ppm Th by instrumental neutron activation analysis (E. Hoffman, pers. comm. 1981). The accuracy limits are not stated, but are probably greater than the detection limits. 24 samples were analysed for U in both the U and Th aliquots, with a reproduceability of ± 1 ppm (usually within ± 0.4 ppm), a variation at least partly due to inhomogeneity in the small sample sizes involved (5g for U, 1g for Th). Nine samples of variably mineralised ignimbrite from a single unit on Dog Island returned relatively uniform Th analyses of 15–20 ppm, despite U contents of 4.5–1240 ppm, showing not only the reproduceability of the analytical results for Th but its relative immobility during uranium mineralisation. Weighing errors are insignificant, being $\pm 0.1\%$. The results are given in Table 7, divided into various lithotypes and geological domains. Badham (1973a) and Robinson (1971) reported a number of uranium analyses from rocks in the Camsell River and Echo Bay areas, which have been incorporated in the tables and discussion.

Weathering and loss of U and Th

Simple averages of these analyses are meaningless, since the loss of uranium by surficial leaching has been well established, at least for granitic and tuffaceous rocks. Stuckless and Nkomo (1978) and Rosholt *et al.* (1973) found recent losses of 70–80% of the uranium in surface samples from Wyoming granites, and Barbier and Ranchin (1969) showed that 65–70% of the uranium in the French St-Sylvestre granite is leachable. In the two-mica St-Sylvestre granite, much of the leachable uranium occurs as accessory uraninite; conversely, 70% of the uranium in French biotite granites occurs in

WHOLE-ROCK URANIUM AND THORIUM ANALYSES

Note: The following abbreviations apply throughout this table:

EXT	Extrusive
INT	Intrusive
SED	Sedimentary
META	Metamorphic
MIN	Probably or definitely mineralised (usually uranium secondary minerals)
GRAN	Granitoid
GAB	Gabbroic
GNE	Gneissic
PEG	Pegmatitic
REG	Regolith
EXO	From the "exotic terrain"

Many analyses appear in more than one section of the table.

<u>Granitoids</u>				
Sample	Uppm	Thppm	Th/U	Sample description
A4F	4.5			Perrault Lake, St.Germain pluton, diorite, INT GRAN
A6Biii	2.2	37.0	16.8	CON quartz monzonite, Hepburn Bath., INT GRAN
A6Diii	510.3			CAM St.Germain pluton, INT GRAN MIN
A6Div	17.6	12.0	0.7	CAM, St.Germain pluton, granite, INT GRAN
A7Dii	7.6	11.0	1.45	BEAR, granite, Hepburn Bath., INT GRAN
A18D	4.9, 5.7	24.0	4.5	Rayrock mine, quartz monzonite, INT GRAN
A20G	1.6, 1.5	5.0	3.2	Bell Island granodiorite, INT GRAN EXO
A21A	2.0, 1.8	9.0	4.7	Bell Island granodiorite, INT GRAN EXO
A37C	2.2			Mountain Lake dark red granodiorite, INT GRAN
A37D	2.2			Mountain Lake dark red granodiorite, INT GRAN
A37E	2.1	39.0	18.6	Mountain Lake dark red granodiorite, INT GRAN
B4E	8.4, 8.8	35.0	4.1	Beaverlodge L. granite, INT GRAN
B7E	3.3, 2.9	21.0	6.8	Beaverlodge L. granite 5e, INT GRAN
B7F	4.9, 4.9	29.0	5.9	Beaverlodge L. granite 5c, INT GRAN
B10A	4.4, 4.6	16, 10	2.9	PITCH 27 granite 5d, INT GRAN
B11C	(7.8), 0.9	2.0	2.2	PITCH 8-10 monzonite 5c, INT GRAN
B14B	6.4, 6.4	14.0	2.2	JB granite 5d, INT GRAN
B15Ai	4.5, 4.7	11.0	2.4	PITCH 8-10 granite 5c, INT GRAN
B15Aii	2.3, 2.4	10.0	4.3	PITCH 8-10 granite 5c, INT GRAN
B15B	6.1, 8.3	22.0	3.1	Granite unit 5a, INT GRAN
B15D	4.1, 4.4	24.0	5.65	Granodiorite unit 5c, INT GRAN
B15F	3.0, 2.8	7.0	2.4	Tonalite, unit 1, INT GRAN EXO
B17C	1.4, 1.3	9.0	6.7	Leith Peninsula granodiorite, INT GRAN EXO
B19C	2.7	14.0	5.2	Leith Peninsula granite, INT GRAN EXO
B21H	4.9	19.0	3.9	Leith Peninsula granite, INT GRAN EXO
B21J	20.3	23.0	1.1	Leith Peninsula aplite, INT GRAN EXO
B24Biii	13.7			HAM tonalite, INT GRAN
B30A	4.5	16.0	3.6	JLD granodiorite, INT GRAN
B34A	9.2	62.0	6.7	JD episyenite, INT GRAN
B34B	4.0	47.0	11.75	JD granite, INT GRAN
B38A	9.2	52.0	5.65	JACKPOT granite, INT GRAN
B43C	3.4	7.0	2.1	Dog Island hornblende monzonite, INT GRAN
B46A	15.2			NORI/RA granodiorite, INT GRAN
C3A	5.9	46.0	7.8	NORI/RA granite, INT GRAN
C3B	3.4			NORI/RA porphyry, INT GRAN

Table 7: Results of neutron activation analysis of uranium and thorium in the country rocks.

<u>Sample</u>	<u>Uppm</u>	<u>Thppm</u>	<u>Th/U</u>	<u>Sample description</u>
<u>Gabbros</u>				
B17J	0.9	3.0	3.3	Leith Peninsula, quartz gabbro, INT GAB EXO
B39C	8.8			JACKPOT quartz gabbro, INT GAB
<u>Extrusive rocks</u>				
McL.Lk.	6.7	53.0	7.9	McLaren Lake porphyries, Sloan Gp., EXT?
A1A	5.0	22.0	4.4	McLaren Lake porphyries, Sloan Gp., EXT?
A4E	1.2	16.0	13.3	Perrault Lake andesite, Dumas Gp., EXT
A4J	13.9			Big Tree Lake (67°N, 117°W), felsic, EXT
A5B	20.9			MAC acid tuff, Dumas Gp., EXT
A5Ci	10.1	58.0	5.74	BESS tuff, Dumas Gp., EXT
A7Ai	260.2	14.0		FC rhyolite, EXT MIN?
A9Aiii	6.0			RHY rhyolite, Labine Gp., EXT
A9Bii	840			RHY rhyolite, Labine Gp., EXT MIN?
A9D	29.9	46.0	1.54	RHY rhyolite, Labine Gp., EXT MIN?
A9Eii	3.3			RHY qtz.-cemented rhyolite breccia, Labine Gp., EXT
A9Fi	4.9	21.0	4.3	SHORE tuff, Labine Gp., EXT
A9Fii	22.2			SHORE volcanic breccia, Labine Gp., EXT
A15Gi	7.9			Mazenod Lake rhodacite ignimbrite, EXT
A16Aiv	38.7			Mazenod Lake hematized ignimbrite, EXT
A16B	11.9	54.0	4.5	Mazenod Lake rhyolite, EXT
A16Hi	7.7			Mazenod Lake ignimbrite, EXT
A16Hiii	22.1			Mazenod Lake ignimbrite w. tourmaline veins, EXT
A16Kii	5.9	40.0	6.8	Mazenod Lake fresh ignimbrite, EXT
A21C	3.2, 3.0	16.0	5.2	Bell Island tuff, EXT EXO?
A22A	3.4, 3.8	13.0	3.6	Bell Island lapilli tuff, EXT EXO?
A40Ai	6.4	42.0	6.6	Coppermine River Gp. ignimbrite, EXT
B1B	7.5, 7.8	22.0	2.9	Beaverlodge Lake felsic porphyry, EXT
B4Ci	2.6, 2.4	5.0	2.0	Beaverlodge Lake dacite, EXT
B8E	2.1, 2.1	2.0	0.9	Beaverlodge Lake dacite, EXT
B11B	8.2, 9.0	24.0	2.8	PITCH 8-10 porphyry, EXT?
B43A	3.6	36.0	10.0	Dog Island bedded tuff, EXT
B43B	1.1	2.0	1.8	Dog Island bedded tuff, EXT
B43Di	33.9	16.0		Dog Island porphyry, EXT MIN
B43Dii	524	17.0		Dog Island porphyry, EXT MIN
B43Diii	106	16.0		Dog Island porphyry, EXT MIN
B43Dv	35.1	17.0		Dog Island porphyry, EXT MIN
B43Dvi	4.5	17.0	3.8	Dog Island porphyry, EXT
B43Dvii	1040	15.0		Dog Island porphyry, EXT MIN
B43Dviii	1240	15.0		Dog Island porphyry, EXT MIN
B44A	6.6	20.0	3.0	Dog Island bedded tuff, EXT
B44B	310	17.0		Dog Island porphyry, EXT MIN
<u>Sedimentary rocks</u>				
A3Fi	2.1			Red Hornby Bay sandstone, Hornby Bay SED
A6Bi	13.8			CON graphitic schist, META SED
A7Aii	220.6			FC black schist, META SED
A9Eiii	3.3			RHY red Labine Gp. sandstone, SED
A16G	7.6			Mazenod Lake siltstone, cream, pre-dating plutonism, SED
A18Hii	2.5			Rayrock, Snare Group meta-calcsilicate, META SED GNE
A20C	1.2, 1.6	3.0		Bell Island black shale, SED EXO?
A20D	9.4, 8.7	100.0		Bell Island placer lens in conglomerate, SED EXO?
A20Ei	14.8, 8.4	38.0		Bell Island placer lens in conglomerate, SED EXO?
A36A	0.5			Mountain Lake dolostone unit 14, SED
A37B	3.1			Mountain Lake grey argillite unit 16, SED
A37Gi	0.6			Mountain Lake red and green regolith, REG SED
A38Di	1.8			Mountain Lake red dolostone unit 9, SED
A39A	1.4			Mountain Lake green dolostone unit 9, SED
A39D	1.6			Mountain Lake white oolite unit 9, SED
B3A	6.8			Beaverlodge Lake green slate/argillite, META SED
B17E	0.8			Leith Peninsula chlorite schist xenolith, META SED EXO
B18C	20.8			Leith Peninsula redox boundary, sandstone, Hornby Bay Gp. SED MIN
B28B	3.4			JD Snare Group siltstone, SED

Table 7 (continued)

<u>Sample</u>	<u>Uppm</u>	<u>Thppm</u>	<u>Th/U</u>	<u>Sample description</u>
<u>Regoliths</u>				
A3A	219.5			Red regolith, Hornby Bay Gp., Hornby Bay REG
A3J	7.4			Red regolith, Hornby Bay Gp., Hornby Bay REG
A3L	2.5			Red regolith, Hornby Bay Gp., Hornby Bay REG
A5Ciii	106.0			Yellow regolith with erythrite, BESS, REG MIN
A37Gi	0.6			Red-green regolith, Mountain Lake, REG SED
B18A	3.6			Leith Peninsula, red regolith, REG EXO
<u>Gneisses, schists</u>				
A7Di	4.1	34.0		BEAR, Hepburn gneiss, GNE
A7F	34.6			BEAR, Hepburn gneiss, GNE
A8C	5.9			TABB, gneiss, GNE
A8E	1600	30.0		SOUTH granitic gneiss, GNE MIN
A8F	0.9			SOUTH amphibolite, GNE
A18Hii	2.5			Rayrock meta-calc-silicate META SED GNE
B23B	10.0			HAM leucogneiss, GNE
B24Ai	2100			HAM magnetite rock, GNE MIN
B25A	12.5			JONES leucogneiss, GNE
B25E	38.5			JONES quartz-magnetite rock, GNE MIN
B25G	1500			JONES magnetite schist, GNE MIN
B29A	34.7	150.0		JLD magnetite rock, GNE MIN
B38Eii	2600	2400		JACKPOT magnetite-gneiss, GNE MIN
B40A	840.0			JACKPOT magnetite-gneiss, GNE MIN
B40D	17.3			JACKPOT magnetite vein cutting paragneiss
B41Bi	175.9			JACKPOT gneiss adjacent to pegmatite, GNE MIN
B41C	175.0			JACKPOT paragneiss, GNE MIN
B47A	2200			NORI/RA biotite-apatite-MoS ₂ schist, GNE MIN
C1F	136.2			NORI/RA apatite-magnetite-biotite rock, GNE MIN
C1H	1100			NORI/RA biotite-tourmaline schist, pegmatite GNE
C2A	8.3			NORI/RA magnetite rock, beyond showings, GNE
C2B	5.7			NORI/RA magnetitic leucogneiss, GNE
C2C	5.8			NORI/RA magnetitic pink leucogneiss, GNE
<u>Metamorphic rocks (others)</u>				
A6Bi	13.8			CON graphitic schist, META SED
A7Aii	220.6			FC black schist, META SED
A7Giii	680			TABB biotite schist, META MIN
A7Gvi	17.6			TABB graphitic schist, META SED
A18Hii	2.5			Rayrock meta-calc-silicate, META SED GNE
A21B	0.8			Bell Island chlorite rock, META EXO?
B3A	6.8			Beaverlodge Lake green slate/argillite, META SED
B17E	0.8			Leith Peninsula, chlorite schist xenolith, META SED EXO
<u>Exotic Terrain</u>				
A20C	1.2, 1.6	3.0		Bell Island black shale, SED EXO?
A20D	9.4, 8.7	100.0		Bell Island placer lens in conglomerate, SED EXO?
A20Ei	14.8, 8.4	38.0		Bell Island placer lens in conglomerate, SED EXO?
A20G	1.6, 1.5	5.0	3.2	Bell Island granodiorite, INT GRAN EXO
A21A	2.0, 1.8	9.0	4.7	Bell Island granodiorite, INT GRAN EXO
A21B	0.8			Bell Island chlorite rock, META EXO?
A21C	3.2, 3.0	16.0	5.2	Bell Island tuff, EXT EXO?
A22A	3.4, 3.8	13.0	3.6	Bell Island lapilli tuff, EXT EXO?
B15F	3.0, 2.8	7.0	2.4	Tonalite, unit 1, INT GRAN EXO
B17C	1.4, 1.3	9.0	6.7	Leith Peninsula, granodiorite, INT GRAN EXO
B17E	0.8			Leith Peninsula, chlorite schist xenolith, META SED EXO
B17J	0.9	3.0	3.3	Leith Peninsula, quartz gabbro, INT GAB EXO
B18A	3.6			Leith Peninsula, regolith, REG EXO
B19C	2.7	14.0	5.2	Leith Peninsula, granite, INT GRAN EXO
B21H	4.9	19.0	3.9	Leith Peninsula, granite, INT GRAN EXO
B21J	20.3	23.0	1.1	Leith Peninsula, aplite, INT GRAN EXO

Table 7 (continued)

Data of Badham (1973a) and Robinson (1971)

<u>Lithology *</u>	<u>U ppm</u>
Basalt, Camsell River (Badham)	0.5
Andesite, Camsell River (Badham)	1.1
Andesite, Echo Bay (Robinson)	0.9 (one value of 22.0 excluded)
Rhyolite, Camsell River (Badham)	1.6
Plutonic rocks, Camsell River (Badham)	3.5
Plutonic rocks, Echo Bay (Robinson)	5.3
Volcaniclastic sediment, Camsell River (Badham)	0.9
Diabase , Camsell River (Badham)	0.4

* All volcanic lithologies are from the Labine Group.

comparatively non-degradable refractory minerals (Rich *et al.* 1977). Zielinski *et al.* (1980) and Walton *et al.* (1981) have shown that tuffs may or may not lose much of their uranium soon after emplacement, depending upon the style of alteration and the alteration products, which may adsorb or incorporate uranium. Walton *et al.* (*op. cit.*) concluded that tuffs only release significant amounts of their uranium when the glass shards are dissolved under vadose conditions, early in the history of the tuff. Most of these studies also showed that remobilised uranium is occasionally concentrated in samples from the weathered zone, either as secondary minerals or by adsorption, which has apparently happened in some of the present samples.

For these reasons, it is suggested that the relatively immobile element Th gives a better indication of the original uranium content of weathered igneous rocks, for which some general Th : U ratios are known. Rogers *et al.* (1978) state that anatectic (or "S-type") granites typically have Th/U ratios below 1, and mantle-derived (or "I-type") granites have ratios above 1, although the classic French two-mica S-type granites of the Massif Central have ratios of 1–3 (Cuney 1978; Leroy 1978). A ratio of 2–3 in the mafic members of a differentiating magmatic suite may typically rise to 5–6 in the more differentiated plutons (Rogers *et al.*, *op. cit.*). Thorium mobility and concentration has occasionally been demonstrated in sedimentary and volcanoclastic rocks (Kimberley 1978) but is not thought to be significant in this study.

It is impossible to predict the amount of uranium loss from the heterogeneous groups of sedimentary and metamorphic rocks, which may be more (or less) permeable, have different oxidation states, and have unpredictable initial Th : U ratios. It is only certain that the assays obtained represent minimum uranium values. It is also impossible to define an "anomalous threshold" value, and the results can only be compared with each other and other published data.

Analytical results

Granitoids

Granitoids from the exotic terrain, excluding the aplitic sample B21J, have mean values of U = 2.55 ppm, Th = 10.5 ppm and Th : U = 4.35. These are far lower than the mean values for the 27 granitic samples from the Great Bear Batholith, which are U = 5.8

ppm, Th = 25.4 ppm and Th : U = 5.7. The four granitoids with Th >40 ppm are all adjacent to the Wopmay Fault, and probably represent anatexis of the U- and Th-bearing Snare Group rocks of the paragneiss belt. The Hottah Lake samples (excluding the exotic terrain), with Th = 13.7 ppm, are obviously Th-deficient and thus probably U-deficient compared to the Beaverlodge Lake samples with Th = 28.3 ppm, despite the fact that both sample suites included granite of unit 5c (McGlynn 1979). The Echo Bay rocks have not been analysed for Th, but they have U contents slightly below the mean, 3.5 to 5.3 ppm; J-type galena from Echo Bay indicates a normal Th : U ratio of 3.7–4.0 in its source (Miller 1982).

Granitoids from the northern areas include plutons from both the Hepburn and Great Bear Batholiths, and have variable U and Th contents; the St. Germain pluton (of the Great Bear Batholith) hornblende–biotite adamellite sample, with a Th : U ratio of only 0.7, suggests an "S-type" origin despite an "I-type" mineralogy, if the sample is representative. The highest Th : U ratio, indicating the most obviously uranium-depleted sample, was found in the basement granodiorite from Mountain Lake, which was also the most altered and hematized pluton sampled. With the fifth highest Th content, this pluton is an obvious possible uranium source for the Mountain Lake deposit.

The average granites reported by Wedepohl *et al.* (1969–1978) commonly contain 10–20 ppm Th, and in all cases less than 33 ppm except for the Triassic Conway granite of New Hampshire (56 ppm). By this criterion, a significant number of the Great Bear Batholith plutons are anomalously Th-rich, and by implication also U-rich. Again, if a loss of only 30% uranium by surficial leaching is assumed, over 25% of all the sampled plutons contained more than 10 ppm U, regarded as the anomalous threshold by Fehn *et al.* (1978). The total evidence suggests that some of the batholith plutons, including those along the Wopmay Fault, at Beaverlodge Lake and at Mountain Lake, are probably anomalously uraniferous. It has not proved possible to correlate particular types of pluton with the U and Th assays; throughout most of the batholith, individual plutons have not been mapped, and not enough samples have been analysed to allow a statistically valid conclusion.

Siliceous extrusive rocks

Siliceous extrusive rocks world-wide have a mean U content of 5 ppm (Rich *et al.* 1977). This is somewhat lower than for granites, perhaps reflecting a loss of uranium with an escaping volatile phase during eruption. The mean Th contents of such rocks do not appear to have been studied, but may reasonably be similar to those of granites. Because, as discussed, the loss of uranium from tuffs is a highly variable process, it is difficult to assess the meaning of the U contents and Th : U ratios obtained. The mean U values found in this study for the Great Bear Batholith rhyolites and ignimbrites is 9.5 ppm, which seems to be a high value. Samples with >40 ppm Th, which might be regarded as anomalous, are, (a) ignimbrites from the basal Coppermine River Group basalts, (b) Mazenod Lake, (c) Achook Island, (d) one from the BESS occurrence near the Coppermine River, and (e) a porphyry of uncertain origin from McLaren Lake, east of Hornby Bay in the north of the batholith. U contents > 10 ppm were again found in samples from Mazenod Lake and Achook Island, and also from several of the Coppermine River deposits. The samples from Echo Bay and Camsell River are extraordinarily low by comparison, being less than 2.0 ppm.

Divided into the volcanic belts, the three Dumas Group samples average 10.7 ppm U, the two Sloan Group samples contain 5.8 ppm U and seven Labine Group samples average 10.6 ppm U, although these are certainly not reliable mean values for the belts. Including the data of Robinson and Badham (*op. cit.*), and considering the likelihood that two anomalous sample from Achook Island contain traces of secondary uranium mineralisation, the true value for the Labine Group is probably less than 5 ppm U and thus less than the later Sloan and Dumas Groups, as might be expected during progressive fractionation. The Th values show a distinct upward trend with time from the Bell Island rhyolites with Th = 13–16 ppm, to the Dog Island tuffs of the Labine Group with Th = 17 ppm, to the Cameron Bay Formation (Labine Group) at Achook Island (33 ppm mean) and higher groups (up to 58 ppm). It is not safe to assume that the original uranium contents were significantly higher, but nevertheless some of the ignimbritic piles of the Great Bear Batholith are certainly credible source rocks, particularly at Mazenod Lake.

Sedimentary rocks

Samples of red regolithic material are not markedly uraniferous (0.6–7.4 ppm U), except for the samples which were anomalously radioactive in the field. Conglomerates from Bell Island, Hottah Lake, containing high levels of heavy detrital minerals such as zircon and oxidised magnetite, have Th = 38–100 ppm and U = 9.0–11.6 ppm. Black shales within the same unit contain only 1.4 ppm U, a surprisingly low amount. These rocks have been tentatively correlated with the earliest stages of the Great Bear Batholith, but could pre-date it (p. 11). Samples of black and graphitic schists from the Akaitcho Group at the Coppermine River contain 13.8 and 220.6 ppm U, which is not unusual for carbonaceous pelites. Six samples of green argillite and dolomites from the Dismal Lakes and Hornby Bay Groups at Mountain Lake contain up to 3.1 ppm U, also not unusual. This does not discount the possibility of local uranium concentrations in black shales or evaporitic units elsewhere in this sedimentary sequence. The samples from Mazenod Lake, Beaverlodge Lake, Achook Island and the JD zone yielded unsurprising, generally low U assays.

Metamorphic rocks

Four samples of the leucocratic paragneiss from the Snare Group belt adjacent to the Wopmay Fault contained from 5.7 to 12.5 ppm U; a mineralised paragneiss sample from the JACKPOT claims shows 2800 ppm U and 2400 ppm Th, confirming the findings of McGlynn (1971). By contrast, a metamorphosed Snare Group calc-silicate from the Rayrock mine contained only 2.5 ppm U. Paragneisses from the Coppermine River area, of the Akaitcho or Snare Groups, contain from 4.1 to 34.6 ppm U, and carbonaceous and graphitic schists from this region contain from 13.8 to 220.6 ppm U. These are all regarded as somewhat high uranium contents. A chlorite schist inclusion from the exotic terrain granite, by contrast, contained only 0.8 ppm U, and has presumably contributed any original uranium to the granite.

D. Regional uranium enrichment

Airborne gamma-ray spectrometry shows that the Great Bear Batholith has a strong regional uranium enrichment, compared to the Hepburn Batholith and the Slave craton, a pattern closely echoed by enrichment in potassium as well (Killeen and

Richardson 1978). A lake-sediment sampling program showed essentially the same *regional* pattern of uranium distribution, although it will be shown (p. 197) that it did not always indicate the known *local* uranium deposits (Cameron and Allan 1973).

The Great Bear Batholith contains higher background levels of uranium and thorium than any other unit of the Canadian Shield. Studies by Burwash and Cumming (1976), Eade and Fahrig (1971) and Shaw (1967) show this quite clearly, and are summarised in Table 8. Burwash and Cumming analysed drill core samples of igneous and metamorphic rocks from the basement of the Alberta-Saskatchewan sedimentary basin, from as much as 230 m beneath the buried basement surface; other workers analysed outcrop samples, representative of all the rock units present. The influence of non-granitic samples is unlikely to account for the lower values found outside the Great Bear Batholith. None of these studies has overcome the problem of surficial loss of uranium, and must still represent only the minimum uranium contents.

Stating that there is a regional enrichment in uranium and thorium still begs the question, why? Higher levels of exposure and lower degrees of metamorphism may be part of the answer, but until the exact sources and style of derivation of the Great Bear Batholith plutons are discovered, the cause of the high uranium and thorium backgrounds will remain purely speculative. It may reflect a uraniferous source material for the granitic magmas, or a uraniferous pre-batholithic cover sequence assimilated by these magmas (such as the Snare Group paragneisses), or it may indicate a high degree of magmatic fractionation (not evident from the petrology of the plutons).

E. Conclusions on the source of uranium

It is impossible to positively identify the sources of uranium in the deposits; one may only assess the various possibilities.

(1) *Background uranium levels.* The Great Bear Batholith as a whole is enriched by a factor of approximately 3 in both uranium and thorium, compared to the rest of the Canadian Shield, and is also enriched compared to world-wide average granites.

(2) *Pre-existing uranium concentrations.* The ^{208}Pb contents of some pitchblende deposits and their geographical location suggest that they may have been derived by the

Uranium and Thorium Contents of Canadian Shield Areas

	<u>U ppm</u>	<u>Th ppm</u>
Western Canada basement (Burwash and Cumming 1976)	4.13	21.1
Canadian Shield, mean (Shaw 1967)	2.45	10.3
Canadian Shield, average weighted according to size of structural province (Eade and Fahrig 1971)	2.1	13.0
Slave Province (Eade and Fahrig 1971)	1.7	8.4
Churchill Province (Eade and Fahrig 1971)	2.6	15.5
Superior Province (Eade and Fahrig 1971)	1.2	9.7
Grenville Province (Eade and Fahrig 1971)	1.2	8.8
Bear Province (Eade and Fahrig 1971)	8.1	35.7

Table 8: Mean U and Th contents of Canadian Shield areas.

remobilisation of the meta-placer uraninite deposits. This might also apply to some of the Hottah Lake deposits, since heavy-mineral lenses from Bell Island, which might pre-date the Great Bear Batholith, are certainly Th-rich and moderately uraniferous. Some pitchblende has apparently been formed by the remobilisation of pre-existing, probably hydrothermal deposits, younger than the meta-placer group.

(3) *Plutons*. Some plutons are certainly possible uranium sources, as defined by high Th or U contents. Some of these are located near the meta-placer deposits, and may have acquired their U and Th by anatexis. At least one pluton has been extensively leached of uranium by weathering, probably during the Helikian era rather than recently, since it is the most hematized and altered pluton seen and immediately underlies the Hornby Bay Group. The Mystery Island I-type plutons at Echo Bay are quite probably not the source of uranium, but no other source can yet be suggested.

(4) *Rhyolitic ignimbrites*. Some of the extrusive suites appear to be feasible uranium sources, notably that at Mazenod Lake. The presence of high $^{208}\text{Pb}/^{204}\text{Pb}$ ratios in the mineralisation, the resorbed pyroxenes and the geographical proximity to the meta-placer belt of the Mazenod Lake ignimbrites and pitchblende mineralisation are all compatible with the suggestion that meta-placer deposits and paragneisses were assimilated into the magmas and accounted for raised uranium concentrations.

(5) *Sedimentary rocks*. It appears that the sedimentary rocks are unlikely sources of uranium if their present-day uranium contents resemble their pre-weathering contents. The only exceptions are some of the Akaitcho group carbonaceous meta-pelites from the Hepburn Batholith, perhaps some heavy-mineral beds from Bell Island, and the meta-placer deposits.

VIII. THE CONTINUITY OF PROCESS : WEATHERING AND OXIDATION

Uniformitarianism is not a strictly applicable philosophy in geology; there is an inverse relationship between the frequency and magnitude of geological events, such that the 2 Ga history of uranium in the Great Bear Batholith cannot be entirely described in terms of events occurring elsewhere today (*e.g.* Dury 1980). Changes must necessarily have taken place on a scale not now seen. For example, although atmospheric oxygen levels had started to rise by 2.0 Ga ago (Cloud 1976), they might not have approached modern values for a substantial further interval, affecting the chemistry of surface waters. Conversely, Schidlowski (1975) has suggested that the partial pressure of CO₂ has not changed significantly since the formation of the oceans. The climate has also ranged from equatorial to polar, and local marine conditions prevailed during Helikian, Palaeozoic and Mesozoic transgressions. Although analogy is a powerful interpretive technique, there is no doubt that in many geological cases there are no precise modern analogues, and too frequently the observed facts are forced into a given model because that model is the only one currently known to be operating.

This study has shown that uranium may be repeatedly remobilised, and is still being remobilised today (but not necessarily redeposited as pitchblende). Uranium is uniquely able to record such events by virtue of its radioactive decay and by the existence of non-uranogenic lead isotopes, and such continual mobility is probably not restricted to uranium: it is simply easier to demonstrate the likelihood of remobilisation for uranium rather than for such elements as copper. This chapter concerns the weathering of the deposits, describing the consequent mineralogy and isotopic characteristics, and speculates on the present mobility of uranium within the batholith.

The remobilisation of uranium requires, (1) the oxidation of the primary tetravalent uranium species such as pitchblende, uraninite, coffinite or refractory species; (2) the solution of the uranyl ions (probably as complexes); and (3) transport of the uranium into a circulating hydrous system. (The quite separate factors which control its subsequent reduction and precipitation have already been considered elsewhere). The deposits seen currently show, in different ways, the stage of oxidation, while the stages of solution and

transport may be deduced. These required steps have never changed with time, only the methods and details of their accomplishment. What must not be assumed is that similar styles of oxidation always occurred in the past, or that the uranium deposits were formed by processes now operative in the Great Bear Batholith.

A. Oxidation and secondary uranium minerals

Although uranium is essentially soluble only in the hexavalent form, not all hexavalent uranium is soluble, for certain anions may precipitate uranyl cations. These are principally the vanadate, phosphate, arsenate and silicate anions, and more rarely molybdate, carbonate, selenate or tellurate anions. There are also a number of uranyl oxides and hydroxides, some incorporating other metals (Morton 1978; Steacy and Kaiman 1978). Such minerals are almost always present in the oxidised zones of uranium deposits, and can precipitate at some distance from the uranium source. They may occasionally form economically important concentrations, such as the duricrust-hosted carnotite deposits at Yeelirrie, Australia (Langford 1978; Mann and Deutscher 1978).

The secondary minerals formed on an outcrop by weathering are controlled by, (1) the mineralogy of the host rocks and the primary uranium deposit; (2) such weathering conditions as mean temperatures and amounts of precipitation; and (3) the chemistry of the water involved. A number of workers have identified uraniferous secondary minerals, but rather fewer have attempted to draw any conclusions from them. This study suggests that a few square centimetres upon an outcrop may constitute an almost closed chemical system or micro-domain, and that this immediate substrate controls the secondary mineralisation. For example, the primary arsenide minerals at Echo Bay do not preclude the formation of uranyl silicates rather than arsenates if primary arsenide phases are not immediately present. Similarly, uranyl oxides may form in preference to silicates only centimetres from suitable silica sources. Beneath the outcrop, as solutions start to mix, more uniformity of the secondary minerals might be predicted, but this concept could not be tested for lack of exposures beneath the outcrop. Probably little of the original tetravalent uranium is retained during its oxidation under the non-arid climate of the Bear Province, most of it eventually dissolving as the host rocks weather away, although the *in situ* replacement of pitchblende will be suggested later.

The secondary minerals identified or previously reported are given in Table 9. Surprisingly, Steacy and Kaiman (1978) state that schoepite and rutherfordine have not been reported from Canada, although both were positively identified, and schoepite in some cases was the commonest component of the oxidised crusts studied. Other apparently unreported minerals are vandendriesscheite and meta-novacekite (uncertain identification); zippeite, reported from Echo Bay (Palache and Berman 1933); and johannite, the JCPDS sample of which came from Great Bear Lake.

The identification of secondary uranium minerals

The technique used herein was primarily X-ray powder diffraction (XRD). Some mineral identifications were subsequently confirmed by qualitative analysis on a scanning electron microscope with an energy-dispersive analytical capability. There are some drawbacks to this approach: (1) many of the minerals are isostructural, and their diffraction patterns are consequently very similar; (2) some "minerals" may not be true species, and others may be solid solutions; (3) some minerals are non-stoichiometric or have variable hydration states, and consequently variable unit cell dimensions; (4) with time, significant amounts of hexavalent uranium may be replaced by divalent lead, distorting the lattice and probably causing the eventual exsolution of a different species; (5) the structures and formulae of some species are still uncertain; (6) as a rule, secondary mineral crusts usually contained several components, and pure phases were comparatively rare. It was also found that certain weaker X-ray reflections were sometimes absent, that the material was sometimes partially amorphous, and that some reflections were significantly displaced.

Morton (1978) has published a table of the principal d-spacings of uranium minerals, although many new data have since been published. Computer file ORDD2 was compiled, containing the largest and the four principal d-spacings of the X-ray diffraction patterns of all the uraniferous minerals currently listed by the JCPDS (1981). Other common supergene minerals, goethite, jarosite, clay minerals, quartz, carbonates and synthetic uranium oxides and hydroxides were also added to the file. Computer searching was used to select possible matches which were then checked manually, which proved to be the fastest method for identifying the XRD patterns. Despite this search

The Chemistry of Secondary Uranium Minerals From the Great Bear Batholith

Becquerelite	$\text{CaU}_6\text{O}_{19} \cdot 11\text{H}_2\text{O}$
Beta-uranophane	$\text{Ca}(\text{UO}_2)_2\text{Si}_2\text{O}_7 \cdot 6\text{H}_2\text{O}$; $\text{Ca}(\text{UO}_2)_2(\text{SiO}_3)_2(\text{OH})_2 \cdot 5\text{H}_2\text{O}$
Billietite	$\text{BaU}_6\text{O}_{19} \cdot 11\text{H}_2\text{O}$
Boltwoodite	$\text{K}_2(\text{UO}_2)_2(\text{SiO}_3)_2(\text{OH})_2 \cdot 5\text{H}_2\text{O}$
Cuprosklodowskite	$\text{Cu}(\text{UO}_2)_2(\text{SiO}_3)_2(\text{OH})_2 \cdot 5\text{H}_2\text{O}$; $\text{Cu}(\text{UO}_2)_2\text{Si}_2\text{O}_7 \cdot 6\text{H}_2\text{O}$
Curite	$\text{Pb}_2\text{U}_5\text{O}_{17} \cdot 4\text{H}_2\text{O}$; $\text{Pb}_3\text{U}_8\text{O}_{27} \cdot 4\text{H}_2\text{O}$
Johannite	$\text{Cu}(\text{UO}_2)_2(\text{SO}_4)_2(\text{OH})_2 \cdot 6\text{H}_2\text{O}$
Liebigite	$\text{Ca}_2\text{U}(\text{CO}_3)_4 \cdot 10\text{H}_2\text{O}$
Metanovacekite	$\text{Mg}(\text{UO}_2)_2(\text{AsO}_4)_2 \cdot 4-8\text{H}_2\text{O}$
Metatorbernite	$\text{Cu}(\text{UO}_2)_2(\text{PO}_4)_2 \cdot 8\text{H}_2\text{O}$
Metazeunerite	$\text{Cu}(\text{UO}_2)_2(\text{AsO}_4)_2 \cdot 8\text{H}_2\text{O}$
Rutherfordine	UO_2CO_3
Schoepite	$\text{UO}_3 \cdot 2\text{H}_2\text{O}$
Sklodowskite	$\text{Mg}(\text{UO}_2)_2\text{Si}_2\text{O}_7 \cdot 6\text{H}_2\text{O}$
Uranophane	$\text{Ca}(\text{UO}_2)_2\text{Si}_2\text{O}_7 \cdot 6\text{H}_2\text{O}$
Vandendriesscheite	$\text{PbU}_7\text{O}_{22} \cdot 12\text{H}_2\text{O}$
Zeunerite	$\text{Cu}(\text{UO}_2)_2(\text{AsO}_4)_2 \cdot 10-16\text{H}_2\text{O}$
Zippeite	$(\text{UO}_2)_2(\text{SO}_4)(\text{OH})_2 \cdot 4\text{H}_2\text{O}$; $\text{K}_2(\text{UO}_2)_6(\text{SO}_4)_3(\text{OH})_{10} \cdot 4\text{H}_2\text{O}$

Table 9: Secondary uranium minerals found in the uranium deposits of the study area.

technique, some patterns were found which were apparently those of secondary uranium minerals but which defied identification. Because the samples frequently contained several minerals, the chemistry of these unidentified phases is not known. Table 10 lists some of the patterns which deviate from published data due to absent, shifted or different-intensity reflections, and also some of the unidentified patterns as deduced after the removal of the reflections of intergrown identified minerals; more than one unidentified mineral may be present in these, and peaks from such minerals which overlap those of identified phases will have been erroneously removed.

The "autunite" and "uranophane" group minerals

The autunite and meta-autunite group minerals have the general formulae $A(\text{UO}_2)_2(\text{XO}_4)_2 \cdot 8-12 \text{ H}_2\text{O}$ and $A(\text{UO}_2)_2(\text{XO}_4)_2 \cdot 4-8 \text{ H}_2\text{O}$ respectively, where $A = \text{K}_2, \text{Na}_2, (\text{NH}_4)_2, \text{Ca}, \text{Ba}, \text{Mg}, \text{Fe}^{2+}, \text{Co}, \text{Cu}, \text{Zn}$ or Mn , and $X = \text{P}, \text{As}$ or V . These minerals are composed of sheets of $(\text{UO}_2\text{XO}_4)_2^{2-}$ or $(\text{UO}_2)_2\text{V}_2\text{O}_8^{2-}$, with interlayer water and cations (Cameron-Schimann 1978). The uranophane group minerals, including sklodowskite, cuprosklodowskite and boltwoodite, are formed of layers of cross-linked chains, again with interlayer cations and water. Clearly there is scope within these structures for variable hydration states and cation exchange. Cameron-Schimann (*op. cit.*), reporting new and previously published analyses, showed the presence of minor Mg replacing Ca in autunite and of Na, Ca, Mg and Fe possibly replacing K in carnotite; species intermediate between meta-torbernite and meta-uranocircite and between autunite and meta-uranocircite were also reported, and Rimsaite (1979) reported uranophane grading into sklodowskite. X-ray diffraction cannot give a positive mineral identification in such cases, and confirmation by electron microprobe or scanning electron microscope techniques should be sought. Mixed phases of these types are probably present in the unidentified material from Echo Bay.

Langmuir (1978b) concluded that uranyl vanadates ("carnotite") are the least soluble of these minerals, even at low V concentrations, in equilibrium with solutions of 1–2 ppb U at intermediate pH levels. Uranyl phosphates are slightly less soluble than uranyl silicates in typical groundwaters, but at least 100 times more soluble than the vanadates. Arsenates were not considered in Langmuir's study. Phosphorus-free

ANOMALOUS AND UNIDENTIFIED SECONDARY MINERALS

Anomalous X-ray diffraction patterns are listed first, together with the published JCPDS powder diffraction patterns, followed by unidentified material. All patterns obtained under identical conditions: quartz sometimes used for a standard: $\text{CuK}\alpha$ radiation, scanning from $2\theta = 4^\circ$ to $<50^\circ$ ($d = 22$ to $>2\text{\AA}$), $1^\circ 2\theta = 1 \text{ cm} = 1$ minute of scanning time. JCPDS references are given.

Langite (with brochantite), Al6Aii

<u>d</u>	<u>I/I° (obtained)</u>	<u>d</u>	<u>I/I° (published, 12-783)</u>
7.83	(hidden)	7.85	10
7.11	100	7.12	100
		5.61	20
		5.32	30
		4.41	20
4.27	15	4.26	30
3.54	45	3.56	80
3.20	(hidden)	3.18	20
		3.01	10
		2.96	20
		2.80	30
2.63	(hidden)	2.65	30
2.60	(hidden)	2.60	40

Notes: Despite interference from brochantite, a number of lines are absent.

Becquerelite, B1E (two patterns)

<u>d</u>	<u>I/I°</u>	<u>d</u>	<u>I/I° (obtained)</u>	<u>d</u>	<u>I/I° (published, 13-405)</u>
7.50	100	7.50		7.44	100
6.60	5	6.56		6.56	4
				6.21	2
				5.59	2
4.71	5	4.70		4.68	6
3.74	20	3.73		3.73	30
3.60	10	3.60		3.61	4
3.55	25	3.55		3.54	20
3.47	10	3.46		3.45	4
3.38	5	3.38		3.37	4
3.21	25	3.20		3.20	35
3.14	15	3.14		3.14	4
2.96	5	2.96		2.96	4
				2.894	4
				2.848	4

Notes: Somewhat variable spacings; some lines absent.

Table 10: The X-ray diffraction d-spacings of anomalous and unidentified secondary uranium minerals found.

Metatorbernite, A16Eiii, B2A

<u>d</u>	<u>I/I° (A16Eiii)</u>	<u>d</u>	<u>I/I° (B2A)</u>	<u>d</u>	<u>I/I° (JCPDS 16-404)</u>
8.70	100	8.67	100	8.71	100
				6.48	40
5.43	10	(hidden)		5.75	25
4.93	15	4.94	70	5.44	75
				4.93	75
4.33	15	4.27	30	4.70	20
3.68	45	3.68	100	4.31	65
3.47	15	3.49	60	3.68	100
3.21	10	3.24	60	3.48	80
				3.23	80
				3.06	40
2.93	5	2.92	60	2.979	15
				2.931	70
2.71	5	2.71	50	2.840	10
2.65	5			2.714	40
				2.667	70

Notes: A number of lines are absent, and intensities vary between samples and with the standard.

Boltwoodite, B35D

<u>d</u>	<u>I/I° (obtained)</u>	<u>d</u>	<u>I/I° (published; 29-1026)</u>
		7.53	20
6.81	100	6.81	100
6.42	40	6.40	50
5.47	25	5.45	50
4.75	25	4.74	40
4.31	15	4.32	40
4.11	5	4.11	20
		3.91	10
		3.75	10
3.53	30	3.54	70
3.39	40	3.40	90
3.13	30	3.13	50
		3.07	10
2.91	35	2.91	70

Notes: 7.53Å line notably completely absent.

UNIDENTIFIED PATTERNS

A33Dvi Yellow and green secondary
uranium minerals.

<u>d</u>	<u>I/I°</u>
10.28	30
8.66	100
6.71	10
5.47	35
5.01	50
4.53	10
4.43	20
4.33	5
4.17	5
3.69	100
3.54	100
3.33	100
3.28	55
3.23	25
3.04	20
2.98	15
2.90	35
2.68	10
2.56	10
2.51	10
2.454	10
2.404	10

A33Dvi Lemon yellow secondary
uranium mineral.

<u>d</u>	<u>I/I°</u>
8.67	100
6.46	30
6.07	20
5.47	10
5.22	10
4.70	10
4.19	20
4.07	10
3.69	20
3.52	20
3.24	60
3.21	30
3.05	15
2.90	20

A34G Yellow-green uranium secondary
mineral (plus quartz)

<u>d</u>	<u>I/I°</u>
10.16	45
8.55	100
7.88	30
4.98	10
4.27	15
3.95	10
3.56	35
3.51	15
3.23	10
3.13	20
2.90	20
2.71	15

B1Ed Yellow uranium secondary
mineral

<u>d</u>	<u>I/I°</u>
8.12	100
6.51	5
5.04	5
4.06	20
3.87	5
3.38	5
3.08	5
3.01	5
2.86	10

Yellow unidentified uranium secondary minerals: probably similar, mixtures.

<u>A30Dv</u>		<u>A30Diii</u>		<u>A30Di</u>	
<u>d</u>	<u>I/I°</u>	<u>d</u>	<u>I/I°</u>	<u>d</u>	<u>I/I°</u>
8.44	100	8.48	100	8.50	(Intensities not obtained, due to changes in scale factor on XRD unit during run)
7.14	50	7.13	40	7.14	
6.44	40	6.42	50	6.46	
4.23(B)	40	4.20(B)	80	4.24	
4.04	20	4.05	30	3.87	
3.87	70	3.88	40		
3.82	20				
3.72	20				
3.66	30				
3.55	30	3.54(B)	80	3.55	
3.29	30			3.29	
		3.25	60		
		3.19	60		
3.14	30	3.13	60	3.14	
3.07	60	3.07	80		
		2.92	150		
2.81	30			2.81	

Notes: The minerals are mixtures, containing uranophane and beta-uranophane; the unidentified phase(s) is probably a mixture too.

meteoric water might be expected to dissolve uranyl phosphates preferentially to uranyl silicates, since the phosphates form the more soluble and stable complexes. Uranyl vanadates were not found in this study, and V is presumably not a significant component of the primary mineralisation or the host rocks.

Uranyl phosphates were rarely found in this study. Although the secondary minerals from the apatite-rich deposits at the NORI/RA claims could not be identified, they do not appear to include uranyl phosphates. Similarly, only uranophane and beta-uranophane were found at the apatite-bearing UGI/DV deposits; however, the immediate substrates of the analysed samples are not phosphatic. Conversely, meta-torbernite was found at the Mazenod Lake and Beaverlodge Lake deposits where no P source is apparent.

Uranyl silicates were found at most of the deposits, and the Ca-bearing minerals uranophane and beta-uranophane are the most common secondary minerals found in this study. They are notably absent from the Helikian sandstone-hosted deposits, and Langmuir (1978a) states that uranophane is typically associated with alkalic igneous rocks. This is probably a response to the release of silica during feldspar breakdown:



(K-feldspar + water = kaolinite + K^+ + $(\text{OH})^-$ + silica)

Cuprosklodowskite appears to form preferentially in the presence of copper; boltwoodite (K-bearing) was only found at the T1 zone deposit, and may reflect an absence of Ca in the alkali-metasomatised host rocks; sklodowskite (Mg-bearing) was found at the Rayrock mine, but in association with cuprosklodowskite, uranophane and beta-uranophane, and the source of Mg is not apparent, nor the relative solubility of sklodowskite. It is not known what conditions favour the formation of beta-uranophane rather than uranophane (Cameron-Schimann 1978), and the two were sometimes found intimately mixed.

Uranyl arsenates were only found in the actual or inferred past presence of primary arsenical ore minerals, and even then not to the exclusion of uranophane at Echo Bay, where possible meta-novacekite was identified.

The uranyl oxide hydrate minerals

Schoepite, apparently not previously recorded from Canada, is not easy to identify, due to the yellow isostructural minerals becquerelite, billietite, compreignacite and meta-vandendriesscheite; other isostructural minerals include fourmarierite, agrinierite, epi-ianthinite, wolsendorfite, masuyite and vandendriesscheite, and possibly bauranoite, calciouranoite and meta-calciouranoite, which range from orange, red and brown to almost black in colour (Christ and Clark 1960; Cameron-Schimann 1978). Three varieties of schoepite, termed I, II and III, were found by Christ and Clark (*op. cit.*); schoepite I is amber brown, altering to schoepite II (metaschoepite) or schoepite III (paraschoepite) by dehydration. Further dehydration leads to the synthetic compound $\text{UO}_2(\text{OH})_2$. Schoepite II is intermediate between types I and III; there is no really diagnostic X-ray reflection to distinguish schoepite III. Becquerelite, billietite and schoepite may be best distinguished by the 002 and 004 reflections, but compreignacite and becquerelite have very similar patterns, and positive identification is probably impossible in the case of mineral mixtures. The X-ray diffraction patterns obtained show considerable variation in the positions and the relative and absolute intensities of the reflections, originally attributed to variations in the unit cell parameters of schoepite, but now regarded as caused by (1) mixtures of various phases, and (2) possible solid solution within the minerals. Such solid solutions may include the exchange of H_3O^+ and M^+ .

The presence of billietite (Ba-bearing) at the JD zone and Beaverlodge Lake showings was unexpected, although minor barite was tentatively identified optically at Beaverlodge Lake, and barite occurs in the French deposits analogous to the JD group, caused by the release of barium from feldspars during alkali metasomatism. Becquerelite (Ca-bearing) and schoepite are probably only formed in silica-poor weathering micro-domains, typically occurring as crusts on massive pitchblende-hematite rock; uranophane and beta-uranophane are more likely to be formed from narrow pitchblende veinlets, immediately adjacent to feldspars releasing silica. The lead-bearing members of this group were not positively identified; it seems likely that they are present, but are masked by more prominent members of the group.

The uranyl carbonate minerals

Rutherfordine and schoepite were found co-existing on blast debris from the ridge crest at Beaverlodge Lake; the debris is composed of hematite and pitchblende without primary carbonate phases. Liebigite was reported from the carbonate-rich uranium deposits at Echo Bay (Lang *et al.* 1959). Rutherfordine is soluble at dissolved uranium totals of some 10^{-6} moles/litre in the $\text{U-H}_2\text{O-CO}_2$ system, or 0.24 ppm U, and is insoluble at 10^{-4} moles U/litre (Hostetler and Garrels 1962). Rainwater in equilibrium with rutherfordine therefore acquires at least 0.24 ppm U in solution. Schoepite is unstable in solutions of $\text{pCO}_2 = 10^{-3.4}$ (equivalent to the atmospheric partial pressure), but the rutherfordine-schoepite equilibrium pCO_2 is very close to this partial pressure.

Other uranyl minerals

Zippeite, a potassium uranyl silicate, has been recorded from Echo Bay, and is probably restricted to deposits rich in sulphides which weather and oxidise to sulphate. Mo-bearing secondary uranyl minerals were expected in material from the molybdenite-bearing material from the NORI/RA claims, but were not found.

Controls on the formation of uranyl minerals

Whereas in arid climates the secondary uranyl minerals may be selectively concentrated in the vadose zone, they are not retained in the Great Bear Batholith but are probably lost proportionately with the host rocks as these erode and weather. Groundwater percolating through a vein containing secondary uranyl phases may eventually become saturated with the mineral, and thus the uranyl mineralogy is in balance between the availability of metals and anions and the solubility of the uranyl phases. Meteoric water percolating through a vein system is not a "typical groundwater", and the data of Langmuir (1978a) on typical groundwaters are not strictly applicable, but one might expect uranyl phosphates and carbonates to be the least stable phases, followed by the oxides, silicates and arsenates, and with vanadates being the most stable oxidised phases. Where uranyl phosphates and carbonates are exposed to rain, percolating meteoric water is probably strongly uraniferous, as at Echo Bay and the Beaverlodge Lake shaft where both mineral types occur. Although the uranyl phosphate and carbonate

minerals were not abundant, their survival suggests that carbonate and phosphate complexes are the predominant uranyl species in at least the local groundwaters.

Rimsaite (1979) found that pitchblende from deposits in Saskatchewan is initially replaced at depth by uranyl lead oxides. Pb is subsequently lost, and uranyl oxide hydrates and silicates are formed, followed by metal-uranyl silicates. The ultimate alteration is to clay minerals, and the co-existing uranyl phases are such as the comparatively soluble sulphates and carbonates. The same general pattern fits the present observations, with the possible exception of lead loss (discussed later).

Coffinite is a somewhat controversial mineral; it contains tetravalent uranium but forms during alteration and silica release. It may also be X-ray-amorphous, either inherently or by metamictisation. Rimsaite (1977) found 16.7% SiO_2 and up to 8% H_2O in coffinite, and up to 13.9% SiO_2 in co-existing pitchblende. Considerable solid solution probably occurs between UO_2 and USiO_4 , and some "coffinite" is probably an amorphous, hydrated, siliceous uranous oxide of no fixed composition.

Uranium in the modern batholith groundwaters is probably present as carbonate and phosphate uranyl complexes, given the reasonably wide distribution of C and P in the country rocks. Any eroded sedimentary cover rocks are more likely to have been calcareous than phosphatic; any incursions of sea-water would also have had a higher dissolved carbonate content than present surficial waters, except where the latter have locally re-equilibrated with carbonate rocks. Consequently the remobilisation of uranium during the tropical climatic interludes (p. 161) was probably accomplished primarily by carbonate complexes, replaced at depth and concomitantly higher temperatures by uranyl hydroxy species.

B. The age and isotopic composition of the secondary mineralisation

Secondary uranium minerals cannot be satisfactorily dated, because they may inherit lead from the parent mineral and yield any apparent date from the parental age to the present. Five samples of uranophane and beta-uranophane forming crusts upon isotopically analysed pitchblende were themselves analysed, and the data are given in Table 11. They were not used for calculating the ages of the deposits. The brief results for the secondary and associated primary mineralisation are as follows:

ISOTOPIC ANALYSES OF SECONDARY URANIUM MINERALS*

Sample	<u>²³⁸U ppm</u>	<u>Total Pb ppm</u>	<u>²⁰⁶Pb/²⁰⁴Pb</u>	<u>²⁰⁷Pb/²⁰⁴Pb</u>	<u>²⁰⁸Pb/²⁰⁴Pb</u>	<u>±Error%</u>	<u>²⁰⁷Pb/²³⁵U</u>	<u>²⁰⁶Pb/²³⁸U</u>
A7Ba	543680	8559.8	847.5	67.63	44.09	1.46	0.1413	0.01633
A7Gi1a	298955	77429	51.04	17.601	37.47	0.07	1.1295	0.13423
A7Givb	469545	44739	340.37	34.09	37.52	0.14	0.7299	0.09225
A8Ea	356585	565.59	565.93	46.23	39.88	0.45	0.0125	0.00162
A9Givb	10757	2669.3	1097.8	109.48	44.61	0.41	3.0256	0.25229

*Uranophane and/or beta-uranophane

Table 11: Isotopic data of the uranium secondary minerals.

The FC showing

A single sample (A7Ba) gave a highly discordant $^{207}\text{Pb}/^{206}\text{Pb}$ age of 700 Ma, compared to a less discordant pitchblende $^{207}\text{Pb}/^{206}\text{Pb}$ age of 660 Ma.

The TABB showing

Two samples were analysed (A7Giia, A7Givb); one yielded a $^{207}\text{Pb}/^{206}\text{Pb}$ age of 510 Ma with very slight negative discordance (the U/Pb ages are 569 Ma and 556 Ma), the other a 640 Ma $^{207}\text{Pb}/^{206}\text{Pb}$ age with marked negative discordance. The pitchblende age is 536 ± 66 Ma.

The SOUTH showing

One sample (A8Ea) gave an extremely discordant $^{207}\text{Pb}/^{206}\text{Pb}$ age of 450 Ma, compared with a pitchblende $^{207}\text{Pb}/^{206}\text{Pb}$ age of 420 Ma with extreme negative discordance.

The SHORE showing

One sample (A9Givb) gave a $^{207}\text{Pb}/^{206}\text{Pb}$ age of 1360 Ma with slight negative discordance (the U/Pb ages were 1450 Ma and 1414 Ma). The pitchblende ages are 1500 ± 10 Ma and 1424 ± 29 Ma.

Each sample analysed gives essentially the age of the parental pitchblende (compare with the pitchblende samples from the same hand specimens, Table 12, Appendix III). Two samples gave almost concordant ages, which may be due to (1) coincidence, (2) to formation at the same time as the pitchblende, and subsequent closed-system behaviour, or (3) to closed system behaviour during the oxidation of pitchblende, at any time but most probably recently. Coincidence is possible, but it is geologically unreasonable that these samples should have survived marine transgressions and weathering under all possible conditions for up to 1400 Ma. The third option, closed-system behaviour, implies that the oxidising groundwater contained enough silica in solution to alter the pitchblende *in situ* with no change in the lead-uranium ratios. This implies further that under the present climatic conditions and with feldspathic host rocks, uranium need not be particularly mobile during weathering if suitable ligands are unavailable. It has been

noted by other workers that lake, stream and sediment sampling has not been a reliable prospecting tool in some areas, an observation perhaps explained by the instantaneous "freezing" of uranium and lead into uranyl silicates. Cameron and Allan (1973), for example, found lake-sediment uranium anomalies in the mid-eastern section of the Great Bear Batholith which approximately followed major lineaments, and which they felt adequately reflected "...the variation of uranium in the underlying crust...". In fact, of the uranium deposits studied within this same section, the HAM/JONES and JACKPOT occurrences approximately correspond to major and minor uranium anomalies, but the JD group has left no anomaly; the paragneiss belt as a whole is also not evident from the lake-sediment analysis.

If the samples are isotopically equivalent to the parental material, formed by recent precipitation from groundwaters leaching the parent or by *in situ* alteration without significant material loss as suggested, they are mathematically equivalent to the parent and could perhaps be used as data points on discordia or lead isochron plots, as was done by Cumming and Rimsaite (1979). The materials generally showed up to twice the common lead content of the pitchblende substrate, showing that some lead from the country rocks was imported into the system during oxidation, compared to the overall loss of uranogenic lead found by Rimsaite (1979).

C. Present day uranium deposition

The Great Bear Batholith extends across regions of continuous and discontinuous permafrost, from some 20 m thick in the south to 50 m or more in the north (Washburn 1973). The latitude has not changed significantly since the early Cretaceous, although milder climates probably prevailed until Oligocene times.

Seasonal groundwater can flow in the thawed ground above the permafrost, and groundwater could continually flow beneath the permafrost under a sufficient hydraulic head. Water is unlikely to cross the ice barrier between the two flow systems; consequently, the uranium presently dissolved during weathering does not significantly penetrate the batholith, but enters the rivers, lakes and muskegs. The annual precipitation must almost entirely become runoff water during the brief summer thaw. It may therefore reach the open ocean by way of the Mackenzie and Coppermine River

systems, or it may be retained by various processes of adsorption or reduction in muskegs and lakes, by organic detritus or "bog-ore" iron and manganese oxy-hydroxides. The Naga Lake swamp (p. 55) is probably an example of such superficial concentration. There is no major recharge area, such as a permafrost-free hill range, which could maintain any significant groundwater flow beneath the permafrost, and this water is probably stagnant, or receives an insignificant contribution from meteoric water during the summer.

It is therefore unlikely that pitchblende is being actively precipitated within the Great Bear Batholith today, although Knipping (1974) suggested such a process at the Rabbit Lake deposit in the Athabasca Basin to the south-east. By extrapolation, the Cretaceous rocks, which at first sight appear to be ideal hosts for roll-front uranium deposits, are in fact unlikely to be significantly mineralised since there has not been a favourable climate or topography for groundwater flow since their formation. It also seems likely that no supergene pitchblende deposits younger than some 200 Ma will be found in the area, and that all the uranium currently being liberated by weathering is being lost.

IX. SUMMARY AND CONCLUSIONS

As a uraniferous metallogenic province, the Great Bear Batholith complex has developed numerous uranium deposits of various types and ages throughout its history, remobilising the metal from older deposits and, ultimately, drawing it from the rocks of the batholith and the pre-batholithic crust.

The formation of a metalliferous deposit requires a metal source, a method of transport and a trap. A comparison of the Great Bear Batholith with the rest of the Canadian Shield suggests that the source is the principal control, for the major uranium transport mechanism is hydrothermal activity triggered by regional igneous and tectonic activity, and the traps appear to be essentially structural, all of which are common phenomena across the entire Shield. The hydrothermal deposits indicate that although the ferrous silicates of mafic rocks form suitable chemical traps, acting as reducing agents for the uranyl-uranous transition, even leucocratic granitoids with dispersed reductants may host hydrothermal pitchblende veins. In contrast, the Great Bear Batholith igneous suites are anomalously enriched in U, Th and K compared to other sectors of the Shield, despite their generally "I-type" characteristics. The dispersed uranium content of the Great Bear Batholith is associated in some way with the high incidence of uranium mineralisation; in this author's view, these are both reflections of an originally uranium-enriched pre-batholithic protolith. In the final analysis, all the uranium in these deposits can probably be traced to the pre-batholithic "protolith", recycled through magmas or older, post-magmatic deposits. Lead isotope studies strongly suggest that the remobilisation of uranium deposits can be traced by the radiogenic lead remobilised with them.

The first level of protolith may be rocks similar to the Snare Group paragneiss belt along the Wopmay Fault, whose anatexis possibly provided uranium to the batholith plutons. The second level would be *their* uranium source, which for the belt mentioned was probably the "Hepburn highlands", although it is conceptually difficult to imagine that the Hepburn Batholith alone provided all the anomalous uranium to the Great Bear Batholith. Such arguments enter the realms of pure speculation at this point.

The hydrothermal and supergene deposition of uranium coincided with periods of tropical climate and igneous or tectonic activity. The uranium deposits of the Great Slave Basin are generally controlled by, and in most cases probably derived from, a series of local monzonite and diorite stocks, and neither support nor refute a climatic correlation. Perhaps these stocks also reflect the hypothetical uraniferous protolith.

The uraninite and pitchblende deposits seen may be classified as supergene, hydrothermal, sandstone-hosted, or metamorphosed palaeo-placer or xerogenic types. Hydrothermal and supergene pitchblende deposits are not easy to distinguish, but criteria such as a carbonate gangue to the pitchblende and a lack of wall-rock alteration may help identify the supergene, "per descensum" occurrences, without being diagnostic of them. None of the supergene deposits is known to have any economic potential, and apparently none have been formed in the batholith within the past 400 Ma.

The hydrothermal deposits are variable in age, metallic chemistry, wall-rock lithology and vein orientation, and show little correlation between these factors. A disproportionate number of supergene and hydrothermal pitchblende deposits have at least one mafic wall-rock, such as a diabase dyke, which can act as a reducing agent during mineralisation, but this relationship is also partly a reflection of the regional north-easterly faults. Dykes have followed these faults, which later movement has re-opened to permit the passage of uraniferous solutions. A similar relationship exists between the giant quartz veins emplaced in the same faults, and the much younger, entirely unrelated uranium mineralisation which may occur within or beside them. In the Ag-U deposits of Echo Bay and the Great Slave Basin, uranium may have been derived from a different source (as yet unidentified) from the remainder of the metals, which were probably concentrated from the "I-type" Mystery Island pluton suite.

The sandstone-hosted deposits in the Helikian Hornby Bay or Dismal Lakes Groups overlying the batholith may be related to syngenetic, stratiform copper deposits, whose sulphides may have been the requisite reducing agents for pitchblende deposition. The largest known deposit, at Mountain Lake, overlies a basement horst, which could have influenced the formation of a copper-bearing horizon, or permitted the introduction of uraniferous solutions along faults. Uranium mineralisation took place beneath at least 5 km of cover rocks at Mountain Lake, which militates against the uraniferous solutions having

percolated downwards from overlying shale or evaporite potential sources; a source in the basement granitoids is considered more likely.

The meta-placer deposits are restricted to iron-rich aluminous bands in a belt of arkosic, potassic paragneisses beside the Wopmay Fault, metamorphosed prior to their intrusion by plutons of the batholith. Although detrital textures and features are often apparent, some might represent metamorphosed duricrust-hosted deposits of autunite or similar minerals, and are rich in boron and halides suggestive of evaporitic or brine environments during their original formation. Deposited originally within the palaeo-xerochore or desert region, these xerogenic deposits pre-date the Great Bear Batholith and probably derived their metallic and volatile elements from the adjacent "Hepburn highlands". They are thought to have donated excess ^{208}Pb to younger, hydrothermal deposits derived from them, and may be a remnant of the uraniferous protolith.

The Helikian sandstones overlying the batholith constitute a classical Proterozoic unconformity, a setting frequently known to have a high potential for uranium deposits. The amount of post-Helikian erosion of the batholith is unknown, although the markedly thin crust suggests that isostasy would have been achieved at a very early date. Much of the northern area may represent the re-exposed Helikian land surface, or not be significantly below it. However, only minor supergene pitchblende deposits along the Coppermine River can be proved to be spatially close to the unconformity.

The methods of transport and deposition of uranium can only be surmised from mineralogical evidence until further studies are carried out, and there is no single general pattern. Earlier studies have shown that a marine fluid was involved in the Echo Bay deposit. The reducing agents have been sulphides in a few deposits, but more usually ferrous minerals, probably silicates, now altered to hematite or sometimes chlorite. Alkali metasomatic wall-rock alteration is a feature of the larger hydrothermal deposits, a process which buffers the pH values of the solutions by the reversible alteration of white micas to feldspars. Contrary to the conclusions of some previous review studies, a significant number of supergene and hydrothermal deposits contain co-precipitated pitchblende and carbonates, indicating that pitchblende could have been precipitated by the loss of CO_2 from a dissolved uranyl carbonate complex. In the higher-temperature

hydrothermal deposits, uranyl ions could combine preferentially with other ligands, so that the problem of the fate of the carbonate in uranyl carbonate solutions may not arise.

Most thesis studies ask more questions than they answer, and this is no exception. In particular, the following further studies might prove fruitful:

- (1) A study of the suggested correlation between uranium remobilisation and palaeo-latitude.
- (2) Regional studies of uranium in other portions of the Canadian Shield, especially the Hepburn Batholith, from which few deposits have been reported.
- (3) A geochronological study of the dyke swarms of the Great Bear Batholith; this might resolve questions concerning the extent of the Western Channel diabases, and the single or multiple nature of the major periods of diabase activity.
- (4) Detailed studies of some specific deposits, using stable isotope and fluid inclusion techniques to investigate the source and nature of the mineralising solutions.
- (5) A metallogenic study of copper in the Great Bear Batholith; this element is closely associated with most of the uranium deposits found, but also forms its own unique deposit suites, and it has the same capacity for continual remobilisation and recycling by redox reactions.
- (6) A study of the source rocks and tectonic setting for the creation of the Great Bear Batholith.

X. REFERENCES CITED

- Ahuja, S.P. 1974. Exploration 1974, Ham mineral claims, Hardisty Lake area. Unpublished in-house report by Trigg, Woollett and Associates Ltd. for Imperial Oil Limited. From DIAND assessment records, Yellowknife (document 080193).
- Allan, R.J. and Cameron, E.M. 1973. Uranium content of lake sediments, Bear-Slave operation. Geol. Surv. Canada map 9-1972, sheet 1.
- Armstrong, R.C. 1969a. Exploration - 1969. KR (CROWN), DAN and JD claims, Wopmay River area, District of Mackenzie, N.W.T. Unpublished in-house report by Trigg, Woollett and Associates. From DIAND assessment records, Yellowknife.
- Armstrong, R.C. 1969b. Exploration - 1969. JD claims, Wopmay River area, District of Mackenzie, N.W.T. Unpublished in-house report by Trigg, Woollett and Associates. From DIAND assessment records, Yellowknife (document 060423).
- Baadsgaard, H., Morton, R.D. and Olade, M.A.D. 1973. Rb-Sr isotopic age for the Precambrian lavas of the Seton Formation, East Arm of Great Slave Lake, Northwest Territories. Can. J. Earth Sci. 10, p. 1579-1582.
- Badham, J.P.N. 1981. Petrochemistry of late Archean (~1.8 Ga) calc-alkaline diorites from the East Arm of Great Slave Lake, N.W.T., Canada. Can. J. Earth Sci. 18, p. 1018-1028.
- Badham, J.P.N. 1978. Magnetite-apatite-amphibole-uranium and silver-arsenide mineralizations in lower Proterozoic igneous rocks, East Arm, Great Slave Lake, Canada. Econ. Geol. 73, p. 1474-1491.
- Badham, J.P.N. 1973a; Volcanogenesis, orogenesis and metallogenesis, Camsell River area, N.W.T. PhD thesis (unpublished), University of Alberta, 334 p.
- Badham, J.P.N. 1973b; Calc-alkaline volcanism and plutonism from the Great Bear Batholith, N.W.T. Can. J. Earth Sci. 10, p. 1319-1327.
- Baillieul, T.A. and Indelicato, G.J. 1981. Uranium in the New Jersey and New York highlands of the Reading Prong. Econ. Geol. 76, p. 167-171.
- Balkwill, H.R. 1971. Reconnaissance geology, southern Great Bear Plain, District of Mackenzie. Geol. Surv. Canada paper 71-11, 47 p., plus map 5-1971 "Norman, and Camsell River".
- Bamford, D. and Prodehl, C. 1977. Explosion seismology and the continental crust-mantle boundary. J. Geol. Soc. London 134, p. 139-151.

- Baragar, W.R.A. and Donaldson, J.A. 1973. Coppermine and Dismal Lakes map-areas (report and maps 1337A and 1338A). Geol. Surv. Canada paper 71-39, 20 p.
- Barbier, J. and Ranchin, G. 1969. Influence de l'altération météorique sur l'uranium à l'état de traces dans le granite à deux micas de St-Sylvestre. *Geochim. et Cosmochim. Acta* 33, p. 39-47.
- Barr, K.G. 1971. Crustal refraction experiment: Yellowknife 1966. *J. Geophys. Res.* 76, p. 1929-1947.
- Barton, P.B. and Skinner, B.J. 1979. Sulphide mineral stabilities. /n: Barnes, H.L. (ed.). *Geochemistry of hydrothermal ore deposits*, 2nd edition. J. Wiley and Sons, p. 278-403.
- Baykal, O. 1967a. Geological report on Beaverlodge-Hottah Lake prosepct. ATOM and TIN claims, N.W.T. Unpublished in-house report of Syracuse Oils Ltd. and Index Construction Co. Ltd. From DIAND assessment records, Yellowknife.
- Baykal, O. 1967b. Geological report on PAL #1 to #10 mineral claims, Sheldon Lake, N.W.T. Unpublished private report. From DIAND assessment records, Yellowknife.
- Bell, R.T. 1978. Uranium in black shales - a review. /n: Kimberley, M.M. (ed.). *Uranium deposits: their mineralogy and origin*. Mineral. Ass. Canada short course, Toronto 1978, p. 307-329.
- Bennison, G.M. and Wright, A.E. 1969. *The geological history of the British Isles*. Arnold Ltd., 406 p.
- Bloy, G.R. 1979. U-Pb geochronology of uranium mineralisation in the East Arm of Great Slave Lake, N.W.T. MSc thesis (unpublished), University of Alberta, 64 p.
- Bond, K. 1976. Assessment report, HONK claims (group 1 & 2). Unpublished in-house report for Uranerz Exploration and Mining Ltd.. From DIAND assessment records, Yellowknife.
- Breyer, J.A. and Ehlmann, A.J. 1981. Mineralogy of arc-derived sediment: siliciclastic sediment on the insular shelf of Puerto Rico. *Sedimentology* 28, p. 61-74.
- Brockamp, O. 1973. Fixation of boron by authigenic and detrital clays. *Geochim. Cosmochim. Acta* 37, p. 1339-1351 (in German; English abstract).
- Burwash, R.A. and Baadsgaard, H. 1962. Yellowknife-Nonacho age and structural relations. *Roy. Soc. Canada Special Publ. No. 4*, p. 22-30.
- Burwash, R.A. and Cape, D.F. 1981. Petrology of the Fort Smith - Great Slave Lake radiometric high near Pilot Lake, N.W.T. *Can. J. Earth Sci.* 18, p. 842-851.
- Burwash, R.A. and Cumming, G.L. 1976. Uranium and thorium in the Precambrian basement

- of western Canada. I. Abundance and distribution. *Can. J. Earth Sci.* 13, p. 284–293.
- Cahen, L., François, A. and Ledent, D. 1971. Sur l'âge des uraninites de Kambove ouest et de Kamoto principal et révision des connaissances relatives aux minéralisations uranifères du Katanga et du copperbelt de Zambia. *Annales de la Soc. Geol. de Belgique* 94, p. 185–198.
- Cameron, E.M. and Allan, R.J. 1973. Distribution of uranium in the crust of the northwestern Canadian Shield as shown by lake-sediment analysis. *J. Geochemical Exploration* 2, p. 237–250.
- Cameron-Schumann, M. 1978. Electron microprobe study of uranium minerals and its application to some Canadian deposits. PhD thesis (unpublished), University of Alberta, 343 p.
- Campbell, D.D. 1955. Geology of the pitchblende deposit of Port Radium, Great Bear Lake, N.W.T. PhD thesis (unpublished), California Inst. of Technology, 323 p.
- Campbell, F.H.A. and Cecile, M.P. 1979. The north-eastern margin of the Aphebian Kilohigok Basin, Melville Sound, Victoria Island, District of Franklin. *Geol. Surv. Canada paper* 79–1A, p. 91–94.
- Cape, D.F. 1977. An investigation of the radioactivity of the Pilot Lake area, N.W.T. MSc thesis (unpublished), University of Alberta, 156 p.
- Chappell, B.W. and White, A.J.R. 1974. Two contrasting granite types. *Pacif. Geol.* 8, p. 173–174 (not seen).
- Charbonneau, B.W. 1980. The Fort Smith radioactive belt, Northwest Territories. *Current Research part C, Geol. Surv. Canada paper* 80–1C, p. 45–57.
- Christ, C.L. and Clark, J.R. 1960. Crystal chemical studies of some uranyl oxide hydrates. *Am. Mineral.* 45, p. 1026–1061.
- Christie, R.L. 1980. Palaeolatitudes and potential for phosphorite deposition in Canada. *Current Research, part B, Geol. Surv. Canada, paper* 80–1B, p. 241–248.
- Climie, J.A. 1975. Geological reconnaissance and airborne radiometric survey of the DIANNE–SUE groups, District of Mackenzie. Unpublished in-house report for Noranda Exploration Company Limited. From DIAND assessment records, Yellowknife (document 080230).
- Cloud, P. 1976. Major features of crustal evolution. *Geol. Soc. S. Africa, Annexure to vol.* 79, 33 p.
- Cook, P.J. and McElhinny, M.W. 1979. A re-evaluation of the spatial and temporal distribution of sedimentary phosphate deposits in the light of plate tectonics. *Econ. Geol.* 74, p. 315–330.

- Craig, J.R. and Scott, S.D. 1974. Sulfide phase equilibria. *In*: Ribbe, P.H. (ed.). Sulfide mineralogy. Mineral. Ass. America short course, p. CS-1 to CS-110.
- Cumming, G.L. 1974. Determination of uranium and thorium in meteorites by the delayed neutron method. *Chemical Geol.* 13, p. 257-267.
- Cumming, G.L. and Richards, J.R. 1975. Ore lead isotope ratios in a continuously changing earth. *Earth and Plan. Sci. Letters* 28, p. 155-171.
- Cumming, G.L. and Rimsaite, J. 1979. Isotopic studies of lead- depleted pitchblende, secondary radioactive minerals and sulphides from the Rabbit Lake uranium deposit, Saskatchewan. *Can. J. Earth Sciences* 16, No. 9, p. 1702-1715.
- Cuney, M. 1978. Geologic environment, mineralogy, and fluid inclusions of the Bois Noirs-Limouzat uranium vein, Forez, France. *Econ. Geol.* 73, p. 1567-1610.
- Dahlkamp, F.J. 1978. Geologic appraisal of the Key Lake U-Ni deposits, northern Saskatchewan. *Econ. Geol.* 73, p. 1430-1449.
- Darnley, A.G., English, T.H., Sprake, O., Preece, E.R. and Avery, D. 1965. Ages of uraninite and coffinite from south-west England. *Min. Mag.* 34, p. 159-176.
- Davidson, A. 1978. The Blachford Lake intrusive suite: an Aphebian alkaline plutonic complex in the Slave Province, Northwest Territories. *Geol. Surv. Canada paper* 78-1A, p. 119-127.
- Day, B. 1950. Preliminary report on the "LOIS" group property. Unpublished private report to Isabella Mining Co. Ltd.. From DIAND assessment records, Yellowknife (document 080788).
- Deer, W.A., Howie, R.A. and Zussman, J. 1963. Rock forming minerals (5 vols.). Longmans.
- Douglas, R.J.W. 1980. Proposals for time classification and correlation of Precambrian rocks and events in Canada and adjacent areas of the Canadian Shield. Part 2: A provisional standard for correlating Precambrian rocks. *Geol. Surv. Canada paper* 80-24, 19 p.
- Dunsmore, H.E. 1977. A new genetic model for uranium-copper mineralisation, Permo-Carboniferous basin, northern Nova Scotia. *Geol. Surv. Canada paper* 77-1B, p. 247-253.
- Dury, G.H. 1980. Neocatastrophism? A further look. *Progress in Physical Geography* 4, p. 391-413.
- Dyck, W. 1978. The mobility and concentration of uranium and its decay products in temperate surficial environments. *In*: Kimberley, M.M. (ed.). Uranium deposits: their mineralogy and origin. Mineral. Ass. Canada, short course Toronto 1978, p. 57-100.

- Eade, K.E. and Fahrig, W.F. 1971. Geochemical evolutionary trends of continental plates – a preliminary study of the Canadian Shield. *Geol. Surv. Canada Bull.* 179, 51 p.
- Easton, R.M. 1981a; Stratigraphy of a Proterozoic volcanic complex at Tuertok Lake, Wopmay Orogen, District of Mackenzie. *Current Research part A, Geol. Surv. Canada paper* 81-1A, p. 305-309.
- Easton, R.M. 1981b; REE, U and Th contents of Proterozoic and Archaean sedimentary rocks from the Bear and Slave structural provinces, N.W.T., Canada. *Geol. Ass. Canada Abstracts* 6 (Joint Annual Meeting 1981), p. A-16.
- Easton, R.M. 1980. Stratigraphy and geochemistry of the Akaitcho Group, Hepburn Lake map area, District of Mackenzie; an initial rift succession in Wopmay Orogen (early Proterozoic). *Current Research part B, Geol. Surv. Canada paper* 80-1B, p. 47-57.
- Erdosh, G. 1979. The Ontario carbonatite province and its phosphate potential. *Econ. Geol.* 74, p. 331-338.
- Erickson, R.L. and Blade, L.V. 1963. Geochemistry and petrology of the alkalic igneous complex at Magnet Cove, Arkansas. *U.S. Geol. Surv. Prof. Paper* #425.
- Faure, G. 1977. *Principles of isotope geology.* John Wiley and Sons, 464 p.
- Fehn, U., Cathles, L.M. and Holland, H.D. 1978. Hydrothermal convection and uranium deposits in abnormally radioactive plutons. *Econ. Geol.* 73, p. 1556-1566.
- Fleet, M.E.L. 1965. Preliminary investigations into the sorption of boron by clay minerals. *Clay Minerals* 6, p. 3-16.
- Fleischer, V.D., Garlick, W.G. and Haldane, R. 1976. Geology of the Zambian Copperbelt. *In: Wolf, K.H. (ed.). Handbook of strata-bound and stratiform ore deposits, Vol.6, p. 223-352, Elsevier.*
- Folinsbee, R.E. 1955. Archaean monazite in beach concentrates, Yellowknife geologic province, Northwest Territories, Canada. *Trans. R. Soc. Canada Ser.3, Section IV, Vol.XLIX, p. 7-24.*
- Fraser, J.A. 1967. Hardisty Lake. *Geol. Surv. Canada map* 1224A.
- Fraser, J.A., Hoffman, P.F., Irvine, T.N. and Mursky, G. 1972. The Bear Province. *Geol. Ass. Canada special paper* No. 11, p. 454-503.
- Frietsch, R. 1978. On the magmatic origin of iron ores of the Kiruna type. *Econ. Geol.* 73, p. 478-485.
- Frith, R., Frith, R.A. and Doig, R. 1977. The geochronology of the granitic rocks along the Bear-Slave structural province boundary, northwest Canadian Shield. *Can. J. Earth Sci.* 14, p. 1356-1373.

- Frith, R.A. 1980. Rb-Sr studies of the Wilson Island group, Great Slave Lake, District of Mackenzie. From: Rb-Sr and U-Pb isotopic age studies. /n: Current Research, part C, Geol. Surv. Canada paper 80-1C, p. 229-233.
- Fronzel, C. 1958. U.S. Geol. Survey Bull. 1064, p. 130-135 (not seen).
- Fuchs, Y. 1980. Sur l'importance des eaux connées pour la formation de certains gisements en milieux évaporitiques. Bull. Cent. Rech. Explor.-Prod. Elf-Aquitaine 4, p. 433-443.
- Furnival, G.M. 1935. The large quartz veins of Great Bear Lake, Canada. Econ. Geol. 30, p. 843-859.
- Gandhi, S.S. 1980. Mountain Lake deposit. /n: Non-hydrocarbon mineral resource potential of parts of northern Canada, Geol. Surv. Canada Open File No. 716, p. 31-32.
- Gandhi, S.S. 1978a. Geological observations and exploration guides to uranium in the Bear and Slave structural provinces and the Nonacho basin, District of Mackenzie. Current Research part B, Geol. Surv. Canada paper 78-1B, p. 141-149.
- Gandhi, S.S. 1978b. Geological setting and genetic aspects of uranium occurrences in the Kaipokok Bay-Big River area, Labrador. Econ. Geol. 73, p. 1492-1522.
- Garrels, R.M. and Christ, C.L. 1965. Solutions, minerals and equilibria. Freeman, Cooper and Co., 450 p.
- Gass, I.G. 1977. The evolution of the Pan African crystalline basement in NE Africa and Arabia. J. Geol. Soc. London 134, p. 129-138.
- Gavshin, V.M. 1972. Accumulation of uranium in natural layer aluminosilicates. Akad. Nauk SSSR Doklady 205, p. 956-959.
- Gill, F.D. 1969a. Evaluation report on the JLD group, Wopmay River area, N.W.T. Unpublished in-house report for Precambrian Mining Services Limited. From DIAND assessment records, Yellowknife (document 060421).
- Gill, F.D. 1969b. Evaluation report on the JD group, Wopmay River area, N.W.T. Unpublished in-house report for Precambrian Mining Services Limited. From DIAND assessment records, Yellowknife.
- Gocht, W. and Pluhar, E. 1981. Type and origin of uranium mineralizations in the Khorat Plateau, Thailand. Econ. Geol. 76, p. 1232-1244.
- Goldhaber, M.B., Reynolds, R.L. and Rye, R.O. 1978. Origin of a south Texas roll-type uranium deposit. II. Sulfide petrology and sulfur isotope studies. Econ. Geol. 73, p. 1690-1705.
- Halliday, A.N. 1980. The timing of early and main stage ore mineralisation in southwest

Cornwall. *Econ. Geol.* 75, p. 752-759.

- Halliday, A.N. and Mitchell, J.G. 1976. Structural, K-Ar and ^{40}Ar - ^{39}Ar age studies of adularia K-feldspars from the Lizard Complex, England. *Earth Plan. Sci. Letters* 29, p. 227-237.
- Hassard, F.R. 1975. Exploration 1975, YUK mineral claims, Mountain Lake (6031), Mackenzie Mining District, Northwest Territories. Unpublished in-house report of Trigg, Woollett and Associates to Imperial Oil Ltd. From DIAND assessment records, Yellowknife (document 080456).
- Hauseux, M.A. 1977. Mode of uranium occurrence in a migmatitic granite terrain, Baie Johan Beetz, Quebec. *Can. Min. Met. Bull.* 70, p. 110-116.
- Heier, K.S. and Adams, J.A.S. 1965. Concentration of radioactive elements in deep crustal material. *Geochim. et Cosmochim. Acta* 29, p. 53-61.
- Heinrich, E.W. 1958. Mineralogy and geology of radioactive raw materials. McGraw-Hill Book Company, Inc., 654 p.
- Henderson, J.F. 1949. Pitchblende occurrences between Beaverlodge and Hottah Lakes, Northwest Territories. *Geol. Surv. Canada paper* 49-16, 17 p.
- Hildebrand, R.S. 1980. Geological map of MacAlpine Channel (86K/5), Vance Peninsula (86K/4) and Echo Bay (86L/1). *Geol. Surv. Canada open file No.* 709.
- Hills, J.H. and Richards, J.R. 1976. Pitchblende and galena ages in the Alligator Rivers region, Northern Territory, Australia. *Mineral. Deposita* 11, p. 133-154.
- Hine, R., Williams, I.S., Chappell, B.W. and White, A.J.R. 1978. Contrasts between I- and S-type granitoids of the Kosciusko Batholith. *J. Geol. Soc. Austral.* 25, p. 219-234.
- Hoeve, J. and Sibbald, T.I.I. 1978. On the genesis of Rabbit Lake and other unconformity-type uranium deposits in northern Saskatchewan, Canada. *Econ. Geol.* 73, p. 1450-1473.
- Hoffman, P.F. 1981. Revision of stratigraphic nomenclature, foreland thrust-fold belt of Wopmay Orogen, District of Mackenzie. *Current Research part A, Geol. Surv. Canada paper* 81-1A, p. 247-250.
- Hoffman, P.F. 1980. On the relative age of the Muskox Intrusion and the Coppermine River basalts, District of Mackenzie. *Current Research part A, Geol. Surv. Canada paper* 80-1A, p. 223-225.
- Hoffman, P.F. 1978a. Age of exotic blocks in diatreme dykes of the Athapuscow Aulacogen, Simpson Islands area, East Arm of Great Slave Lake, District of Mackenzie. *Geol. Surv. Canada paper* 78-1A, p. 145-146.

- Hoffman, P.F. 1978b. Sloan River, 1 : 125000 map. Geol. Surv. Canada Open File No. 535.
- Hoffman, P.F. 1969. Proterozoic palaeocurrents and depositional history of the East Arm fold belt, Great Slave Lake, Northwest Territories. *Can. J. Earth Sci.* 6, p. 441-462.
- Hoffman, P.F. and Bell, I. 1975. Volcanism and plutonism, Sloan River map-area (86K), Great Bear Lake, District of Mackenzie. Geol. Surv. Canada paper 75-1A, p. 331-337.
- Hoffman, P.F., Bell, I.R. and Tirrul, R. 1976. Sloan River map-area (86K), Great Bear Lake, District of Mackenzie. Geol. Surv. Canada paper 76-1A, p. 353-358.
- Hoffman, P.F. and Cecile, M.P. 1974. Volcanism and plutonism, Sloan River map-area (86K), Great Bear Lake, District of Mackenzie. Geol. Surv. Canada paper 74-1A, p. 173-177.
- Hoffman, P.F., and McGlynn, J.C. 1977. Great Bear Batholith; a volcano-plutonic depression. Geol. Ass. Canada, special paper No. 16, p. 169-192.
- Hoffman, P.F. and St-Onge, M.R. 1981. Contemporaneous thrusting and conjugate transcurrent faulting during the second collision in Wopmay Orogen: implications for the sub-surface structure of post-orogenic outliers. Current Research part A, Geol. Surv. Canada paper 81-1A, p. 251-257.
- Hoffman, P.F., St-Onge, M., Carmichael, D.M. and de Bie, I. 1978. Geology of the Coronation Geosyncline (Aphebian), Hepburn Lake sheet (86J), Bear Province, District of Mackenzie. Current Research part A, Geol. Surv. Canada paper 78-1A, p. 147-151.
- Hoffman, P.F., St-Onge, M.R., Easton, R.M., Grotzinger, J. and Schulze, D.E. 1980. Syntectonic plutonism in north-central Wopmay Orogen (early Proterozoic), Hepburn Lake map area, District of Mackenzie. Current Research part A, Geol. Surv. Canada, paper 80-1A, p. 171-177.
- Hoste, J., Op De Beeck, J., Gijbels, R., Adams, F., Van Den Winkel, P. and De Soete, D. 1971. Instrumental and radiochemical activation analysis. Chemical Rubber Company Press, 148 p.
- Hostetler, P.B. and Garrels, R.M. 1962. Transportation and precipitation of uranium and vanadium at low temperatures, with special reference to sandstone-type uranium deposits. *Econ. Geol.* 57, p. 137-167.
- Irving, E. 1979. Paleopoles and paleolatitudes of North America and speculations about displaced terrains. *Can. J. Earth Sci.* 16, p. 669-694.
- Irving, E., Donaldson, J.A. and Park, J.K. 1972. Palaeomagnetism of the Western Channel diabase and associated rocks, Northwest Territories. *Can. J. Earth Sci.* 9, p. 960-971.

- James, W.C., Mack, G.H. and Suttner, L.J. 1981. Relative alteration of microcline and sodic plagioclase in semi-arid and humid climates. *J. Sed. Pet.* 51, p. 151-164.
- Jonasson, I.R. and Dunsmore, H.E. 1979. Low grade uranium mineralisation in carbonate rocks from some salt domes in the Queen Elizabeth Islands, District of Franklin. *Current Research part A, Geol. Surv. Canada paper 79-1A*, p. 61-70.
- Jory, L.T. 1964. Mineralogical and isotope relations in the Port Radium pitchblende deposit, Great Bear Lake, Canada. PhD thesis (unpublished), California Inst. Tech., 275 p.
- Kanasewich, E.R. 1968. The interpretation of lead isotopes and their geological significance. *In: Hamilton, E.I. and Farquhar, R.M., eds.; Radiometric dating for geologists.* Wiley Interscience Publishers, 506 p.
- Kerswill, J.A. and McConnell, J.W. 1979. The Grenville of Labrador: a possible target for uranium exploration in light of recent geological and geochemical investigations. *Current Research part B, Geol. Surv. Canada paper 79-1B*, p. 329-339.
- Kidd, D.F. 1933. Great Bear Lake area, Northwest Territories. *Geol. Surv. Canada Summary Report 1932, Part C*, p. 1-36.
- Kieller, B.J. 1962. Mineralogy of the No.2 zone, Eldorado Mine, Port Radium, Northwest Territories. Unpub. M.Sc. thesis, University of Alberta, 106 p.
- Killeen, P.G. and Richardson, K.A. 1978. The relationship of uranium deposits to metamorphism and belts of radioelement enrichment. *Geol. Surv. Canada paper 78-1B*, p. 163-168.
- Kimberley, M.M. 1978. Origin of stratiform uranium deposits in sandstone, conglomerate, and pyroclastic rocks. *In: Kimberley, M.M. (ed.). Uranium deposits: their mineralogy and origin.* Min. Ass. Canada short course, Toronto 1978, p. 339-381.
- Knipping, H.D. 1974. The concepts of supergene versus hypogene emplacement of uranium at Rabbit Lake, Saskatchewan, Canada. *In: Formation of uranium ore deposits.* I.A.E.A. Vienna, STI/PUB/374, p. 531-549.
- Kretz, R. 1968. Study of pegmatite bodies and enclosing rocks, Yellowknife-Beaulieu region, District of Mackenzie. *Geol. Surv. Canada Bull.* 159, 109 p.
- Kullerud, G. 1967. Sulfide studies. *In: Abelson, P.H. (ed.). Researches in Geochemistry*, vol. 2, p. 286-321. J. Wiley and Sons.
- Lambert, R. StJ. 1975. Archaean thermal regimes, crustal and upper mantle temperatures, and a progressive evolutionary model for the earth. *In: Windley, B.F. (ed.). The early history of the earth.* Wiley, p. 363-373.
- Lang, A.H. 1951. Canadian deposits of uranium and thorium (interim account). *Geol. Surv.*

Canada paper 51-10.

- Lang, A.H., Griffith, J.W. and Steacy, H.R. 1959. Canadian deposits of uranium and thorium. Geol. Surv. Canada, Economic Geology Series No. 16 (second edition), 324 p.
- Langford, F.F. 1978a. Uranium deposits in Australia. / *n*: Kimberley, M.M. (ed.). Uranium deposits: their mineralogy and origin. Mineral. Ass. Canada short course, Toronto 1978, p. 205-216.
- Langford, F.F. 1978b. Mobility and concentration of uranium in arid surficial environments. / *n*: Kimberley, M.M. (ed.). Uranium deposits: their mineralogy and origin. Mineral. Ass. Canada short course, Toronto 1978, p. 383-394.
- Langmuir, D. 1978a. Uranium solution-mineral equilibria at low temperatures with applications to sedimentary ore deposits. / *n*: Kimberley, M.M. (ed.). Uranium deposits: their mineralogy and origin. Mineral. Ass. Canada short course, Toronto 1978, p. 17-55.
- Langmuir, D. 1978b. Uranium solution-mineral equilibria at low temperatures with applications to sedimentary ore deposits. *Geochim. et Cosmochim. Acta* 42, p. 547-569.
- Leech, G.B., Lowdon, J.A., Stockwell, C.H. and Wanless, R.K. 1963. Age determinations and geologic studies (including isotopic ages - report 4). Geol. Surv. Canada paper 63-17.
- Legagneur, G.P. 1969. Geophysical report, DV claim group. Unpublished in-house report for Giant Yellowknife Mines Limited. From DIAND assessment records, Yellowknife.
- Leroy, J. 1978. The Margnac and Fanay uranium deposits of the La Crouzille district (western Massif Central, France): geologic and fluid inclusion studies. *Econ. Geol.* 73, p. 1611-1634.
- Lord, C.S. 1942. Snare River. Geol. Surv. Canada map 690A.
- Lord, C.S. and Parsons, W.H. 1952. Camsell River. Geol. Surv. Canada map 1014A.
- Loveridge, W.D. 1980. Rubidium-strontium and uranium-lead isotopic age studies, report 3. / *n*: Geol. Surv. Canada paper 80-1C, p. 161-246.
- Lowdon, J.A. 1963. Age determinations and geological studies: Part 1 - isotopic ages, report 4. Geol. Surv. Canada, paper 63-17, 140 p.
- Lowdon, J.A. 1962. Age determinations by the Geological Survey of Canada. Report 3: isotopic ages. Geol. Surv. Canada paper 62-17, 140 p.
- Lowdon, J.A. 1961. Age determinations by the Geological Survey of Canada: Report 2 - isotopic ages. Geol. Surv. Canada paper 61-17, 127 p.

- Lowdon, J.A. 1960. Age determinations by the Geological Survey of Canada. Report 1: isotopic ages. Geol. Surv. Canada paper 60-17, 51 p.
- Ludwig, K.R., Nash, J.T. and Naeser, C.W. 1981. U-Pb isotope systematics and age of mineralisation, Midnite mine, Washington. Econ. Geol. 76, p. 89-110.
- Mann, A.W. and Deutscher, R.L. 1978. Genesis principles for the precipitation of carnotite in calcrete drainages in Western Australia. Econ. Geol. 73, p. 1724-1737.
- Martineau, M.P. 1970. The petrology of the Big Spruce Lake complex. PhD thesis (unpublished), Oxford University, 93 p.
- Martineau, M.P. and Lambert, R.St-J. 1974. The Big Spruce Lake nepheline-syenite/carbonatite complex, N.W.T. /n: Geol. Ass. Canada/Mineral. Ass. Canada Joint Meeting, Programs with Abstracts, 1974, p. 59.
- McConnell, D. 1973. Apatite. Springer-Verlag, 111 p.
- McGlynn, J.C. 1979. Geology of the Precambrian rocks of the Riviere Grandin and in part of the Marian River map areas, District of Mackenzie. Current Research part A, Geol. Surv. Canada paper 79-1A, p. 127-131.
- McGlynn, J.C. 1977. Geology of Bear-Slave structural provinces, District of Mackenzie, scale 1 : 1,000,000. Geol. Surv. Canada Open File map no. 445.
- McGlynn, J.C. 1976. Geology of the Calder River (86 F) and Leith Peninsula (86 E) map-areas, District of Mackenzie. Current Research part A, Geol. Surv. Canada paper 76-1A, p. 359-361.
- McGlynn, J.C. 1971. Metallic mineral industry, District of Mackenzie, Northwest Territories. Geol. Surv. Canada, paper 70-17.
- McGlynn, J.C. 1968. Tumi Lake. Geol. Surv. Canada map 1230A.
- McGlynn, J.C. and Henderson, J.B. 1972. The Slave Province. Geol. Ass. Canada, special paper no.11, p. 506-526.
- McMorland, D. 1955. Geological report, NORI group of claims, Culbert Lake, N.W.T. Unpublished in-house report for Radiore Uranium Mines Limited. From DIAND assessment records, Yellowknife (document 017383).
- Meneghel, L. 1981. The occurrence of uranium in the Katanga System of northwestern Zambia. Econ. Geol. 76, p. 56-68.
- Miller, A.R. and Kerswill, J.A. 1980. Elemental associations within Aphebian clastic redbeds, northern half of the Richmond Gulf area, New Quebec. Current Research, part A, Geol. Surv. Canada paper 80-1A, p. 271-279.

- Miller, R.G. 1982. The geochronology of uranium deposits in the Great Bear Batholith, Northwest Territories. *In press*, Can. J. Earth Sci.
- Miller, R.G. 1981. Kawazulite $\text{Bi}_2\text{Te}_2\text{Se}$, related bismuth minerals and selenian covellite from the Northwest Territories. *Can. Mineralogist* 19, p. 341–348.
- Morton, R.D. 1978. The identification of uraniferous minerals. *In*: Kimberley, M.M. (ed.). Uranium deposits: their mineralogy and origin. Mineral. Ass. Canada short course, Toronto 1978, p. 141–183.
- Morton, R.D. 1974. Sandstone-type uranium deposits in the Proterozoic strata of northwestern Canada. *In*: Formation of uranium ore deposits. I.A.E.A. Vienna, STI/PUB/374, p. 255–273.
- Moss, R.D. and Marten, B.E. 1975. Geological investigation of BRUCE, MIKE, TIM, JEFF and ROD claims, Dismal Lakes area, Northwest Territories. Unpublished in-house report of B.P. Minerals Limited. From DIAND assessment records, Yellowknife, (document 080594).
- Munday, R.J. 1979. Uranium mineralisation in northern Saskatchewan. *Can. Min. Met. Bull.* 72, no. 804, p. 102–111.
- Mursky, G. 1973. Geology of Port Radium map-area, District of Mackenzie. *Geol. Surv. Canada Memoir* 374, 40 p.
- Mylrea, F.H. 1953. Report on the ME, PB claims, Marian River Area. Unpublished in-house report for Goldcrest Mines Ltd.. From DIAND assessment records, Yellowknife.
- Nielsen, P.A. 1978. Metamorphism of the Arseno Lake area, Northwest Territories. *Geol. Surv. Canada paper* 78–10, p. 115–122.
- Notholt, A.J.G. 1979. The economic geology and development of igneous phosphate deposits in Europe and the U.S.S.R. *Econ. Geol.* 74, p. 339–350.
- Overstreet, W.C. 1967. The geologic occurrence of monazite. *U.S.G.S. Professional Paper* no. 530, 327 p.
- Palache, C. and Berman, H. 1933. Oxidation products of pitchblende from Bear Lake. *Am. Mineral.* 18, p. 20–24.
- Palache, C., Berman, H. and Frondel, C. 1944–1962. Dana's system of mineralogy, 7th edition, 3 volumes. John Wiley and Sons.
- Parak, T. 1975. Kiruna iron ores are not "Intrusive-magmatic ores of the Kiruna type". *Econ. Geol.* 70, p. 1242–1258.
- Patchett, P.J., Bylund, G. and Upton, B.G.J. 1978. Palaeomagnetism and the Grenville orogeny: new Rb–Sr ages from dolerites in Canada and Greenland. *Earth and*

Plan. Sci. Letters 40, p. 349-364. "

- Paterson, J. 1976(a); Assessment report, FXO claim group (1-16). Unpublished in-house report for Uranerz Exploration and Mining Limited. From DIAND assessment records, Yellowknife.
- Paterson, J. 1976(b); Assessment report, UGI claim group (1-17, 19, 20). Unpublished in-house report for Uranerz Exploration and Mining Limited. From DIAND assessment records, Yellowknife (document 080484).
- Paterson, J. 1976(c); Assessment report, JONES group (1-40). Unpublished in-house report for Uranerz Exploration and Mining Limited. From DIAND assessment records, Yellowknife (document 080572).
- Paterson, J. 1976d. BERNI group (1-8), Mackenzie mining district. Unpublished in-house report for Uranerz Exploration and Mining Ltd.. From DIAND assessment records, Yellowknife (document 080589).
- Paterson, J. 1975(a); Assessment report, FXO claim group. Unpublished in-house report for Uranerz Exploration and Mining Limited. From DIAND assessment records, Yellowknife (document 080194).
- Paterson, J. 1975(b); Assessment report, UGI group 1-9, 10-17, 19 + 20. Unpublished in-house report for Uranerz Exploration and Mining Limited. From DIAND assessment records, Yellowknife (document 080231).
- Philpotts, A.R. 1967. Origin of certain iron-titanium oxide and apatite rocks. *Econ. Geol.* 62, p. 303-315.
- Rafalskiy, R.P., Vlasov, A.D. and Nikol'skaya, I.V. 1963. On the possibility of simultaneous transport of U^{6+} and S by hydrothermal solutions (from experimental data). *Akad. Nauk SSSR Doklady* 151, p. 432-434 (in Russian).
- Rakovic, M. 1970. Activation analysis (English translation edited by D. Cohen). Iliffe Books Ltd., London, 339 p.
- Ramdohr, P. 1969. The ore minerals and their intergrowth. 3rd edition. Pergamon Press, 1174 p.
- Rich, R.A., Holland, H.D. and Petersen, U. 1977. Hydrothermal uranium deposits. Elsevier, 264 p.
- Rimsaite, J. 1979. Petrology of basement rocks at the Rabbit Lake deposit and progressive alteration of pitchblende in an oxidation zone of uranium deposits in Saskatchewan. *Geol. Surv. Canada paper* 79-1B, p. 281-299.
- Rimsaite, J. 1977. Mineral assemblages at the Rabbit Lake uranium deposit, Saskatchewan: a preliminary report. *Geol. Surv. Canada paper* 77-1B, p. 235-246.

- Ripley, E.M., Lambert, M.W. and Berendsen, P. 1980. Mineralogy and paragenesis of red-bed copper mineralisation in the lower Permian of south central Kansas. *Econ. Geol.* 75, p. 722-729.
- Robertson, D.S., Tilsley, J.E. and Hogg, G.M. 1978. The time-bound character of uranium deposits. *Econ. Geol.* 73, p. 1409-1419.
- Robertson, J.A. 1978. Uranium deposits in Ontario. *In*: Kimberley, M.M. (ed.), *Uranium deposits: their mineralogy and origin*. Mineral. Ass. Canada short course, Toronto 1978, p. 229-280.
- Robinson, B.W. 1971. Studies on the Echo Bay silver deposit, Northwest Territories, Canada. PhD thesis (unpublished), University of Alberta, 229 p.
- Robinson, B.W. and Morton, R.D. 1972. The geology and geochronology of the Echo Bay area, Northwest Territories, Canada. *Can. J. Earth Sci.* 9, p. 158-171.
- Robinson, B.W. and Ohmoto, H. 1973. Mineralogy, fluid inclusions and stable isotopes of the Echo Bay U-Ni-Ag-Cu deposits, Northwest Territories, Canada. *Econ. Geol.* 68, p. 635-656.
- Roed, M.A. 1968. Economic geology of the LKS claims. Unpublished in-house report for Anaconda Petroleum Ltd. From DIAND assessment records, Yellowknife.
- Rogers, J.J.W., Ragland, P.C., Nishimori, R.K., Greenberg, J.K. and Hauck, S.A. 1978. Varieties of granitic uranium deposits and favorable exploration areas in the eastern United States. *Econ. Geol.* 73, p. 1539-1555.
- Rosholt, J.N., Zartman, R.E. and Nkomo, I.T. 1973. Lead isotope systematics and uranium depletion in the Granite Mountains, Wyoming. *Bull. Geol. Soc. America* 84, p. 989-1002.
- Runnells, D.D. 1969. The mineralogy and sulphur isotopes of the Ruby Creek copper prospect, Bornite, Alaska. *Econ. Geol.* 64, p. 75-90.
- Russell, R.D. and Farquhar, R.M. 1960. Lead isotopes in geology. Interscience Publishers, 243 p.
- Ruzicka, V. 1979. Uranium and thorium in Canada, 1978. Current Research part A. *Geol. Surv. Canada paper* 79-1A, p. 139-155.
- St-Onge, M.R. and Hoffman, P.F. 1980. "Hot-side-up" and "hot-side-down" metamorphic isograds in north-central Wopmay orogen, Hepburn Lake map area, District of Mackenzie. Current Research, part A, *Geol. Surv. Canada paper* 80-1A p. 179-182.
- Sawiuk, M.J. and Williams-Jones, A.E. 1981. Evidence for the pre-metamorphic concentration of uranium at Karpinka Lake, Saskatchewan. *Geol. Ass. Canada, Abstracts 6 (Joint Annual Meeting 1981)*, p. A-50.

- Schidlowski, M. 1975. Archaean atmosphere and evolution of the terrestrial oxygen budget. *In*: Windley, B.F. (ed.). The early history of the earth. Wiley, p. 525-535.
- Shaw, D.M. 1967. U, Th and K in the Canadian Precambrian Shield and possible mantle compositions. *Geochim. et Cosmochim. Acta* 31, p. 1111-1113.
- Smith, D.G.W. 1965. The chemistry and mineralogy of some emery- like rocks from Sithean Sluaigh, Strachur, Argyllshire. *American Mineralogist* 50, p. 1982-2022.
- Smith, D.G.W. and Gold, C.M. 1979. EDATA2: a Fortran IV computer program for processing wavelength- and/or energy-dispersive electron microprobe analyses. *In*: Newbury, D.E. (ed.), 1979. Microbeam analysis. San Francisco Press, p. 273-278.
- Smith, E.E.N. 1974. Review of current concepts regarding vein deposits of uranium. *In*: Formation of uranium ore deposits. I.A.E.A. Vienna, STI/PUB/374, p. 515-529.
- Smith, F.G. 1955. Sampling of main showing of PITCH 27-28 group. Unpublished in-house report by N.W. Byrne. From DIAND assessment records, Yellowknife.
- Snelling, A.A. 1980. A geochemical study of the Koongarra uranium deposit, Northern Territory, Australia. PhD thesis (unpublished), University of Sydney.
- Stacey, J.S. and Kramers, J.D. 1975. Approximation of terrestrial lead isotope evolution by a two-stage model. *Earth and Plan. Sci. Letters* 26, p. 207-221
- Steady, H.R. and Kaiman, S. 1978. Uranium minerals in Canada: their description, identification and field guides. *In*: Kimberley, M.M. (ed.). Uranium deposits: their mineralogy and origin. Mineral. Ass. Canada short course, Toronto 1978, p. 107-140.
- Steiger, R.H. and Jäger, E. 1977. Subcommittee on Geochronology: convention on the use of decay constants in geo- and cosmochemistry. *Earth and Plan. Sci. Letters* 36, p. 359-362.
- Stockwell, C.H. 1973. Revised Precambrian time scale for the Canadian Shield. *Geol. Surv. Canada paper* 72-52, 4 p.
- Stockwell, C.H. 1964. Fourth report on structural provinces, orogenies, and time-classification of rocks of the Canadian Precambrian shield. *Geol. Surv. Canada paper* 64-17 pt. II, p. 1-29.
- Stuckless, J.S. and Nkomo, I.T. 1978. Uranium-lead isotope systematics in uraniferous alkali-rich granites from the Granite Mountains, Wyoming: implications for uranium source rocks. *Econ. Geol.* 73, p. 427-441.
- Thorpe, R.I. 1978. Sill of Western Channel diabase, Port Radium, District of Mackenzie. *In*: Wanless, R.K. and Loveridge, W.D., 1978. Rubidium-strontium isochron

- age studies, report 2. Geol. Surv. Canada paper 77-14, p. 4-6.
- Thorpe, R.I. 1974. Lead isotope evidence on the genesis of the silver-arsenide vein deposits of the Cobalt and Great Bear Lake areas, Canada. *Econ. Geol.* 69, p. 777-791.
- Thorpe, R.I. 1972. Mineral exploration and mining activities, mainland Northwest Territories, 1966-1968. Geol. Surv. Canada paper 70-70, 204 p.
- Thorpe, R.I. 1971. Lead isotope evidence on age of mineralisation, Great Bear Lake, District of Mackenzie. Geol. Surv. Canada paper 71-1B, p. 72-75.
- Tilsley, J.E. 1978. Uranium mineralisation in shallow intrusive environments. *In*: Kimberley, M.M. (ed.). Uranium deposits: their mineralogy and origin. Mineral. Ass. Canada short course, Toronto 1978, p. 281-289.
- Troger, W.E. 1979. Optical determination of rock-forming minerals, 4th edition. Revised by Bambauer, H.U., Taborszky, F. and Trochim, H.D., English edition. E. Schweizerbart'sche Verlagsbuchhandlung, Stuttgart, 188 p.
- Turner, F.J. 1968. *Metamorphic Petrology*. McGraw-Hill, 403 p.
- Uytenbogaardt, W. and Burke, E.A.J. 1971. Tables for microscopic identification of ore minerals, 2nd edition. Elsevier, 430 p.
- Valloni, R. and Maynard, J.B. 1981. Detrital modes of recent deep-sea sands and their relation to tectonic setting: a first approximation. *Sedimentology* 28, p. 75-83.
- van Schmus, W.R. and Bowring, S.A. 1980. Chronology of igneous events in the Wopmay Orogen, Northwest Territories, Canada. *In*: Abstracts with Programs, Geol. Soc. America, 12, no.7, p. 540.
- Walker, R.R. 1977. The geology and uranium deposits of Proterozoic rocks, Simpson Islands, Northwest Territories. MSc thesis (unpublished), University of Alberta.
- Walton, A.W., Galloway, W.E. and Henry, C.D. 1981. Release of uranium from volcanic glass in sedimentary sequences: an analysis of two systems. *Econ. Geol.* 76, p. 69-88.
- Wanless, R.K. and Loveridge, W.D. 1972. Rubidium-strontium isochron age studies, report 1. Geol. Surv. Canada paper 72-23, 77 p.
- Wanless, R.K., Stevens, R.D., Lachance, G.R. and Delabio, R.N. 1979. Age determinations and geological studies: K-Ar isotopic ages, report 14. Geol. Surv. Canada paper 79-2, 67 p.
- Wanless, R.K., Stevens, R.D., Lachance, G.R. and Delabio, R.N. 1978. Age determinations and geological studies: K-Ar isotopic ages, report 13. Geol. Surv. Canada

paper 77-2, 60 p.

- Wanless, R.K., Stevens, R.D., Lachance, G.R. and Delabio, R.N. 1974. Age determinations and geological studies: K-Ar isotopic ages, report 12. Geol. Surv. Canada paper 74-2, 72 p.
- Wanless, R.K., Stevens, R.D., Lachance, G.R. and Delabio, R.N. 1973. Age determinations and geological studies: K-Ar isotopic ages, report 11. Geol. Surv. Canada paper 73-2, 139 p.
- Wanless, R.K., Stevens, R.D., Lachance, G.R. and Delabio, R.N. 1972. Age determinations and geological studies: K-Ar isotopic ages, report 10. Geol. Surv. Canada paper 71-2, 96 p.
- Wanless, R.K., Stevens, R.D., Lachance, G.R. and Delabio, R.N. 1970. Age determinations and geological studies. K-Ar isotopic ages, report 9. Geol. Surv. Canada paper 69-2A, 78 p.
- Wanless, R.K., Stevens, R.D., Lachance, G.R. and Edmonds, C.M. 1967. Age determinations and geological studies: K-Ar isotopic ages, report 8. Geol. Surv. Canada paper 67-2 (part A), 141 p.
- Wanless, R.K., Stevens, R.D., Lachance, G.R. and Edmonds, C.M. 1966. Age determinations and geological studies: K-Ar isotopic ages, report 7. Geol. Surv. Canada paper 66-17, 120 p.
- Wanless, R.K., Stevens, R.D., Lachance, G.R. and Rimsaite, J.Y.H. 1965. Age determinations and geological studies. K-Ar isotopic ages, report 6. Geol. Surv. Canada paper 65-17, 101 p.
- Wanless, R.K., Stevens, R.D., Lachance, G.R. and Rimsaite, J.Y.H. 1964. Age determinations and geological studies: Part 1: isotopic ages, report 5. Geol. Surv. Canada paper 64-17 (part 1), 126 p.
- Washburn, A.L. 1973. Periglacial processes and environments. Edward Arnold Ltd., 320 p.
- Wedepohl, K.H. 1969, 1970, 1972, 1974, 1978. Handbook of geochemistry (editor). Springer-Verlag, Berlin.
- Wilson, J.T. and Lord, C.S. 1942. Ingray Lake. Geol. Surv. Canada map 697A.
- Windley, B.F. 1977. The crust-mantle boundary in space and time. J. Geol. Soc. London 134, p. 99-102.
- Winkler, H.J.F. 1979. Petrogenesis of metamorphic rocks. Springer-Verlag, 348 p.
- Withers, R.L. 1979. Mineral deposits of the Northrim mine and a brief enquiry into the genesis of veins of the (Ag, Bi, Ni, Co, As) type. MSc thesis (unpublished), University of Alberta, 271 p.

Zielinski, R.A., Lindsey, D.A. and Rosholt, J.N. 1980. The distribution and mobility of uranium in glassy and zeolitised tuff, Keg Mountain area, Utah, U.S.A. *Chemical Geol.* 29, p. 139–162.

XI. APPENDIX I: KEY TO SAMPLE NUMBERING

To identify any sample referred to, *e.g.* B31Ciiib:

B31 refers to field note-book B, p. 31.

C refers to the third outcrop described on this page.

iii refers to the third sample from this outcrop.

b indicates the second of two or more analyses performed on this sample (generally restricted to the isotopic analyses).

LOCATION OF SAMPLES

A1-A4:	Hornby Bay area, Great Bear Lake
A5-A8:	Coppermine River showings
A9:	Achook Island
A15-A16:	Mazenod Lake
A17-A20B:	Rayrock mine
A20C-A22A:	Bell Island, Hottah Lake
A23-A27:	Dease Lake area
A28-A31:	UGI/DV claims
A32-A35:	Echo Bay
A36-A42:	Mountain Lake
B1-B9:	Beaverlodge Lake
B10:	PITCH 27-28
B11-B16:	PITCH 8-10, JB and LOIS claims, and general Hottah Lake area
B17-B21:	Leith Peninsula
B23-B27:	HAM and JONES showings
B28A-C, B30D-B37:	JD group of showings
B28D-B30B:	JLD showings
B38-B42:	JACKPOT showing
B43-B44:	Dog Island, Conjuror Bay
B45-C4:	NORI/RA showings

XII. APPENDIX II: ANALYTICAL TECHNIQUES

Electron microprobe analyses

The standard operating conditions and the techniques for the energy-dispersive analyses (EDA) are described in Miller (1981) (Appendix IV) and will not be repeated. Pseudobrookite (nominally Fe_2TiO_5) and uraninite (nominally UO_2 to U_3O_8) were quantitatively analysed. Standards for U and Th were metal oxides; for Pb, a Pb-Si glass; for Fe, hematite; for Ti, rutile or ilmenite; for the rare earths, a variety of artificial glasses and a monazite; for Nb, niobium metal; for Y, yttrium metal or a Y-Fe "garnet"; and for other trace elements, a variety of ordinary silicate minerals. The principles of overlap correction, background fitting and detection limits are also briefly described in Appendix IV.

For the rare earth elements, overlap coefficients are large and difficult to obtain, since standards and samples generally contain several rare earths, each of which has some three major and three other significant L emission lines. Wave-length dispersive analysis (WDA) was used for the uraninite samples containing rare earth elements. The data-reduction programme EDATA2 (Smith and Gold 1979) can simultaneously handle EDA and WDA data, so that other elements could be analysed by EDA.

Reflectivity and hardness measurements

The details of reflectivity and microhardness measurement are detailed in Appendix IV and will not be repeated here.

Neutron activation analysis

The determination of U and Th by neutron activation analysis is in increasing use, and is a rapid, sensitive, accurate and cheap method of analysing trace levels of these elements in geological materials. The general principles of neutron activation are detailed by Rakovic (1970) and Hoste *et al.* (1971), and the details of some procedures for U and Th by Cumming (1974).

The delayed neutron technique depends upon inducing fission in fissionable nuclides, which in practice are only ^{232}Th , ^{235}U and ^{238}U . The fission products subsequently decay by neutron emission after a beta-minus decay. These emitters have half-lives in the range of 1 – 60 seconds, compared to the prompt neutrons emitted during the fission process. The only other delayed neutron emitters are ^9Li and ^{17}N . ^9Li , with a half-life of 0.17 seconds, is produced from the reaction $^9\text{Be}(n,p)^9\text{Li}$; Be is not a significant component in most rocks, and the rapid decay of the ^9Li makes this insignificant after a few seconds. ^{17}N , with a half-life of 4.2 seconds, is produced by the reaction $^{17}\text{O}(n,p)^{17}\text{N}$. Oxygen being a major component of most rocks, and the half-life being significant, this is the only likely interference to occur, and Cumming (*op. cit.*) showed that it may be ignored for 10 g samples, using a 25 second cooling time and a 64 second counting time, except for determining Th at levels below 1 ppm.

Thermal (slow) neutrons are necessary to fission ^{235}U , and fast neutrons to fission ^{232}Th and ^{238}U . Thus a sample must be irradiated twice, once to determine ^{235}U and hence ^{238}U , the second time by fast neutrons to determine ^{232}Th (using the known U content to correct for ^{238}U). The sensitivity for Th analyses is about 1% of that for U, and can only be increased by increasing the irradiation time in the reactor to a point where the sample becomes too hot to handle.

The analyst, Dr. E. Hoffman of McMaster University, Ontario, reports detection limits of 0.1 ppm U by this technique. Thorium was determined by instrumental neutron activation analysis (INAA), whereby the isotope ^{233}Th is produced from ^{232}Th , decaying by beta-minus decay with a half-life of 22.2 minutes. The gamma-ray emission during the beta decay is measured to obtain the Th concentration by comparison with a Th standard.

XIII. APPENDIX III: ISOTOPIC AGES OF THE DEPOSITS

This appendix comprises a pre-print copy of a paper accepted for publication by the Canadian Journal of Earth Sciences. All figures and references are as they will appear in print, except that the figure and table numbers have been altered to run consecutively with the body of this thesis.

THE GEOCHRONOLOGY OF URANIUM DEPOSITS IN THE GREAT BEAR BATHOLITH,
NORTHWEST TERRITORIES

ABSTRACT

The oldest uranium mineralisation found in the Great Bear Batholith during this study may be hydrothermal pitchblende-hematite veins at Hottah Lake. Their apparent age of 2058 ± 34 Ma can also be explained by the contamination of deposits only 440 ± 57 Ma old, the age of pitchblende veins nearby. Numerous pendants of metamorphosed, uraninite-bearing "black sand" placers in a north-trending belt west of the Wopmay Fault are 1860 ± 20 Ma old, the age of the granites which intrude them. Mineralisation at Echo Bay is from 1500 ± 10 Ma to 1424 ± 29 Ma old, and extends up to 30 kilometres north and 40 kilometres south of Echo Bay. The JD claims contain small quartz vein deposits dated at 535 ± 164 Ma and 1092 ± 115 Ma. At Mountain Lake, pitchblende in Helikian sandstones overlying the batholith is 1076 ± 96 Ma old. Polymetallic veinlets at Mazenod Lake are 457 ± 26 Ma old. Pitchblende in a giant quartz vein at the Rayrock mine is 511 ± 86 Ma old. Small pitchblende veins east of the batholith along the Coppermine River are between 400 and 660 Ma old.

All the deposits are either between some 400 and 660 Ma old, or indicate remobilisation during this interval. These events may be related to a marine transgression and regression, approximately 600 and 350 Ma ago respectively.

A. Introduction

Middle and Late Proterozoic rocks are frequently uraniferous metatexites in many parts of the world. In Canada, a widespread late Aphebian (~1800 Ma) unconformity in such areas as the Athabasca Basin is recognised as generally favourable for unconformity-associated uranium mineralisation, this mineralisation ranging in age from 1800 Ma to recent (*e.g.* Hoeve *et al.* 1981; Cumming and Rimsaite 1979). Although the Great Bear Batholith (1850–1875 Ma) lacks a widespread cover sequence, it also hosts a number of uranium deposits. This study suggests that late Aphebian hydrothermal deposits and pre-batholithic uraninite-bearing placers, emplaced in the margins of the Great Bear Batholith, are among the original sources of uranium, and that subsequent remobilisation of these under tropical weathering regimes has produced the range of deposit types and ages seen today.

B. Regional geology

The Great Bear Batholith is a late Aphebian complex of acidic ignimbrites, flows and plutons, separated from the Wentzel and Hepburn Batholiths by the Wopmay Fault (Fig. 29). Together these batholiths form part of the Wopmay Orogen (Hoffman and St-Onge 1981). Zircon U–Pb geochronology has given ages of 1890 ± 20 Ma for the Hepburn Batholith, at least 1875 Ma for the base of the Great Bear Batholith, and 1860 ± 10 Ma for the upper Great Bear Batholith (van Schmus and Bowring 1980). Granodiorite from a block of "exotic terrain" between Great Bear Lake and Hottah Lake has been dated at 1920 ± 10 Ma (van Schmus and Bowring *op. cit.*; Hoffman and St-Onge *op. cit.*; McGlynn 1979). Current interpretations of the tectonic structure suggest an older subduction zone at approximately 1900 Ma dipping west beneath the present Great Bear Batholith, followed by a younger subduction zone at approximately 1850 Ma dipping east beneath it (Hoffman and St-Onge 1981).

Numerous remnants of pre-batholithic sedimentary rocks occur as narrow, north-trending belts of biotitic paragneiss and migmatite, just west of the Wopmay Fault, but their full extent is unknown. Granitoid plutons in the southern part of the Great Bear Batholith contain sedimentary and volcanic roof pendants, which have either been loosely classified with the Snare Group, or ascribed to syn-orogenic deposition, or simply left

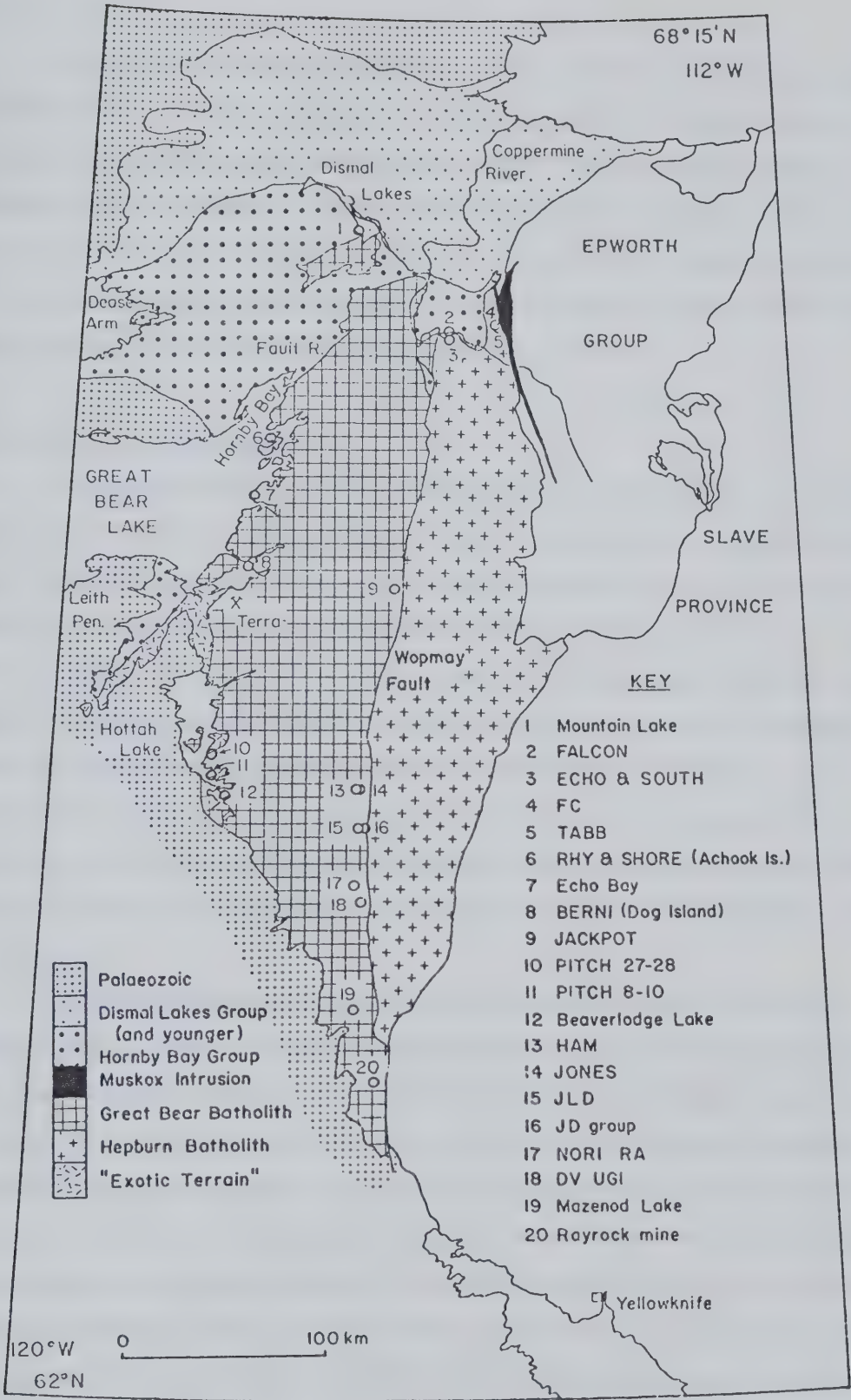


Figure 29: General geology and sample location map, Great Bear Batholith.

unclassified.

The Hornby Bay Group is the basal unit of the Amundsen Basin, a post-Hudsonian structure which accumulated shallow-water marine sediments throughout much of the Helikian and Hadrynian. In places it has a basal regolith, overlying rather rugged topography, before passing up into a sequence of sandstones, shales and stromatolitic dolomites. This group predates the Coppermine River basalts, the MuskoX Intrusion and the Mackenzie diabase swarm, all approximately 1200 Ma old (Hoffman 1980; Douglas 1980; Patchett *et al.* 1978; Wanless *et al.* 1964).

C. Sample sites and geology

The deposits (Fig. 29) are either named after major lakes, or by present claim names, or by the claim names current when reports were filed with the Department of Indian Affairs and Northern Development, Yellowknife. Acknowledgement must be made to the public company reports in the DIAND Yellowknife office, which are too numerous to list individually. The use of the words deposit, showing and occurrence implies nothing concerning their economic viability. The genetic classification of uranium deposits is still a matter of opinion and local geology, and they are classified here simply as metamorphosed palaeo-placers, vein deposits, sandstone-hosted deposits and hematite-pitchblende fels, which is a fine-grained, hydrothermal vein material. Gandhi (1978) has described some of the uranium deposits and regional mineralisation patterns in the area.

At Mountain Lake, uranium mineralisation is hosted by the so-called unit 11 sandstone, at the contact of the Hornby Bay Group and the overlying Dismal Lakes Group. Showings in the Hornby Bay sandstones were also sampled on Leith Peninsula, at Dease Lake (between Hornby Bay and Dease Arm) and near Fault River, but only sulphides and secondary uranium mineralisation were found at surface. The Mountain Lake pitchblende samples came from five pieces of drill core provided by Trigg, Woollett Consulting Ltd., and the data should not be extrapolated to primary mineralisation elsewhere in these sandstones. The core samples contain siliceous pitchblende and coffinite, both slightly phosphatic. Chemical and optical variations could not be positively linked to a paragenetic sequence. Minor Fe-Cu sulphides and Co-Ni sulph-arsenides accompany the uranium.

Along the Coppermine River are several small pitchblende vein occurrences (2–5, Fig. 29), generally hosted by igneous rocks and paragneiss of the Hepburn Batholith, just beneath the unconformity with the Hornby Bay Group. Since the uranium may have been transported out of the Great Bear Batholith, or may have been derived from pre- or post-batholithic rocks common to both batholiths, it is appropriate to include these deposits in this paper. The styles of mineralisation are diverse, and only nine pitchblende samples from four showings were analysed.

The well-known hydrothermal veins of the Echo Bay and Eldorado mines at Echo Bay carry U/Ag/Bi/Cu/Co/Ni/As minerals in a quartz and carbonate gangue (Robinson and Ohmoto 1973; Robinson and Morton 1972). The hydrothermal fluid was probably sea-water circulating through a diabase sheet 1392 ± 48 Ma old (Robinson and Ohmoto *op. cit.*; age revised after Thorpe 1978). Badham (1973) showed that the silver deposits of the Camsell River, such as at the Terra mine, resemble those of Echo Bay, and Thorpe (1974) confirmed some lead isotope similarities. The RHY and SHORE claims on Achook Island, Great Bear Lake, contain small quartz veins mineralised with pitchblende, copper sulphides and cobalt–nickel arsenides. The low-grade mineralisation at the BERNI claims on Dog Island, Conjuror Bay, is very fine-grained pitchblende or coffinite, deposited with hematite and carbonate around small clasts in veins of brecciated ignimbrite. The Achook Island deposits are hosted by rhyolitic ignimbrites of the Cameron Bay Formation, while the remainder occur generally within felsic extrusives of the Port Radium and Echo Bay Formations (Hildebrand 1980; Hoffman *et al.* 1976).

The meta-placer deposit group comprises uraninite showings in amphibolite facies metasedimentary rocks, intruded by granitic plutons along the west side of the Wopmay Fault. The deposits sampled are on the NORI/RA and UGI/DV claim groups at DeVries Lake, the HAM and JONES claims at Hailstone Lake, the JACKPOT claims and the JLD claims. These are thought to be metamorphosed palaeo-placers derived from the Hepburn Batholith, and are characterised by recrystallised magnetite with variable heavy mineral suites (including zircon, apatite, xenotime, ilmenite and allanite), detrital uraninite grains and paragenetically late pyrite and chalcopyrite. Similar deposits elsewhere have been described by Burwash and Cape (1981) and Baillieul and Indelicato (1981); the latter proposed a non-placer origin for their material.

Unsuccessful mining attempts were made between 1950 and 1956 at the PITCH 8–10 claims on Hottah Lake, and at Beaverlodge Lake (not to be confused with Beaverlodge Lake, Saskatchewan). The Beaverlodge Lake deposits are veins and lenses of pitchblende or hematite–pitchblende fels, hosted by volcanic and sedimentary pendants of unknown age in granites of the Great Bear Batholith (McGlynn 1979). Some 10 kilometres north of Beaverlodge Lake lies the PITCH 8–10 mine, where quartz–carbonate veins in a diabase dyke of unknown age carry pitchblende, and 10 kilometres north again are the PITCH 27–28 claims, where pitchblende cements a brecciated quartz vein cutting granite of the Great Bear Batholith. The PITCH 27–28 claims are at the border of the exotic terrain basement complex.

The JD deposit is a quartz vein system containing metabasalt–hosted pitchblende veinlets, adjacent to a giant quartz vein west of the Wopmay Fault. The T1 and Main Zone veins appear to be granite–hosted branches of the JD vein system, but there are consistent isotopic differences, particularly in the $^{208}\text{Pb}/^{204}\text{Pb}$ ratios. The veins are some 4 kilometres east of the JLD meta–placer showing (*q.v.*).

The Mazenod Lake Cu–U occurrence contains polymetallic veinlets within a breccia pipe, hosted by ignimbrites of the Great Bear Batholith. The material contains a finely intergrown mixture of coeval pitchblende, hematite and Bi–Cu–Pb–S–Se–Te minerals (Miller 1981).

The deposits mined at Rayrock were pitchblende–hematite veins, hosted by a quartz stockwork which branches from the Marion River Fault (McGlynn 1971). This fault also contains a quartz stockwork, and could be classed as a giant quartz vein. The materials analysed were thin veins and disseminations of pitchblende in quartz and silicified granodiorite country rocks of the batholith.

Echo Bay Geochronology

The general geochronology of the Echo Bay deposits has not been reviewed since the acceptance of revised decay constants (Steiger and Jager 1977), and it is appropriate to do so here (Fig. 30). The adjacent granodioritic Hogarth pluton was dated at 1790 ± 30 Ma by zircon U–Pb geochronology (revised after Jory 1964), but recent analyses suggest approximately 1850–1860 Ma (S. Bowring, pers. comm. 1981). It cuts

ECHO BAY: REVISED GEOCHRONOLOGY

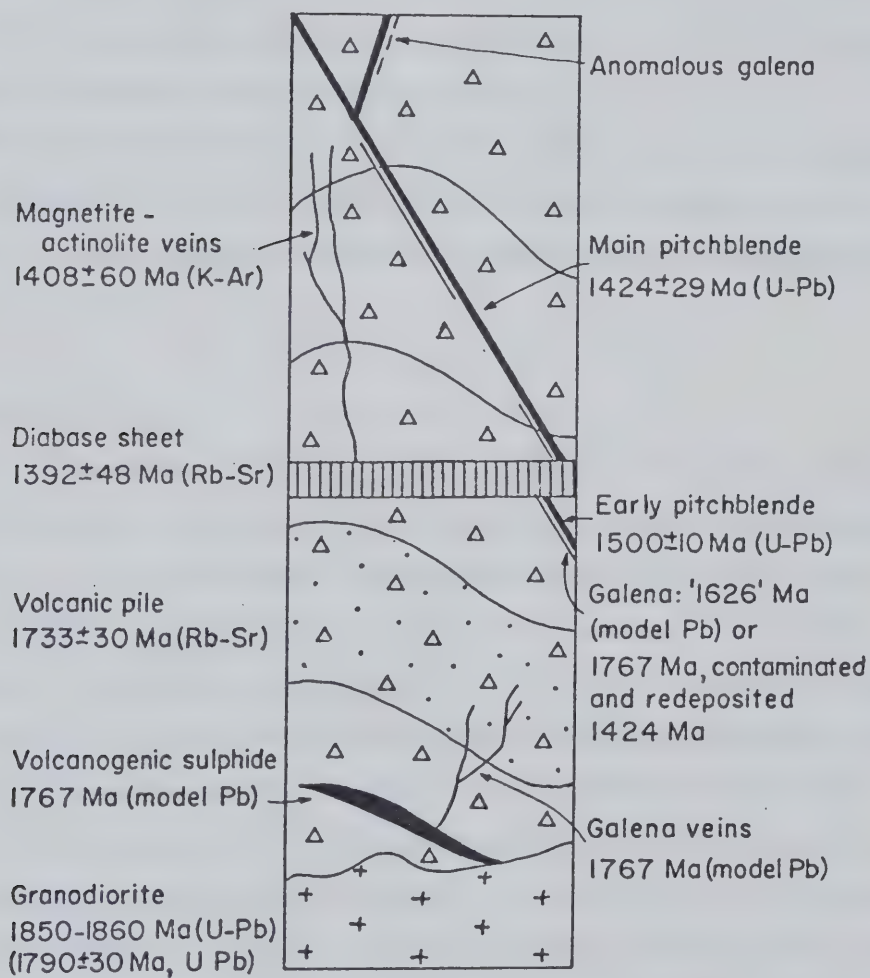


Figure 30: Echo Bay: general geochronology.

apparently coeval volcanic equivalents with a whole-rock Rb–Sr age of 1733 ± 30 Ma or 1772 ± 90 Ma (both revised after Robinson 1971). The volcanic and intercalated sedimentary rocks host the mineralised veins. A Rb–Sr isochron age of 1392 ± 48 Ma was obtained for a diabase sheet at Port Radium (revised from Thorpe 1978), while possibly related magnetite–actinolite veins have a K–Ar age of 1408 ± 60 Ma (revised after Robinson 1971). Similar magnetite–actinolite–apatite pods at the Terra mine, however, may be older than the felsic volcanism (Badham 1973).

Robinson and Morton (1972) noted that the K–Ar ages which they obtained for the granodiorite and its related extrusives are about 1650 Ma, markedly lower than their Rb–Sr age. Loss of argon during burial and minor metamorphism was suggested as the cause of the lower ages.

D. Techniques: Sampling

Nearly all the samples have been studied in polished and thin section. Samples were first slabbed and a radioluxograph, regarded as a prerequisite for such studies, taken of the cut surface. On the basis of the radioluxograph, selected chips were marked, sawn out and crushed, then hand-picked under a binocular microscope; a sand-size grain of pitchblende is usually sufficient. This eliminates secondary uranium minerals and yields reliable samples from disseminated pitchblende mineralisation. The risk of simultaneously sampling several generations of mineralisation was reduced by reference to the polished sections, by using fewer, larger grains, and by analysing physically distinct pitchblende varieties separately. In the accompanying tables, different samples from the same hand specimen are indicated by final lower-case letters in the catalogue numbers; roman numerals designate different hand specimens from the same outcrop. Duplicate samples from single crushings were sometimes used, since two single grains need not have lost identical amounts of lead. Only when some ten or more grains are required for a single analysis does this approach prove unhelpful, since homogeneity is then being achieved by mixing.

For a few specimens, preliminary concentration with heavy liquids was necessary. For magnetite-rich material, containing as little as 300 ppm uranium, a rock chip or a mass of unpicked heavy concentrate was taken, since uraninite could not be physically or

optically distinguished in the concentrate.

Pb and U Isotope Measurements

Samples were weighed and decomposed in nitric acid, with up to 10% hydrochloric- or hydrofluoric-acid as necessary to achieve total decomposition of the mineralisation and any gangue. Lead and uranium were isolated by ion exchange. ^{208}Pb and ^{235}U were used as tracers for the quantitative determinations by isotope dilution. Galena was dissolved in hydrochloric acid, but other sulphides were at first dissolved in nitric acid, and lead may have been lost as the insoluble sulphate. Later sulphide samples were roasted in air to remove the sulphur as oxides, although some lead might be lost by volatilisation by this technique. No common lead samples were analysed for uranium.

Isotopes were analysed on a 30 cm. radius, solid source Micromass-30 mass spectrometer at the University of Alberta. Lead chloride was loaded by the conventional phosphoric acid/silica gel technique on a central rhenium filament, and uranium nitrate was loaded directly on to a side rhenium filament. The lead isotopes were measured using ^{206}Pb as the index. The precision for $^{207}\text{Pb}/^{206}\text{Pb}$ and spiked $^{208}\text{Pb}/^{206}\text{Pb}$ ratios was generally better than $\pm 0.03\%$, but the $^{204}\text{Pb}/^{206}\text{Pb}$ and unspiked $^{208}\text{Pb}/^{206}\text{Pb}$ ratios may have errors as high as 50% in extreme cases, due to the very low levels of ^{204}Pb and ^{208}Pb present. At these trace isotope levels, such errors have no effect on the age calculation. The unspiked $^{208}\text{Pb}/^{204}\text{Pb}$ ratios have the lowest precision, which is unfortunate since this ratio can often serve as a "fingerprint" to identify related mineralisation. Blanks were negligible, being 10–20 ng of Pb and less than 3 ng of U. Pb/U ratios have estimated total precisions of better than 1%.

The decay constants used herein are those recommended by Steiger and Jäger (1977): $\lambda^{235}\text{U} = 9.8485 \times 10^{-10}\text{yr}^{-1}$, $\lambda^{238}\text{U} = 1.55125 \times 10^{-10}\text{yr}^{-1}$, $\lambda^{232}\text{Th} = 4.9475 \times 10^{-11}\text{yr}^{-1}$, $\lambda^{87}\text{Rb} = 1.42 \times 10^{-11}\text{yr}^{-1}$, $\lambda^{40}\text{K}\beta = 4.962 \times 10^{-10}\text{yr}^{-1}$, $\lambda^{40}\text{K}\alpha + \lambda'^{40}\text{K}\alpha = 0.581 \times 10^{-10}\text{yr}^{-1}$. The mantle model of Stacey and Kramers (1975) was used for all model lead calculations, and gives results essentially similar to those using the model of Cumming and Richards (1975). In age calculations for phases with radiogenic lead, the "cumulative age" assumes that lead accumulated in the source until it was extracted relatively recently, and it is the maximum possible age for the source (Russell and Farquhar 1960). The

"instantaneous age" denotes the moment when uranium was producing lead with the measured $^{207}\text{Pb}/^{206}\text{Pb}$ ratio, and is the maximum possible age of the lead mineral (Russell and Farquhar *op. cit.*).

Treatment of Lead Isotope Data

The samples analysed contain measurable amounts of common or contaminant lead trapped during mineralisation, indicated by the non-radiogenic isotope ^{204}Pb . A so-called ordinary common lead is one isotopically similar to lead from the mantle. However, when uranium is remobilised and redeposited, uranogenic ^{206}Pb and ^{207}Pb (the daughters of ^{238}U and ^{235}U) may be mobilised with it, and extra ^{208}Pb may similarly be incorporated into the common lead from a thorium-bearing source.

A correction for the common lead is necessary for concordia plots, but its composition must be assumed if it cannot be directly measured from a coeval, uranium-free, lead-bearing phase. If the common lead has inherited unsuspected, older uranogenic lead and is present in large amounts, the sample gives a spuriously high apparent age, and in such cases the Pb-Pb isochron and U-Pb discordia ages of a sample suite may differ. Such older lead will scatter the analyses towards higher $^{207}\text{Pb}/^{235}\text{U}$ values, and always to a *greater* apparent age. A least-squares fit discordia will then generally be biased to a greater age at the upper intersection and a lesser age at the lower, and may also be rotated in either sense. Excess uranogenic lead is indicated when an isochron passes above the mantle lead growth curve, for which a μ value of approximately 9 is indicated at Echo Bay (Thorpe 1974). If the discordia and isochron ages disagree markedly, the isochron age is regarded as more reliable, although less precise; if they agree, the mean value has been taken. A measured $^{206}\text{Pb}/^{204}\text{Pb}$ ratio of >700 in the uraninite or pitchblende samples generally indicated low levels of common lead, that the concordia plot was insensitive to its actual composition, and that it could consequently be treated as having an ordinary lead composition. At ratios <700 , the common lead composition becomes critical. For all deposits, an ordinary common lead of the sample's $^{207}\text{Pb}/^{206}\text{Pb}$ age was initially assumed, calculated from the Stacey and Kramers (1975) mantle model. Any excess uranogenic lead that then remains uncorrected can be interpreted, in simple cases, on the concordia plot.

Much use has been made of the $^{207}\text{Pb}/^{206}\text{Pb}$ isochron for radioactive samples.

Unlike the concordia plot, knowledge of the common lead composition is unnecessary for this, and in uraninite and pitchblende, unlike zircon and similar minerals, this is not always negligible. This technique only applies to systems which have been closed to U and Pb until recent times, but this condition seems to have applied in the younger deposits, as indicated by the concordia plots. Its use is restricted to samples with lower $^{206}\text{Pb}/^{204}\text{Pb}$ ratios, since this ratio cannot be measured accurately when ^{204}Pb is only present at trace levels.

^{208}Pb was not used as the isochron reference isotope, because (1) in a sample group of uniform $^{208}\text{Pb}/^{204}\text{Pb}$ ratios, it is equivalent to using ^{204}Pb , and (2) there is the possibility of small additions of radiogenic ^{208}Pb . Ordinary lead 0–1800 Ma old has a $^{208}\text{Pb}/^{204}\text{Pb}$ ratio of 35–39. A higher ratio in a pitchblende or uraninite sample indicates either thorium in the material or excess ^{208}Pb in the common lead. It was assumed that if thorium was present, then the material would have an approximately uniform Th : U ratio, and the measured $^{206}\text{Pb}/^{204}\text{Pb}$ and $^{208}\text{Pb}/^{204}\text{Pb}$ ratios would exhibit similar variations between samples. This only occurred in the meta-placer deposits. For all the other deposits, the $^{208}\text{Pb}/^{204}\text{Pb}$ ratio (1) was either invariable, or (2) varied independently of the $^{206}\text{Pb}/^{204}\text{Pb}$ ratio, and any contribution from thorium in the sample is therefore probably small. In both cases, the ^{208}Pb was therefore part of the common lead, which may be homogeneous in the first case and must be inhomogeneous in the second. The results confirm these assumptions, particularly concerning the homogeneity of common lead (which is crucial to the successful interpretation of isochrons).

All age errors are 2σ errors, multiplied by $\sqrt{\text{MSWD}}$ when MSWD is >2 . This somewhat *ad hoc* approach is taken to reflect the geological scatter in the data, which exceeds the statistical scatter and measurement error.

E. Results

From the analytical results (Table 12) the deposits fall into two categories: (1) isotopically simple deposits, where the isochron and discordia ages agree (the Mountain Lake, Coppermine River, Echo Bay, meta-placer and Rayrock deposits); and (2) isotopically complex deposits, where the two techniques yield different ages (the

Sample	Source ^f	Mineral ²	238U(ppm)	Total Pb(ppm)	Pb isotope ratios			Pb-U ratios	
					206/204	207/204	208/204	Error% ⁴	207/235 206/238
EB1	1	Pi	443058	38609	100.04	20.776	36.42	0.22	0.3930 0.04872
EB2	1	Pi	523134	47363	103.04	20.812	36.45	0.13	0.3361 0.04346
EB3	1	Pi+As?	1049.3	945.96	45.327	17.575	36.443	0.25	3.6887 0.36501
ML1a	2	Pi	160584	9068.0	1879.0	148.95	45.07	0.81	0.5844 0.05914
ML1b	2	Pi	175507	9996.2	2176.3	170.42	48.43	0.37	0.5929 0.05994
ML2a	2	Pi	395019	1088.5	605.07	57.88	49.97	2.29	0.0271 0.00273
ML2b	2	Pi	332451	966.13	556.14	52.91	45.46	2.40	0.0275 0.00287
ML3a	2	Pi	238822	14020	20492	1420.7	46.93	6.09	0.5988 0.06328
ML3b	2	Pi	349752	21595	23697	1738.3	43.55	8.76	0.6656 0.06635
ML4a	2	Pi	343870	8165	1410.4	93.61	47.38	0.21	0.1942 0.02514
ML4b	2	Pi	269826	6962	1470.8	96.98	47.82	0.43	0.2102 0.02721
ML5a	2	Pi	485793	16009	3671.1	291.72	46.88	1.72	0.3641 0.03494
ML5b	2	Pi	525675	21679	4019.3	327.04	46.78	0.73	0.4679 0.04360
A6A	4	Gn	-	-	17.310	15.482	35.533	0.02	- -
A6Cf	5	Pi	233173	25065	518.05	43.457	38.72	0.17	0.8272 0.10764
A6Cff	5	Pi	497697	35921	692.9	53.052	38.51	0.14	0.5687 0.07430
A6Cfff	5	Pi	242740	17405	708.8	53.948	38.60	0.34	0.5676 0.07414
A7Bb	6	Pi	122055	8414.5	1394.7	100.24	45.80	0.56	0.6112 0.07209
A7Gi	7	Pi	278468	20904	140.17	22.759	37.23	0.08	0.4915 0.06072
A7Gif	7	Pi	309618	25258	115.54	21.112	37.29	0.05	0.4823 0.06177
A7Gifb	7	Pi	706493	54102	188.74	25.504	37.38	0.02	0.5347 0.06676
A7Giva	7	Pi	51758	7396.7	82.729	19.348	37.20	0.02	0.7788 0.09719

Table 12: All isotopic data.

A8Eb	8	Pi	13080	65448	527.7	43.773	38.94	0.05	39.031	5.1194
A9C11i	9	Dj	-	-	7974.5	523.3	58.78	1.46	-	-
A9G1a	10	Pi	342584	75574	6623	631.3	43.94	1.48	2.9710	0.23111
A9G1b	10	Pi	285572	69732	5249	504.3	45.14	0.74	3.2891	0.25532
A9G11i	10	Pi	460481	74072	6662	604.5	42.76	0.68	2.0664	0.16907
A9G1va	10	Pi	205620	42977	8410	762.8	45.06	2.41	2.7106	0.22079
A9G1vc	10	Pi	622162	136207	20000	1785.8	42.94	4.82	2.8307	0.23175
A9G1vd	10	Pi	207933	42944	4545.4	416.87	43.96	0.46	2.6495	0.21679
A16D11a	11	Pi	356041	13991	397.71	38.092	56.16	0.06	0.3089	0.03780
"	11	Pi	"	"	"	"	"	"	0.2777 ³	0.03543 ³
A16D11b	11	Pi	378745	16632	998.60	70.778	56.16	0.20	0.3474	0.04477
"	11	Pi	"	"	"	"	"	"	0.3330 ³	0.04367 ³
A16D11c	11	Pi	434119	16434	695.51	54.386	55.805	0.17	0.3011	0.03814
"	11	Pi	"	"	"	"	"	"	0.2835 ³	0.03680 ³
A16D11fa	11	Pi	168175	29931	72.686	19.592	55.64	0.03	0.8609	0.08495
"	11	Pi	"	"	"	"	"	"	0.3627 ³	0.04695 ³
A16D11fb	11	Pi	257681	32492	85.448	20.324	55.76	0.15	0.6910	0.07119
"	11	Pi	"	"	"	"	"	"	0.3547 ³	0.04559 ³
A16D11fc	11	Pi	117734	33561	64.457	19.158	55.74	0.08	1.3845	0.12995
"	11	Pi	"	"	"	"	"	"	0.4911 ³	0.06221 ³
A17Aa	12	Pi	92679	6351.2	1497.7	101.80	63.86	0.71	0.5792	0.07209
A17Ab	12	Pi	237648	8471.8	3468.6	205.81	58.14	1.87	0.2923	0.03845
A17AC	12	Pi	195340	7718.6	2378.7	146.55	43.95	5.10	0.3229	0.04221

Table 12 (continued)

A17B1	12	P1	265050	12451	9242.1	511.65	50.75	7.88	0.3791	0.05113
A17B1a	12	P1	57939	4030.3	1092.7	75.13	61.32	0.90	0.5486	0.07182
A17B1b	12	P1	324752	10996	7401.9	414.78	60.97	1.96	0.2739	0.03674
A17B1f1	12	P1	11593	978.1	2170.6	137.00	61.18	2.31	0.6966	0.08957
A18B1a	12	P1	203940	4216.6	3333.3	199.39	46.50	4.53	0.1712	0.02240
A18B1b	12	P1	238559	26218	14306	833.36	50.12	18.5	0.9444	0.11968
A18B1c	12	P1	350002	18372	6038.6	370.13	59.09	0.91	0.4593	0.05657
A19F1v	12	P1	36485	2207.8	3985.7	296.71	41.54	0.68	0.6309	0.06458
A19G1f	12	P1	512248	21243	19802	1094.4	46.60	5.65	0.3404	0.04528
A19G1f1	12	P1	531958	17324	111111	6138.0	80.17	36.4	0.2707	0.03562
A19H1f	12	P1	390504	11150	25445	1342.6	41.18	3.42	0.2252	0.03129
A26F	13	Cp	-	-	113.39	21.911	44.50	0.56	-	-
A26G	13	Cp	-	-	831.39	72.54	42.73	1.98	-	-
A28G1f	14	Ur	11529	3735.7	57803	6591.5	1094.1	45.4	5.1822	0.33027
A30C1	14	Ur	13439	2066.9	18484	1845.9	209.11	1.88	2.1847	0.15986
B1Ea	16	P1/He	237366	12133	15129	839.44	55.52	3.77	0.4190	0.05574
B1Eb	16	P1/He	406251	16830	24331	1319.8	52.66	8.16	0.3350	0.04529
B5B1b	16	P1	373666	1210.0	1988.1	124.46	42.90	2.44	0.0266	0.00349
B5B1f	16	P1	565998	4644.9	2460.6	150.72	38.32	2.16	0.0670	0.00879
B6A	16	P1	579107	19389	1974.3	130.32	50.30	0.48	0.2863	0.03541
B6C	16	P1/He	130885	7421.6	4231.9	284.19	37.53	2.56	0.5353	0.06091
B6D1f1	16	P1/He	25376	1960.1	872.91	83.602	39.92	4.08	0.8605	0.07842
B7B1	16	P1/He	338916	16934	4948.0	279.29	38.24	0.50	0.4016	0.05446

Table 12 (continued)

B7B1i	16	Pi/He	574931	24331	25316	1418.3	50.53	2.60	0.3537	0.04619
B7B1ii	16	Pi/He	107970	6976.5	6038.6	453.46	55.91	7.25	0.6914	0.06894
B10Ca	17	Pi	367454	39789	599.74	69.24	73.22	0.04	1.2672	0.09960
B10Cb	17	Pi	258924	39247	317.46	43.59	71.68	0.13	1.6865	0.13061
B11Ji	18	Pi	318302	9206.1	493.39	42.81	49.92	0.38	0.2240	0.02837
B11Jiii	18	Pi	567033	60260	201.00	29.093	36.83	0.05	0.9247	0.09078
B11Jv	18	Pi	474889	77721	142.74	25.435	50.02	0.02	1.3471	0.12356
B11Jvi	18	Pi	537486	24621	4288.2	247.10	49.15	5.86	0.3695	0.04943
B11Jvii	18	Pi	471824	22868	3152.6	186.07	53.87	0.73	0.3904	0.05206
B11Jviii	18	Pi	476296	19208	1763.4	108.41	41.02	0.60	0.3154	0.04301
B11Jxiii	18	Pi	641960	28217	1101.7	78.99	55.21	0.07	0.3630	0.04500
B11Jxiv	18	Pi	571932	29501	755.46	57.01	72.97	0.14	0.3909	0.05047
B11Jxv	18	Pi	562110	17637	2187.2	132.58	65.30	5.64	0.2477	0.03331
B13A	18	Pi	625447	27683	7446.0	426.46	52.56	1.82	0.3662	0.04802
B24Ai	19	Ur	2814.5	752.95	20576	2316.7	149.15	15.2	4.2581	0.27590
B25G	20	Ur	5457.9	2790.1	16000	1831.9	126.20	1.29	8.2416	0.52594
B29D	21	Ur	307.31	95.259	1612.1	194.24	51.13	2.06	4.8346	0.31280
B30D	22	Pi	522461	47534	571.04	57.459	39.41	0.05	0.9362	0.08969
B31D	22	Pi	370913	46878	94.23	21.804	36.77	0.05	0.9197	0.08151
B31Ea	22	Pi	459126	11573	1482.8	98.92	36.40	0.37	0.2095	0.02671
B31Eb	22	Pi	431306	69398	119.55	24.315	36.76	0.03	1.4780	0.12437
B31Ec	22	Pi	149312	25777	89.52	22.138	36.78	0.07	1.4604	0.11517
B31Ed	22	Pi	407369	29890	304.72	34.017	36.75	0.03	0.6125	0.06909
B31Ee	22	Pi	518285	30425	470.65	46.041	36.84	0.06	0.5384	0.05803

Table 12 (continued)

B31Ef	22	Gn	-	-	69.21	21.06	36.74	0.39	-	-
B31Eg	22	Pf	489708	82008	134.31	25.626	36.64	0.10	1.6501	0.13832
B31Gb	22	Pf	36089	15863	60.86	19.656	36.87	0.14	3.3016	0.25016
B33Aa	22	Pf	564845	54492	455.37	52.54	38.76	0.11	1.0822	0.09284
B33Ab	22	Pf	522738	56083	459.90	52.95	38.81	0.26	1.2138	0.10403
B33Ac	22	Pf	398675	38105	481.56	53.83	38.86	0.11	1.0509	0.09234
B35C	23	Pf	14730	887.55	2936.0	221.34	59.40	6.77	0.6197	0.06374
B35E	23	Pf	8260	591.82	1895.0	118.37	58.89	10.7	0.5734	0.07595
B35F	23	Pf	181208	7022.3	11628	782.63	53.83	8.31	0.3808	0.04180
B36A	23	Pf	103489	3293.4	3256.3	226.17	54.71	1.39	0.3033	0.03383
B36C	24	Pf	6058.9	330.81	524.47	51.39	36.68	0.19	0.5215	0.05349
B38Ella	25	Py	-	-	207.24	36.71	53.71	0.14	-	-
B38Ellb	25	Ur	202862	58066	44053	4909.1	993.6	7.08	4.4657	0.29145
B38Ellc	25	Ur	27510	7006.7	8305.6	919.80	234.4	4.60	3.8850	0.25825
B40B	25	Cp	-	-	21.47	16.08	37.56	0.30	-	-
B41Da	25	Ur	1592.8	503.22	7627.8	873.56	110.4	19.4	5.0320	0.32369
B43Dvlla	26	Pf	3890.8	306.06	784.31	72.59	42.50	0.11	0.8184	0.07978
B43Dvllb	26	Pf	10483	699.60	763.88	69.64	43.24	0.04	0.6768	0.06771
B45A1	27	Py	-	-	89.68	24.83	61.84	4.03	-	-
B45A1f	27	Py	-	-	55.06	19.29	46.14	0.28	-	-
B48A	27	Py	-	-	413.26	62.46	44.48	2.15	-	-
B48B	27	Ur	34678	9859.2	104167	11734	123.8	29.7	4.5729	0.29477
B48C	27	Ur	11032	3387.8	38462	4384.7	88.77	4.00	4.9790	0.31773
C1B	27	Ur	6176.3	1170.4	9920.6	1123.0	75.93	1.41	3.0105	0.19523

Table 12 (continued)

C1 (Jory) 28	Pi	592245	106100	5770	515	67.81	-	2.2680	0.1894
C2 (Jory) 28	Pi	656274	106900	4620	436	94.89	-	2.1516	0.1703
C3 (Jory) 28	Pi	642873	154900	6090	560	47.84	-	3.1531	0.2551
C4,5,6 (Jory) 28	Pi	481460	87900	21600	1953	39.46	-	2.3961	0.1935
C7 (Jory) 28	Pi	683672	157900	8260	755	50.19	-	3.0235	0.2445
C8 (Jory) 28	Pi	415544	41800	3120	260	43.17	-	1.1686	0.1075

¹Sources: 1 = Echo Bay (mine dump), 2 = Mountain Lake borehole core, 4 = FALCON, 5 = ECHO, 6 = FC, 7 = TABB, 8 = SOUTH, 9 = RHY, 10 = SHORE, 11 = Mazenod Lake, 12 = Rayrock, 13 = Dease Lake, 14 = DV/UGI, 16 = Beaverlodge Lake, 17 = PITCH 27-28, 18 = PITCH 8-10 (mine dump), 19 = HAM, 20 = JONES, 21 = JLD, 22 = JD, 23 = T1, 24 = Main Zone, 25 = JACKPOT, 26 = BERNI, 27 = NORI/RA, 28 = Echo Bay mine (Jory 1964)

²May contain gangue minerals. Pi = pitchblende, As = arsenides, Py = pyrite, Cp = chalcopyrite, Gn = galena, Dj = djurleite, Ur = uraninite, Pi/He = hematite-pitchblende fels.

³After modelled lead corrections as described in text.

⁴₂-sigma errors are quoted for 206/204 values only, but are generally applicable to 207/204 values too. 208/204 errors for radioactive phases will be greater. 207/235 and 206/238 ratio errors are assumed to be 0.5% and 0.7% respectively.

Table 12 (concluded)

Mazenod Lake, Hottah Lake and JD group deposits). The second group may be amenable to analysis using non-ordinary common lead models. Only one deposit in the first category is treated in detail, and the results for all deposits are listed in Table 13.

Meta-placer Deposits

The meta-placer deposits illustrate the isotopically simple group, having similar ages on a concordia plot of uraninite and an isochron plot of sulphide concentrates. The eleven uraninite samples analysed from six deposits contained negligible common lead, and a model mantle lead correction was assumed. Although slightly different discordant ages were found for three claim groups (Table 13), two distinct trends emerge on the concordia plot, being JACKPOT + JLD with intercepts of 1849 ± 12 and 396 ± 102 Ma (four samples), and HAM + UGI/DV + NORI/RA (two of three samples) with intercepts of 1872 ± 8 and 394 ± 24 Ma (five samples) (Fig. 31). Their mean values, 1860 ± 20 Ma and 395 ± 100 Ma, may be taken as representative of the group as a whole. The 395 Ma age may either reflect the regional Palaeozoic remobilisation event described later, or may simply be due to diffusive lead loss and therefore geologically meaningless.

These ages reflect the time of granite intrusion (1860 ± 10 Ma to 1875 Ma), but are also similar to the age of the proposed source of uraninite, the Hepburn Batholith (1890 ± 20 Ma). The 1849 Ma and 1872 Ma trends may indicate separate intrusive pulses. It seems strange that the uraninite crystals should have apparently survived metamorphism without retaining a trace of pre-metamorphic lead, supporting the suggestion that their source was little older than the Great Bear Batholith. Since the meta-placer bodies can contain detrital zircons, which in turn may have entered the granite as xenocrysts, a note of mild caution should be sounded concerning the granite geochronology despite the initially satisfying agreement.

The sample $^{208}\text{Pb}/^{204}\text{Pb}$ ratios of 51–1094 approximately correlate with the $^{206}\text{Pb}/^{204}\text{Pb}$ ratios within individual deposits, showing that much ^{208}Pb was generated by Th in the uraninite rather than entering with the common lead. Th was detected during microprobe analyses.

Pyrite and chalcopyrite concentrates from several deposits were analysed for lead. On a $^{207}\text{Pb}/^{204}\text{Pb}$ vs. $^{206}\text{Pb}/^{204}\text{Pb}$ plot (Fig. 32), the analyses yield a line with a slope of

DEPOSIT	Pb-Pb		DISCORDIA INTERSECTIONS		ISOLATED OR ANOMALOUS	
	ISOCHRON AGE (Ma)	MSWD ¹	AGES (Ma)	MSWD ¹	Pb/Pb AGES (Ma)	INTERPRETATION
Mountain Lake	1076±96	25	1029±75	224	450	1076±96 (mineralisation)
ECHO showing	408±22	0.02	431±12	0.004	-	415±29 (mineralisation)
TABB showing	535±36	158	538±64	41	-	536±66 (mineralisation)
SOUTH showing	-	-	-	-	420	
FC showing	-	-	-	-	660	
RHY/SHORE	-	-	1500±10	0.3	-	1500±10 (mineralisation)
Echo Bay mine	1373 (no error assigned)	-	1424±29	13	-	1424±29 (mineralisation) (1419?)
BERRI	-	-	-	-	-	339±22 (episodic lead loss)
JACKPOT	-	-	1850±15	0.004	-	
NORI/RA	-	-	1853±19	4.4	-	
UGI/DV	1836±32	27	1864±14	(two samples)	-	1860±20 (metamorphism?)
JLD	(sulphides)	-	-	-	1830	395±100 (episodic lead loss)
HAM	-	-	-	-	1830	
JONES	-	-	-	-	1860	
Group 1: JLD + JACKPOT	-	-	1849±12	0.04	-	
Group 2: UGI/DV + HAM + NORI/RA	-	-	1872±8	0.86	-	

JD showing	535±164	4232	1428±18	140±9	5	-	1428±18 (uranogenic lead source?)
T1 Zone	960±454	2.5	1092±115	99±34	23	400	1092±115 (mineralisation)
Main Zone	-	-	-	-	-	-	535±164 (mineralisation)
PITCH 27-28	1444	(2 samples)	1546±40	73±42	(2 samples)	-	2058±34 (uranogenic lead source?)
PITCH 8-10: a)	-	-	1330-1530	300	(estimated)	-	1450±150? (mineralisation,
b)	422±38	224	449±48	-0.3±4.8	147	-	uranogenic lead source?)
Beaverlodge Lake:							
a) Pitchblende	No isochron		2058±34	340±4	1.9	-	440±57 (mineralisation)
b) Hematite-							
pitchblende fels							
Mazenod Lake	457±26	44	a) 1201±62 (ordinary common lead)	184±10	26	-	1201±62 (uranogenic lead source?)
			b) 494±73 (modelled common lead)	42±73	21	-	457±26 (mineralisation)
Rayrock mine	517±80	8	484±59	69±49	97	950	511±86 (mineralisation)

Note: all errors are 2σ , and have been multiplied by \sqrt{MSWD} when $MSWD > 2$.

Discordia error envelopes calculated after Ludwig (1980).

$$MSWD = \frac{\text{mean square weighted deviates} = \frac{\text{sum of squared residuals}}{\text{degrees of freedom}}}{\text{degrees of freedom}}$$

Table 13: Isotopic dates of the deposits.

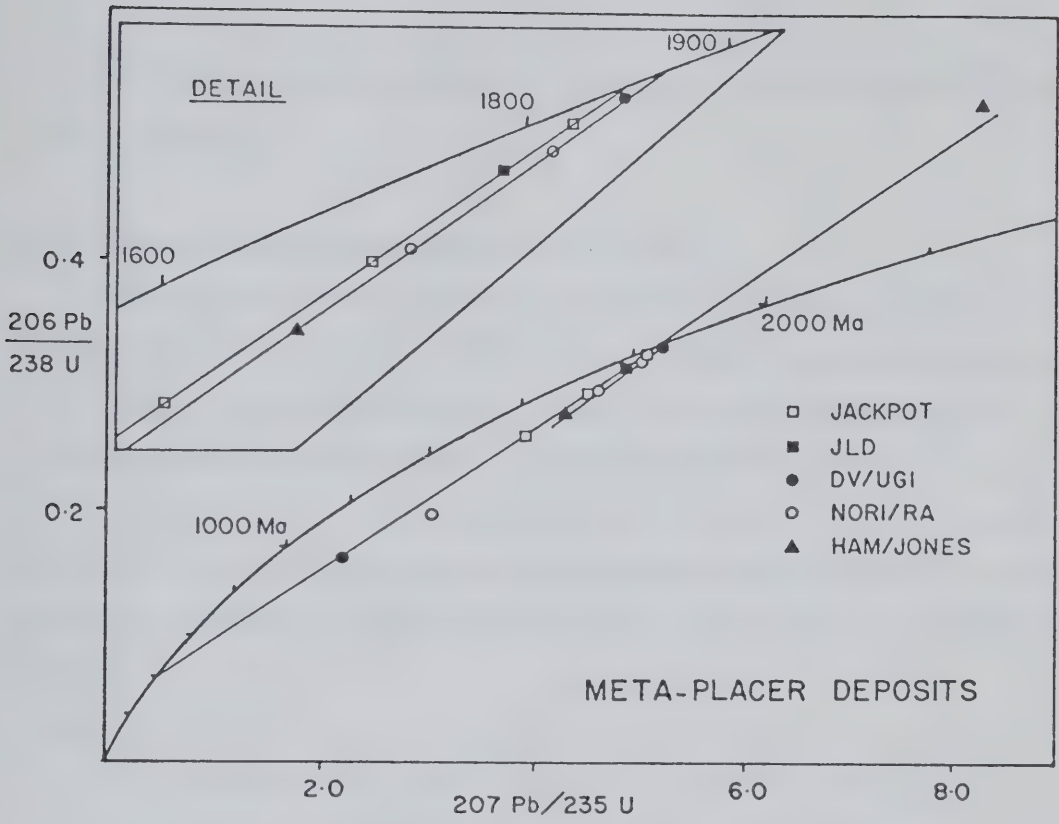


Figure 31: Meta-placer deposits: concordia plot of uraninite.

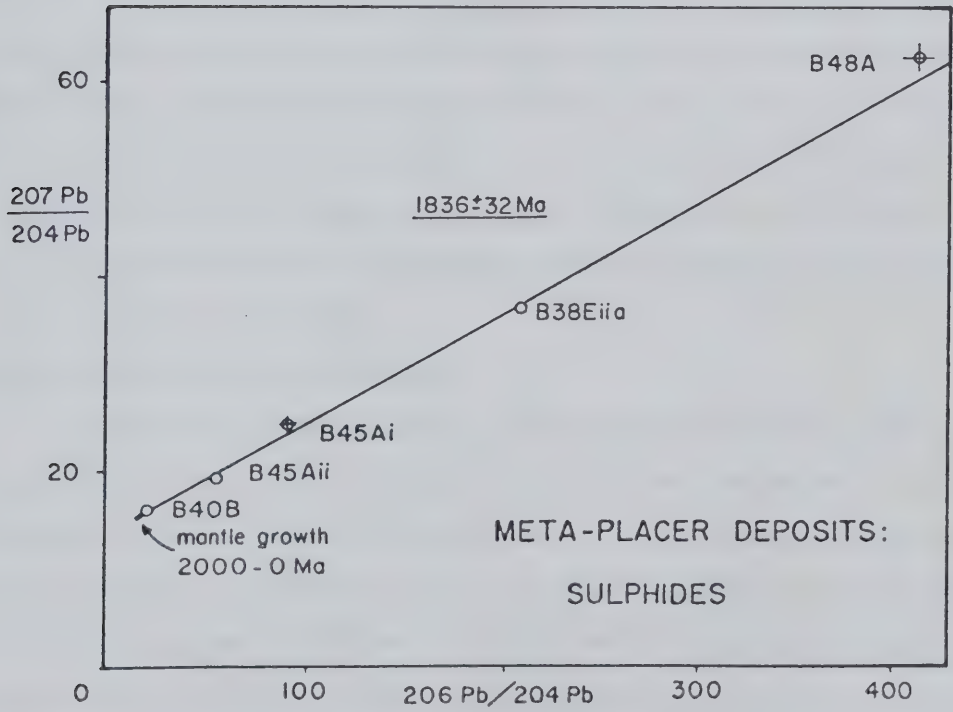


Figure 32: Meta-placer deposits: isochron plot of pyrite and chalcopyrite lead.

0.1123, or 1836 ± 32 Ma, MSWD = 27, interpreted as a $^{207}\text{Pb}/^{206}\text{Pb}$ isochron generated by uranium impurities.

Other Isotopically Simple Deposits: Mountain Lake

Pitchblende from each of the five drill-core specimens from the Mountain Lake deposit was analysed in duplicate. The analyses, omitting the samples from core ML4, form a poorly-defined isochron (Fig. 33) and discordia (Fig. 34) but with similar results for each, namely 1076 ± 96 Ma and 1029 ± 75 Ma respectively. The isochron value of 1076 ± 96 Ma is preferred because of the much lower MSWD (Table 13). Uranium deposition at this time would have occurred beneath some 5.4 kilometres of cover rocks (Baragar and Donaldson 1973). The ML4 samples both have discordant $^{207}\text{Pb}/^{206}\text{Pb}$ ages of 450 Ma.

Coppermine River

Pitchblende from four minor deposits in the Coppermine River area was analysed. Three samples from the ECHO showing have isochron and discordia ages of 408 ± 22 Ma and 431 ± 12 Ma (mean value = 415 ± 29 Ma), while four samples from the TABB showing have isochron and discordia ages of 535 ± 36 Ma and 538 ± 64 Ma (mean value = 536 ± 66 Ma) (Figs. 35,36). Single samples from the FC and SOUTH showings have $^{207}\text{Pb}/^{206}\text{Pb}$ ages of 660 Ma and 420 Ma respectively, the latter analysis showing extreme negative discordance. A galena sample was analysed from a fifth occurrence, the FALCON (sample A6A, Table 12). The galena occurs in a quartz-carbonate cemented, diatreme-like, brecciated gneiss, and its lead is slightly evolved from an ordinary lead at least 850 Ma old. It cannot be interpreted with any certainty, and further speculation is unwarranted without more data.

Echo Bay, Achook Island, Dog Island

The six analyses of pitchblende from Echo Bay made by Jory (1964) do not statistically form a good discordia (Fig. 37). Three pitchblende samples with unavoidable sulphides or arsenides from the Echo Bay mine dump were therefore analysed; one was rejected, containing insufficient Pb and U, and the others are extremely discordant. However, six analyses of pitchblende from the SHORE occurrence, Achook Island, appear to add significant information when combined with Jory's data. Nine samples now

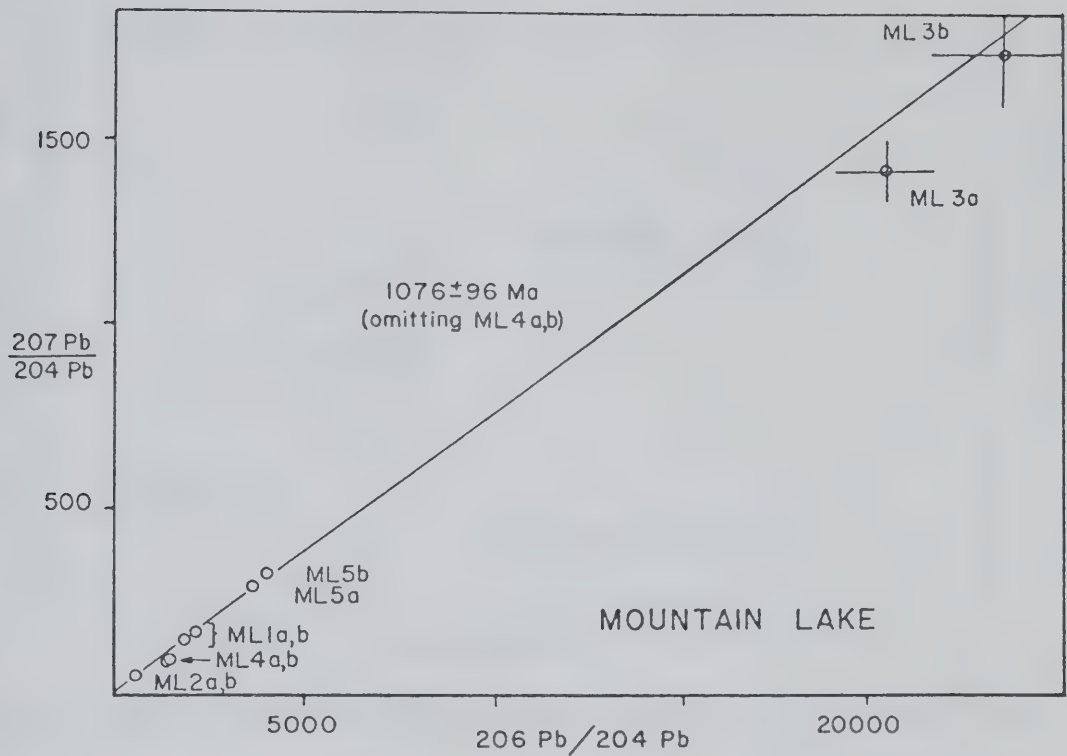


Figure 33: Mountain Lake: isochron plot of pitchblende.

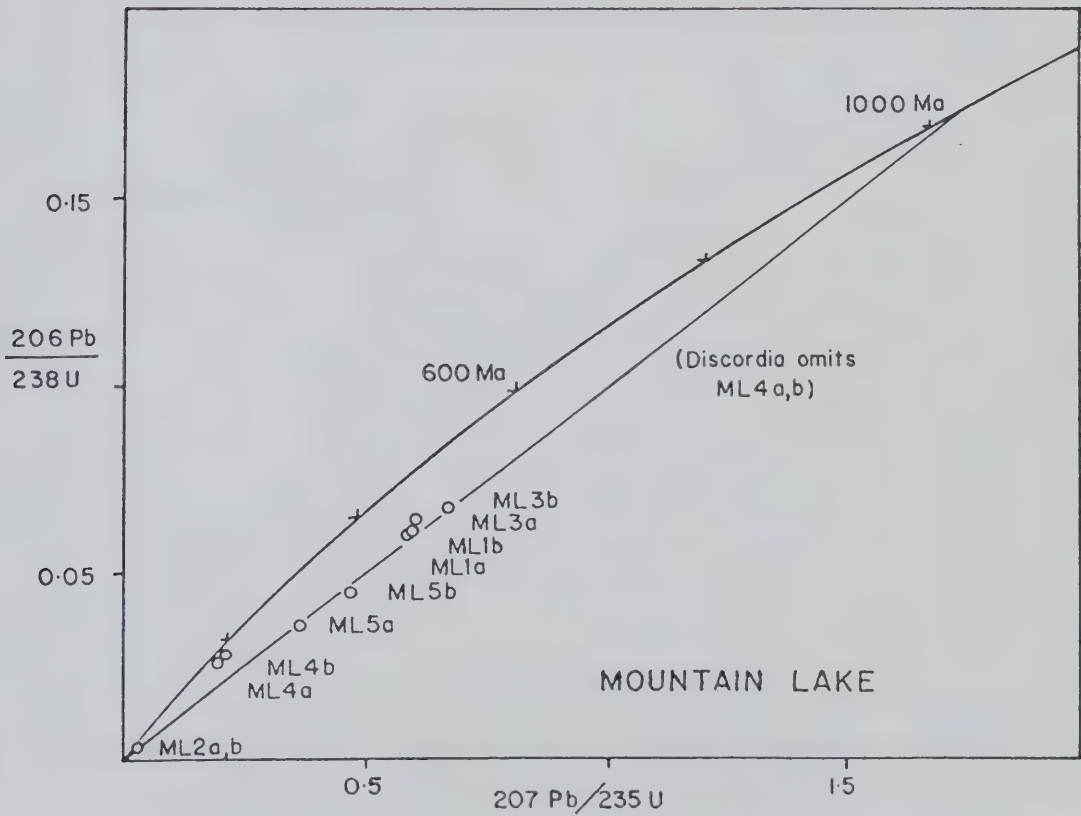


Figure 34: Mountain Lake: concordia plot of pitchblende.

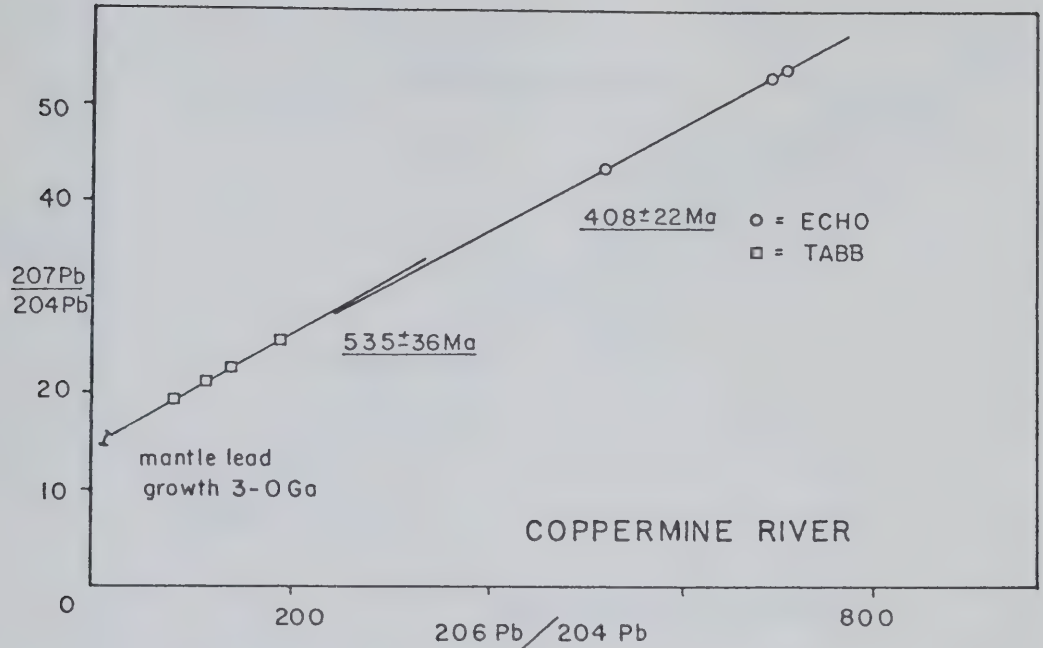


Figure 35: Coppermine River: isochron plot of pitchblende from the ECHO and TABB showings.

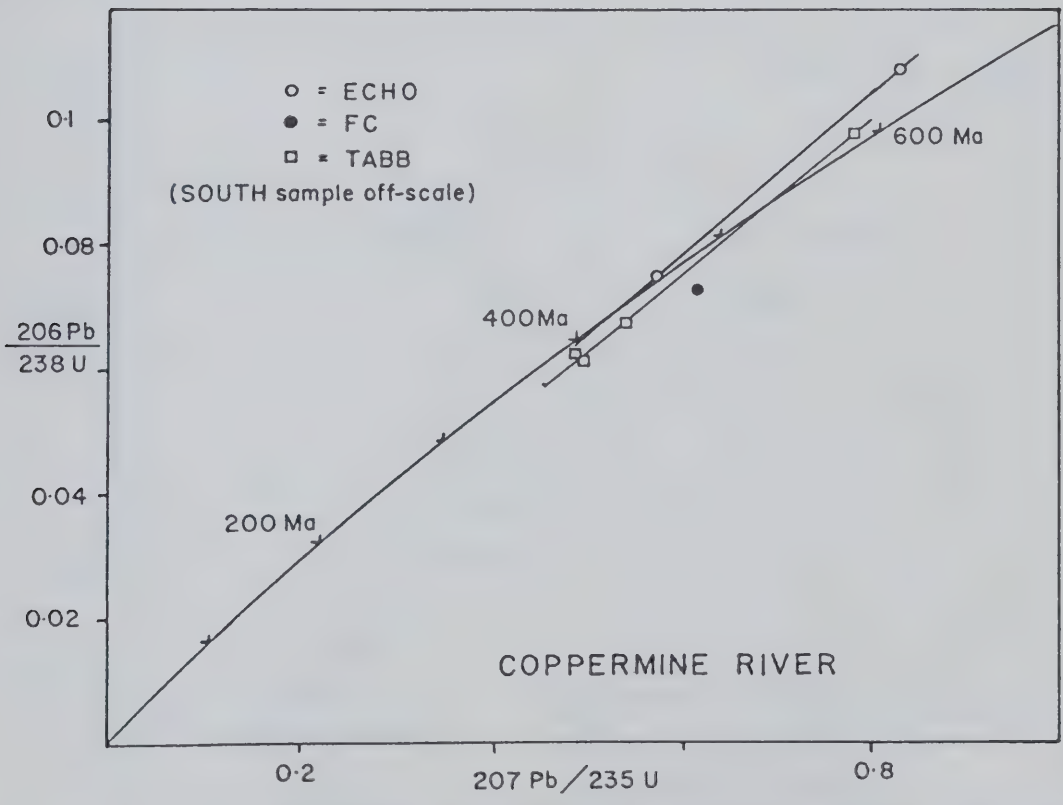


Figure 36: Coppermine River: concordia plot of pitchblende from the ECHO, TABB and FC showings.

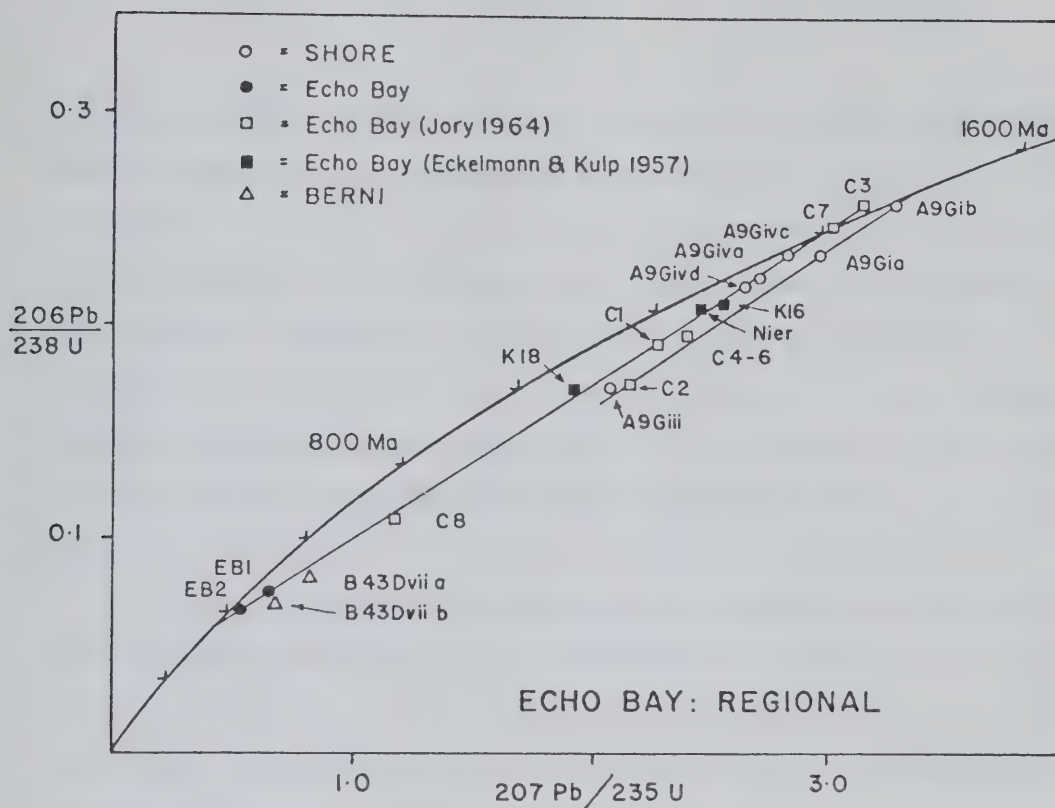


Figure 37: Echo Bay, BERNI and SHORE claims: concordia plot of pitchblende.

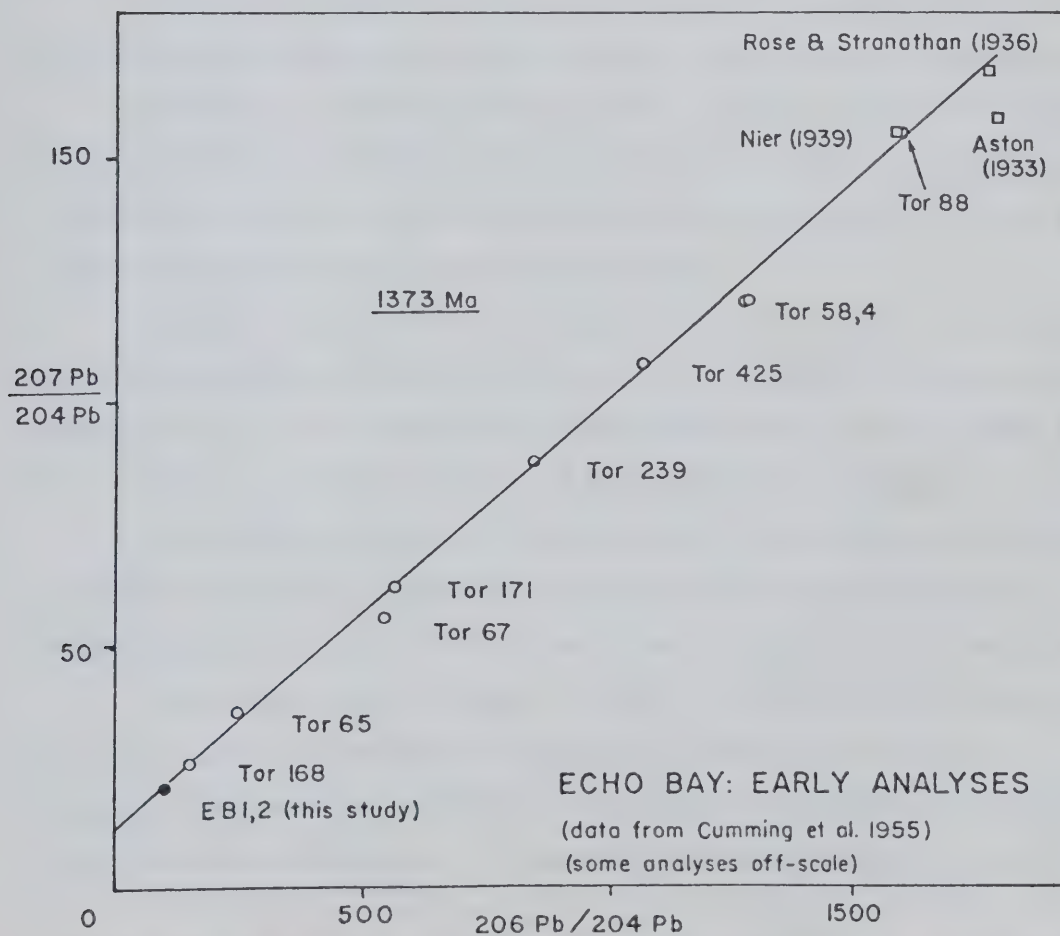


Figure 38: Echo Bay and Eldorado mine: isochron plot of pitchblende analyses from Cumming *et al.* (1955).

yield a discordia with intersections at 1424 ± 29 Ma and 339 ± 22 Ma. (As Jory (1964) noted, his virtually concordant samples C3 and C7 bracket the concordia, with identical (revised) $^{207}\text{Pb}/^{206}\text{Pb}$ ages of 1419 Ma, which stands as the most accurate age estimation). Three more samples, one almost concordant, suggest another discordia between 1500 ± 10 Ma and 125 ± 48 Ma, but the lower intersection involves too large an extrapolation to be meaningful. The two remaining analyses (A9Giii and C 4–6) fall between these discordia, representing either a mixture, a continuum of mineralisation or combined episodic and diffusive lead loss from 1500 Ma old material. Three analyses listed by Eckelmann and Kulp (1957) were not used in the computation.

The 1500 Ma event may be restricted to Achook Island if Jory's sample C2 is only coincidentally on this discordia. The 339 Ma lower discordia intersection is defined by the two new Echo Bay analyses, but these are critically affected by the choice of common lead. 339 ± 22 Ma is therefore less precise than the error margin implies, but still suggests a Palaeozoic lead loss event, with or without continuous diffusive loss.

The data from the BERNI claims were not used in the computation, due to the different style of mineralisation, but the analyses fall close to the 1424 Ma discordia.

Cumming *et al.* (1955) collated their own and previous workers' lead isotope data for pitchblende from the Eldorado mine. The isochron for the fourteen suitable analyses by Cumming *et al.* gives an age of 1373 Ma (Fig. 38). No precise age error can be assigned since measurement errors were not stated.

A sample of djurleite ($\text{Cu}_{1.96}\text{S}$) in a silicate matrix from the RHY claims contains primarily uranogenic lead (sample A9Ciii, Table 12). The computed instantaneous age is about 400 Ma, and the cumulative age is about 730 Ma. There is no independent evidence for a source of uranium 400–730 Ma old, and no meaningful interpretation is possible.

Jory (1964) and Thorpe (1974) analysed twenty-four samples of lead-bearing sulphides, mostly galena, from the Echo Bay–Camsell River area, and these are reconsidered here in the light of the revised decay constants and mantle lead model.

Two ordinary galena lead ages are defined at 1767 Ma and 1626 Ma (or some 50 Ma younger using the Cumming and Richards (1975) mantle model) (Table 14).

Geologically, however, the "1626" Ma old galena postdates the 1428 Ma pitchblende (Jory 1964). The material with a 1767 Ma model age, which includes a possible

<u>$^{206}\text{Pb}/^{204}\text{Pb}$</u>	<u>$^{207}\text{Pb}/^{204}\text{Pb}$</u>	<u>$^{208}\text{Pb}/^{204}\text{Pb}$</u>	<u>$^{207}\text{Pb}/^{206}\text{Pb}$</u>	<u>Sample and interpretation</u>
15.66	15.32	35.29	0.9783	Ordinary lead, 1767 Ma model age (3 samples)
15.92	15.37	35.66	0.9655	Ordinary lead, 1626 Ma model age (8 samples)

Data after Thorpe (1974) and Jory (1964)

Table 14: Common lead isotopic data from Echo Bay, from Thorpe (1974) and Jory (1964).

volcanogenic exhalative sulphide (Thorpe *op. cit.*), is presumably related to the volcanism, while the 1626 Ma age is probably due to a mixture of 1767 Ma old lead with younger lead from the 1392 Ma diabase sheet previously mentioned. Since this mixing model satisfies all the data, there are no longer grounds for doubting the general validity of model-lead ages, based on the apparent 1626 Ma age, or for trying to make this fit the age of the pitchblende mineralisation (and vice versa) as has been proposed (Thorpe 1974, 1971).

A group of anomalous J-type leads contain radiogenic lead, compared to the two ordinary lead compositions. The $^{205}\text{Pb}/^{206}\text{Pb}$ ratio of the radiogenic component indicates a normal Th/U ratio in its source rock of about 3.7–4.0. The $^{207}\text{Pb}/^{206}\text{Pb}$ ratio of the radiogenic component is 0.1085 ± 0.007 , representing a cumulative age of 1774 ± 123 Ma and an instantaneous age of 1032 ± 81 Ma. These samples could be interpreted as the relatively recent deposition of lead from the volcano-sedimentary host rocks, although geologically this does not appear totally satisfactory (Thorpe 1974).

Finally, two samples analysed by Jory (1964) contained small amounts of uranogenic lead. PR3 was a uraniferous tetrahedrite-chalcopyrite assemblage, and can be interpreted as a uranium-lead system 1576 Ma old. Slight contamination by older lead would bring this age to the general pitchblende ages. The $^{207}\text{Pb}/^{206}\text{Pb}$ ratio of the uranogenic component in galena sample PR42 provides virtually no age restraints.

Rayrock Mine

Fourteen pitchblende samples from the Rayrock mine were analysed. One sample, A19Fiv, is anomalous, and the remainder define an isochron age of 517 ± 80 Ma and a discordia age of 484 ± 59 Ma (Fig. 39,40). The mean value of 511 ± 86 Ma is assumed.

Isotopically Complex Deposits: Mazenod Lake

Three samples were analysed from each of two hand-specimens, A16Dii and A16Diii, from Mazenod Lake. The $^{206}\text{Pb}/^{204}\text{Pb}$ ratios are 398–999 and 64–85 for the two rocks, while the $^{208}\text{Pb}/^{204}\text{Pb}$ ratios are 56.04 ± 0.24 and 55.71 ± 0.07 respectively. The six analyses yield an isochron age of 457 ± 26 Ma (Fig. 41), given previously as 460 ± 30 Ma (Miller 1981). The $^{208}\text{Pb}/^{204}\text{Pb}$ data suggest that the common lead may vary marginally between the two rocks, but it is homogeneous to a first approximation.

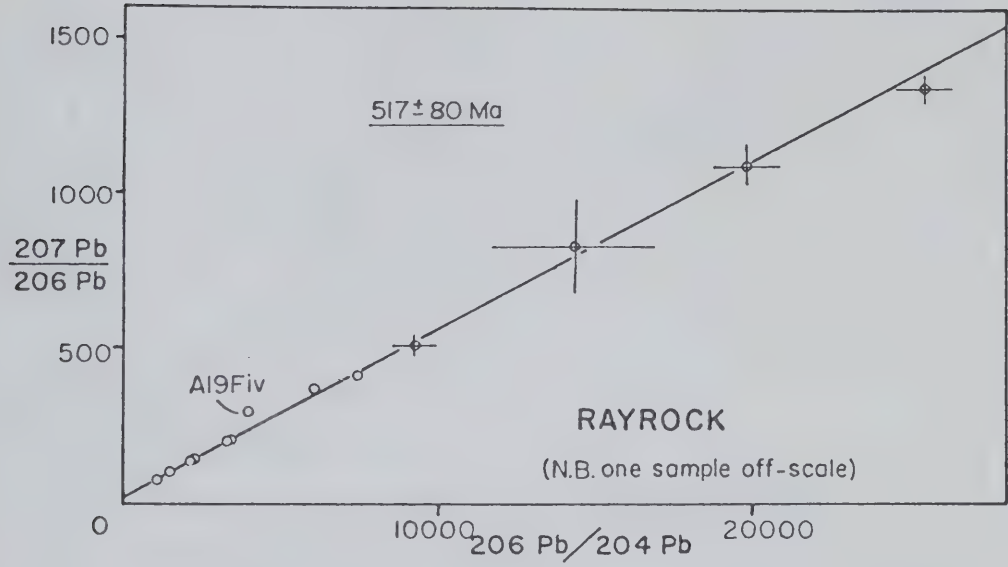


Figure 39: Rayrock mine: isochron plot of pitchblende.

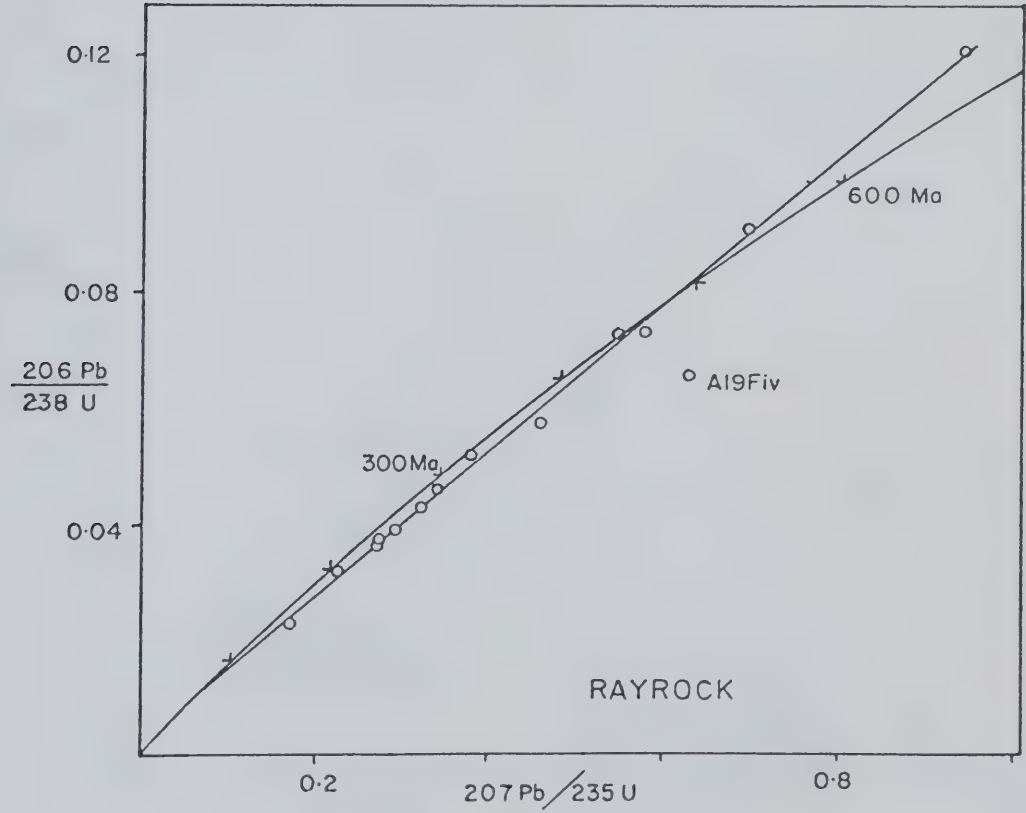


Figure 40: Rayrock mine: concordia plot of pitchblende.

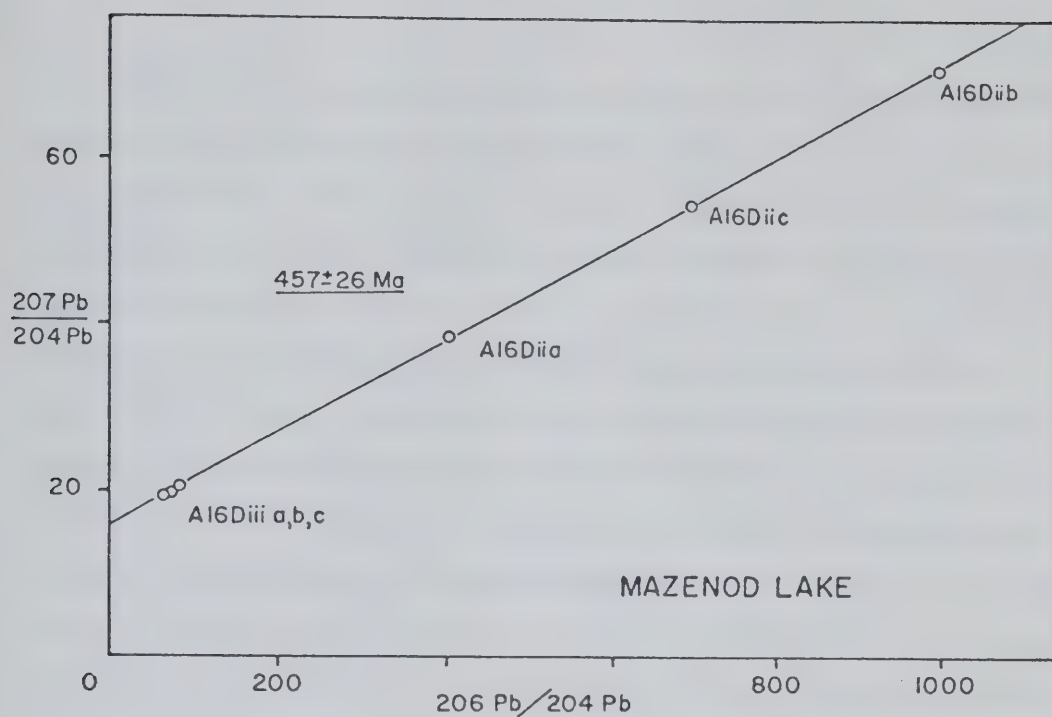


Figure 41: Mazenod Lake: isochron plot of pitchblende.

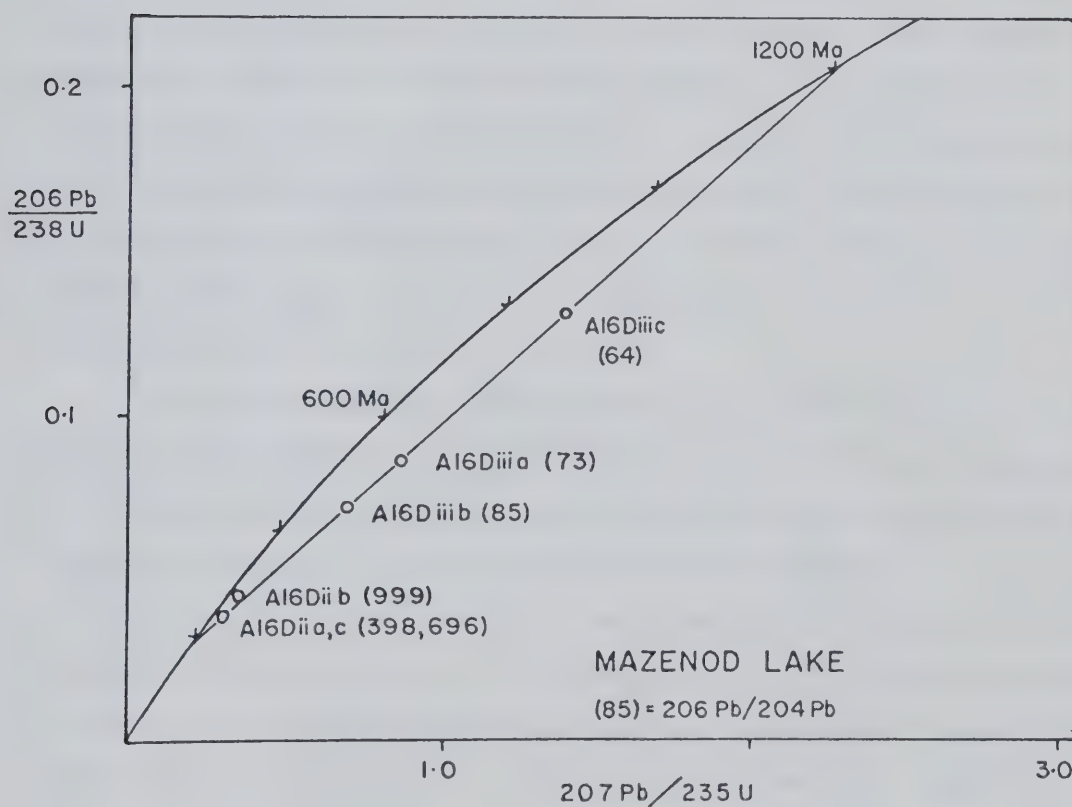


Figure 42: Mazenod Lake: concordia plot of pitchblende, using ordinary common lead correction.

Using an ordinary mantle lead correction, five of the six analyses form a good discordia with intersections of 1201 ± 62 Ma and 184 ± 10 Ma (Fig. 42). As the common lead increases (and the $^{206}\text{Pb}/^{204}\text{Pb}$ ratios fall), the samples plot closer to the upper discordia intersection, implying that the common lead contains a large, old uranogenic component which has not been corrected out. The samples with less common lead plot at the young end of the discordia, since radiogenic lead created since 457 Ma is predominant. The lower intersection of the discordia lies below 457 Ma because of the combined effects of diffusive lead loss and the postulated uranogenic lead contaminant. Although the 1201 Ma intersection is ascribed to uranogenic lead contamination, an alternative interpretation is of original pitchblende deposition at 1201 Ma, and intense lead loss at 184 Ma. This is rejected for three reasons; first, the trend of increasing common lead along the discordia; second, the disagreement between isochron and discordia ages; third, the common lead was homogeneous at 457 Ma, to an extent virtually impossible without complete dissolution and mixing. The contaminant uranogenic lead could have been derived from a precursor uranium deposit now 1201 Ma old, remobilised to form the 457 Ma old deposit. However, radiogenic lead from the approximately 1850 Ma old country rocks may also have been added in unknown amounts, in which case the hypothetical precursor would be <1201 Ma old, and the 1201 Ma intersection geologically meaningless. Furthermore, diffusive lead loss has occurred, which can rotate the discordia, so that even if the upper discordia intersection does represent a precursor uranium deposit, the statistical measurement error of 62 Ma would be less than the true error.

To illustrate the effect of the composition of the common lead correction for the discordia, a model contaminant was constructed. On the x-y plot, the contaminant must lie on the sample isochron, below the last sample analysis (Fig. 43). It must also have a $^{207}\text{Pb}/^{206}\text{Pb}$ ratio less than the 1850 Ma instantaneous ratio of about 0.21, or lie to the right of a line of this slope drawn from the mantle lead composition (assumed to be 1850 Ma old, the maximum host rock age). Lead extracted 500 Ma ago from a uranium deposit now 1200 Ma old was chosen as the uranogenic component. It has a $^{207}\text{Pb}/^{206}\text{Pb}$ ratio of 0.0951, and the mixing line of this lead with 1200 Ma old (or 1850 Ma old) model mantle lead intersects the isochron at approximately $^{206}\text{Pb}/^{204}\text{Pb} = 41.6$, $^{207}\text{Pb}/^{204}\text{Pb}$

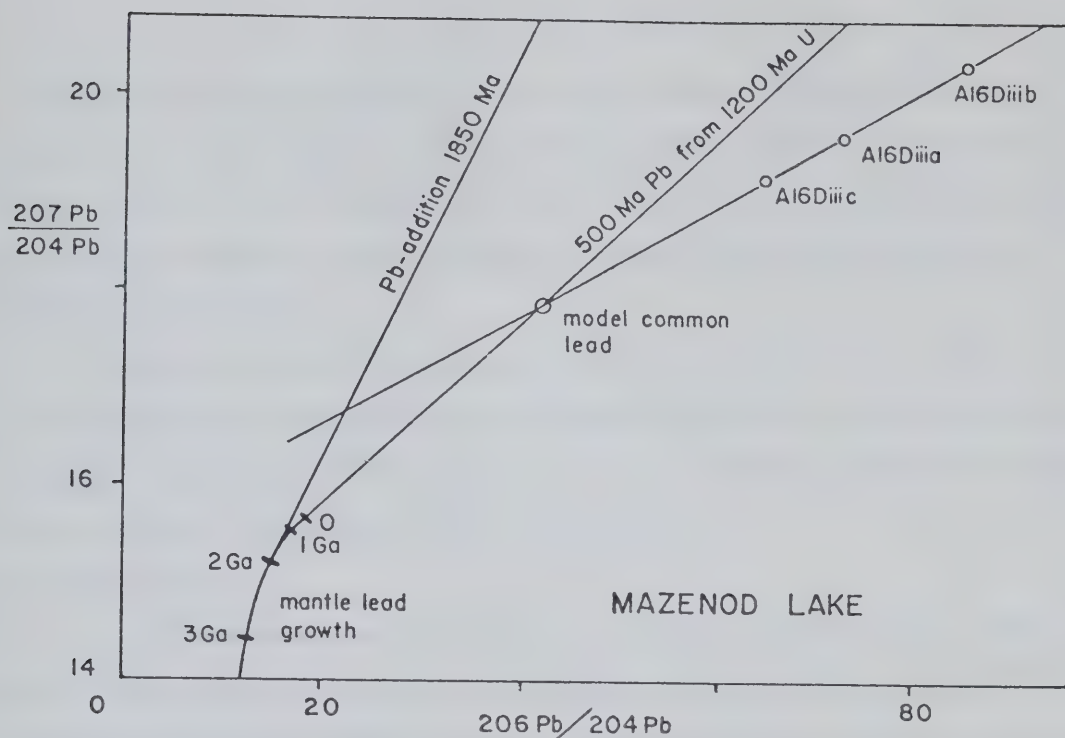


Figure 43: Mazenod Lake: construction of a model lead composition, using a uranogenic lead component extracted 500 Ma ago from a source now 1200 Ma old.

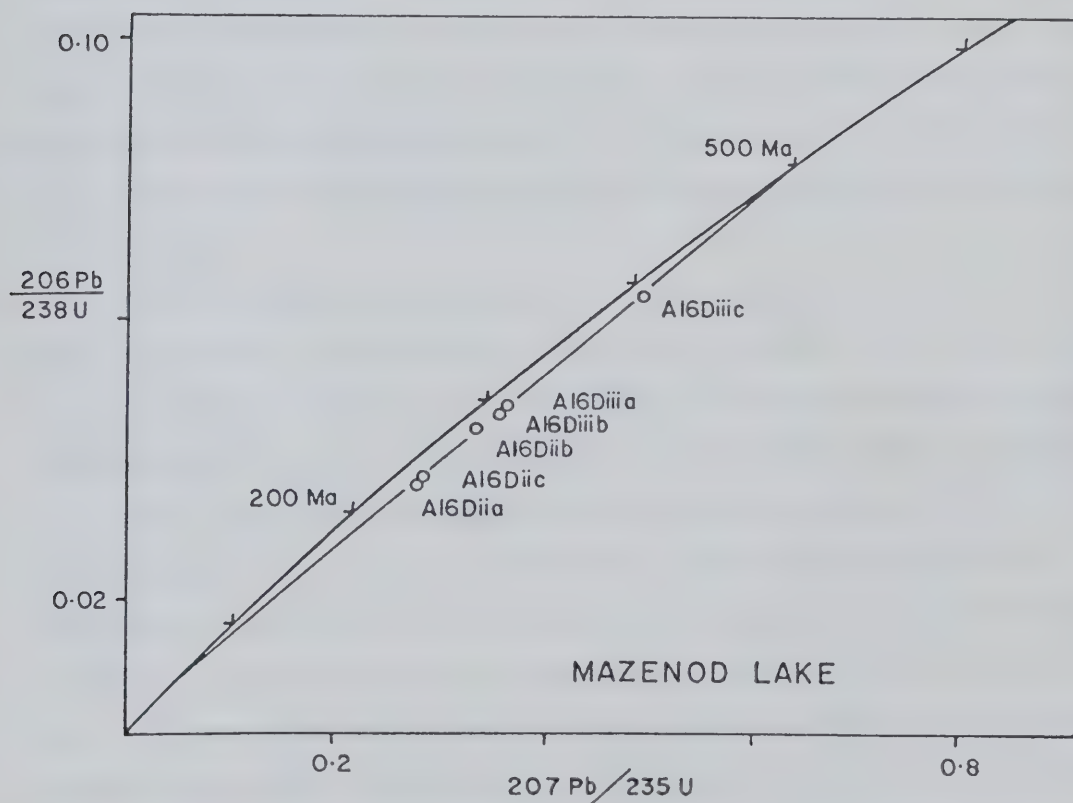


Figure 44: Mazenod Lake: concordia plot of pitchblende, using modelled common lead correction.

= 17.85. This composition was tried as the common lead correction, and the result is a discordia (six samples) with intersection ages of 494 ± 73 Ma and 42 ± 73 Ma (Fig. 44). Further model refinement would bring this age closer to 457 Ma, the preferred isochron age. The 42 Ma intersection age is ascribed to diffusive lead loss and is therefore geologically meaningless.

To sum up, the samples are thought to be 457 ± 26 Ma old, and to contain a common lead, hosted perhaps by coeval sulphosalts, made up of a mantle component and a radiogenic component. This may have come from a uranium source about 1201 ± 62 Ma old, or may be an uninterpretable mixed contaminant.

JD Claims Group

The JD mineralised vein system has two subsidiary branches, the so-called T1 and Main Zones. One galena and seventeen pitchblende samples have been analysed. The pitchblende samples have $^{208}\text{Pb}/^{204}\text{Pb}$ ratios of 36–37 or 39 at the JD showing, 54–59 at the T1 showing and 37 at the Main Zone (one sample), so evidently a number of different common-leads are involved. The galena and six pitchblende samples from specimen B31E have been brecciated and recemented by quartz, and are not necessarily coeval, while the three pitchblende samples from specimen B33A are coeval but with different lustres. The galena contains more radiogenic lead than some pitchblende, and is also apparently too young to be used as a common lead correction (modelling suggests a maximum age of some 1000 Ma).

The $^{206}\text{Pb}/^{204}\text{Pb}$ ratios are very low for the JD samples (*i.e.* they have large amounts of common lead) but are fairly high for the T1 and Main Zone material. Using an ordinary mantle lead composition for the common lead correction, the data are scattered on a concordia plot (Fig. 45), but seven of the twelve JD samples plotted are collinear with discordia intersections at 1428 ± 18 Ma and 140 ± 9 Ma, and four of the five T1 and Main Zone analyses form a discordia intersecting at 1092 ± 115 Ma and 99 ± 34 Ma. Other tantalising but unjustified discordia can be drawn by integrating all the data. Both discordia probably have some real significance, particularly the 1092 Ma line, taken as the true age of the T1 and Main Zone samples since the $^{206}\text{Pb}/^{204}\text{Pb}$ ratios imply (but do not prove) low contaminant lead contents. Sample B35E (T1 zone) plots in isolation, with slight reverse discordance and a $^{207}\text{Pb}/^{206}\text{Pb}$ age of 400 Ma. Other samples which plot off the two

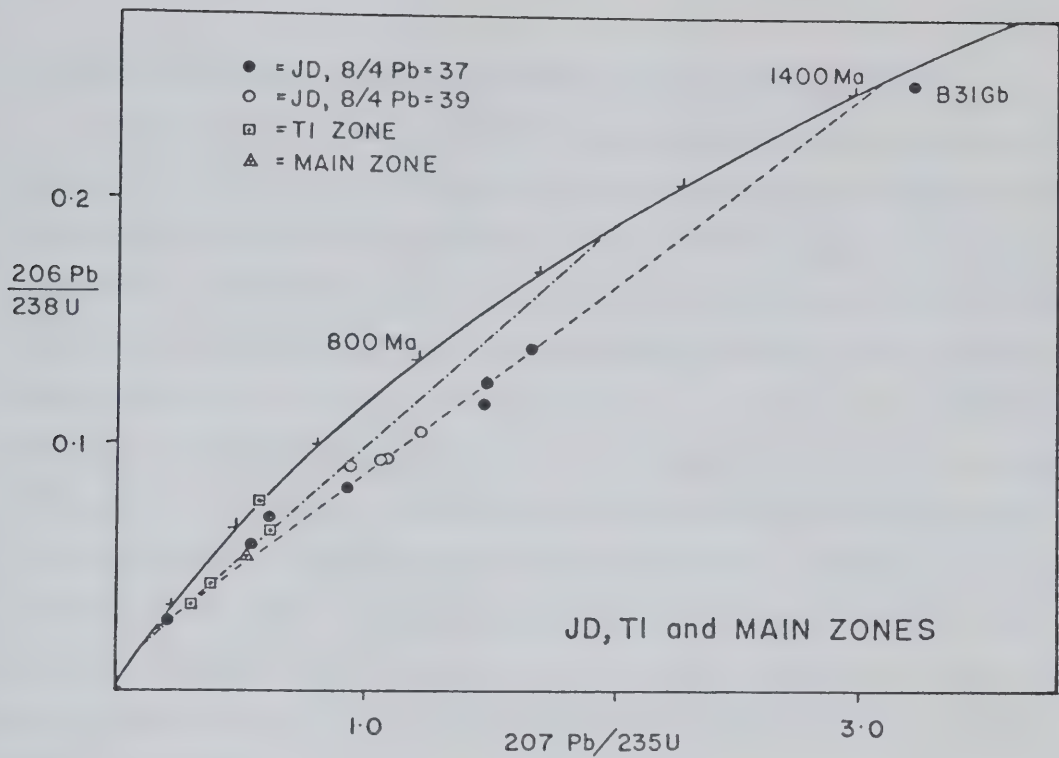


Figure 45: JD claims: concordia plot of pitchblende.

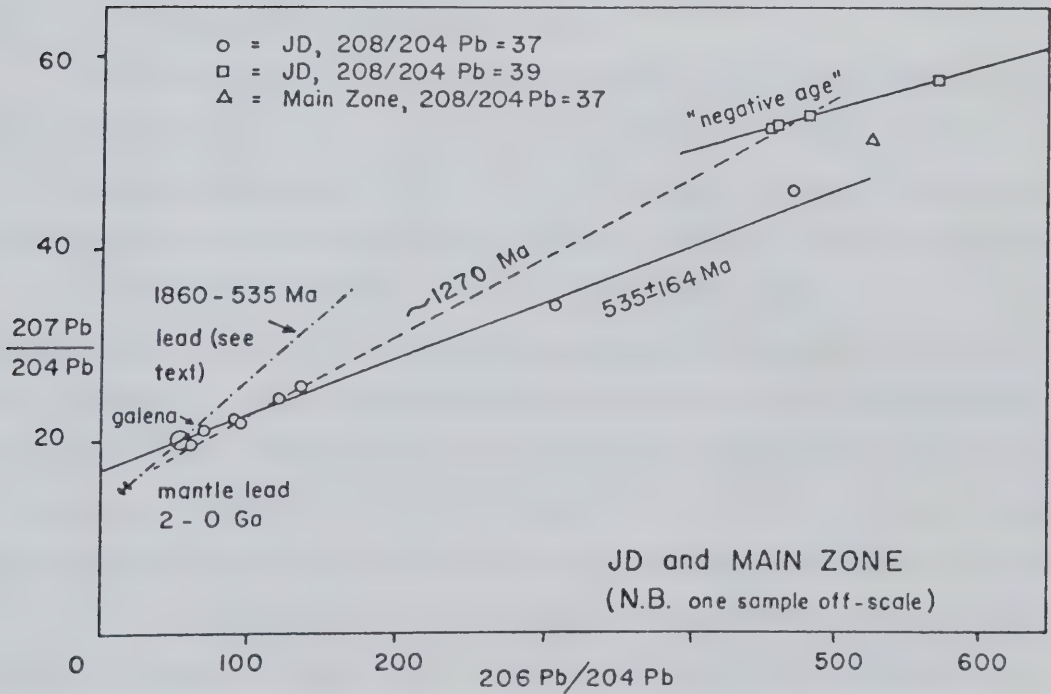


Figure 46: JD claims: isochron plot of pitchblende and one galena from the JD and Main Zone showings.

discordia may have been updated or contaminated with older uranogenic lead.

A number of "isochrons" are possible, depending on how much significance is attached to the sample groups as defined by their $^{208}\text{Pb}/^{204}\text{Pb}$ ratios. The eight pitchblende samples (and the galena) from the JD showing with $^{208}\text{Pb}/^{204}\text{Pb}$ ratios of 36–37 define a "scatterchron" of 535 ± 164 Ma (Fig. 46). The four JD showing samples with $^{208}\text{Pb}/^{204}\text{Pb}$ ratios of approximately 39 define a line of slope 0.0417 ± 0.0003 , which represents a negative age (Fig. 46). The four T1 Zone samples form a "scatterchron" of 960 ± 454 Ma (Fig. 47). The single Main Zone sample is distinct. These are the only *a priori* justifiable sample groups. If all twelve pitchblendes from the JD showing are considered, eight form a line of approximate slope age 1270 Ma; using ^{208}Pb as a reference isotope, which as noted is not thought to be quite as reliable, the same eight analyses form a line of approximate slope age 1200 Ma. In the same $^{206}\text{Pb}/^{208}\text{Pb}$ vs. $^{207}\text{Pb}/^{208}\text{Pb}$ coordinate system, other lines may be drawn if the JD, Main and T1 zone samples are mixed, but there is no justification for this.

The most radiogenic sample from the JD showing, B31Ea, has a $^{207}\text{Pb}/^{206}\text{Pb}$ age of 490 Ma; this compares with the 400 Ma $^{207}\text{Pb}/^{206}\text{Pb}$ age given for the reverse discordant sample B35E. The most radiogenic sample of all, B35F (T1 Zone) has a $^{207}\text{Pb}/^{206}\text{Pb}$ age of 810 Ma, and contains insignificant common lead.

The JD showing "isochrons" pass well above the model lead growth curve, except for the 1270 Ma line drawn by mixing the sample groups, so that the samples contain an uncorrected uranogenic component in the common lead (little if any ^{208}Pb appears to have been added). The suite must therefore be interpreted as was the Mazenod Lake material; the 1428 Ma discordia intersection may represent an almost thorium-free uranium source or deposit of that age, or it may be geologically meaningless and caused by a mixed contaminant. Figure 46 shows the mixing line of an ordinary mantle lead with uranogenic lead extracted at 535 Ma from a source now 1860 Ma old, and the position on that line of a possible common lead composition (the 535 Ma – 1428 Ma model yields too radiogenic a common lead). Using this model common lead composition of $^{206}\text{Pb}/^{204}\text{Pb} = 48$, $^{207}\text{Pb}/^{204}\text{Pb} = 19.7$, a new concordia plot of the eight "535 Ma old" pitchblendes was drawn. The data are very scattered, with a best-fit six-point discordia age of 805 ± 190 Ma, and the model is evidently inadequate.

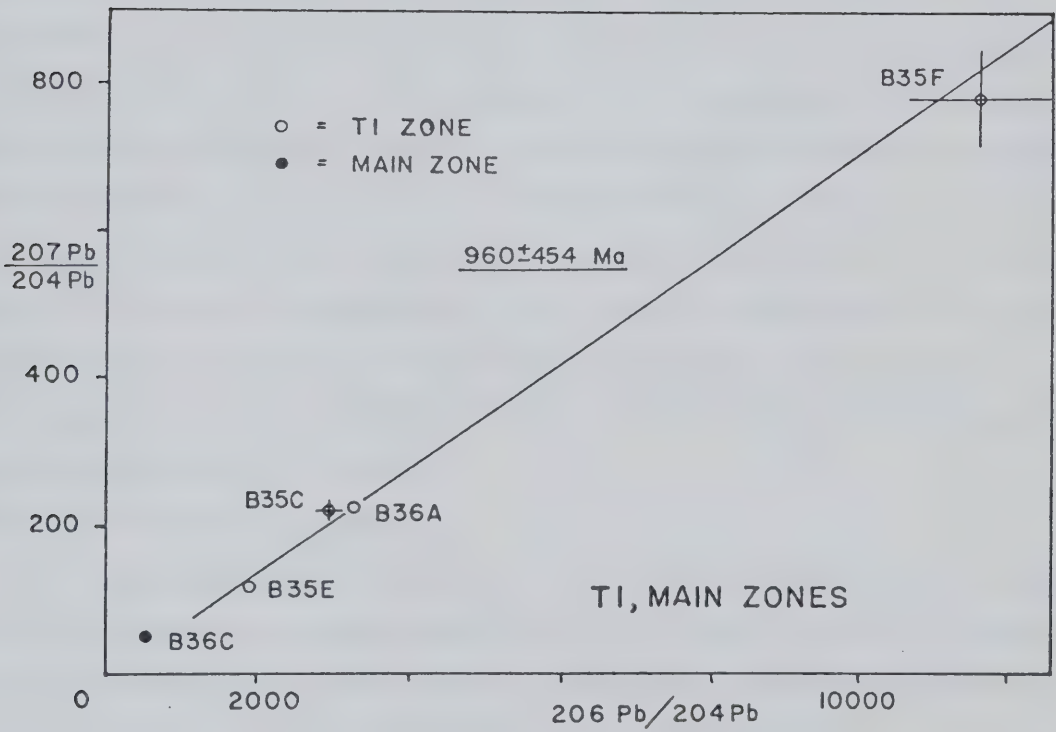


Figure 47: JD claims: isochron plot of pitchblende from the Main Zone and T1 Zone showings.

The line of "negative age" must be some type of mixing line, particularly since three samples are cogenetic and the $^{208}\text{Pb}/^{204}\text{Pb}$ ratios are distinctive. Because samples which define a discordia should contain the same components in their common leads (barring coincidences), mixing models which also permit the cogenetic samples to plot on the 1428 Ma discordia are cumbersome and geologically unlikely, and the line cannot yet be satisfactorily explained.

There is more to the history of the JD group of uranium deposits than this study can define. The general age of the JD mineralisation is probably 535 ± 164 Ma while pitchblende in the T1 and Main Zones is some 1092 ± 115 Ma old (the discordia age is preferred to the isochron age, due to the high $^{206}\text{Pb}/^{204}\text{Pb}$ ratios and greater precision). The 1428 Ma discordia intersection is of unknown significance, but using it for common lead modelling was unsuccessful. The complexity of the common lead may stem from a multistage origin, since these deposits are only three or four kilometres from the 1860 Ma old meta-placer uranium deposits on the JLD claims (*q.v.*). Remobilisation of this at 1092 Ma and 535 Ma is quite sufficient to render the common lead extremely inhomogeneous. The T1 zone $^{208}\text{Pb}/^{204}\text{Pb}$ ratios of 54–59 may reflect the thorogenic lead typical of the meta-placer deposits.

Hottah and Beaverlodge Lakes

Twenty-eight analyses of pitchblende and pitchblende-hematite fels from Hottah and Beaverlodge Lakes, including six by Cumming *et al.* (1955), have $^{208}\text{Pb}/^{204}\text{Pb}$ ratios of 37–43, 49–56 and 72–73. The excess ^{208}Pb is ascribed to a contaminating lead rather than to thorium in the samples. At least two original common leads are therefore involved, mixed in varying degrees. The three $^{208}\text{Pb}/^{204}\text{Pb}$ ratio groups do not correlate with the geography, style of mineralisation, apparent age or $^{206}\text{Pb}/^{204}\text{Pb}$ ratio, and may even vary within an outcrop. A concordia plot of all the samples, using an ordinary lead correction, produces four possible discordia (Fig. 48), with intersection ages of 2058 ± 34 and 340 ± 4 Ma, approximately 1330–1530 and 300 Ma, 449 ± 48 and -0.3 ± 4.8 Ma, and 1546 ± 40 and 73 ± 42 Ma (two cogenetic samples).

The 2058 Ma discordia is defined by five of seven pitchblende-hematite fels samples from Beaverlodge Lake, and, perhaps coincidentally, one of the two cogenetic samples from a specimen of pitchblende cement from the PITCH 27–28 claims. All seven

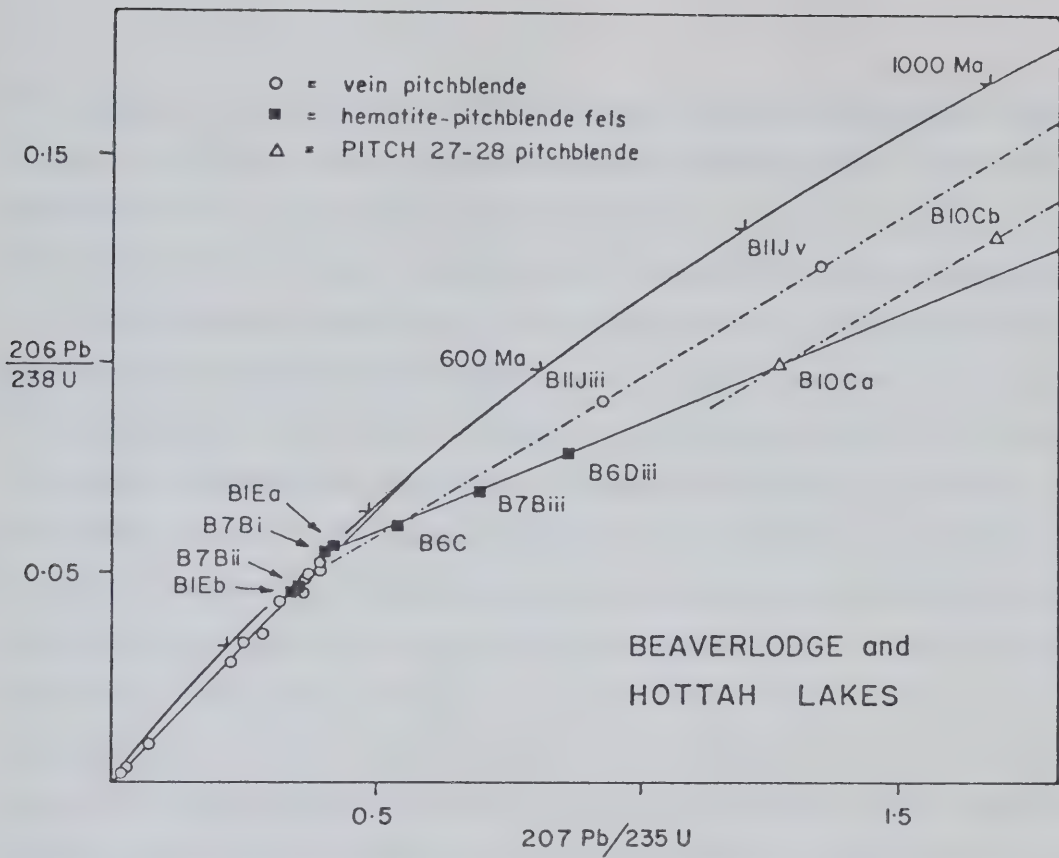


Figure 48: Hottah and Beaverlodge Lakes: concordia plot of pitchblende.

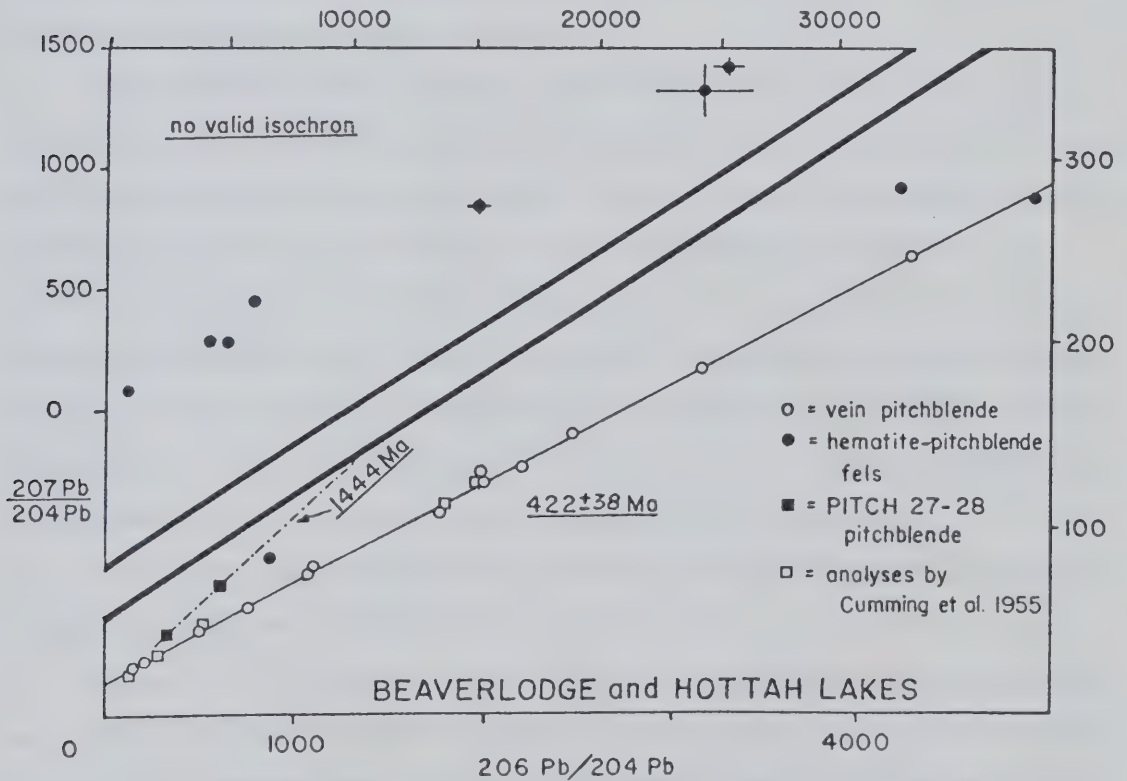


Figure 49: Hottah and Beaverlodge Lakes: isochron plots of (i) pitchblende veins from Hottah and Beaverlodge Lakes, and (ii) hematite-pitchblende fels from Beaverlodge Lake.

fels samples could be reasonably interpreted as old material showing partial or total updating at 340 Ma. However, a trend of decreasing $^{206}\text{Pb}/^{204}\text{Pb}$ ratios along the discordia suggests that, as in the Mazenod Lake suite, the upper intersection actually represents a uranogenic lead contaminant. Similarly, the least contaminated samples, essentially devoid of common lead, have $^{207}\text{Pb}/^{206}\text{Pb}$ ages of only some 400 Ma. It must nevertheless be observed that, (1) it is geologically possible for the pitchblende–hematite fels to be 2058 Ma old, being hosted by undated roof pendants, although not for the PITCH 27–28 pitchblende; (2) the trend of decreasing $^{206}\text{Pb}/^{204}\text{Pb}$ ratios is not perfect, and they are surprisingly high for this interpretation (6039 in one sample); (3) the statistical fit of the discordia is excellent. Emplacement at 2058 Ma and remobilisation at 340 Ma is a real possibility for the pitchblende–hematite fels; more probably it is somewhat older than 340 Ma and contaminated with lead from a uranium source at least 2058 Ma old. As at Mazenod Lake, combined contamination and diffusive lead loss would have reduced the 340 Ma lower discordia intersection in this case (from the 440 Ma age suggested later). In either case, a very old uranium source is indicated in the area, either country rocks or a uranium deposit, although diffusive lead-loss patterns or slight errors could raise or lower the 2058 Ma intersection considerably.

The estimated 1330–1530 Ma discordia intersection is an artifact induced by contamination, and is defined by two vein pitchblende samples and the cluster of analyses near 340 Ma on the concordia. The samples' $^{206}\text{Pb}/^{204}\text{Pb}$ ratios are the lowest of all, and decrease towards the upper intersection, as in the Mazenod Lake example. The two pitchblende samples from the PITCH 27–28 claims have high common lead contents and identical high $^{208}\text{Pb}/^{204}\text{Pb}$ ratios; their two-point discordia age (1546 Ma) approximately matches their more reliable two-point isochron age (1444 Ma) and the 1350–1550 Ma intersection mentioned above. Although these are all two-point lines, the coincidences suggest some type of mineralisation event of an uncertain age and nature.

The 449 ± 48 Ma discordia was calculated for twelve vein pitchblende samples from Beaverlodge Lake and the PITCH 8–10 claims.

On the $^{207}\text{Pb}/^{206}\text{Pb}$ isochron plot (Fig. 49), the vein pitchblendes from Beaverlodge and Hottah Lakes, together with the analyses by Cumming *et al.* (1955), form an isochron of age 422 ± 38 Ma with some slight scatter, equivalent to the 449 ± 48 Ma discordia. The

mean value of 440 ± 57 Ma is taken as the best age estimate. The pitchblende–hematite fels analyses are somewhat scattered; since the $^{208}\text{Pb}/^{204}\text{Pb}$ ratios show them to have different common leads, drawing an isochron through them is not justified.

To summarise, both types of mineralisation show the 440 ± 57 Ma event, during which the pitchblende veins at the PITCH 8–10 claims and Beaverlodge Lake were deposited. Pitchblende at the PITCH 27–28 claims is about 1450 Ma old, and two vein pitchblende samples from the PITCH 8–10 claims could have inherited lead from a source of that age. The pitchblende–hematite fels at Beaverlodge Lake indicates an event at about 2058 ± 34 Ma, but the geological nature of this event has not been established. It may be related in some way to the exotic terrain or other pre-batholithic supracrustal material.

F. Conclusions

Uranium has been introduced at least twice into the margins of the Great Bear Batholith from external sources, by way of the 2058 Ma old uranium source near the exotic terrain at Hottah Lake and the 1860 Ma old meta-placer deposits. A third source, a specific group of plutons, may have provided metals for the Echo Bay Ag–U deposits (Hoffman *et al.* 1976). Such sources have probably been remobilised repeatedly to produce the array of uranium deposit types and ages seen today, which still reflect the original perimetric distribution of the first deposits. This does not preclude the possibility that uranium has also been remobilised from other rocks within the batholith.

Pendants of pre-batholithic supracrustal rocks are widespread, but the meta-placer types are restricted to the single belt along the Wopmay Fault. The original placer minerals were probably shed westwards from the Hepburn Batholith, to accumulate as alluvial fans, beach-sand placers or aeolian placers at the old continental margin. Such uraninite-bearing deposits, perhaps updated by the intrusion of the Great Bear Batholith plutons at 1860 Ma, are a credible source of remobilised uranium for all the deposits of the eastern batholith margin, from the Rayrock mine to the Coppermine River.

The mid-Proterozoic, 2058 Ma old uranium source (whatever its nature), adjacent to the exotic terrain welded to the western margin of the batholith, is a possible source

material for the younger deposits in the Hottah Lake area. The full extent of this terrain, northwards beneath Great Bear Lake and southwards beneath the Palaeozoic cover, is completely speculative. A northern extension, assimilated into the Great Bear Batholith plutons and its uranium then recycled hydrothermally into the vein systems at Echo Bay, is unlikely, since Robinson and Morton (1972) indicated a sub-crustal origin for extrusives co-magmatic with these plutons.

Until the Palaeozoic era, all remobilisation of the original sources was a purely parochial affair. The first known remobilisation events occurred at Echo Bay, at 1500 and 1424 Ma (Fig. 50). The older event has not been found elsewhere, while the younger, triggered by a diabase intrusion at Echo Bay, may have extended as far as Hottah Lake and the Wopmay Fault (at the JD claims), where it is seen as the possible age for contaminant lead sources and for the PITCH 27–28 pitchblende. Major mafic igneous activity occurred throughout the batholith from some 1300 to 1200 Ma (Douglas 1980), but this had surprisingly little immediate impact on uranium mineralisation systems. At the Mountain Lake deposit (1076 ± 96 Ma old), uranium may have been mobilised and transported by hydrothermal activity following the extrusion of the overlying Coppermine River basalts at 1257 Ma; a hydrothermal updating event at 1108 Ma has been proposed for these lavas (Douglas *op. cit.*). The T1 deposit, 1092 ± 115 Ma old, and a possible precursor deposit at Mazenod Lake about 1201 ± 62 Ma old, are the only other manifestations of this event. In contrast, the pitchblende deposits of the Athabasca Basin have principal components 1345, 1299 and 1077 Ma old (Hoeve *et al.* 1981). The Great Bear Batholith was apparently at the outer limit of the uranium-mobilising effects of the Grenville Orogeny, which had ceased by 1000 Ma (Douglas *op. cit.*).

All the deposits covered in this study are either between 400 and 660 Ma old, or indicate remobilisation or lead loss within this time interval. A major marine transgression at the base of the Cambrian (600 Ma ago) and subsequent regression at the end of the Devonian (350 Ma ago) are known to have occurred, and the Coronation Sills and Franklin dyke swarm in the north of the batholith are about 650 Ma old (Douglas *op. cit.*). Submergence would have had profound effects on the groundwater regimes, introducing brines to levels previously above the water table, and the Franklin event suggests minor tectonic and igneous activity associated with the transgression. Resultant hot brines are

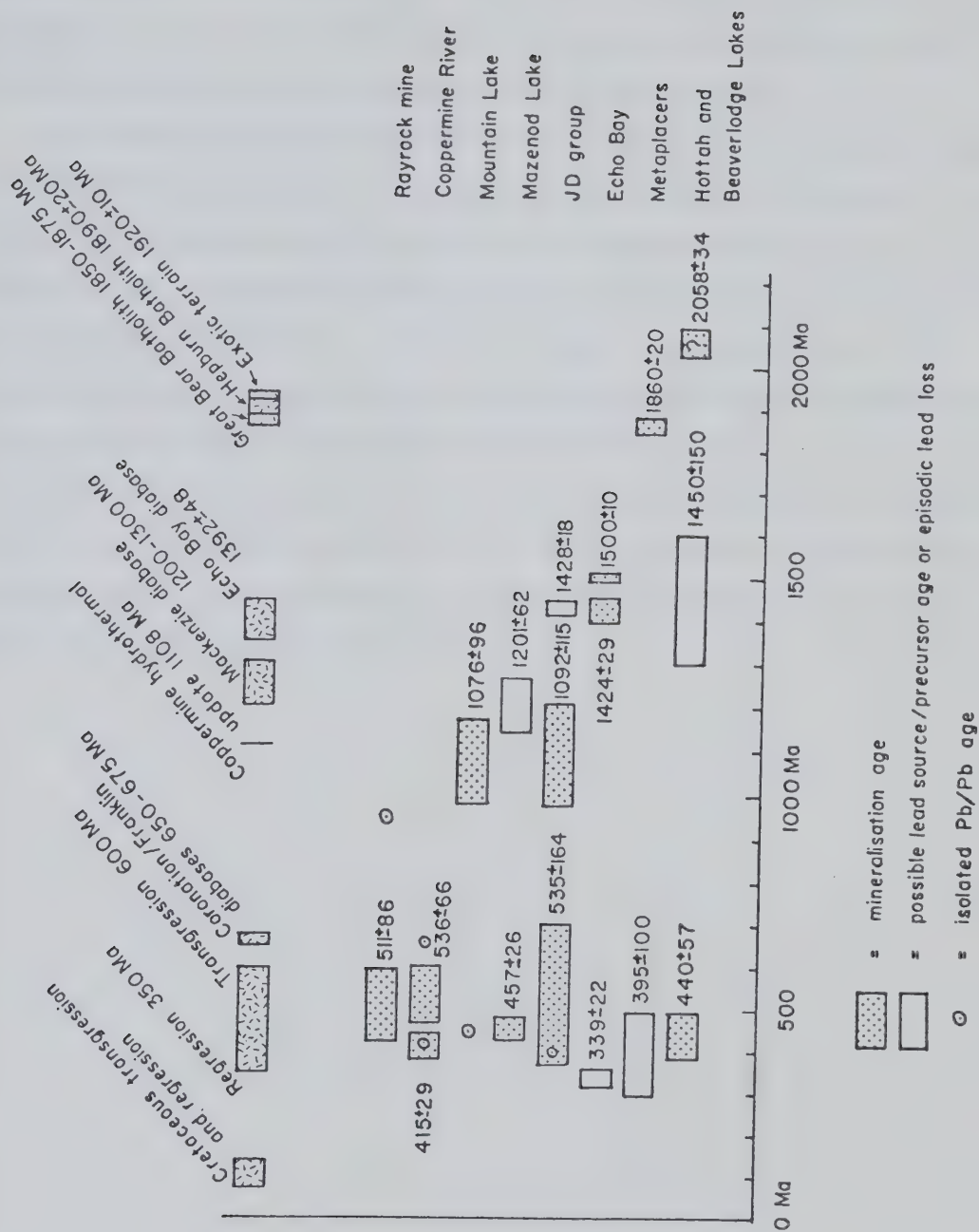


Figure 50: Correlation of the dates obtained with the known geological events within the batholith.

suggested as the agent for the widespread remobilisation which occurred in this period. Hoeve *et al.* (1981) have found lower discordia intersections at 411–515 Ma in pitchblende deposits 1077–1345 Ma old in the Athabasca Basin. This period has not been previously known as a time of mineralisation and remobilisation, but may prove to be even more extensive than the Great Bear Batholith deposits suggest.

From the palaeolatitudes suggested by Irving (1979) from palaeomagnetic data, a reference location at Mazenod Lake lay within 20° of the Equator in the periods 1830–1700 Ma, perhaps 1500–1310 Ma (there is a data gap for the period 1450–1650 Ma), 1100–960 Ma, 740–630 Ma and 580–370 Ma. It is interesting that the hydrothermal deposits dated fall within these intervals, with the exceptions of the undetermined 2058 Ma event and the 1201 Ma discordia date obtained at Mazenod Lake. Tropical weathering conditions may have caused extensive leaching of uranium, which then entered hydrothermal systems. It is also apparent that the Cretaceous palaeolatitude resembled today's, perhaps explaining why the Cretaceous marine transgression and regression (Balkwill 1971) apparently did not produce uranium deposits, whereas the Palaeozoic transgression cycle apparently did.

G. Acknowledgements

This study forms part of a doctoral thesis at the University of Alberta. Fieldwork was funded by the Department of Indian and Northern Affairs, Yellowknife, courtesy of Dr. W. Padgham. Numerous company geologists provided hospitality, transport and geological information in the field. Isotopic analyses were funded by NSERC grant A1168 to Dr. H. Baadsgaard of the University of Alberta, and performed on instruments maintained by Dr. G.L. Cumming of the Earth and Planetary Physics Institute, University of Alberta. Drs. Baadsgaard and Cumming also kindly provided the computer programs used. The constructive criticism of the manuscript by Dr. R.D. Morton and Dr. H. Baadsgaard is gratefully acknowledged.

REFERENCES

- BADHAM, J.P.N. 1973. Volcanogenesis, orogenesis and metallogenesis. Camsell River, N.W.T. PhD thesis (unpublished), University of Alberta, 334 p.
- BAILLIEUL, T.A. and INDELICATO, G.J. 1981. Uranium in the New Jersey and New York Highlands of the Reading Prong. *Economic Geology*, 76, p. 167-171.
- BALKWILL, H.R. 1971. Reconnaissance geology, southern Great Bear Plain, District of Mackenzie. Geological Survey of Canada paper 71-11, 47 p.
- BARAGAR, W.R.A. and DONALDSON, J.A. 1973. Coppermine and Dismal Lakes map-areas. Geological Survey of Canada paper 71-39, 20 p.
- BURWASH, R.A. and CAPE, D.F. 1981. Petrology of the Fort Smith - Great Slave Lake radiometric high near Pilot Lake, N.W.T. *Canadian Journal of Earth Sciences*, 18, p. 842-851.
- CUMMING, G.L. and RICHARDS, J.R. 1975. Ore lead isotope ratios in a continuously changing earth. *Earth and Planetary Science Letters*, 28, p. 155-171.
- CUMMING, G.L. and RIMSAITE, J. 1979. Isotopic studies of lead-depleted pitchblende, secondary radioactive minerals and sulphides from the Rabbit Lake uranium deposit, Saskatchewan. *Canadian Journal of Earth Sciences*, 16, p. 1702-1715.
- CUMMING, G.L., WILSON, J.T., FARQUHAR, R.M. and RUSSELL, R.D. 1955. Some dates and subdivisions of the Canadian Shield. *Proceedings of the Geological Association of Canada*, 7, Pt.2, p. 27-79.
- DOUGLAS, R.J.W. 1980. Proposals for time classification and correlation of Precambrian rocks and events in Canada and adjacent areas of the Canadian Shield. Part 2: A provisional standard for correlating Precambrian rocks. Geological Survey of Canada paper 80-24, 19 p.
- ECKELMANN, W.R. and KULP, J.L. 1957. Uranium-Lead method of age determination. *Bulletin of the Geological Society of America*, 68, p. 1117-1140.
- GANDHI, S.S. 1980. Mountain Lake deposit. *in* Geological Survey of Canada, Open File no. 716, p. 31-32.
- GANDHI, S.S. 1978. Geological observations and exploration guides to uranium in the Bear and Slave structural provinces and the Nonacho Basin, District of Mackenzie. Current Research, part B, Geological Survey of Canada paper 78-1B, p. 141-149.

- HILDEBRAND, R.S. 1980. Geological map of MacAlpine Channel, Vance Peninsula and Echo Bay. Open File No. 709, Geological Survey of Canada.
- HOEVE, J., CUMMING, G.L., BAADSGAARD, H. and MORTON, R.D. 1981. Geochronology of uranium metallogenesis in Saskatchewan. Program with Abstracts: Canadian Institute of Mining and Metallurgy, Uranium Symposium (Saskatoon), September 1981, p. 11.
- HOFFMAN, P.F. 1980. On the relative age of the Muskox Intrusion and the Coppermine River basalts, District of Mackenzie. Current Research part A, Geological Survey of Canada paper 80-1A, p. 223-225.
- HOFFMAN, P.F., BELL, I.R. and TIRREL, R. 1976. Sloan River map-area, Great Bear Lake, District of Mackenzie. Geological Survey of Canada paper 76-1A, p. 353-358.
- HOFFMAN, P.F. and ST-ONGE, M.R. 1981. Contemporaneous thrusting and conjugate transcurrent faulting during the second collision in Wopmay Orogen: implications for the sub-surface structure of post-orogenic outliers. Current Research part A, Geological Survey of Canada paper 81-1A, p. 251-257.
- IRVING, E. 1979. Paleopoles and paleolatitudes of North America and speculations about displaced terrains. Canadian Journal of Earth Sciences, 16, p. 669-694.
- JORY, L.T. 1964. Mineralogical and isotope relations in the Port Radium pitchblende deposit, Great Bear Lake, Canada. PhD thesis (unpublished), California Institute of Technology, 275 p.
- LUDWIG, K.R. 1979. Calculation of uncertainties of U-Pb isotope data. Earth and Planetary Science Letters 46, p. 212-220.
- MCGLYNN, J.C. 1971. Metallic Mineral Industry, District of Mackenzie, Northwest Territories. Geological Survey of Canada paper 70-17.
- MCGLYNN, J.C. 1979. Geology of the Precambrian rocks of the Riviere Grandin and in part of the Marian River map areas, District of Mackenzie. Current Research part A, Geological Survey of Canada paper 79-1A, p. 127-131.
- MILLER, R.G. 1981. Kawazulite $\text{Bi}_2\text{Te}_2\text{Se}$, related bismuth minerals and selenian covellite from the Northwest Territories. Canadian Mineralogist, 19, p. 341-348.
- PATCHETT, P.J., BYLUND, G. and UPTON, B.G.J. 1978. Palaeomagnetism and the Grenville orogeny: new Rb-Sr ages from dolerites in Canada and Greenland. Earth and Planetary Science Letters 40, p. 349-364.
- ROBINSON, B.W. 1971. Studies on the Echo Bay silver deposit, Northwest Territories, Canada. PhD thesis (unpublished), University of Alberta, 229 p.
- ROBINSON, B.W. and MORTON, R.D. 1972. The geology and geochronology of the Echo Bay area, Northwest Territories, Canada. Canadian Journal of Earth Sciences,

9, p. 158–171.

- ROBINSON, B.W. and OHMOTO, H. 1973. Mineralogy, fluid inclusions and stable isotopes of the Echo Bay U–Ni–Ag–Cu deposits, Northwest Territories, Canada. *Economic Geology*, 68, p. 635–656.
- RUSSELL, R.D. and FARQUHAR, R.M. 1960. Lead isotopes in geology. Interscience Publishers Inc., 243 p.
- STACEY, J.S. and KRAMERS, J.D. 1975. Approximation of terrestrial lead isotope evolution by a two-stage model. *Earth and Planetary Science Letters*, 26, p. 207–221.
- STEIGER, R.H. and JAGER, E. 1977. Subcommittee on Geochronology: convention on the use of decay constants in geo- and cosmochemistry. *Earth and Planetary Science Letters*, 36, p. 359–362.
- THORPE, R.I. 1978. Sill of Western Channel Diabase, Port Radium; *in* Wanless, R.K. and Loveridge, W.D. 1977; Rubidium–strontium isochron age studies, Report 2. Geological Survey of Canada paper 77–14, p. 4–6.
- THORPE, R.I. 1974. Lead isotope evidence on the genesis of the silver–arsenide vein deposits of the Cobalt and Great Bear Lake areas, Canada. *Economic Geology*, 69, p. 777–791.
- THORPE, R.I. 1971. Lead isotope evidence on age of mineralisation, Great Bear Lake, District of Mackenzie. Geological Survey of Canada paper 71–1B, p. 72–75.
- VAN SCHMUS, W.R. and BOWRING, S.A. 1980. Chronology of igneous events in the Wopmay Orogen, Northwest Territories, Canada. *in* Abstracts with Programs, Geological Society of America, 12, no.7, p. 540.
- WANLESS, R.K., STEVENS, R.D., LACHANCE, G.R. and RIMSAITE, J.Y.H. 1964. Age determinations and geological studies: Part 1: isotopic ages, report 5. Geological Survey of Canada paper 64–17.

XIV. APPENDIX IV: MAZENOD LAKE DEPOSIT MINERALOGY

This appendix consists of a publication on the metallic mineralogy of the Mazenod Lake pitchblende deposits, which is located in the back pocket.

KAWAZULITE $\text{Bi}_2\text{Te}_2\text{Se}$, RELATED BISMUTH MINERALS AND SELENIAN COVELLITE FROM THE NORTHWEST TERRITORIES

RICHARD MILLER

Department of Geology, University of Alberta, Edmonton, Alberta T6G 2E3

ABSTRACT

Kawazulite, tellurobismuthite and selenian *blau-bleibend* covellite are associated with pitchblende and hematite in a breccia pipe that cuts Aphebian dacitic ignimbrites at Mazenod Lake, Northwest Territories. Electron-microprobe analyses of kawazulite give $\text{Bi}_{2.13}\text{Te}_{1.96}\text{Se}_{1.04}$ and $\text{Bi}_{2.13}\text{Te}_{2.01}\text{Se}_{0.99}$, with minor Cu and Fe. Three unidentified bismuth minerals (*A*, *B*, *C*), with the general formula $\text{Bi}_2(\text{S}, \text{Se}, \text{Te})_3$, were also found. Anisotropy for kawazulite is distinct, with polarization colors bluish grey to brownish grey; its measured reflectivity is 60.0 to 61.6% (547-591 nm). Tellurobismuthite and mineral *A* have measured reflectivities of 61.6 to 62.0% and 51.1 to 51.6%, and micro-indentation hardness values (VHN_{50}) of 155 to 180 and 199 to 205, respectively. This is not only the first reported Canadian occurrence, but also the first recorded occurrence of kawazulite outside Japan. The covellite, which exhibits weak anisotropy, contains up to 15 wt. % Se. Associated digenite and chalcopyrite have normal compositions and optical properties.

Keywords: kawazulite, tellurobismuthite, guanajuatite, covellite, Se, Te, Bi, Mazenod Lake, Bear Province, Northwest Territories, hardness, reflectivity, microprobe.

SOMMAIRE

Kawazulite, tellurobismuthite et covelline *blau-bleibend* sélénifère sont associées à la pitchblende et à l'hématite dans une brèche en pipe qui recoupe des ignimbrites dacitiques d'âge Aphébien au lac Mazenod (Territoires du Nord-Ouest). La kawazulite possède la composition $\text{Bi}_{2.13}\text{Te}_{1.96}\text{Se}_{1.04}$ et $\text{Bi}_{2.13}\text{Te}_{2.01}\text{Se}_{0.99}$ avec un peu de Cu et de Fe (déterminations par microsonde électronique). Trois minéraux de bismuth, non-identifiés (*A*, *B* et *C*), de formule idéalisée $\text{Bi}_2(\text{S}, \text{Se}, \text{Te})_3$, sont aussi présents. La kawazulite est grise, anisotrope de bleuâtre à brunâtre entre nicols croisés. On mesure une réflectivité de 60,0 à 61,6% (de 547 à 591 nm). Pour la tellurobismuthite et l'espèce *A*, la réflectivité a les valeurs 61,6-62,0% et 51,1-51,6% et la dureté (par micro-indentation, VHN_{50}), 155-180 et 199-205, respectivement. C'est la première fois qu'on trouve la kawazulite ailleurs qu'au Japon. La covelline, légèrement anisotrope, contient jusqu'à 15% de Se (en poids). Les cristaux de digénite et de

chalcopyrite associés ont des propriétés optiques et des compositions normales.

(Traduit par la Rédaction)

Mots-clés: kawazulite, tellurobismuthite, guanajuatite, covelline, Se, Te, Bi, lac Mazenod, province de l'Ours, Territoires du Nord-Ouest, dureté, réflectivité, microsonde.

INTRODUCTION

A small U-Cu deposit occurs at Mazenod Lake, Northwest Territories, on the so-called Dianne mineral claims of the Noranda Exploration Company Limited (Long. $116^{\circ}55'W$, Lat. $63^{\circ}45'30''N$). A breccia pipe several hundred metres in diameter, defined by tourmaline veinlets and a large aeromagnetic anomaly, cuts dacitic ignimbrites of the Great Bear plutonic-volcanic suite. These intensely hematized host rocks are occasionally cut by small (1 to 2 mm across) veinlets of hematite-pitchblende that also host the Bi-Cu-Pb-S-Se-Te mineralization. Primary and secondary hematite can be distinguished in the veinlets; primary hematite has a platy habit, whereas secondary hematite, produced by the oxidation of magnetite, is present as equidimensional grains with relict magnetite cores. The pipe exhibits extensive superficial copper-rich oxidation products.

METHODOLOGY

Reflectivity measurements were made with a photometer calibrated to a tungsten carbide standard (Carl Zeiss no. 47 42 53). Reflectivity is 46.1% at 546 nm and 45.7% at 589 nm, with an accuracy of $\pm 1.5\%$. Monochromatic filters were used to obtain the wavelengths required. The reflectivity values given are the highest of four or more measurements. Freshly polished material was always used, since mineral *A* and tellurobismuthite both showed significant brown tarnishing after a period of a month.

Micro-indentation hardness was measured with a Vickers diamond indenter. The VHN numbers so obtained have been corrected by

reference to a calibration curve, constructed by comparing the measured and actual hardnesses of a range of six standard minerals. This led to a corrected value about 15% lower than the apparent value at $VHN_{50} = 100$.

The electron-microprobe analyses all involve the energy-dispersion technique and were made on an ARL EMX instrument fitted with an ORTEC energy-dispersion analyzer. The data were processed by the program EDATA2 (Smith & Gold 1979). Count times were 400 seconds for both the standards and the samples, with full-spectrum total counts of 1.5 to 2.5 million. The accelerating voltage was 15 kV in all cases.

Two sets of standards were used on different runs. One set comprised silver-bismuth selenide, cobalt telluride, chalcopyrite, pitchblende and lead-silica glass. The second set comprised a gold-silver alloy, Bi, Se and Te metals, chalcopyrite, pitchblende and lead-silica glass. As and Sb might be expected to be present, but a check by wavelength-dispersion techniques did not reveal them.

EDATA2 calculates the background continuum radiation for the average atomic number of the specimen; experience to date confirms that this procedure is entirely satisfactory (Smith & Gold 1979). Computer plots of the spectra after removal of the calculated background showed no significant residuals. The background calculation is based upon a "normative background", derived from a diamond sample, which models precisely the efficiency characteristics of the particular detector.

The program is set to reject concentrations of less than 0.03% as being below detection limits. In practice, elements analyzed on high-energy lines (*i.e.*, 5 kV and up) under these conditions have lower detection limits than this. In the suite of elements sought, major overlaps occur between the spectra of S, Pb and Bi, ranging from 26 to $\approx 100\%$. Overlap coefficients were calculated from the standards; the close approach to 100% totals (with the exception of analyses 7-9) indicates that these coefficients are correct. However, the detectability of these elements is no longer of the order of 0.03%. For example, analysis 1, on tellurobismuthite, had 301,134 counts in the Bi $M\beta$ region of analysis. Of these counts, 26%, or 78,294, fall in the S region of analysis. The statistical variation of these counts, *i.e.*, the square root (at the 1 σ level), is 280 counts. At the 2.58 σ or 99% confidence level, a peak of 722 counts could therefore register in the S region, owing to Bi, which sets the limit on S detectability in the presence of this amount of

Bi. A comparison with the analysis of digenite suggests that this represents about 0.05% S, although its different atomic weight makes direct comparison uncertain. I suggest that a detection limit of 0.1% is reasonable for S in a matrix of 50-60% Bi, with an analytical accuracy of ± 0.2 wt. %. Similar logic gives slightly higher values for Pb in a Bi- or S-rich matrix. Se, Te, Fe and Cu are not subject to interference in this suite, and a detection limit of perhaps 0.05% with an accuracy of $\pm 0.1\%$ is reasonable. The situation for S deteriorates further in the Pb-bearing phase, mineral *A*. The analytical X-ray lines were $K\alpha$ for S, Fe and Cu; $L\alpha$ for Se, Ag and Te; $M\beta$ for Pb and Bi.

MINERALOGY

The bismuth minerals found in this study all have the general formula $Bi_2(S,Se,Te)_3$ and similar optical properties. They were identified during routine electron-microprobe studies and cannot be distinguished optically except by reflectivity measurements. Kawazulite was first reported and described by Kato (1970), whose type material came from the Kawazu mine, Japan. It has not apparently been reported in the literature since then.

The Canadian kawazulite occurs in trace amounts, intimately associated with selenian covellite. The anhedral grains do not exceed 25 micrometres in diameter, so that X-ray-diffraction analyses and micro-indentation-hardness measurements are not practicable. Trace amounts of a similar phase occur nearby and form a very fine intergrowth with pitchblende and primary hematite. These grains are of the order of one micrometre in size and may be a different bismuth mineral. Kawazulite is also found as myrmekitic, submicrometre inclusions within the covellite; it has either exsolved from covellite or coprecipitated with it.

Tellurobismuthite has coprecipitated with about 50% pitchblende and is associated with some primary hematite. It is anhedral, forming grains generally less than 20 μm in diameter. It is also found as interstitial blebs, up to 100 μm in diameter, between grains of secondary hematite. There are trace amounts of chalcopyrite, bornite and, rarely, covellite, but these are not closely associated with the tellurobismuthite.

Mineral *A* was found in one veinlet as blebs up to 100 μm or more in diameter, interstitial to primary hematite. Although these blebs are large enough for microprobe analysis, they nearly all contain exsolved rods of covellite, up to 10 μm long and 0.3 μm in diameter. Oc-

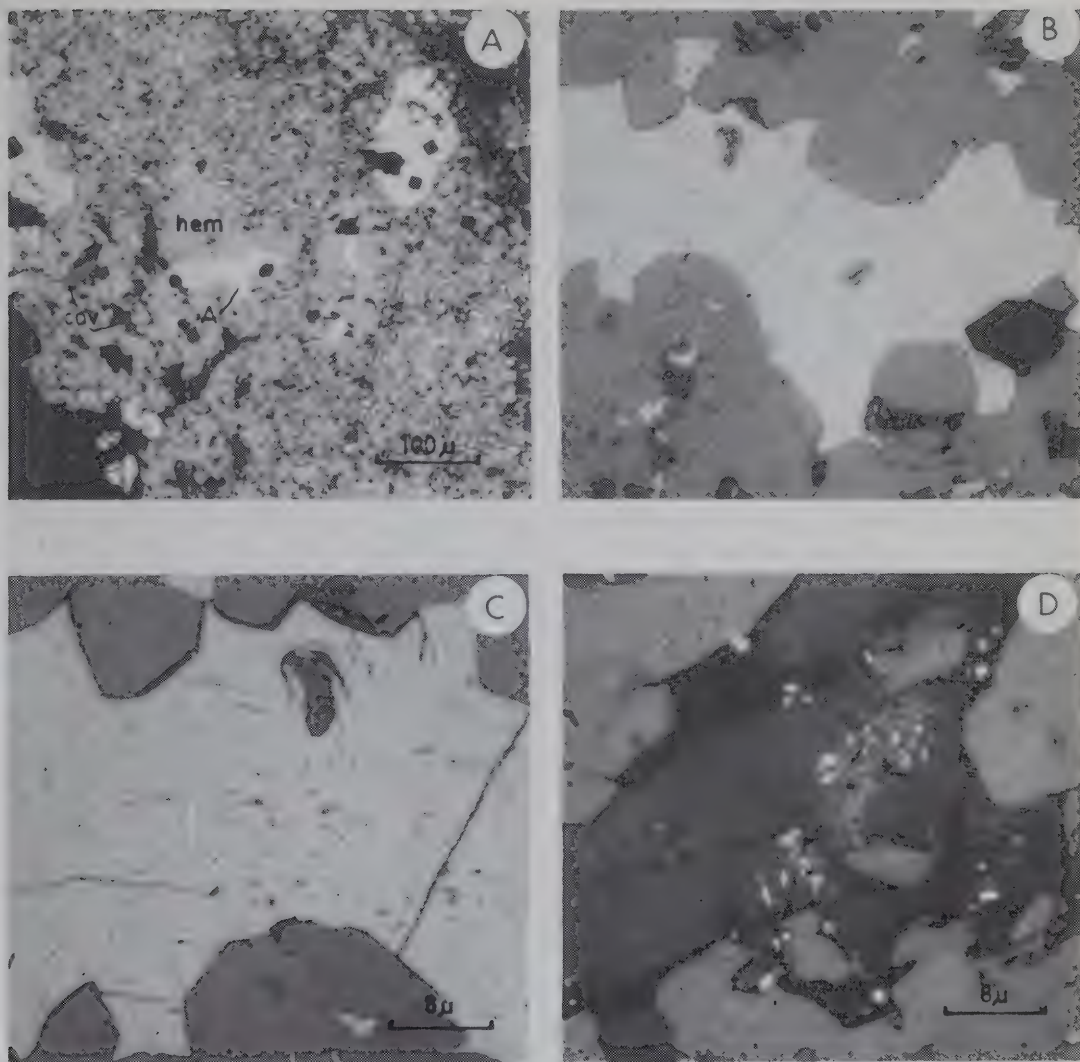


FIG. 1. A. Mineral *A* (white) and minor covellite (medium grey) in hematite (light grey) and silicate (black); x8 objective, photographed under oil immersion (as B, C and D). B. Central grain of mineral *A* in Figure 1A, x40 objective: exsolution rods of covellite are barely resolved at left, and three exsolution lamellae of mineral *B* (white) are at top. C. Left-hand section of grain of mineral *A* in Figure 1B, x100 objective: exsolution rods of covellite, in long and cross sections. D. Covellite grain, same scale as Figure 1C, 100 μm from the grain of mineral *A*, shows myrmekitic exsolution of mineral *A*.

casionally, the reverse relationship can also be seen. Like the kawazulite, mineral *A* was precipitated simultaneously with covellite, and the exsolution that resulted indicates a high-temperature solid solution between covellite and $\text{Bi}_2(\text{Se},\text{Te})_3$. It is possible that this covellite is the selenian analogue, klockmannite, which has similar optical properties (Uytendogaardt &

Burke 1971). Figure 1 illustrates the distribution of this phase.

Mineral *B* occurs as a few exsolution blebs in mineral *A*. These blebs are about $2 \times 10 \mu\text{m}$ on average and have a rather higher reflectivity than the host.

Mineral *C* occurs as a few single grains up to $4 \mu\text{m}$ in diameter, intergrown with pitchblende

or primary hematite. The veinlet in which it was found adjoins the one containing kawazulite.

The selenian *blaubleibend* covellite commonly occurs as grains up to 100 μm across; it is a primary mineral. A little secondary covellite forms alteration rims around chalcopyrite and bornite, which both occur as much smaller grains. Chalcopyrite exsolution lamellae occur within the bornite, which was not analyzed. Digenite was identified optically, but Goble & Smith (1973) studied very similar material and concluded that it was perhaps anilite that had been converted to a digenite-like material by the polishing process; the same may also be true in this case.

The first of these minerals to be deposited at Mazenod Lake was magnetite, although nothing indicates the stage at which it was subsequently oxidized. Some primary hematite followed, before the main period of hematite formation and U-Cu-Bi-Pb-S-Se-Te mineralization. Isotopic analyses by the author give an age of $460 \pm 30 \text{ Ma}$ for the veins. A general age of 1800 Ma is assigned to the igneous rocks of the Great Bear batholith.

RESULTS

Kawazulite

Analyses 2 and 3 (Tables 1, 2) are essentially

TABLE 1. COMPOSITION OF BISMUTH MINERALS

	Bi	Cu	Pb	Fe	Ag	S	Se	Te	Total*	Mineral
1)	52.6	(ND)	(ND)	0.45	(ND)	(ND)	0.26	46.3	99.95	Tellurobismuthite (this study)
2)	56.4	1.38	(ND)	0.48	(ND)	(ND)	10.4	31.8	100.99	Kawazulite (this study)
3)	56.3	(ND)	(ND)	0.37	(ND)	(ND)	9.92	32.4	99.33	Kawazulite (this study)
4)	48.8	6.35	10.7	1.02	(ND)	(ND)	32.9	0.90	101.08	Mineral A (this study)
5)	46.7	6.40	10.4	0.90	0.10	(ND)	33.6	0.79	99.19	Mineral A (this study)
6)	47.1	6.14	10.2	2.01	0.23	(ND)	33.5	0.93	100.34	Mineral A (this study)
7)	56.2	0.30	(ND)	2.24	(ND)	(ND)	20.1	17.6	96.57	Mineral B (this study)
8)	52.5	5.53	(ND)	0.37	(ND)	1.47	18.8	17.4	96.26	Mineral B (this study)
9)	55.1	0.69	(ND)	1.63	(ND)	(ND)	14.6	25.1	97.25	Mineral C (this study)

Compositions are expressed in weight %; ND: not detected. * Minor deviations from listed totals are due to minor Si (less than 0.2%) or U (less than 0.4%). The first may be due to an error in background fitting, the second to a halo effect from surrounding pitchblende.

TABLE 2. COMPOSITION OF $\text{Bi}_2(\text{S}, \text{Se}, \text{Te})_3$ MINERALS

	Bi	Cu	Pb	Fe	Ag	S	Se	Te	Mineral
1)	2.06	(ND)	(ND)	0.07	(ND)	(ND)	0.03	2.97	Tellurobismuthite (this study)
2)	2.13	0.17	(ND)	0.07	(ND)	(ND)	1.04	1.96	Kawazulite (this study)
3)	2.13	(ND)	(ND)	0.05	(ND)	(ND)	0.99	2.01	Kawazulite (this study)
4)	1.65	0.71	0.37	0.13	(ND)	(ND)	2.95	0.05	Mineral A (this study)
5)	1.55	0.70	0.35	0.11	0.01	(ND)	2.96	0.04	Mineral A (this study)
6)	1.56	0.67	0.34	0.25	0.02	(ND)	2.95	0.05	Mineral A (this study)
7)	2.06	0.04	(ND)	0.31	(ND)	(ND)	1.94	1.06	Mineral B (this study)
8)	1.80	0.62	(ND)	0.05	(ND)	0.33	1.70	0.97	Mineral B (this study)
9)	2.07	0.09	(ND)	0.23	(ND)	(ND)	1.45	1.55	Mineral C (this study)
10)	2.18#	-	-	-	-	3.00	-	tr	Bismuthinite (Durembergová & Kratochvíl 1977)
11)	2.22#	-	0.10	-	-	1.30	-	1.70	Tetradymite (Durembergová & Kratochvíl 1977)
12)	1.73	-	-	0.05	-	1.13	tr	1.86	Tetradymite (Timofeevskii 1972)
13)	1.77	-	-	0.05	-	1.04	tr	1.95	Tetradymite (Timofeevskii 1972)
14)	1.82	-	-	-	-	1.14	0.22	1.64	Tetradymite (Guha & Darling 1972)
15)	1.73	-	-	-	-	1.26	0.48	1.27	Tetradymite (Guha & Darling 1972)
16)	2.17	-	-	-	-	1.14	0.46	1.40	Tetradymite (Sarkar & Deb 1969)
17)	2.03	-	-	-	-	1.00	-	2.00	Tetradymite (Kashkaï et al. 1974)
18)	2.30	(ND)	(ND)	(ND)	-	1.10	(ND)	1.90	Tetradymite (Harada et al. 1972)
19)	1.88	-	-	-	-	0.93	0.18	1.89	Tetradymite (Palache et al. 1944, p. 162 analysis 8)
20)	1.79	-	0.03	-	-	1.16	-	1.84	Tetradymite (Plimer 1977)
21)	1.60	-	0.40	-	-	1.61	-	1.38	Plumbian tetradymite (Plimer 1977)
22)	1.92#	0.02	0.01	0.12	-	2.98	0.02	(ND)	Bismuthinite (Harada et al. 1972)
23)	2.00	-	-	-	-	2.40	0.60	-	Bismuthinite (Palache et al. 1944, p. 276 analysis 7)
24)	1.96	0.05	-	0.02	-	2.96	-	0.04	Bismuthinite (Palache et al. 1944, p. 276 analysis 4)
25)	2.01	-	-	-	-	0.18	-	2.82	Tellurobismuthite (Palache et al. 1944, p. 160 analysis 4)
26)	2.01	-	-	-	-	0.03	0.02	2.94	Tellurobismuthite (Palache et al. 1944, p. 160 analysis 6)
27)	1.83	-	0.17	-	-	2.47	-	0.53	Plumbian csiklovaite (Plimer 1977)
28)	2.05	-	-	-	-	0.14	2.86	-	Guanajuatite (Palache et al. 1944, p. 278 analysis 2)
29)	1.89	-	-	-	-	1.21	1.79	-	Guanajuatite (Palache et al. 1944, p. 278 analysis 4)

These values are (Bi+Sb). Atomic proportions, S+Se+Te = 3. ND not detected, - no data.

identical, except for a little Cu in the former. This may be due to copper in the kawazulite lattice rather than to exsolved covellite, since sulfur was not detected. If the exsolution product is klockmannite rather than covellite, however, this could produce copper contamination without sulfur.

The optical properties of the kawazulite are: reflectivity = 60.0% at 547 nm and 61.6% at 591 nm [*cf.*, type material: 45 to 50% (Kato 1970)]; color white; bireflectance, twinning and internal reflections not observed; anisotropy strong, with colors bluish grey to brownish grey (*cf.*, type material: grey to reddish brown-grey); *VHN* not obtainable, but the material is markedly softer than covellite; one good cleavage locally visible.

The reflectivity and reddish anisotropy reported for type kawazulite (Kato 1970) are consistent with a poor-quality polish, reducing the reflectivity and giving false anisotropy colors. Although X-ray-diffraction data exist for synthetic $\text{Bi}_2\text{Te}_2\text{Se}$ (PDF 29-247), it has not been possible to confirm that the mineral from Mazenod Lake is structurally identical to kawazulite. However, the electron-microprobe analyses, coupled with the generally strong physical resemblance to the other minerals of the group, support the identification.

Tellurobismuthite

The tellurobismuthite (analysis 1) is interesting only because of the absence of Se from the analysis, despite the Se-bearing minerals elsewhere. This suggests that there is no solid solution between tellurobismuthite and kawazulite.

The measured reflectivity of the tellurobismuthite is 61.6% at 547 nm and 62.0% at 591 nm, both marginally below previously reported values; $VHN_{50} = 155\text{--}180$, compared with reported values of $VHN_{10-20} = 32\text{--}93$ (Uytendogaardt & Burke 1971).

Mineral A

Analyses 4, 5 and 6 (Tables 1, 2) are essentially identical. The grains commonly have exsolved covellite (or klockmannite) rods in them; although visually clear areas were selected for analysis, similar rods may have been present below the sample surface but within the analyzed volume. However, the consistent Cu and Pb contents suggest that both of these elements are contained within the mineral lattice.

The best-fitting formula from the analyses is

$\text{Bi}_9\text{Cu}_4\text{Pb}_2\text{Se}_{18}$, with minor Te substituting for Se. Alternatively, the mineral may have a paraganajuatite structure, presumed to be analogous to the tetradymite and tellurobismuthite structures (Harker 1934, Brown & Lewis 1962), in which Bi has been replaced by $0.75(\text{Pb} + 2\text{Cu})$. However, these structures comprise hexagonal layers of close-packed, identical atoms in a five-layer sandwich; for paraganajuatite this is (Se-Bi-Se-Bi-Se), with metallic bonding within layers and van der Waals bonds between adjacent Se layers. There is no space in the structure for the extra atoms required for the suggested substitution, unless voids are created in the Se layers or unless Bi, Cu or Pb can substitute for Se.

Brown & Lewis (1962) have shown that a high degree of solid solution can occur in the Bi-Te system. The extra atoms are probably accommodated by the addition of extra layers to the structure, such as those shown by Strunz (1963) in the system Bi-Se. Until more data are obtained, this mineral should perhaps be regarded as a Cu-Pb-bearing variety of guanajuatite or paraganajuatite. "Mineral S" (Čech & Vavřín 1978), $\text{PbCuBi}(\text{S}, \text{Se}, \text{Te})_3$, is the closest published analogue found by the author. It has the same property of being derivable from a $\text{Bi}_2(\text{S}, \text{Se}, \text{Te})_3$ formula by the substitution of $\text{Pb} + \text{Cu}$ for Bi, so that ionic charges would be balanced.

The measured reflectivity of mineral A is 51.1% at 547 nm and 51.6% at 591 nm; $VHN_{50} = 199\text{--}205$.

Mineral B

Analyses 7 and 8 (Tables 1, 2) are less reliable than others in Table 1 because mineral B, which exists as exsolved patches in mineral A, is too small to avoid significant contamination during analysis by radiation from mineral A as well as from adjacent hematite (analysis 7) and covellite (analysis 8). These patches or lamellae were also visibly affected by the electron beam; they turned brown. The other bismuth phases were not markedly affected.

Both analyses of mineral B give low totals (96.6 and 96.3%). A grain was checked qualitatively by wavelength-dispersion methods to look for As or Sb, which could be hidden by the Se and Te X-ray peaks, respectively; none was found. The low analyses could be due to oxidation of the mineral surface during analysis or to slight volatilization and crater formation under the beam. Mineral B is a relatively minor product of exsolution; it possibly has the

formula $\text{Bi}_2\text{Se}_2\text{Te}$, which would make it a previously unrecorded member of this mineral group.

Mineral C

Analysis 9 (Tables 1, 2) represents the composition $\text{Bi}_4\text{Se}_3\text{Te}_3$, a previously unrecorded species. As the grain analyzed is small, confirmation of the composition would be desirable. It may be a member of a solid solution whose observed Se:Te ratio of 1:1 is a matter of coincidence, but this ratio also suggests an ordered phase. If we fit the formula to Harker's (1934) structural model as discussed, the logical possibilities are that each Te or S layer of Harker is filled with an ordered mixture of Se and Te, or that there are alternating layers of (Te-Bi-Se-Bi-Te) and (Se-Bi-Te-Bi-Se), or that there are alternating five-layer sandwiches of Bi_2Se_3 and Bi_2Te_3 .

Selenian covellite

Selenian *blaubleibend* covellite occurs closely associated with the bismuth minerals and as exsolution bodies within them. There is evidently a solid solution between covellite and $\text{Bi}_2(\text{Se},\text{Te})_3$. As discussed, some of the smaller exsolution bodies may in fact be klockmannite, but are far too small to analyze. It is notable that the digenite has comparatively little Se, and that the chalcopyrite has no detectable Se at all. Te is probably incapable of entering these lattices by virtue of its greater ionic size.

Ramdohr (1969) has attributed the *blaubleibend* effect to solid solution with Cu_2S , which is borne out by the excess Cu in the structural formulae (Tables 3, 4). Goble & Smith (1973)

analyzed suites of anilite and *blaubleibend* covellite and concluded that there are two varieties of the covellite, with the formulae $\text{Cu}_{1.12 \pm 0.03}\text{S}$ and $\text{Cu}_{1.32 \pm 0.04}\text{S}$ [yarrowite and spionkopite, respectively, of Goble (1980)]. The present study duplicates the yarrowite data, with the formula $\text{Cu}_{1.12 \pm 0.07}(\text{S},\text{Se})$. The digenite-like altered anilite of Goble & Smith (1973) gave an average composition of $\text{Cu}_{1.76 \pm 0.06}\text{S}$; the digenite of this study may well be similar, with the composition $\text{Cu}_{1.73}(\text{S},\text{Se})$.

The covellite is notable for its subdued birefractance, whereas its anisotropy under crossed nicols is much reduced, or even absent in a number of grains. Under oil, it remains blue in unpolarized or plane-polarized light. The adjacent digenite, bornite and chalcopyrite have normal optical properties.

DISCUSSION

Solid solution is known to exist in the series Bi_2S_3 - Bi_2Te_3 and Bi_2S_3 - Bi_2Se_3 , despite the different crystal structures involved in the latter series. Named minerals in these series are bismuthinite Bi_2S_3 , orthorhombic; csiklovaite $\text{Bi}_2\text{S}_2\text{Te}$, "undetermined" (Roberts *et al.* 1974); tetradyomite $\text{Bi}_2\text{Te}_2\text{S}$, rhombohedral (Harker 1934); tellurobismuthite Bi_2Te_3 , hexagonal or rhombohedral (Kato 1970); guanajuatite/paraguanajuatite Bi_2Se_3 (Palache *et al.* 1944), orthorhombic/hexagonal [but note that Strunz (1963) gave paraguanajuatite as $\text{Bi}_4(\text{Se},\text{S})_5$; Henley *et al.* (1975) gave guanajuatite as $\text{Bi}_2\text{Se}_2\text{S}$; Roberts *et al.* (1974) and others gave $\text{Bi}_2(\text{Se},\text{S})_3$ for both)]; kawazulite $\text{Bi}_2\text{Te}_2\text{Se}$, rhombohedral (Bland & Basinski 1961). Bland & Basinski showed that synthetic $\text{Bi}_2\text{Te}_2\text{Se}$ is isostructural with tetradyomite, whose structure was determined by Harker (1934).

Although solid solutions occur between the S and Se, and S and Te end-members (Fig. 2), apparently no analyses have been reported along the Se-Te tieline apart from kawazulite. This study suggests the existence of two other minerals along this line, $\text{Bi}_2\text{Se}_2\text{Te}$ (mineral B) and $\text{Bi}_4\text{Se}_3\text{Te}_3$ (mineral C). Of the five bismuth minerals found in this study, tellurobismuthite was found in one veinlet, kawazulite and mineral C coexist in a second, and mineral A and exsolved mineral B occur in a third. This suggests that there is no solid solution between kawazulite and mineral C, nor between mineral B and mineral A (possibly guanajuatite). It is also likely that there is no solid solution between tellurobismuthite and kawazulite, nor between mineral B and mineral C. Although these pairs were

TABLE 3. COMPOSITION OF SELENIAN COVELLITE

	Cu	Fe	Pb	S	Se	Te	Total*	Mineral
30)	61.2	1.06	0.87	25.7	9.4	0.07	98.46	Covellite (this study)
31)	58.0	3.57	1.28	21.5	15.7	0.05	100.45	Covellite (this study)
32)	60.4	3.98	2.57	20.5	12.4	0.13	100.00	Covellite (this study)
33)	60.3	1.83	1.77	21.7	13.7	(ND)	99.49	Covellite (this study)
34)	61.3	2.65	2.23	22.0	12.5	(ND)	100.79	Covellite (this study)
35)	74.1	1.13	1.00	20.2	3.3	(ND)	99.89	Digenite (this study)
36)	33.3	31.6	0.78	34.7	(ND)	(ND)	100.44	Chalcopyrite (this study)

Expressed in weight %. * Minor deviations from the listed totals are due to traces of Si (less than 0.2%) or U (less than 0.4%). The first may be due to an error in background fitting, the second may be a halo effect from adjacent pitchblende.

TABLE 4. COMPOSITION OF SELENIAN COVELLITE

	Cu	Fe	Pb	S	Se	Te	Mineral
30)	1.05	0.02	tr	0.87	0.13	tr	Covellite (this study)
31)	1.05	0.07	0.01	0.77	0.23	tr	Covellite (this study)
32)	1.19	0.09	0.02	0.80	0.20	tr	Covellite (this study)
33)	1.11	0.04	0.01	0.80	0.20	(ND)	Covellite (this study)
34)	1.14	0.06	0.01	0.81	0.19	(ND)	Covellite (this study)
35)	1.73	0.03	0.01	0.94	0.06	(ND)	Digenite (this study)
36)	0.97	1.05	0.01	2.00	(ND)	(ND)	Chalcopyrite (this study)

Expressed in atomic proportions, S+Se+Te = 1.

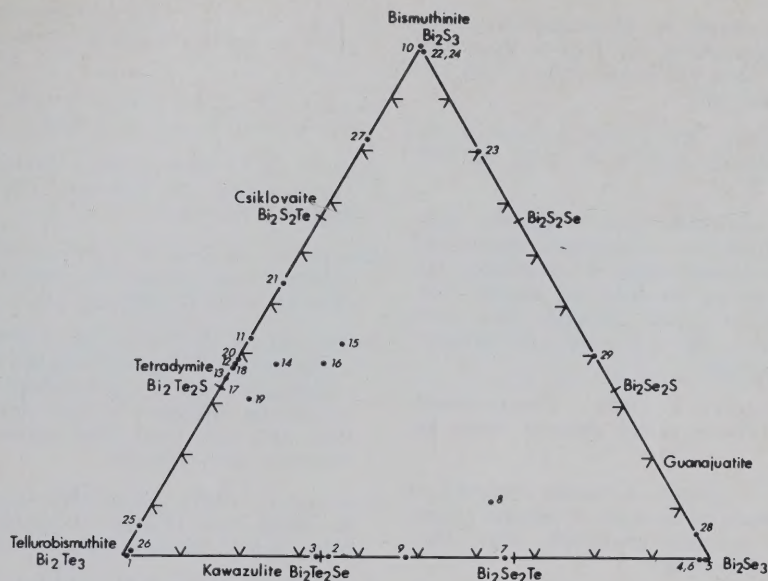


FIG. 2. Reported analyses of $\text{Bi}_2(\text{S,Se,Te})_3$ minerals; for key to individual analyses, see Table 2.

not found coexisting, the common origin and proximity of the veinlets, coupled with the almost perfect ratios of Se to Te, support this view.

Despite the presence of sulfur in the veinlets, as shown by the copper sulfides, there is virtually no sulfur in the bismuth minerals. This does not necessarily indicate a miscibility gap between minerals along the Bi_2Te_3 – Bi_2Se_3 tieline and Bi_2S_3 , but rather that chalcopyrite and digenite are intolerant of Se, whereas covellite is more tolerant and the bismuth minerals are more tolerant still. Under conditions of higher sulfur availability, sulfur may well enter the lattice of kawazulite and the unidentified minerals.

ACKNOWLEDGEMENTS

I extend particular thanks to Mr. S. Launspach, microprobe operator at the University of Alberta. The microprobe facilities are supported by NSERC grant A4254 to D.G.W. Smith. Optical work was made possible by NSERC grant A4242 to R.D. Morton. Noranda Exploration Company Limited kindly allowed access to their property; field expenses were met by the Department of Indian Affairs and Northern Development, Yellowknife. The manuscript benefited from critical reading by Roger Morton, Dorian Smith and anonymous referees.

REFERENCES

- BLAND, J.A. & BASINSKI, S.J. (1961): The crystal structure of $\text{Bi}_2\text{Te}_2\text{Se}$. *Can. J. Phys.* 39, 1040-1043.
- BROWN, A. & LEWIS, B. (1962): The systems bismuth–tellurium and antimony–tellurium and the synthesis of the minerals hedleyite and wehrliite. *J. Phys. Chem. Solids* 23, 1597-1604.
- ČECH, F. & VAVŘÍN, I. (1978): Poubaite, $\text{PbBi}_2(\text{Se, Te, S})_4$, a new mineral. *Neues Jahrb. Mineral. Monatsh.*, 9-19.
- DUREMBERGOVÁ, D. & KRATOCHVÍL, F. (1977): Bismuth- and tellurium-bearing minerals from Smolotely near Příbram. *Časopis Mineral. Geol.* 22, 407-410 (in Czech.; see also *Mineral. Abstr.* 29, 78-4909).
- FANDER, H.W. (1967): Selenium at Peko and Cobar. *Aust. Mineral. Dev. Lab. (AMDEL) Bull.* 2, 73-75 (see also *Mineral. Abstr.* 18, 281).
- GOBLE, R.J. (1980): Copper sulfides from Alberta: yarrowite Cu_8S_8 and spionkopite $\text{Cu}_{39}\text{S}_{28}$. *Can. Mineral.* 18, 511-518.
- & SMITH, D.G.W. (1973): Electron microprobe investigation of copper sulphides in the Precambrian Lewis series of S.W. Alberta, Canada. *Can. Mineral.* 12, 95-103.
- GUHA, J. & DARLING, R. (1972): Ore mineralogy of the Louvem copper deposit, Val D'Or, Quebec. *Can. J. Earth Sci.* 9, 1596-1611.

- HARADA, K., NAGASHIMA, K., MIYOKAWA, K. & YUI, S. (1972): Bismuthinite and cosalite from Agenosawa mine, Akita Prefecture, Japan. *Geol. Soc. Japan J.* 78, 485-488.
- HARKER, D. (1934): The crystal structure of the mineral tetradymite, $\text{Bi}_2\text{Te}_2\text{S}$. *Z. Krist.* 89, 175-181.
- HENLEY, K.J., SCHULTZ, P.K. & BROWN, R.N. (1975): Contributions to Australian mineralogy. 7. The compositional range of seleniferous bismuth sulphosalts in the Juno ore deposit, Tennant Creek, N.T. *Aust. Mineral. Dev. Lab. (AMDEL) Bull.* 20, 1-18 (see also *Mineral. Abstr.* 27, 76-3649).
- HEY, M.H. & EMBREY, P. (1972): Twenty-seventh list of new mineral names. *Mineral. Mag.* 38, 987-1001.
- & ——— (1974): A second appendix to the second edition of an index of mineral species and varieties arranged chemically. *Brit. Mus. (Nat. Hist.) Publ.* 725.
- KASHKAI, M.A., MAKHMUDOV, A.I. & MAGRIBI, A.A. (1974): Tetradymite and hessite from chalcoppyrite and pyrite ores from the Kashkachi deposit in the Dashkesan region of the Azerbaidzhan SSR. *Dokl. Akad. Nauk Azerb. S.S.R.* 30, 62-66 (in Russ.; see also *Mineral. Abstr.* 27, 76-844).
- KATO, A. (1970): In Introduction to Japanese Minerals. *Geol. Surv. Japan* 1970, 87-88.
- PALACHE, C., BERMAN, H. & FRONDEL, C. (1944): *Dana's System of Mineralogy. I. Elements, Sulfides, Sulfosalts, Oxides.* J. Wiley & Sons, New York.
- PLIMER, I.R. (1977): Bismuth minerals from quartz pipes in eastern Australia. *Aust. Mineral.* 10, 41-43.
- RAMDOHR, P. (1969): *The Ore Minerals and Their Intergrowths.* Pergamon, London.
- ROBERTS, W.L., RAPP, G.R. & WEBER, J. (1974): *Encyclopaedia of Minerals.* Van Nostrand & Reinhold, New York.
- SARKAR, S.C. & DEB, M. (1969): Tetradymite and wehrilite from Singhbhum copper-belt, India. *Mineral. Mag.* 37, 423-425.
- SMITH, D.G.W. & GOLD, C.M. (1979): EDATA2: a Fortran IV computer program for processing wavelength- and/or energy-dispersive electron microprobe analyses. In *Microbeam Anal. Soc. Proc. 14th Ann. Conf.* (San Antonio 1979; D.E., Newbury, ed.), 273-278.
- STRUNZ, H. (1963): Homöotypie Bi_2Se_2 - Bi_2Se_3 - Bi_3Se_4 - Bi_4Se_5 usw. (Plätynit, Ikunolith, Laitakarit). *Neues Jahrb. Mineral. Monatsh.*, 154-157.
- TIMOFEEVSKII, D.A. (1972): Bismuth sulfotellurides in the Darasun ore field, eastern Transbaikalia. *Zap. Vses. Mineral. Obshchest.* 101, 24-35 (in Russ.; see also *Mineral. Abstr.* 23, 72-3330).
- UYTENBOGAARDT, W. & BURKE, E. (1971): *Tables for Microscopic Identification of Ore Minerals.* (2nd ed.). Elsevier, Amsterdam.

Received October 1980, revised manuscript accepted February 1981.

B30340